UAB
Universitat Autònoma de Barcelona

yellow-in-the-dark mutants meet the omics era to unravel light and retrograde signaling in the green algae Chlamydomonas reinhardtii

Mariano Andrés De Silvio

ADVERTIMENT. L'accés als continguts d'aquesta tesi doctoral i la seva utilització ha de respectar els drets de la persona autora. Pot ser utilitzada per a consulta o estudi personal, així com en activitats o materials d'investigació i docència en els termes establerts a l'art. 32 del Text Refós de la Llei de Propietat Intel·lectual (RDL 1/1996). Per altres utilitzacions es requereix l'autorització prèvia i expressa de la persona autora. En qualsevol cas, en la utilització dels seus continguts caldrà indicar de forma clara el nom i cognoms de la persona autora i el títol de la tesi doctoral. No s'autoritza la seva reproducció o altres formes d'explotació efectuades amb finalitats de lucre ni la seva comunicació pública des d'un lloc aliè al servei TDX. Tampoc s'autoritza la presentació del seu contingut en una finestra o marc aliè a TDX (framing). Aquesta reserva de drets afecta tant als continguts de la tesi com als seus resums i índexs.

ADVERTENCIA. El acceso a los contenidos de esta tesis doctoral y su utilización debe respetar los derechos de la persona autora. Puede ser utilizada para consulta o estudio personal, así como en actividades o materiales de investigación y docencia en los términos establecidos en el art. 32 del Texto Refundido de la Ley de Propiedad Intelectual (RDL 1/1996). Para otros usos se requiere la autorización previa y expresa de la persona autora. En cualquier caso, en la utilización de sus contenidos se deberá indicar de forma clara el nombre y apellidos de la persona autora y el título de la tesis doctoral. No se autoriza su reproducción u otras formas de explotación efectuadas con fines lucrativos ni su comunicación pública desde un sitio ajeno al servicio TDR. Tampoco se autoriza la presentación de su contenido en una ventana o marco ajeno a TDR (framing). Esta reserva de derechos afecta tanto al contenido de la tesis como a sus resúmenes e índices.

WARNING. The access to the contents of this doctoral thesis and its use must respect the rights of the author. It can be used for reference or private study, as well as research and learning activities or materials in the terms established by the 32nd article of the Spanish Consolidated Copyright Act (RDL 1/1996). Express and previous authorization of the author is required for any other uses. In any case, when using its content, full name of the author and title of the thesis must be clearly indicated. Reproduction or other forms of for profit use or public communication from outside TDX service is not allowed. Presentation of its content in a window or frame external to TDX (framing) is not authorized either. These rights affect both the content of the thesis and its abstracts and indexes.

UNIVERSITAT AUTÒNOMA DE BARCELONA
FACULTAT DE BIOCIÈNCIES

PhD in Plant Biology and Biotechnology

yellow-in-the-dark mutants meet the omics era to unravel light and retrograde signaling in the green algae Chlamydomonas reinhardtii

---

Dissertation presented by Mariano Andrés De Silvio for the degree of PhD in Plant Biology and Biotechnology at the Autonomous University of Barcelona. This work was carried out at the Centre for Research in Agricultural Genomics (CRAG)

Thesis director

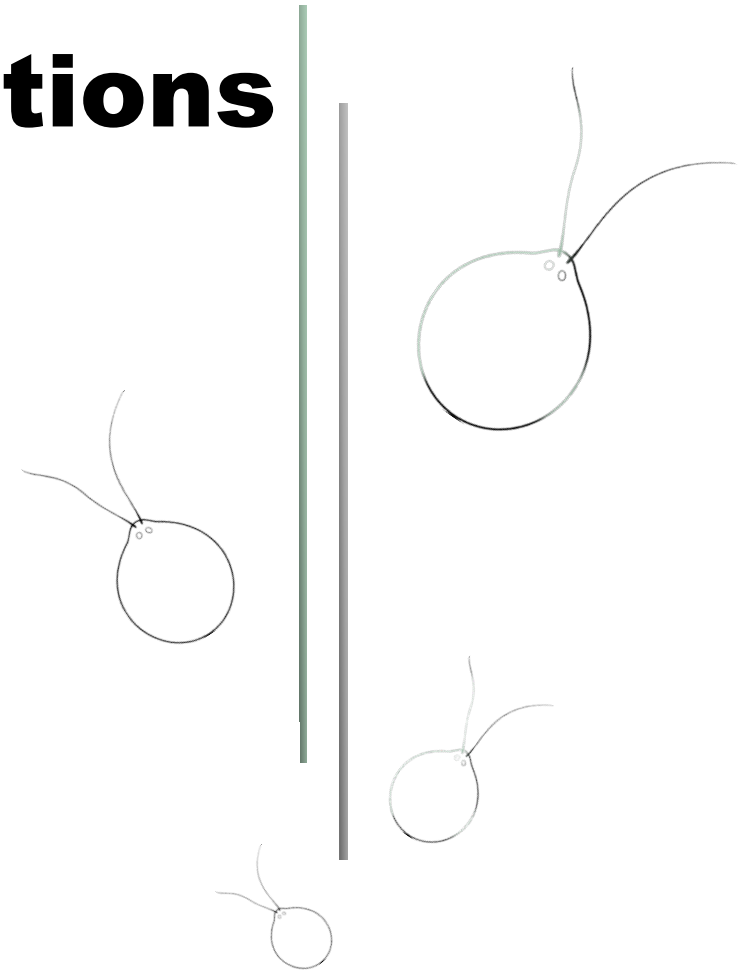
Dr. Elena Monte Collado

PhD candidate

Mariano Andrés De Silvio

Barcelona,
May 2024

Abbreviations



APA: active phyA-binding (PIF motif)

APB: active phyB-binding (PIF motif)

At: *Arabidopsis thaliana* / Arabidopsis

At Light: de-etiolation of Arabidopsis seedlings (Burko et al., 2020)

AUX: auxin influx carrier

BBX: B-BOX protein (i.e. BBX16)

BR: brassinosteroid

BZR1: BRASSINAZOLE-RESISTANT 1 (brassinosteroid receptor)

CCE: CRY C-TERMINAL EXTENSION (cryptochromes domain)

CCM: carbon concentrating mechanism

Chlide: chlorophyllide

Ci: inorganic carbon (CO_2 or HCO_3^-)

CLiP: Chlamydomonas Library Project

***CpANGs*/Cp**: chloroplast-associated nuclear genes

cpUPR: chloroplast unfolded protein response

Cre/CR: *Chlamydomonas reinhardtii* / Chlamydomonas

COP1: CONSTITUTIVE PHOTOMORPHOGENESIS 1

cry: cryptochromes

CTT: CONSTANS, CO-like and TOC1 domain

CUL1: CULLIN 1

CUL4: CULLIN 4

DASH: Drosophyla-Arabidopsis-Synechocystis-Human

DDB1: DAMAGE SPECIFIC DNA BINDING PROTEIN 1

DE (*DEGs*): differential expression / differentially expressed genes

DELLA: DELLA protein (aspartic acid - glutamic acid - leucine - leucine - alanine)

DGDG: di-galactosyldiacylglycerol (galactolipids from chloroplast membranes)

DPOR: light-independent (Dark) Protochlorophyllide Oxidoreductase

E2: ubiquitin-conjugating enzymes

EBF: EIN3 BINDING F-BOX (i.e. EBF1 / EBF2)

EIN3: ETHYLENE INSENSITIVE 3

ET: ethylene

ETF: early transcription factor

FA: fatty acid

FAD: flavin adenine dinucleotide (chromophore of blue light receptors)

FC: ferrochelatase (i.e. FC1 / FC2)

FKF1: FLAVIN-BINDING, KELCH REPEAT, F-BOX 1

GA: Gibberellin

GARP: GOLDEN2 (*Zea mays*), ARR-B (*Arabidopsis thaliana*), Psr1 (*Chlamydomonas reinhardtii*)

GCN: gene co-expression network

GID1: GIBBERELLIN-INSENSITIVE DWARF1 (GA receptor)

GLK: GOLDEN2-LIKE (i.e. GLK1 / GLK2)

GRAS: generally recognized as safe

GRN: gene regulatory networks

GRF7: GROWTH REGULATING FACTOR 7

GuCy: guanylyl cyclase encoding gene (Cre16.g688638_4532)

GUN: GENOMES UNCOUPLED (i.e. GUN1-6)

HE (VHE): highly (and very highly) expressed genes

HFR1: LONG HYPOCOTYL IN FAR-RED

HSC70-1: HEAT SHOCK COGNATE PROTEIN 70-1

HSP22E/F: HEAT SHOCK PROTEIN 22 E/F

HY5: ELONGATED HYPOCOTYLS 5

IFT: intraflagellar transport

L+Lin: Light plus lincomycin

LAF1: LONG AFTER FAR-RED LIGHT 1

LHCSR1/3A/3B: LIGHT HARVESTING COMPLEX STRESS-RELATED 1/3A/3B

LIN/linco: Lincomycin

LKP2: LOV KELCH PROTEIN 2

LOV: LIGHT OXYGEN VOLTAGE

LPOR (POR1): Light-dependent Protochlorophyllide Oxidoreductase

LinRGs: lincomycin responsive genes

LLRGs: light and lincomycin responsive genes

LRGs: light responsive genes.

LRTFs: light responsive transcription factors

LTF: late transcription factor

MARS1: MUTANT AFFECTED IN RETROGRADE SIGNALING 1

MGDG: mono-galactosyldiacylglycerol (galactolipids from chloroplast membranes)

MgProto: Mg-protoporphyrin IX

MORF2: MULTIPLE ORGANELLAR RNA EDITING FACTOR 2

MTF: mid transcription factor

NAB1: NUCLEIC ACID BINDING 1

NEP: NUCLEAR ENCODED POLYMERASE (Chloroplast RNA polymerase)

NF: Norflurazon

PAP: PEP-ASSOCIATED PROTEIN

PBE: PIF-binding E-box (CACATG)

Pchlide: protochlorophyllide

PEP: PLASTID ENCODED POLYMERASE (Chloroplast RNA polymerase)

PhANG: Photosynthesis-associated nuclear genes

PhAPG: Photosynthesis-associated plastid genes

PHOT: phototropin

PIF: PHYTOCHROME INTERACTING FACTOR

PHR: photolyase homologous region

pifq: *PIF* quadruple mutant (*pif1345*)

phy: phytochromes

PIN: auxin efflux carrier

PLB: prolamellar bodies

Pp: *Physcomitrella patens*

PT: prothylakoids

PSY: PHYTOENE SYNTHASE

R / FR: red / far-red

RBX1: RING BOX PROTEIN 1

RS: retrograde signaling

RT-qPCR: Reverse Transcription – Quantitative Polymerase Chain Reaction

RuBiSco: ribulose-1,5-biphosphate carboxylase/oxygenase

SCE: stored curvature elastic (stress)

SCF: SKP1-CULLIN1-F-BOX

SIG: SIGMA factor

SLY1: SLEEPY 1

SKP1: S-PHASE KINASE ASSOCIATED PROTEIN 1

SPA: SUPPRESSOR OF PHYA-105

TEM: transmission electron microscopy

TFs: transcription factors

TIC: TRANSLOCON AT THE OUTER MEMBRANE OF THE CHLOROPLAST

TOC: TRANSLOCON AT THE INNER MEMBRANE OF THE CHLOROPLAST

UVR8: Ultraviolet receptor 8

VIPP1/2: VESICLE INDUCING PLASTID PROTEIN 1/2

VP: valine-proline motif

wt: wild type

wt12 Light: dark-to-light transition of wt cells grown in 12:12 photoperiod (Strenkert et al., 2019)

wt Dark: wild type CC-124 cells grown in dark conditions

wt Dark + Linco: wild type CC-124 cells grown in dark conditions and lincomycin treatment

y: *yellow-in-the-dark mutant*

y-1: Sager's original *yellow-in-the-dark* mutant (Sager & Palade, 1954)

y-2: *yellow-in-the-dark* mutant with a more stable locus (Ford & Wang, 1982)

y-4: *yellow-in-the-dark chlL* mutant (*chlL*) (Suzuki & Bauer, 1992)

***y-4* Dark/D0**: *y-4* etiolated cells in dark conditions

***y-4* Dark + Linco**: y-4 etiolated cells in dark and lincomycin treatment

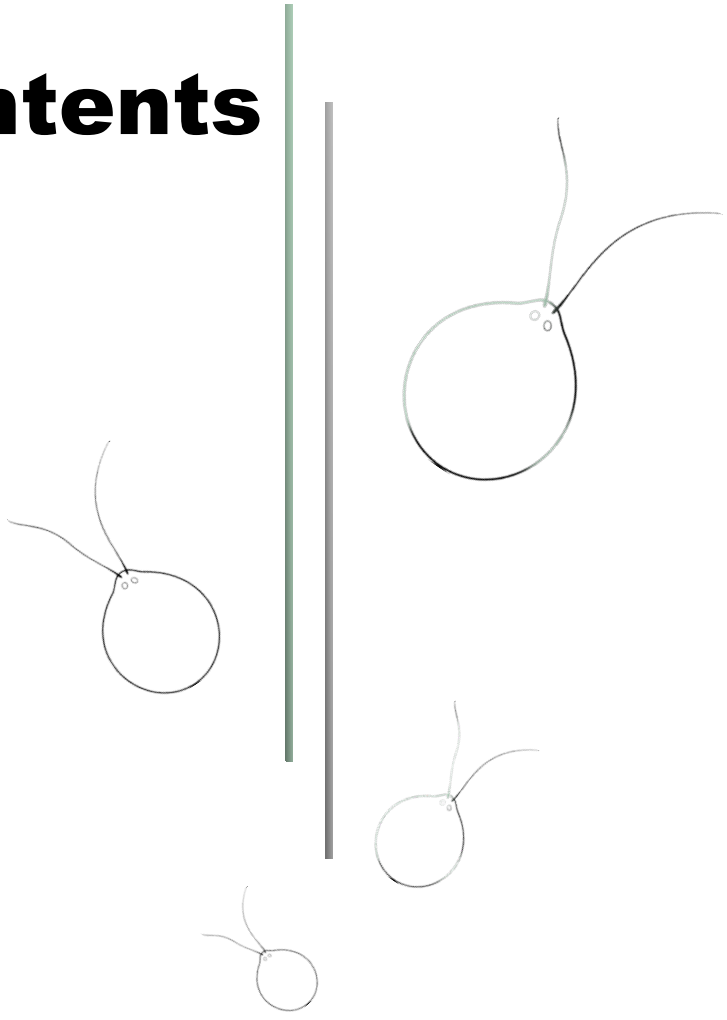
***y-4* Light**: de-etiolation of *y-4* cells in light

***y-4* Light + Linco**: de-etiolation of *y-4* cells in light and lincomycin treatment

***y-4* AL**: *y-4* cells always-grown in light conditions

ZTL: ZEITLUPE

Table of Contents



Summary ---------- *XV*

CHAPTER 1 - *General Introduction* ---------- *1-30*

Objectives ---------- *30-34*

CHAPTER 2 - *Setup of a y mutant based de-etiolation system* ---------- *35-62*

CHAPTER 3 - *Transcriptome analysis: LIGHT SIGNALING* ---------- *63-114*

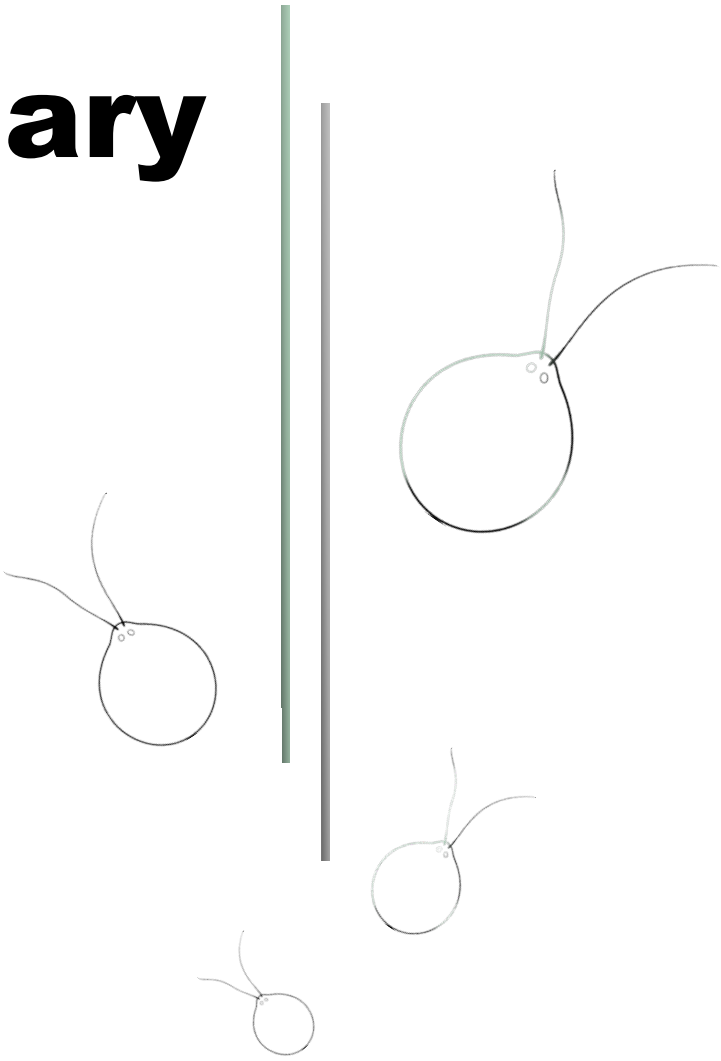
CHAPTER 4 - *Transcriptome analysis: RETROGRADE SIGNALING* ---------- *115-148*

General Discussion ---------- *149-154*

Conclusions ---------- *155-158*

References ---------- *159-172*

Summary



Seedling de-etiolation is characterized by the transition from skotomorphogenesis (elongated hypocotyl, presence of hook and closed cotyledons, limited root growth) to photomorphogenesis (short hypocotyl, open and expanded cotyledons, lateral root growth); during this shift, dark-adapted non-photosynthetic plastids (etioplasts) transform into fully functional photosynthetic chloroplasts upon transfer to light. This process is regulated by complex but exquisite light signaling pathways that involve photoreceptors (mainly phytochromes and cryptochromes), and several key transcriptional regulators (PIFs, HY5, GLKs and B-BOX proteins. In addition, the plastid itself can act as an environmental sensor and send retrograde signals (RS) to the nucleus to fine-tune its development during de-etiolation. How RS are sent to the nucleus remains a mystery, but it has been shown that GUN1 is a central regulator of this pathway. Importantly, light and chloroplasts signals converge to regulate chloroplast biogenesis and other aspects of seedling development such as cotyledon separation. De-etiolation has been traditionally studied in angiosperm plants, thanks to their ability to etiolate in the dark. In contrast, gymnosperms can synthesize chlorophyll in darkness and always feature a fully developed chloroplast. Interestingly, yellow-in-the-dark (y) mutants of the green microalgae *Chlamydomonas reinhardtii* are unable to synthesize chlorophylls in the dark and form undifferentiated chloroplasts with no photosynthetic activity under prolonged darkness. Upon exposure to light, they are able to fully restore a functional chloroplast. Remarkably, they lack essential components of light and RS pathways in angiosperms, including PIFs, GLKs and GUN1.

In this work, we developed a y mutant based de-etiolation system that allowed us to transcriptomically study and characterize main light and RS events. Comparative analysis with Arabidopsis showed that light and RS regulate similar biological processes in both species. We found that photosynthesis-associated genes are already accumulated at high levels in y etiolated cells and are slightly induced by light, while RS strongly but transiently repress these genes. Our results suggest that PIFs and GLKs evolved in angiosperm plants to confer a higher degree of regulation to these genes, and that GUN1 might have evolved to keep sustained repression of these genes. Moreover, combined physiological and transcriptomic data suggests that chloroplast biogenesis is achieved in two distinct phases in y mutants, similarly to angiosperm plants. Finally, by building gene co-expression networks we identified potential novel transcription factors that regulate chloroplast biogenesis in Chlamydomonas. This work provides new insights in the regulation of light and RS during de-etiolation.

Introduction

CHAPTER 1

Introduction

From dark to light: de-etiolation 3

A complex light signaling pathway regulates de-etiolation 4-12

Light signaling starts with perception of light by plant photoreceptors 4-6

Active photoreceptors repress the activity of COP1-SPA E3 ubiquitin ligases and PIF transcription factors to trigger de-etiolation response 7-11

Regulation of seedling de-etiolation by phytohormones 11-12

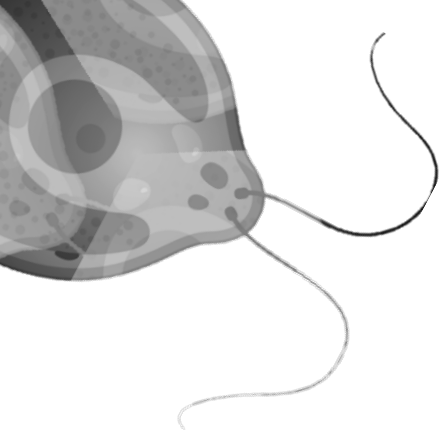
Etioplast-to-chloroplast transition: the hallmark of de-etiolation response 13-16

GUN1-mediated chloroplast-to-nucleus retrograde signals regulate de-etiolation in Arabidopsis 17-19

Etiolation does not take place in non-angiosperm plants, but key light and retrograde signaling components involved in de-etiolation are conserved at different degree 20-24

Chlamydomonas reinhardtii: how a green microalga has become a widely established model for basic and applied research 24-27

Chlamydomonas yellow-in-the-dark mutants: a model to study early light and retrograde signaling during chloroplast biogenesis 27-30



1 Chapter

Light is surely the most important environmental factor during a plant life cycle. On one hand, as photoautotrophic organisms, plants need light to produce their own energy source in the form of sugars, and since they are sessile organisms, they need to constantly adapt their morphology to maximize light capture; on the other hand, light is also a source of information for plants about their growth environment: light quality, quantity and duration inform them about seasons, time of day, or presence of neighbors, and determine most of developmental and physiological responses, including photomorphogenesis, the entrainment of an oscillating circadian clock, flowering, phototropism, and shade avoidance (Arsovski et al., 2012).

From dark to light: de-etiolation

Plants are constantly seeking light since the beginning of their life after seed germination (Figure 1.1): in Arabidopsis, a newly emerging seedling fueled by seed reserves rapidly elongates the hypocotyl and forms an apical hook that protects the shoot apical meristem from damaging, while cotyledons and roots remain undeveloped; this process occurs in dark and is called skotomorphogenesis. Once the seedling reaches the surface and encounters light, development switches to photomorphogenesis: hypocotyl stops elongating, the hook opens and cotyledons expand; in this process, the seedling gains photosynthetic competence and becomes autotrophic. Other dicot species, such as tomato or bean, feature a similar developmental transition. Skotomorphogenic to photomorphogenic growth in all these species, is coupled at the cellular level with a transition from dark-developed plastids, called etioplasts, to light-developed chloroplasts, and this switch in developmental programs is called de-etiolation. This also marks a profound change in metabolism: etioplasts do not contain chlorophylls, nor active photosystem complexes, while dark conditions force etiolated seedlings to grow heterotrophically, fueled by lipids and protein reserves present in the cotyledons; upon light exposure, etioplasts develop into chloroplasts that contain thylakoids (a network of internal membranes where all the components of the electron transport chain are assembled), and start performing photosynthesis, thus establishing seedling autotrophy (Armarego-Marriott et al., 2019, Gommers & Monte, 2017).

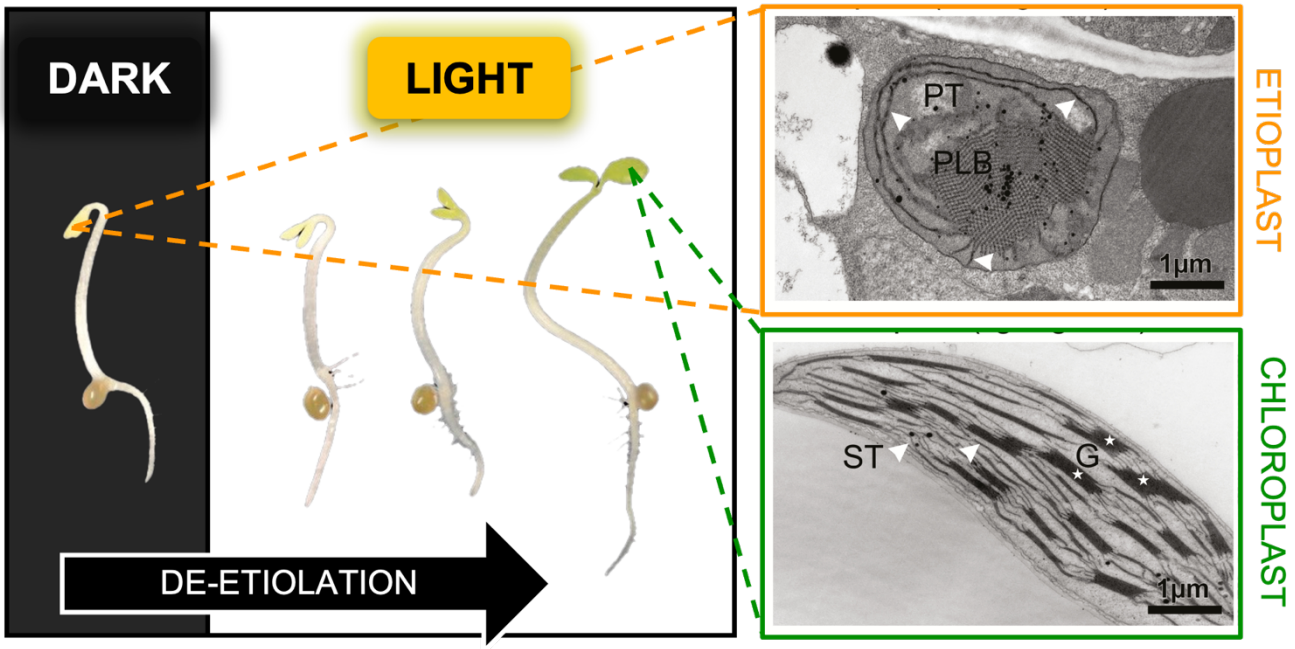


Figure 1.1: De-etiolation is characterized at the seedling level by a transition from skotomorphogenesis (long hypocotyl, close cotyledons, apical hook) in the dark to photomorphogenesis (expanded cotyledons, repression of hypocotyl elongation, root development) in light; at the cellular level dark-developed etioplasts (which lack photosynthetic machinery, and feature prolamellar bodies and prothylakoids) transform into chloroplasts (featuring photosynthetic machinery incorporated into thylakoids, and grana stacks) upon light exposure. PT: prothylakoid; PLB: prolamerllar bodies; ST: stroma thylakoids; G: grana stacks. Electron microscopy images taken from Armarego-Marriott et al., 2020. See also section "*Etioplast-to-chloroplast transition: the hallmark of de-etiolation response*".

A complex light signaling pathway regulates de-etiolation

Many genetic and biochemical studies of de-etiolation have been conducted in angiosperm plants and have shown that this process is regulated by a very complex but exquisite light signaling pathway, which starts with light detection by photoreceptors, followed by a signal transduction mechanism that involves E3 ubiquitin ligases and many transcription factors and regulators (Xu, 2019).

Light signaling starts with perception of light by plant photoreceptors

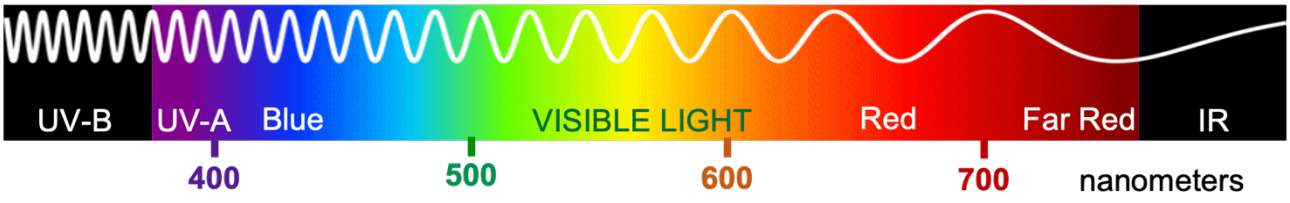
To trigger de-etiolation and other light-dependent physiological responses, plants have developed photoreceptors, each one capable of detecting light at specific wavelengths. There are 5 classes of photoreceptors in plants (Table 1.1): phytochromes for red /far-red light (600-750 nm), cryptochromes, F-box containing Flavin binding proteins and phototropins for blue / UV-A light (320-500 nm), and UVR8 photoreceptor for UV-B light (280-320 nm) (Paik & Huq, 2019).

The red / far-red light cytoplasmic receptor phytochromes are homodimers, each monomer being a chromoprotein which consists of an apoprotein of 125 kD covalently attached to a phytochromobilin tetrapyrrole ring. This molecule acts as the chromophore, since it can isomerize in response to red / far-red light, inducing changes in protein structure. Phytochromes are present in two interconvertible forms: Pr and Pfr, the biological inactive and active states, and are able to respond to red and far-red light, respectively. When they perceive red light, active Pfr phytochromes migrate from the cytoplasm

to the nucleus, where they can regulate physiological responses by interacting with other protein regulators (Paik & Huq, 2019). In Arabidopsis, five types of phytochromes have been described, named phyA-E; phyA and phyB are the main phys and are necessary for the perception of far-red and red light, respectively, and, whereas phyB is the most abundant phytochrome, in light-grown plants, phyA is most abundant in dark-grown seedlings (Quail et al., 1995). When photoactivated phytochromes migrate to the nucleus, they localize together with their interactors in specific nuclear foci called photobodies. These are transiently formed, and their number and size is dynamic, and vary in response to the level of Pfr; the exact function of photobodies is unclear, but they are speculated to be sites of phytochrome signaling, protein turnover, or chromatin remodeling (Chen & Chory, 2011). More recently, it has been shown that photobodies are generated by light-induced liquid-liquid phase separation (LLPS), and that phyB photobodies are comprised of a first group of proteins which directly interact with phyB, readily localizing to the photobody, and a second group of proteins each one interacting with a member of the first group when co-expressed with it (Chen et al., 2022; Kim et al., 2023). Phytochromes have been involved in multiple plant physiological responses including germination, seedling de-etiolation, gravitropism and flowering, and also in the entrainment of the circadian clock (Legris et al., 2019).

Cryptochromes are blue / UV-A light photoreceptors, involved in many physiological responses such as, de-etiolation, floral induction, stomata opening, gravitropism and in the entrainment of the circadian clock. Cryptochromes feature a flavin adenine dinucleotide (FAD) chromophore, while their structure consists of a conserved FAD-binding photolyase homologous region (PHR) and a divergent C-terminal extension (CCE). They are present in the form of inactive monomers in the dark; the absorption of photons by FAD triggers a change in protein structure, followed by their homooligomerization; in this state, they can interact with other cryptochrome-interacting proteins to modulate plant growth and development (Ahmad & Cashmore, 1996; Wang & Lin, 2020). Three cryptochromes have been identified in Arabidopsis (CRY1, CRY2 and CRY3): CRY1 is biologically active in both cytoplasm and nucleus, with specific functions (Wu & Spalding, 2007), while CRY2 is more abundant in the nucleus, where it completes its posttranslational life cycle (Yu et al., 2007); CRY3, instead is different from the first two, since it is part of the CRY-DASH (Drosophyla, Arabidopsis, Synechocystis, human) class of cryptochromes, and is localized to the chloroplast and mitochondria, but its precise function has not yet been clarified (Kiontke et al., 2020). Interestingly, activated cryptochromes can also form photobodies: similarly to phys, CRY2 photobodies are the result of LLPS, and, in particular, CRY2 has been shown to recruit enzymes involved in mRNA methylation, that change stability of mRNAs encoding CIRCADIAN CLOCK ASSOCIATED 1 (CCA1), a central circadian-oscillator protein, affecting circadian rhythm (Quail, 2021).

Two other blue / UV-A light photoreceptors have been described in Arabidopsis: F-box proteins and phototropins. Phototropins have a role in phototropism, as the name indicates, but also are involved in stomatal opening and chloroplast movement. In these functions the two phototropins identified in



UV-B photoreceptor	*Cryptochromes*	*Phototropins*	*F-box proteins*	*Phytochromes*
UV-B [280-320 nm]	Blue / UV-A [320-500 nm]	Blue / UV-A [320-500 nm]	Blue / UV-A [320-500 nm]	Red / Far Red [600-750 nm]
UVR8	CRY1-3	PHOT1 / PHOT2	ZTL / FKF1 / LKP2	PHYA-E
UV-B acclimation, Photoprotection, Stomatal Opening	De-etiolation, Flowering, Stomata opening, Gravitropism, Entrainment of the circadian clock	Phototropism, Stomatal opening, Chloroplast movement	Entrainment of the circadian clock, Flowering	Germination, De-etiolation, Gravitropism, Flowering, Entrainment of the circadian clock

Table 1.1: The 5 classes of photoreceptors in Arabidopsis. For each class, it is indicated the absorption spectrum (line 1), name of the photoreceptor members (line 2), main functions in which they are involved (line 3). IR: Infrared.

Arabidopsis, PHOT1 and PHOT2, have partially overlapping functions. In contrast to cryptochromes, phototropins, are plasma membrane photoreceptors, and consist in two Light-Oxygen-Voltage (LOV) domains at the N-terminal, which mediate light sensing through the FAD chromophore, and a C-terminal kinase domain. In the presence of blue light, photoexitation of LOV domains, causes autophosphorylation of the photoreceptor, which in turn triggers phototropins signaling through kinase activity (Christie, 2007). F-box proteins, specifically ZEITLUPE (ZTL), FLAVIN-BINDING, KELCH REPEAT, F-BOX 1 (FKF1), and LOV KELCH PROTEIN2 (LKP2), are similar to phototropins, since they all feature a single LOV domain with a FAD chromophore for light sensing; but they differ structurally in the presence of an F-box and six C-terminal Kelch repeats, and mechanistically in the regulation of F-box-interacting proteins through the regulation of their stability. This is achieved primarily by the interaction of these unique domains to the SKP1–CUL1-F-BOX (SCF) E3 ligase complex, affecting its activity. F-box proteins are associated with the regulation of circadian clock and flowering (Ito et al., 2012).

UVR8 is the only photoreceptor that is capable of sensing UV-B light. It forms inactive homodimers in the ground state, which monomerize upon UV-B light absorption via tryptophan residues. Once activated, UVR8 monomers can 1) interact with CONSTITUTIVELY PHOTOMORPHOGENIC 1 (COP1), a key repressor of plant photomorphogenesis in plants, or 2) bind with specific transcription factors, affecting their transcriptional activity. UVR8 is mainly involved in UV-B acclimation, photoprotection and stomatal opening (Podolec et al., 2021).

Active photoreceptors repress the activity of COP1-SPA E3 ubiquitin ligases and PIF transcription factors to trigger de-etiolation response

Of the mentioned photoreceptors, phytochromes (phy) and cryptochromes (cry) are the main regulators of seedling de-etiolation in Arabidopsis. In response to red and blue light, active photoreceptors initiate the light signaling cascade by repressing the activity of two key components of this pathway (Figure 1.2), the COP1-SUPPRESSOR OF PHYA-105 (SPA) ubiquitin E3 ligase complex and PHYTOCHROME INTERACTING FACTORS (PIF) (Xu, 2019).

The COP1-SPA ubiquitin E3 ligase complex is a master regulator of light signaling in plants. Whereas COP1 is widely distributed across eukaryotes, SPA is specific to plant lineages. The Arabidopsis genome encodes one *COP1* and four *SPA* (*SPA1-4*) genes, which are structurally similar in the presence of a central coiled coil (CC) domain and a C-terminal WD40 repeat domain; at the N-terminal COP1 features a Really Interesting New Gene (RING) domain, whereas SPA family contains a kinase-like domain. COP1 and SPA form tetrameric complexes composed of two COP1 and two SPA1-4 proteins, that interact in correspondence of the CC domain. COP1-SPA in turn recruits the components of the E3 ubiquitin ligase complex (Figure 1.2), DAMAGE SPECIFIC DNA BINDING PROTEIN 1 (DDB1), CULLIN 4 (CUL4) and RING BOX PROTEIN 1 (RBX1), which mediate interaction with ubiquitin-conjugating enzymes (E2) (Chen et al., 2006). This multimeric complex negatively regulates light induced gene expression in the dark by targeting many positive regulators of de-etiolation and photomorphogenesis, such as ELONGATED HYPOCOTYLS (HY5), LONG AFTER FAR-RED LIGHT 1 (LAF1), and LONG HYPOCOTYL IN FAR-RED (HFR1), causing their ubiquitination and promoting their degradation via the 26S proteasome system (Han et al., 2020). Upon light, active phytochromes and cryptochromes repress COP1-SPA mainly by three different mechanisms: first they interact with the E3 ubiquitin ligase complex detaching COP1 and SPA; second, they can trigger COP1-mediated degradation of SPA; third they can also inactivate this complex by excluding COP1 from the nucleus, through an as yet unknown mechanism. In all cases, positive light signaling factors are stabilized and can promote photomorphogenic response (Podolec & Ulm, 2018). As a proof of the key role of COP1 in negative regulation of seedling de-etiolation is the so called constitutive photomorphogenic (*cop*) phenotype of *cop1* mutants in Arabidopsis in the dark (Figure 1.3 A,a,B,b; Table 1.2), characterized by short hypocotyls, open cotyledons with partial plastid differentiation, resembling light-grown wild type seedlings (Deng & Quail, 1992). Similarly, *spa1234* quadruple mutants (Table 1.2) show a strong *cop* phenotype in the dark (Laubinger et al., 2004).

Activation of photomorphogenesis during seedling de-etiolation is also dependent on the repression of PIFs (Figure 1.2), a subset of basic helix-loop-helix (bHLH) transcription factors which accumulate in dark-grown seedlings, and are rapidly degraded by light, mainly by photoactivated phytochromes (Shen et al., 2008). In Arabidopsis eight different PIFs have been identified, all of them featuring an

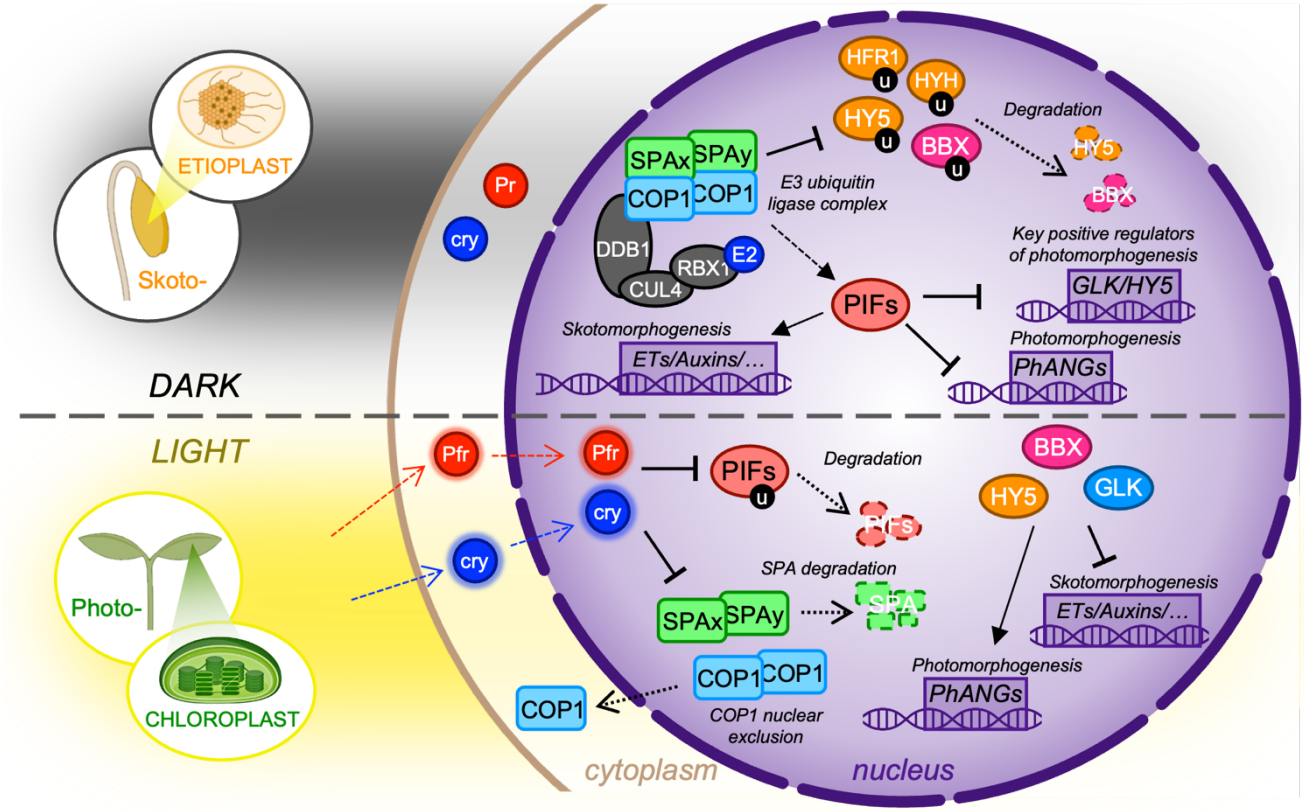


Figure 1.2: A simplified model of light signaling in Arabidopsis. In the dark, two COP1 and two SPA subunits associate together with DDB1, CUL4, RBX1 and E2 to form the COP1-SPA ubiquitinase E3 ligase complex, that targets main positive regulators of photomorphogenesis, such as HY5 and BBX, causing their degradation by ubiquitination; also, PIFs accumulate in the dark (stabilized by COP1-SPA) and suppress photomorphogenesis by repressing the expression of both key positive regulators, such as *GLK* and *HY5*, and other downstream targets, such as *PhANGs*, but also induce skotomorphogenesis genes. Light activates phy (that switches from Pr to active Pfr form) and cry photoreceptors, which migrate to the nucleus causing degradation of PIFs by ubiquitination; also, active phys and crys repress COP1-SPA complex by 1) detaching COP1 from SPA, 2) inducing SPA degradation or 3) inducing COP1 nuclear exclusion; consequently, key transcriptional regulators of photomorphogenesis (HY5, BBX, GLK) accumulate, inducing photomorphogenesis genes and repressing skotomorphogenesis.

APB (active phy-B binding) motif, which allows phyB interaction, while PIF1 and PIF3 feature an additional APA (active phyA-binding) motif, which allows phyA interaction with these two specific PIFs. Thus, upon light exposure photoactive phytochromes in the Pfr form migrate to the nucleus and interact with PIFs through APB and APA binding domains, leading to PIF phosphorylation. Phosphorylated PIFs are then targeted for ubiquitination with subsequent proteasome-mediated degradation or can be retained in the cytoplasm, inhibiting their activity (Favero, 2020). Genetic studies performed in mutants of the PIF quartet, *pifq* (*pif1*, *pif3*, *pif4* & *pif5*) have brought striking evidence of their role as repressors of photomorphogenesis in dark: the *pifq* mutant, in fact, features a *cop*-like phenotype (Figure 1.3 C,c,D,d; Table 1.2), with short hypocotyls, expanded and enlarged cotyledons and partial etioplast differentiation in dark conditions (Leivar et al., 2008). In the dark, all four PIF quartet members regulate the expression of many target genes by binding to a core G-box (CACGTG) in their promoter region, or additionally to a PIF-binding E-box (PBE-box) (CACATG)

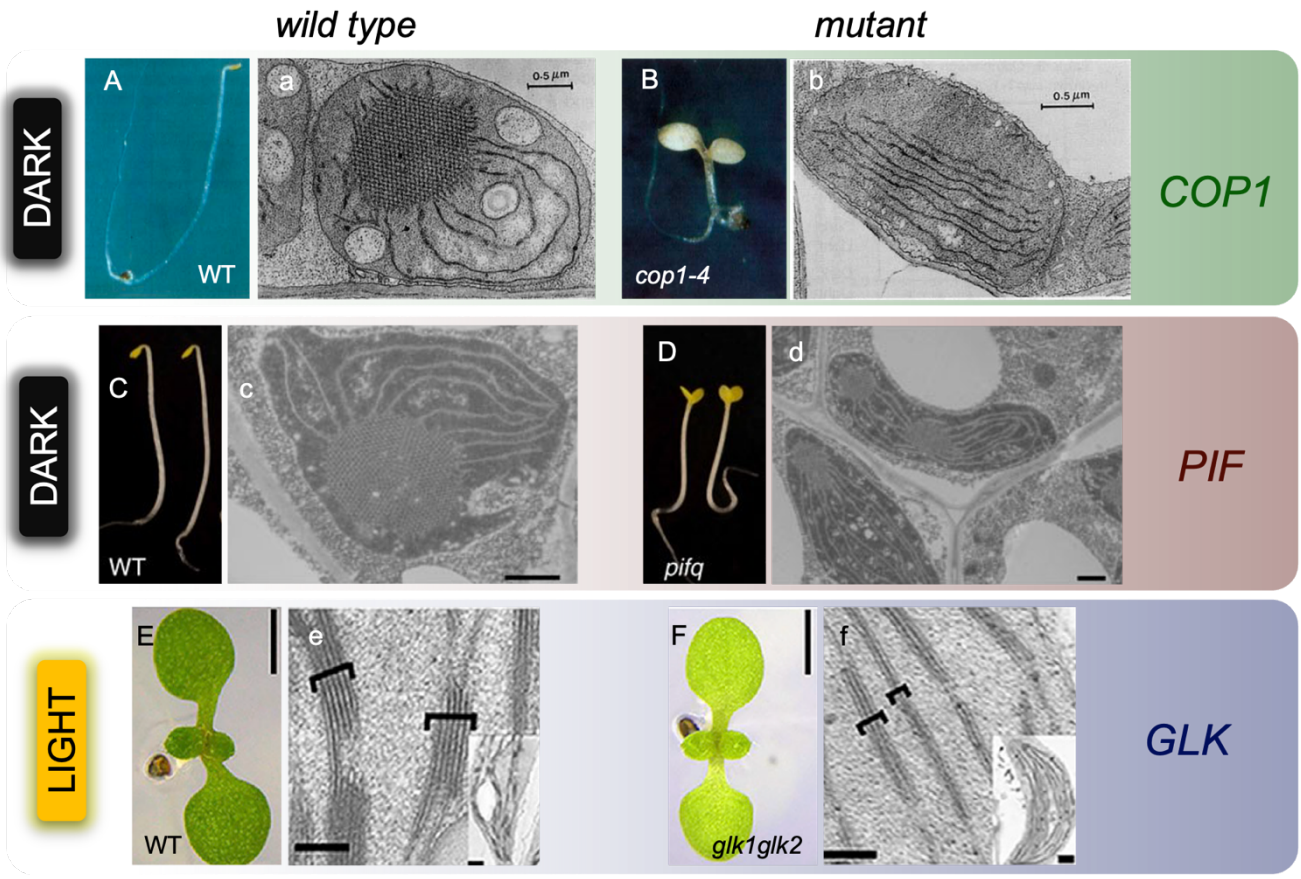


Figure 1.3: Phenotypes of *cop1*, *pif* and *glk* mutants in Arabidopsis, at the seedling level, in capitals (A-F), and cellular level, in lower case (a-f). TEM images were captured in the cotyledons. In the dark, wt seedlings (left side) feature elongated hypocotyls, closed cotyledons, and an etioplast with characteristic PLB and PT; *cop1* and *pifq* mutants (right side) feature a constitutive photomorphogenic phenotype in this condition, characterized by open cotyledons, short hypocotyls, and a partially differentiated plastid, with part of PLB disassembled (*pifq*) or with total absence of PLB (*cop1*), evidencing the key role of COP1 and PIFs as repressors of photomorphogenesis in the dark. In the light, wt seedlings feature expanded cotyledons, chlorophyll accumulation and developed chloroplasts; *glk1glk2* double mutants (right side) show defects in greening, due to lower chlorophyll levels, and thinner thylakoid membranes, indicating the key role of GLKs in promoting chloroplast development. Images were retrieved from Quail & Deng, 1992 (COP1, TOP), Martín et al., 2016 (PIF, MIDDLE) and Zhang et al., 2021 (GLK, BOTTOM).

(Martinez-Garcia et al., 2000; Pfeiffer et al., 2014; Zhang et al., 2013). Transcriptomic studies of *pifq* have shown that the vast majority of the alterations in gene expression in dark, caused by absence of PIFs, are normally triggered by phy signaling when dark-grown wild type seedlings are exposed to light for de-etiolation; also, early light PIF-quartet regulated genes are enriched in *loci* that encode many diverse transcription factors. Altogether, these data suggest the presence of a broadly acting, PIF-regulated transcriptional cascade during de-etiolation (Leivar et al., 2009; Pfeiffer et al., 2014). More recently, it has been shown that also cryptochromes can interact with PIFs, specifically PIF4 and PIF5, to repress their function under limiting blue light conditions (Pedmale et al., 2016).

Light triggered suppression of COP1-SPA complexes and PIF activity cause derepression of key positive regulators of photomorphogenesis. Perhaps the best characterized one that falls in this category is HY5, a bZIP transcription factor that controls the expression of one third of the genes throughout the whole genome (Lee et al., 2007). As the name indicates, first studies showed that *hy5*

Gene Name	*At ID*	*Mutant type*	*Seedling phenotype*	*Plastid phenotype*	Light conditions	*References*
COP1	AT2G32950	*cop1-4*	cop phenotype: open cotyledons, short hypocotyl	Plastid differentiation, absence of PLB, thylakoids, no greening	DARK	Deng & Quail, 1992
SPA1 *SPA2* *SPA3* *SPA4*	AT2G46340 AT4G11110 AT3G15354 AT1G53090	*spa1234* *spa134* *spa123* *spa124*	*spa1234*: strong cop phenotype *spa134*: wild type *spa123, spa134*: mild cop phenotype	-	DARK	Laubinger et al., 2004
PIF1 *PIF3* *PIF4* *PIF5*	AT2G20180 AT1G09530 AT2G43010 AT3G59060	*pifq (pif1345)* and all the combinations	*pifq*: strong cop phenotype Any combination with *pif1* features a mild cop phenotype with separated cotyledons	*pifq*: partially differentiated plastids, with reduced PLB area and longer PT *pif1 & pif3*: partially differentiated plastids with Pchlide accumulation	DARK	Leivar et al., 2008 Leivar et al., 2009 Stephenson et al., 2009
HY5	AT5G11260	*hy5-1*	Elongated hypocotyl, altered root morphology	Developed chloroplasts, same morphology as wt	LIGHT	Oyama et al., 1997
GLK1 *GLK2*	AT2G20570 AT5G44190	*glk1, glk2 (single)* *glk1glk2 (double)*	*glk1* and *glk2* undistinguishable from wt; *glk1glk2* pale green and overall smaller plants	*glk1glk2* chloroplasts show reduced chlorophyll levels, thinner thylakoids and reduced grana levels	LIGHT	Fitter et al., 2002 Zhang et al., 2021

Table 1.2: Summary table of main key regulators of light signaling during seedling de-etiolation in Arabidopsis, with the mutant phenotypes described in the literature (at both seedling and plastid level). At: Arabidopsis; wt: wild type.

mutants are characterized by drastically elongated hypocotyls in light conditions (Table 1.2), thus indicating its involvement in positive regulation of photomorphogenesis (Oyama et al., 1997). Other studies have implicated this factor in controlling, besides hypocotyl growth, root growth, chloroplast development, the accumulation of anthocyanins, carotenoids and chlorophylls, and hormonal responses during de-etiolation; more importantly, it has been shown that the degree of the photomorphogenic response is proportional to the amount of accumulated HY5 in the nucleus, which affects directly or indirectly the expression of over 3000 genes (Burko et al., 2020). This explains why HY5 stability needs to be tightly regulated by the COP1-SPA complex. There are two ways this regulation is achieved. First, HY5 stability is dependent on light (Figure 1.2): as previously indicated, HY5 is repressed by COP1-SPA in the dark, while in light active photoreceptors migrate to the nucleus and repress COP1-SPA through different mechanisms, favoring the accumulation of HY5 (Podolec & Ulm, 2018). Additionally, HY5 stability is dependent on its phosphorylation status: COP1-SPA complexes in fact have higher binding affinity for dephosphorylated HY5 forms, which are accumulated in light and are physiologically active; in contrast, phosphorylated forms are more stable, accumulate in the dark and are physiologically inactive. Recently, it has been shown that SPA proteins have kinase activity and are necessary for the generation of HY5 phosphorylated forms, suggesting a COP1-SPA-HY5 negative feedback loop that occurs in light to fine-tune photomorphogenesis

(Wang et al., 2021). Moreover, HY5 activity is also strictly coordinated with PIFs; these two factors work antagonistically, positively and negatively regulating, respectively, the expression of common gene targets, through direct binding to G-boxes. These factors can coexist and associate in PIF-HY5 regulatory modules, with more inductive or repressive activity depending on light conditions, to perfectly tune photomorphogenic response (Chen et al., 2013; Toledo-Ortiz et al., 2014). HY5 activity is also modulated by B-BOX proteins, zinc-finger transcription factors which feature DNA-binding properties and the ability to interact with other proteins through the B-BOX domains. There are 32 B-BOX members in Arabidopsis, divided into five different structural groups, depending on the presence of one or two B-BOX domains, and the presence or absence of CTT and VP domains (Gangappa & Botto, 2014). Many B-BOX proteins are involved in regulating HY5 activity working as rate-limiting cofactors: specifically, BBX20, BBX21, BBX22 and BBX23 interact with HY5 and enhance its transcriptional activation activity, while BBX24, BBX25, BBX28 and BBX29 repress HY5 function by forming BBX-HY5 inactive heterodimers. HY5 and BBOX proteins are not alone in promoting photomorphogenesis: GOLDEN2-LIKE (GLK) proteins, GLK1 and GLK2, two transcription factors belonging to the GARP superfamily, have been involved in regulating chloroplast development during de-etiolation (Figure 1.3 E,e,F,f; Table 1.2). Genetic evidence has shown that Arabidopsis light- grown *glk1glk2* double mutant seedlings feature pale green chloroplasts in all photosynthetic tissues with severe reduction in thylakoids and grana (Fitter et al., 2002). A more recent study has shown that PIFs regulate GLKs by directly repressing the expression of *GLK1* in dark-grown Arabidopsis seedlings and that photoactivated phyB reverses this inhibition upon light exposure (Martín et al., 2016); moreover, in the same study, it has been demonstrated that *glk1* mutants feature longer hypocotyls and less open cotyledons in light, extending the role of GLK1 as a regulator not only of chloroplast biogenesis but of whole seedling development (Martín et al., 2016).

Regulation of seedling de-etiolation by phytohormones

Not less important is the role of phytohormones in regulating seedling de-etiolation (Figure 1.4). Auxin promotes growth, and therefore its transport throughout whole seedling is tightly controlled during this process; this is achieved by auxin influx AUXIN RESISTANT 1 (AUX1) and efflux PIN-FORMED (PIN) carriers. In darkness, PIFs induce auxin synthesis, while PIN4 and PIN7 create an auxin gradient at the top of the hypocotyl which results in the characteristic apical hook (Hornitschek et al., 2012); at the same time, COP1 by locally suppressing PIN1 cause low auxin levels in the shoot and root systems (Sassi et al., 2012). Gibberellin (GA) signaling is also fundamental for de-etiolation: in the dark PIFs induce GA synthesis, and GAs in turn repress DELLA proteins, key transcriptional regulators of GA-mediated developmental responses, promoting growth. GA signaling starts with their interaction with GA receptor, GIBBERELLIN INSENSITIVE DWARF 1 (GID1) forming GA-GID1 complex, and this in turn interacts with DELLA forming GA-GID1-DELLA ternary complex, which recruits $SCF^{SLY1/GID2}$ complex for DELLA ubiquitination and degradation (Sun, 2011), although it has

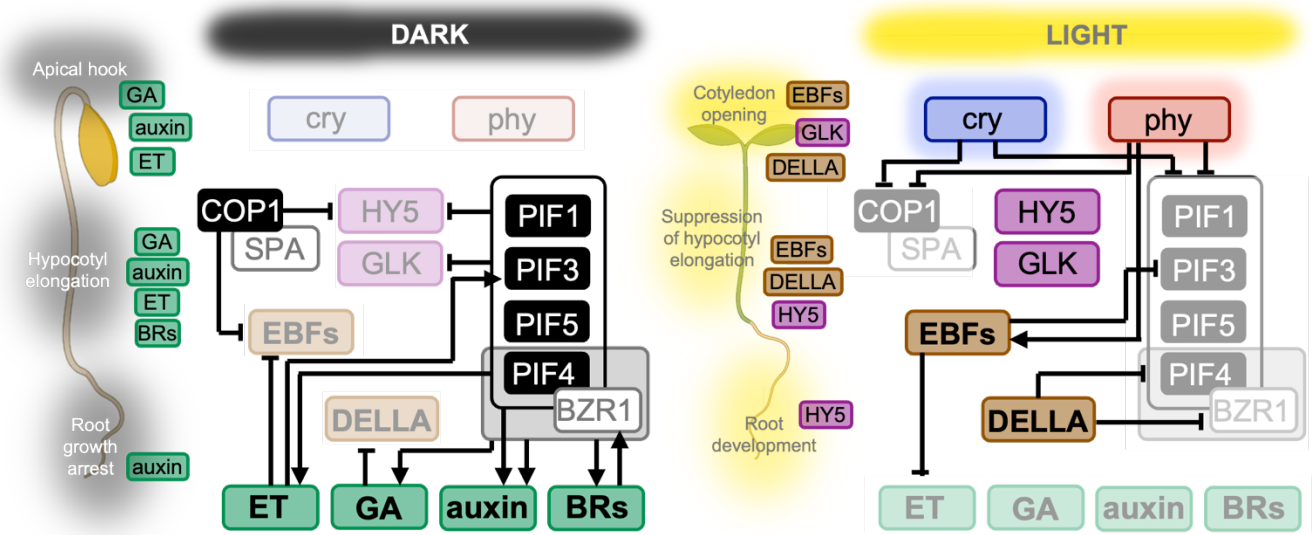


Figure 1.4: Simplified model for phytohormone regulation of light signaling. In the dark, PIFs induce phytohormone production, responsible, at different degree, for the characteristic phenotypes of the skotomorphogenic development (apical hook, hypocotyl elongation and suppression of root growth): for instance, ET and GA are necessary for the local expression of *PIN* genes at the top of the hypocotyl, which in turn cause the auxin gradient responsible for the formation of the apical hook. At the same time COP1 favors ET signaling by repressing EBFs; also, COP1 in cooperation with PIFs, repress HY5 and GLK. Light activates crys and phys which repress COP1 and PIFs, thus inhibiting phytohormone production; consequently, DELLAs (repressed by GAs), EBFs, GLK and HY5 can trigger the photomorphogenic response: DELLAs and EBFs act as PIF repressors favoring cotyledon opening, and also suppression of hypocotyl elongation; HY5 favors root development and suppression of hypocotyl elongation, whereas GLK is involved in proper chloroplast development. This figure was inspired in another figure of an excellent de-etiolation review by Gommers & Monte (2018) (Box 2 Figure).

also been shown that COP1 can destabilize DELLAs, independently of GAs (Blanco-Touriñan et al., 2020). Upon light exposure, levels of bioactive GAs decrease allowing DELLAs to perform their biological function, which is promoting photomorphogenesis; phenotypical evidence, in fact, showed that DELLA deficient mutants feature elongated hypocotyls in light (Achard et al., 2007); also, genetic and molecular evidence has shown that this is achieved predominantly by DELLAs physically interacting and repressing PIF activity during de-etiolation (de Lucas et al., 2008; Feng et al., 2008). Brassinosteroids (BR) are essential for skotomorphogenesis, as shown by the *cop* phenotype in dark of BR-deficient mutants (Li et al., 1996). In this condition, BRs stabilize BRASSINAZOLE-RESISTANT 1 (BZR1), a key transcription factor of BR-signaling, which in turn interacts with PIF4. PIF4-BZR1 module triggers skotomorphogenesis by inducing auxin signaling, and BR and GA synthesis in the dark (Oh et al., 2012), while upon exposure to light BZR1 is repressed by DELLAs, inducing photomorphogenesis (Bai et al., 2012). Ethylene (ET) is another positive regulator of skotomorphogenesis: ethylene biosynthesis is induced in the dark by PIFs, while COP1 and ET destabilize two F-box proteins that act in SCF complexes, EIN3 BINDING FACTOR 1 and 2 (EBF1 and 2), which are suppressors of ETHYLENE INSENSITIVE 3 (EIN3), a transcription factor that upregulates the expression of the above mentioned PIN and PIF3. Photoactivated phyB in light induces EBFs-mediated EIN3 and PIF3 degradation (Zhong et al. 2010).

Etioplast-to-chloroplast transition: the hallmark of de-etiolation response

When seedlings grow under the soil surface in the dark, embryonic proplastids present in the seed transition into non-photosynthetic etioplasts in the cotyledons. Very distinctive of these plastids, are paracrystalline lipid-pigment-protein structures called prolamellar bodies (PLB), in which chlorophyll precursor protochlorophyllide (Pchlide) is associated to the light-dependent protochlorophyllide oxidoreductase (LPOR), responsible for its conversion (Solymosi & Schoefs, 2010). These plastids also contain lamellar prothylakoid membranes (PT); they do not feature light-harvesting complex proteins, or if present it is in very low amounts and not embedded in the plastid membranes (Müller & Eichacker, 1999). Upon light exposure, PLBs disassemble and are reformed into thylakoids, light-harvesting complex proteins are synthetized, while LPOR rapidly converts the accumulated Pchlide into chlorophyll, which is incorporated into the assembling photosystems, establishing photosynthetic competence in the differentiating chloroplast (Solymosi & Schoefs, 2010). The majority of the chloroplast proteins including photosystem components are encoded in the nucleus and require their import from the cytoplasm into the assembling chloroplast (Figure 1.5); this function is carried out by the chloroplast protein import machinery, specifically the TRANSLOCON AT THE OUTER-INNER MEMBRANE OF THE CHLOROPLAST (TOC-TIC) through the recognition of a specific transit peptide by TOC receptors (Richardson & Schnell, 2019). Chloroplast encoded proteins instead are synthesized by the plastid own expression system (Dobrogojski et al., 2020). Lipids are also an essential component of thylakoid membranes: reminiscent of their cyanobacterial origin, chloroplast membranes are poor in phospholipids and rich in galactolipids in the form of MGDG and DGDG (mono- and di-galactosyldiacylglycerol) which can be synthesized from the endoplasmic reticulum or the own plastid, being the eukaryotic and prokaryotic pathway, respectively (Ohlrogge & Browse, 1995). During chloroplast biogenesis, thylakoid membranes may be formed from the inner envelope membrane through a VIPP1 (VESICLE INDUCING PLASTID PROTEIN) regulated vesicle-budding system (Vothknecht et al., 2012). A recent work showed that the overall etioplast-to-chloroplast transition during seedling de-etiolation occurs in two distinct phases: a “structure establishment phase” characterized by gradual formation of thylakoid membranes, and an initial increase of photosynthesis-related proteins and galactolipids, followed by a “chloroplast proliferation phase” characterized by an increase in chloroplast number and grana stacking, in parallel with cell expansion (Pipitone et al., 2021). A critical aspect of de-etiolation is the production of pigments. For instance, production of chlorophylls occurs very rapidly since accumulated Pchlide in the dark can cause lethal bleaching upon light exposure (Reinbothe et al., 1996). Besides, chlorophylls are needed for the assembly of both photosystem I and II super complexes, which in turn are required for the biogenesis of thylakoid membranes and formation of grana stacks (Pribil et al., 2014). Also important in this process are carotenoids, which are synthesized by phytoene synthase (PSY), the central carotenoid biosynthesis enzyme. These pigments have a photoprotective role and help minimize photooxidative

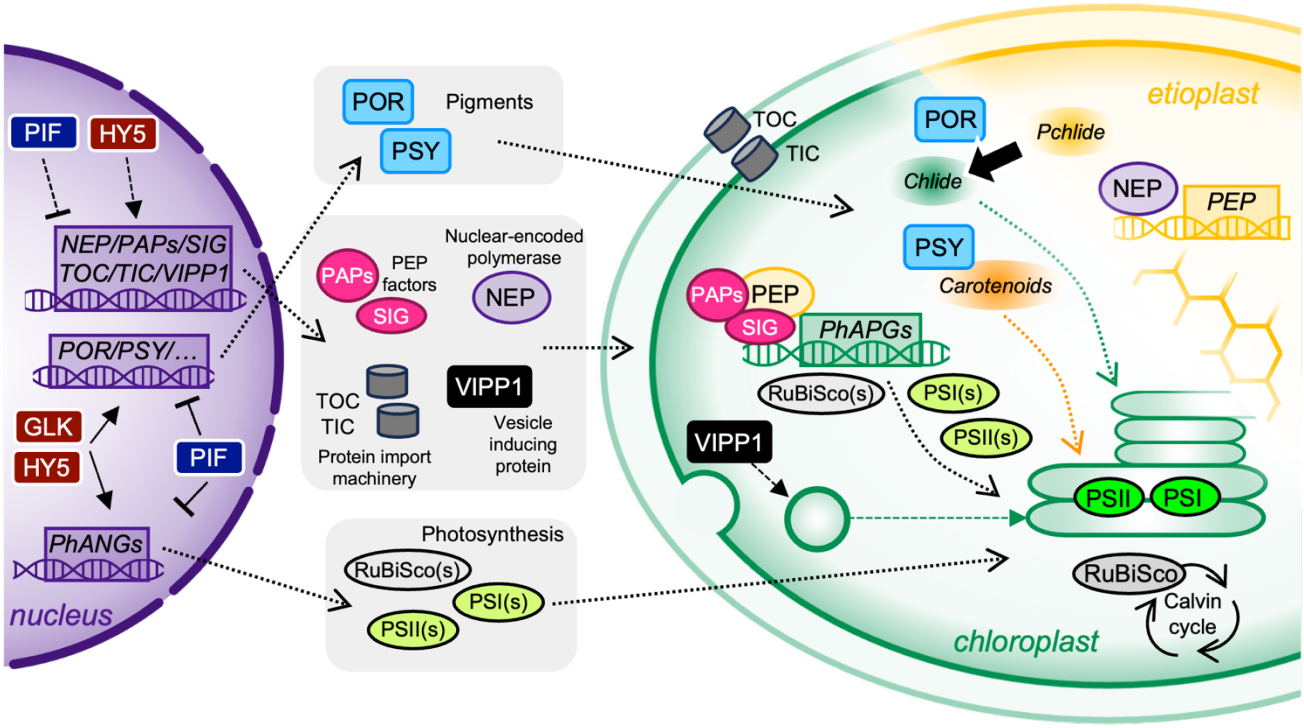


Figure 1.5: Comprehensive illustration of all the main factors required for chloroplast biogenesis. Upon transfer to light, GLKs and HY5 induce the expression of *PhANGs* and genes encoding for enzymes of the chlorophyll and carotenoid biosynthetic pathways (these genes are repressed in the dark by PIFs). Also, many other fundamental components encoded in the nucleus need to be expressed, including *TOC-TIC* chloroplast protein import machinery, the nuclear-encoded plastid polymerase (*NEP*), *PAPs* and *SIG* factors required for PEP polymerase activity and *VIPP1*; these components are likely regulated by the PIF-HY5 module. All these components are synthesized in the cytoplasm and imported through the TOC-TIC import machinery. Also, chloroplast biogenesis requires the expression of plastid genes including, *PhAPGs*: these are expressed through PEP polymerase, whose expression depends on NEP activity, whereas his activity depends on the association with PAPs and SIG factors. Import of POR and PSY is fundamental for the biosynthesis of chlorophylls and carotenoids, which are incorporated to the assembling photosystems composed of both nuclear-encoded and plastid-encoded subunits (s). VIPP1 likely is involved in the assembly of thylakoid membranes by an inner membrane budding mechanism. Also, RuBiSCo is assembled using both nuclear and plastid-encoded subunits, proving the capacity of CO_2 fixation.

damage (Cazzonelli et al., 2020). Due to the importance of chlorophylls and carotenoids in this process, biosynthesis of both pigments is strictly controlled by many of the above mentioned transcriptional regulators. The PIF-HY5 module directly regulates the expression of *PSY* by binding to the common G-box motif (Toledo-Ortiz et al., 2014). This module also affects the expression of many genes encoding enzymes (and associated factors) of the chlorophyll biosynthesis pathway (Figure 1.6), such as, *LPOR* (*PORA*, *PORC* subunits), glutamyl t-RNA reductase (*HEMA1*), *GENOMES UNCOUPLED 4* (*GUN4*) and Mg-chelatase subunit H (*CHLH*) (Lee et al., 2007; Monte et al., 2004; Moon et al., 2008). GLKs are involved in the regulation of chlorophyll production and, also, control carotenoid biosynthesis by regulating the expression of *PSY*, but in contrast to PIF-HY5 module, this is an indirect regulation mediated by a G-box Binding Factor (Sun et al., 2022; Waters et al., 2009). DELLAs play also a key role in this context: these proteins accumulate in the cotyledons in dark to promote formation of PLB, and by promoting the expression of LPOR in the dark, prevents photobleaching; also, by interacting with PIFs they regulate chlorophyll biosynthesis and PSY

expression in the dark (Cheminant et al., 2011). BR and ET-signaling also control pigment production during de-etiolation: etiolated seedlings of *det2* BR-deficient mutants accumulate excess Pchlide in the dark, and PIF4-BZR1-GROWTH REGULATING FACTOR 7 (GRF7) interact with each other to tightly regulate the expression of chlorophyll biosynthesis genes, including *HEMA1*, *HEMB1* subunit of 5-aminolevulinic acid dehydratase (ALAD), Mg-chelatase subunit D (*CHLD*), *CHLH*, and *GUN4* (Wang et al. 2020); moreover, EIN3 activates PIF3 in the dark to inhibit Pchlide accumulation, which allows the seedling to avoid photodamage after prolonged periods under the soil (Zhong et al., 2014). Chloroplast biogenesis requires not only the expression of photosynthesis associated nuclear genes (*PhANGs*), which are mainly induced by HY5 and GLK transcription factors after exposure to light, but also the expression of photosynthesis associated plastid genes (*PhAPGs*) (Figure 1.5). Transcription of these genes is carried out by the PLASTID ENCODED POLYMERASE (PEP), and more importantly the activity of PEP is also regulated by light, through a nuclear-to-chloroplast anterograde signal, although the underlying mechanism has not been fully elucidated. Many evidences support the involvement of the PIF-phy module in the regulation of PEP activity: a) gene expression and protein levels of PEP negatively correlate with PIF, and positively correlate with PIF-repressed SIGMA factors (SIG); b) many PEP-ASSOCIATED PROTEIN (PAPs), such as HEMERA (HMR), as well as other nuclear encoded chloroplast proteins that regulate PEP activity, such as SIG, are necessary for the assembly of phy photobodies in the nucleus; c) the promoter regions of all these nuclear-encoded PEP-associated proteins contain a PIF3 binding motif (Dubreuil et al., 2017; Hernández-Verdeja et al., 2020; Hwang et al., 2022). The Arabidopsis plastid genome harbors 85 protein encoding genes: the majority of them (54) are related to photosynthesis functions, and include 6 genes of the cytochrome b6f complex, 5 genes of the photosystem I (PSI), 15 genes of the photosystem II (PSII), 6 genes of the chloroplast ATPase, 12 genes of the NADH dehydrogenase subunit and one gene encoding the RuBisCo large subunit; the other 31 genes encode proteins that mediate plastid gene expression, and include 25 ribosomal proteins and 4 PEP subunits. Not only anterograde signals, but also chloroplast-to-nucleus retrograde signals represent an essential part of de-etiolation response, and are necessary for proper chloroplast development. As the components of all protein complexes that perform photosynthesis are encoded in both nuclear and chloroplast genomes, their expression need to be coordinated to ensure successful assembly of these complexes in the developing chloroplast. In particular, given that free pigments are extremely phototoxic, efficient assembly of photosystem complexes is necessary for proper incorporation of chlorophyll and accessory pigments that are being synthesized in the chloroplast (Hernández-Verdeja et al., 2020; Jarvis & López-Juez, 2013).

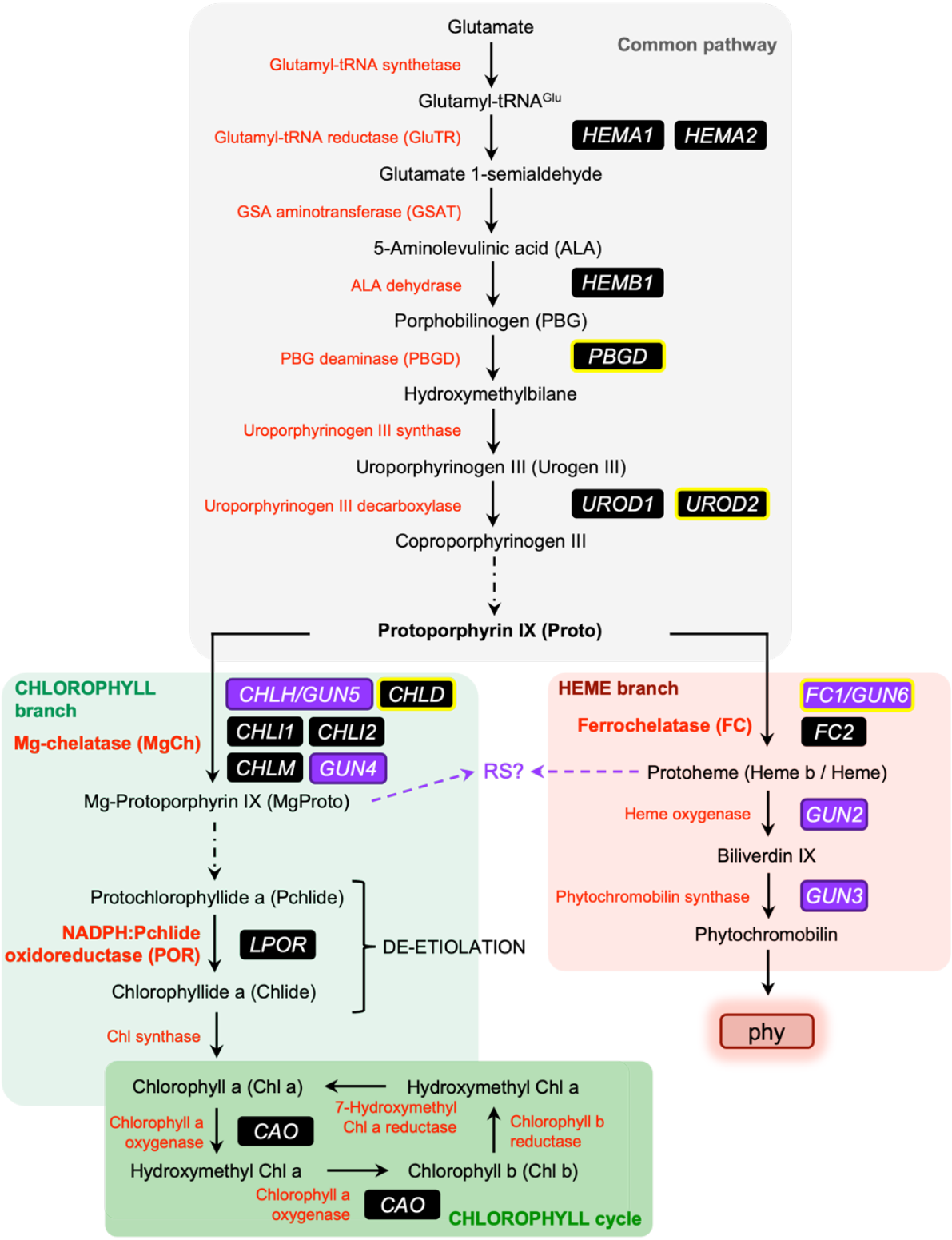


Figure 1.6: Tetrapyrrole biosynthesis pathway. Tetrapyrroles are synthesized from glutamate through a series of enzymatic reactions until is converted to Proto IX, the common precursor of both chlorophyll and heme biosynthesis branches. The chlorophyll branch starts with the addition of Mg^{2+} catalyzed by MgCh complex to form MgProto, and features a light-dependent step of Pchlide reduction to Chlide, which is critical for de-etiolation. Chlide is esterified to form Chl a which can be reversibly converted to Chl b in the chlorophyll cycle. In the heme branch a Fe^{2+} is added instead, by the FC enzyme, to form protoheme (here referred as heme) which is converted in a series of two reactions to phytochromobilin, the chromophore of phys. Many enzymes of this pathway have been involved in RS: GUN4/5 of the chlorophyll branch and GUN2/3/6 of the heme branch (shown in purple). Consequently, MgProto and heme have been hypothesized as mobile RS, although this is still objected to debate. Moreover, it has been found that GUN1 interacts with components of this pathway: PBGD, UROD2, CHLD and FC1 (yellow borders).

GUN1-mediated chloroplast-to-nucleus retrograde signals regulate de-etiolation in Arabidopsis

Chloroplast-to-nucleus retrograde signaling (RS) emerged with photosynthetic eukaryotes, in a complex process of domestication of a photosynthetic symbiont: exchange of metabolites with the host was accompanied by massive gene transfer, which eventually required the development of a host-symbiont communication system. Today's green organisms from algae to plants have evolved a complex RS pathway that fine-tunes chloroplast development and environmental responses (Calderon & Strand, 2021).

During de-etiolation, chloroplast communicates its physiological status to the nucleus via RS, and this produces changes in gene expression which ultimately feed back to the chloroplast, and fine-tunes its development. This is the so called "biogenic control" (in contrast to the "operational control" RS that operates in mature chloroplasts of adult plants) (Shimizu & Masuda, 2021). Major advances in the elucidation of biogenic RS came from the observation that treatment with compounds that specifically affect chloroplast function negatively affects the expression of *PhANGs*. Two compounds have been used for this purpose: norflurazon (NF), a potent inhibitor of carotenoid biosynthesis, and lincomycin (LIN), which impairs chloroplast protein translation. This finding established the basis for a genetic screen which led to the identification of many RS mutants, named GENOMES UNCOUPLED (*gun*), which retained *PhANGs* expression after treatment with norflurazon (NF). Interestingly, *gun2-5* are mutants of tetrapyrrole biosynthesis genes (Figure 1.6,1.7), specifically two of the heme branch, heme oxygenase (*GUN2*) and phytochromobilin synthase (*GUN3*), and two of the chlorophyll branch, regulator of the Mg-chelatase CHLH subunit (*GUN4*) and CHLH subunit itself (*GUN5*) (Larkin et al., 2003; Mochizuki et al., 2001; Susek & Chory, 1992; Susek et al., 1993). Consequently, intermediates of the tetrapyrrole biosynthesis pathway have been hypothesized as the RS that modulates nuclear gene expression. At first, Mg-protoporphyrin IX (Mg-Proto), the first tetrapyrrole intermediate of the chlorophyll branch obtained from the conversion of Protoporphyrin-IX (Proto-IX) by Mg-Chelatase, was postulated as the molecule that accomplishes this function, since *gun2* and *gun5* accumulate high levels of this precursor after NF treatment; however, it was argued that other mutants of this pathway which also accumulate Mg-Proto in the presence of NF, do not feature a *gun* phenotype (Strand et al., 2003; Pontier et al., 2007). Alternatively, heme has been proposed as the RS. This hypothesis was supported by the later identification of the dominant *gun6* mutant which overexpresses ferrochelatase 1 (FC1) (Woodson et al., 2011). Ferrochelatases generate heme from the conversion of Proto-IX precursor. Arabidopsis encodes two isoforms of this enzyme which are differentially localized in the chloroplast: whereas FC2, the most abundant isoform, is mainly localized in the thylakoids, FC1 is predominantly localized in the chloroplast envelope. Interestingly, overexpression of FC1 but not FC2 produces a *gun* phenotype, and therefore it was proposed that a specific pool of heme generated by FC1 may leave the plastid and act as a positive

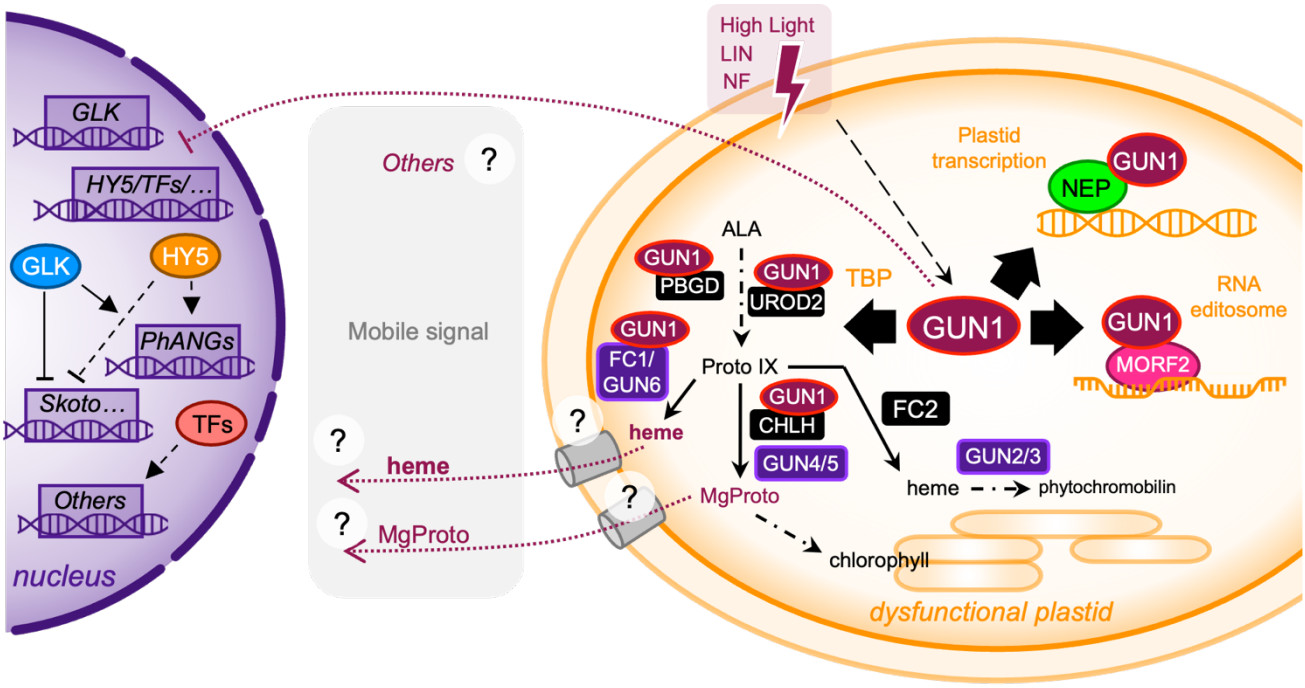


Figure 1.7: Simplified model for biogenic retrograde signaling. The plastid can act as a sensor of environmental stresses that impair chloroplast activity and send RS to the nucleus to regulate nuclear gene expression, according to plastid needs. During de-etiolation, RS are regulated mainly by GUN1, which is considered a hub, being involved in multiple different responses. These include modulation of plastid gene expression by favoring NEP activity over PEP, RNA editing through MORF2, and regulation of tetrapyrrole biosynthesis pathway (TBP), likely achieved by its interaction with several enzymes (FC1, CHLH, UROD2, PBGD). Moreover, the TBP includes many other *gun* mutants (in purple), which are enzymes of the chlorophyll branch (GUN4/5) or the heme branch (GUN2/3/6). A controversial matter in RS field is the identity of the mobile RS: TBP intermediates have been postulated for this function, such as MgProto and heme. The latter is thought to be part of a pool of heme synthesized by FC1/GUN6 (in contrast to plastid heme synthesized by FC2). Regardless of the identity of mobile signals, these are sent to the nucleus by a yet unknown mechanism; GUN1-dependent signals are known to repress many important transcription factors, including the positive regulators of photomorphogenesis *GLK1* and *HY5*.

RS (Fan et al., 2023; Terry & Smith, 2013). However, how heme is transported outside the chloroplast and the mechanism by which heme acts as an intracellular signaling factor are far from being understood (Richter et al., 2023).

An additional level of complexity in our understanding of RS is given by the characterization of *gun1* (Figure 1.7). Unlike *gun2-6* mutants, *gun1* is not an enzyme of the tetrapyrrole biosynthesis pathway, but it is required for RS caused by defects in the carotenoid biosynthesis pathway or by inhibition of chloroplast protein translation; lack of repression of *PhANGs* in *gun1* mutant, in fact, have been shown in both NF and lincomycin (LIN) treatment (Koussevitzky et al., 2007). GUN1 encodes a chloroplast protein that features a pentatricopeptide repeat (PPR) and a MutS-related domain. Originally, it was thought that these two domains confer GUN1 the ability to bind nucleic acids, but no evidence of such function has been found *in vivo*. However, there are increasing evidences that postulate a role for GUN1 in regulating plastid gene expression. For instance, it has been shown that GUN1 interacts with NUCLEAR ENCODED POLYMERASE (NEP) favoring its activity over PEP in LIN stress conditions (Tadini et al., 2019). GUN1 was also postulated to regulate chloroplast transcript editing during RS, as 1) this process is affected in *gun1* mutants grown in NF, 2) GUN1 was shown to interact

with the RNA-editosome component MULTIPLE ORGANELLAR RNA EDITING FACTOR 2 (MORF2), and 3) overexpression of MORF2 cause a *gun* phenotype (Zhao et al., 2019). However, 1) and 3) could not be reproduced by a later work, where the authors show striking evidence for GUN1 RNA-binding function *in vivo* and *in vitro*, and postulate a role for GUN1 in regulating RNA maturation, rather than editing (Tang et al., 2024). Moreover, GUN1 could be implicated in regulating chloroplast protein homeostasis, through regulation of the TOC-TIC chloroplast protein import complex: it was demonstrated that GUN1 interacts with the chloroplast chaperone HEAT SHOCK COGNATE PROTEIN 70-1 (HSC70-1), which helps TIC protein import function, and also GUN1 regulates the expression of TOC-TIC subunits under LIN treatment (Tadini et al., 2019). Finally, a link between GUN1 and tetrapyrrole biosynthesis has been evidenced by the interaction of GUN1 with many enzymes of this pathway, including CHLD, PBG deaminase (PBGD), Urogen III decarboxylase (UROD2), and FC1, but the consequences of these interactions are not well understood (Tadini et al., 2016).

Ever since its first identification, GUN1 has been involved in regulation of seedling de-etiolation and chloroplast biogenesis. First studies, in fact, showed that, although *gun1* mutants and wild type seedlings of Arabidopsis are indistinguishable in dark, during de-etiolation *gun1* fails to complete apical hook opening and cotyledon expansion upon light exposure; moreover, *gun1* mutants feature delayed chloroplast differentiation and accumulate less chlorophylls and nuclear transcripts encoding photosynthesis components compared to the wild type (Mochizuki et al., 1996). It has been suggested that GUN1 upregulates *LPOR* expression and contributes to reduce accumulation of phototoxic Pchlide, which could explain the delayed chloroplast biogenesis of *gun1* mutants (Xu et al., 2016). More recently, it has been shown that GUN1 accumulates in etioplasts of dark grown seedlings and mediates a negative RS which restricts chloroplast biogenesis during dark and early light response (Hernández-Verdeja et al., 2022). Many studies have demonstrated a link between light and RS during de-etiolation. For instance, both *hy5* and *cry1* mutants show a *gun* phenotype (Ruckle et al., 2007); also, overexpression of *GLK1* and *GLK2* results in a *gun* phenotype upon both NF and LIN treatment, and is more pronounced in *GLK1* (Leister & Kleine, 2016; Martín et al., 2016). Moreover, it has been shown that GUN1-mediated RS and phy-PIF mediated light signals antagonistically regulate the expression of *GLK1.* Here, GUN1-mediated repression of *GLK1* under excess light may serve to repress photomorphogenic development and protect against photo-oxidative damage (Martín et al., 2016). This repression is mediated by BBX16 downstream of GLK1 (Veciana et al., 2022). The expression of these and other key transcriptional regulators of light signaling and chloroplast development are regulated by GUN1 in dark and during the initial de-etiolation phase, including PIFs, GLK1, BZR1 and HY5. This, together with the accumulation of GUN1 in non-photosynthetic tissues suggest a role of GUN1 in maintaining non-photosynthetic plastid types, and beyond in controlling organ-specific *PhANG* expression and chloroplast development (Hernández-Verdeja et al., 2022).

Etiolation does not take place in non-angiosperm plants, but key light and retrograde signaling components involved in de-etiolation are conserved at different degree

The de-etiolation process, as well as the above described light and RS mechanism that triggers it, have been extensively described in Arabidopsis and other angiosperm plants. The ability to etiolate, in fact, is characteristic of these species and relies in the "inability" to synthesize chlorophyll in the dark (Figure 1.8). In this condition, chlorophyll production is blocked at the Pchlide stage, and this precursor and the LPOR enzyme responsible for its light-dependent conversion to chlorophyllide are accumulated in the PLBs of the forming etioplasts. Light photons activate the LPOR, leading to chlorophyll production, while a complex light and RS program regulates chloroplast development in the de-etiolating organism. This does not apply to non-angiosperm plants, which feature a light-independent POR enzyme, called DPOR, responsible for Pchlide conversion in the dark. Consequently, non-angiosperm species form chloroplasts in the dark after germination, and are not able to etiolate even after prolonged growth periods in absence of light (Armarego-Marriott et al., 2019; Reinbothe et al., 2010). However, etiolated-like phenotypes have been observed in several non-angiosperm lineages, including ferns, lycophytes, mosses and even algae. For instance, dark-grown mosses elongate and are pale, ferns have elongated cells in the dark, and in some cases chlorophyll is not synthesized; also R/FR reversible chlorophyll biosynthesis has been observed in brown, red and green algae (Mathews, 2006). However, it is argued that these phenotypes cannot be defined "etiolated", which strictly means having etioplasts (Armarego-Marriott et al., 2019). What could fall in this definition are members of anciently derived gymnosperm groups. For instance, dark-grown seedlings of *Ginkgo biloba* do not contain chlorophylls and feature typical etioplasts, with PLB and PT (Rascio et al., 1984). Even so, its genome encodes for subunits of the DPOR enzyme and phylogenetic studies show that DPOR gene loss occurred in the early evolution of angiosperms (Vedalankar & Tripathy, 2018).

Although acquisition of de-etiolation capacity in angiosperms is a recent evolutionary event, the main components of light signaling pathway involved in this process are conserved at different degree in earlier evolutionary lineages (Figure 1.9). The most conserved components of the light signaling pathway include photoreceptors, COP1, SPA and HY5. Whereas cryptochromes are present in all major evolutionary lineages from bacteria to plants, phytochromes are specific of both land plants and marine algae: FR/R photoreversible responses, as well as their light-dependent translocation to the nucleus have been well documented in charophyte algae (Duanmu et al., 2014; Wang & Lin, 2020). Of the E3 ubiquitin ligase machinery, COP1 is the most conserved component being present in all eukaryotes, while SPA is specific of land plants, charophytes and some green algae (Han et al., 2019). Their role in regulating light-mediated responses has been studied in the moss *Physcomitrella*

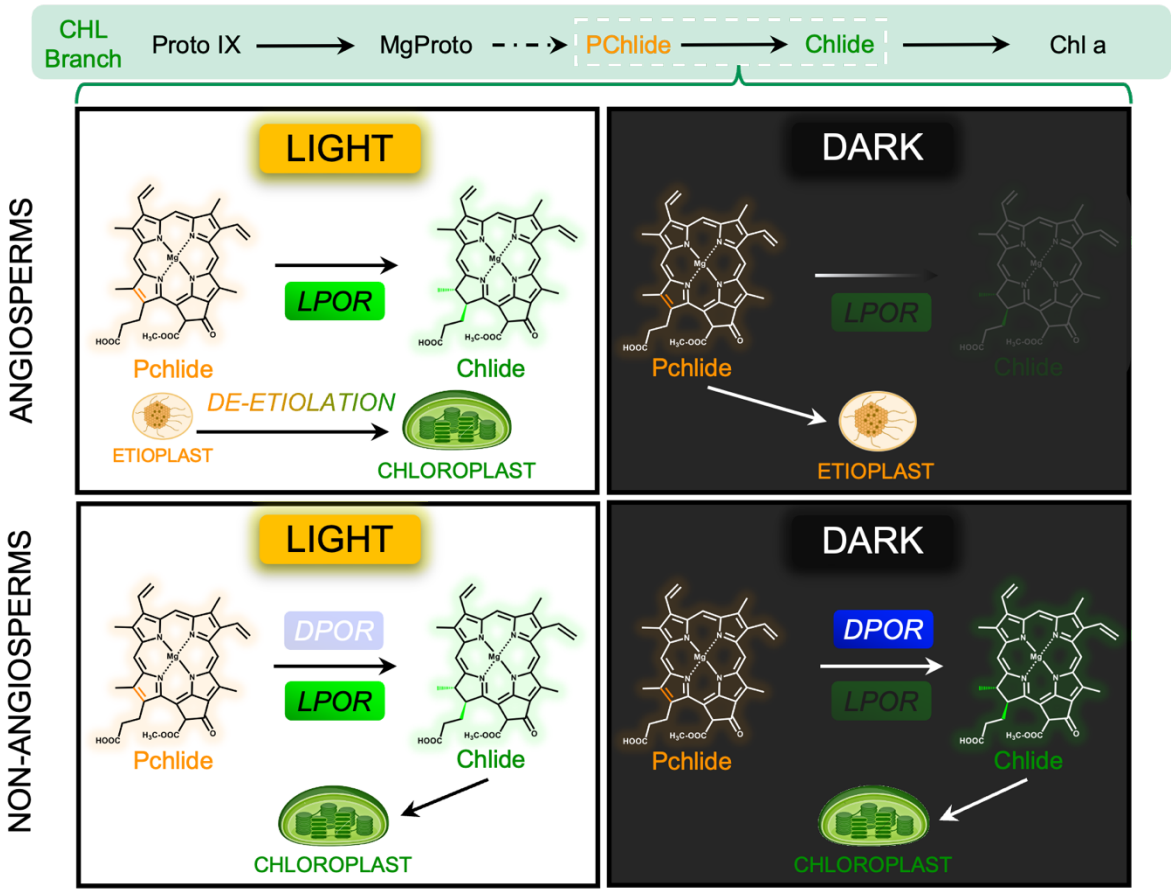


Figure 1.8: Schematic view of Pchlide to Chlide conversion in angiosperm and non-angiosperm plants. Chloroplast biogenesis relies on plants capacity to produce chlorophyll, which is in turn determined by their ability to reduce Pchlide into Chlide, by the protochlorophyllide oxidoreductase enzyme (POR). Angiosperm plants only feature a light-dependent POR (LPOR), responsible for this conversion in the presence of light; consequently, these plants accumulate Pchlide in the dark and form the etioplast, while light induces Chlide production required to complete de-etiolation. In contrast, non-angiosperm plants synthesize chlorophyll also in the dark, as they feature an additional light-independent version of the POR called dark POR (DPOR), responsible for Pchlide to Chlide conversion in this condition; therefore, these plants are not able to etiolate, and feature a functional chloroplast in the dark.

patens: while PpCOP1 can rescue the *cop1* phenotype in Arabidopsis, PpSPA1 fails to rescue the *spa*123 mutant, suggesting functional divergence of SPA genes during evolution of land plants (Han et al., 2020; Ranjan et al., 2014). Homologs of the key photomorphogenesis positive regulator HY5 have been also described in *P. patens*, and suggest that the role of HY5 as a photomorphogenesis promoter is conserved in land plants: PpHY5 is highly destabilized in the dark and interacts with PpCOP1; also a truncated *PpHY5* expressed in wild type Arabidopsis seedlings in short day conditions exhibits a short hypocotyl (Artz et al., 2019; Yamawaki et al., 2011). Phylogenetic studies indicate that HY5 originated in chlorophytes (Han et al., 2019): in particular, in the green microalgae *Chlamydomonas reinhardtii* it has a role in acclimation under light stress (Wulf et al., 2023). PIFs are also rather conserved in green plants, as phylogenetic studies showed its charophyte origin; moreover, PIF studies in *P. patens* indicate the phy-PIFs signaling module is conserved in land plants: in particular, PpPIFs are able to complement *pifq* mutant in Arabidopsis (Inoue et al., 2017; Possart

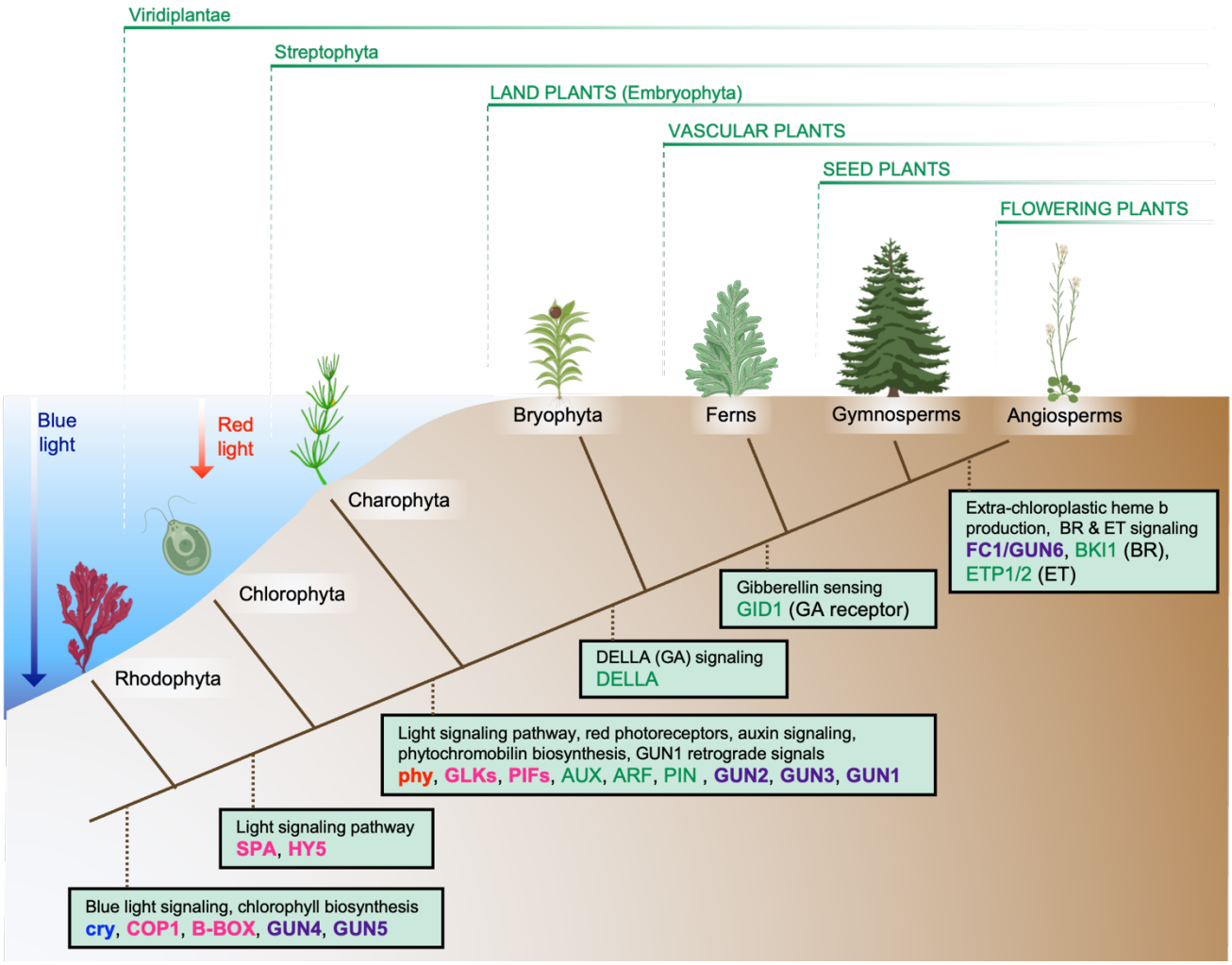


Figure 1.9: Evolution of light and retrograde signaling components. Light, retrograde and phytohormone signaling components are indicated in pink, purple and green, respectively. Phytochromes and cryptochromes are indicated in red and blue, respectively. Red algae conserve main chlorophyll branch enzymes (despite they don't synthesize chl b), blue light receptors and COP1, the latter shared in all eukaryotes. The key light signaling components SPA and HY5 have been described in green microalgae, with a role in photoprotection. Most light and retrograde signaling components have emerged before land colonization, including phys, GLKs, PIFs, GUN2, GUN3, and also a potential *GUN1* homolog, which has been identified in *C. braunii* but not in *K. nitens*. In addition, main components of auxin synthesis and transport have been identified in *K. nitens*, including PIN, AUX and AUXIN RESPONSE FACTOR (ARF). Phylogenetic analysis showed DELLAs emerged with land colonization, but the ability to respond to GAs was acquired later with vascularity. Finally, only angiosperm plants feature BRI1 KINASE INHIBITOR (BKI1) and EIN2-TARGETING PROTEIN (ETP1/2), two essential components of BR and ET signaling pathways; whereas BKI1 emerged shortly after gymnosperms and angiosperm divergence, ETP1/2 emerged later, likely after dicotyledonous divergence. Also, angiosperms specifically feature FC1, which is presumably involved in extra-chloroplastic heme production, that has been hypothesized as a mobile RS. Image adapted from Han et al., 2019 (Figure 1).

et al., 2017). Finally, although GLK sequences have been found in algal genomes (Hernández-Verdeja & Lundgren, 2023), a conserved GLK function has only been demonstrated for land plants. In *P. patens*, *glk* mutants are pale green and their chloroplast show impaired thylakoid stacking (Yasumura et al., 2005); in *Marchantia polymorpha*, *glk* mutants show reduced chlorophyll levels, and also smaller chloroplasts with rudimentary thylakoids and reduced grana (Yelina et al., 2023).

More recent is the emergence of phytohormone signaling (Figure 1.9). GA-responses are specific of vascular plants, but phylogenetic studies show DELLAs evolutionary origin coincides with land adaption (Hernández-García et al., 2019). Phylogenetic analysis indicate that auxin signaling and transport has originated in charophytes, as the core components have been identified in *Klebsormidium nitens* (Wang et al., 2015). In contrast, although many components of brassinosteroid signaling have been found in algal genomes, and BR receptors have been characterized in ferns, BRs canonical signaling pathway has been probably originated after the split of gymnosperms and angiosperms (Wang et al., 2015; Zheng et al., 2022). Ethylene signaling pathway seems to be the most recent of the phytohormones in evolution, having originated after the emergence of angiosperms but before divergence of monocots and dicots (Wang et al., 2015).

Regarding RS, its emergence occurred with early evolutionary green lineages, as many evidences of chloroplast-to-nucleus communication have been found in *C. reinhardtii*, and indicate the involvement of tetrapyrrole biosynthesis components, similarly to Arabidopsis. The first evidence of RS in *C. reinhardtii*, in fact, showed that the accumulation of MgProto in green algae causes changes in gene expression (Kropat et al., 1997). More recently, bilins have been shown to generate changes in gene expression which are fundamental for greening and phototropic growth (Wittkopp et al., 2017). However, other studies showed that RS may also be triggered by the chloroplast unfolded protein response (cpUPR) (Theis et al., 2020). Whether bilin- or cpUPR-dependent, the identity of the RS molecule, and the mechanism by which the RS exits the chloroplast and regulate gene expression (directly or through putative interacting partners) have not been identified and are objected to debate. Interestingly, phylogenetic studies showed that the central regulator GUN1 is absent in early green lineages: a GUN1 homolog was identified in the charophytan algae *Chara braunii* but not in *K. nitens*, suggesting that GUN1-mediated RS has emerged with the Phragmoplastophyta clade (Nishiyama et al., 2018). But this has been recently refuted by a study which showed that in *M. polymorpha* MpGUN1 is not involved in *PhANGs* repression as a consequence of the inhibition of plastid translation, suggesting GUN1 role in RS has emerged more recently (Honkanen & Small, 2022). Therefore, it would be illuminating to identify the main regulator(s) of the ancestral RS mechanism, and how this evolved to regulate chloroplast biogenesis during de-etiolation in angiosperm plants.

Altogether, despite variable conservation of light and RS pathways through photosynthetic lineages, de-etiolation only occurs in angiosperm and in some gymnosperm species. Therefore, it is definitely a surprise when realizing that the first chloroplast biogenesis studies were conducted in *C. reinhardtii*. This was possible by using *yellow-in-the-dark* (*y*) mutant strains, which are unable to produce chlorophyll in the dark and present an undifferentiated plastid lacking thylakoid membranes, which is restored to a functional chloroplast upon exposure to light (Sager & Palade, 1954; Ohad et al., 1967). In this sense they resemble angiosperm species, and were the organism of choice for this early chloroplast biogenesis studies, mainly for its ability to grow non-photosynthetically with acetate as the only energy source (Harris, 2001). However, *C. reinhardtii* lacks many of the key signaling

components such as GLKs, PIFs or GUN1 as I will describe later, opening the intriguing question of what ancestral light and RS mechanisms regulate chloroplast biogenesis.

Chlamydomonas reinhardtii: how a green microalga has become a widely established model for basic and applied research

Unicellular green microalgae, including *C. reinhardtii* (hereafter called Chlamydomonas), belong to the Chlorophyta lineage which diverged from Streptophyta (charophytan algae and land plants) over a billion years ago. Chlamydomonas and higher plants share many genes acquired from the common ancestor of Viridiplantae species, mainly related to photosynthesis and plastid functions. However, a common feature derived from animal-plant ancestor that has been lost in the evolution of angiosperm plants is the eukaryotic flagellum and its basal body (Yoon et al., 2004). Consequently, Chlamydomonas has always represented a powerful model species for photosynthesis, flagellar structure and function, and cell motility (Harris, 2001). In the field of photosynthesis, Chlamydomonas was established as a model species in the middle of the 20th century, boosted by Ruth Sager work, who acquired one of the first transmission electron microscopy (TEM) images of the chloroplast, and also significantly contributed to our understanding of chloroplast biogenesis (Sager & Palade, 1954). This was favored by the suitability of Chlamydomonas as a laboratory species, given that: a) it can be maintained axenically using synthetic media; b) its grow conditions are very flexible, since it can be propagated in the dark under heterotrophic conditions with acetate supplemented media, or in light under both autotrophy (in minimal media) or mixotrophy (in acetate supplemented media) conditions, and also in a wide range of temperatures, performing well from 20 to 28ºC; c) it is haploid, which allows mutant phenotypes to be expressed immediately (Davies & Grossman, 1998). Of these features, the ability to retain a developed chloroplast in dark while growing on carbon supplemented media represents an advantage compared to Arabidopsis, and helped to identify mutants impaired in photosynthesis and chloroplast biogenesis, and the key regulators involved, which are more difficult to study in higher plants (Gutman & Niyogi, 2004). For example, the identification of *stt7* mutant of the photosynthetic regulatory mechanism called state transition in Chlamydomonas (Fleischmann et al., 1999), helped their later identification in Arabidopsis (Depège et al., 2003).

The power of Chlamydomonas as a model species has been further elevated by the establishment of its genome sequence (Merchant et al., 2007) which has been updated last year (Craig et al., 2023), by the development of many tools for genetic transformation, including CRISPR (Greiner et al., 2017), and a collection of genome-wide T-DNA insertional mutants, called Chlamydomonas Library Project (CLiP) (Li et al., 2016), and also by the many protocols for heterologous gene expression being developed (Kindle et al., 1989; Weiner et al., 2018). Still, it is worth mentioning that all tools for the generation of mutants and heterologous gene expression are to date far from being efficient. For instance, *CLiP* mutants are prone to false positives (Tran & Kaldenhoff, 2020), while CRISPR

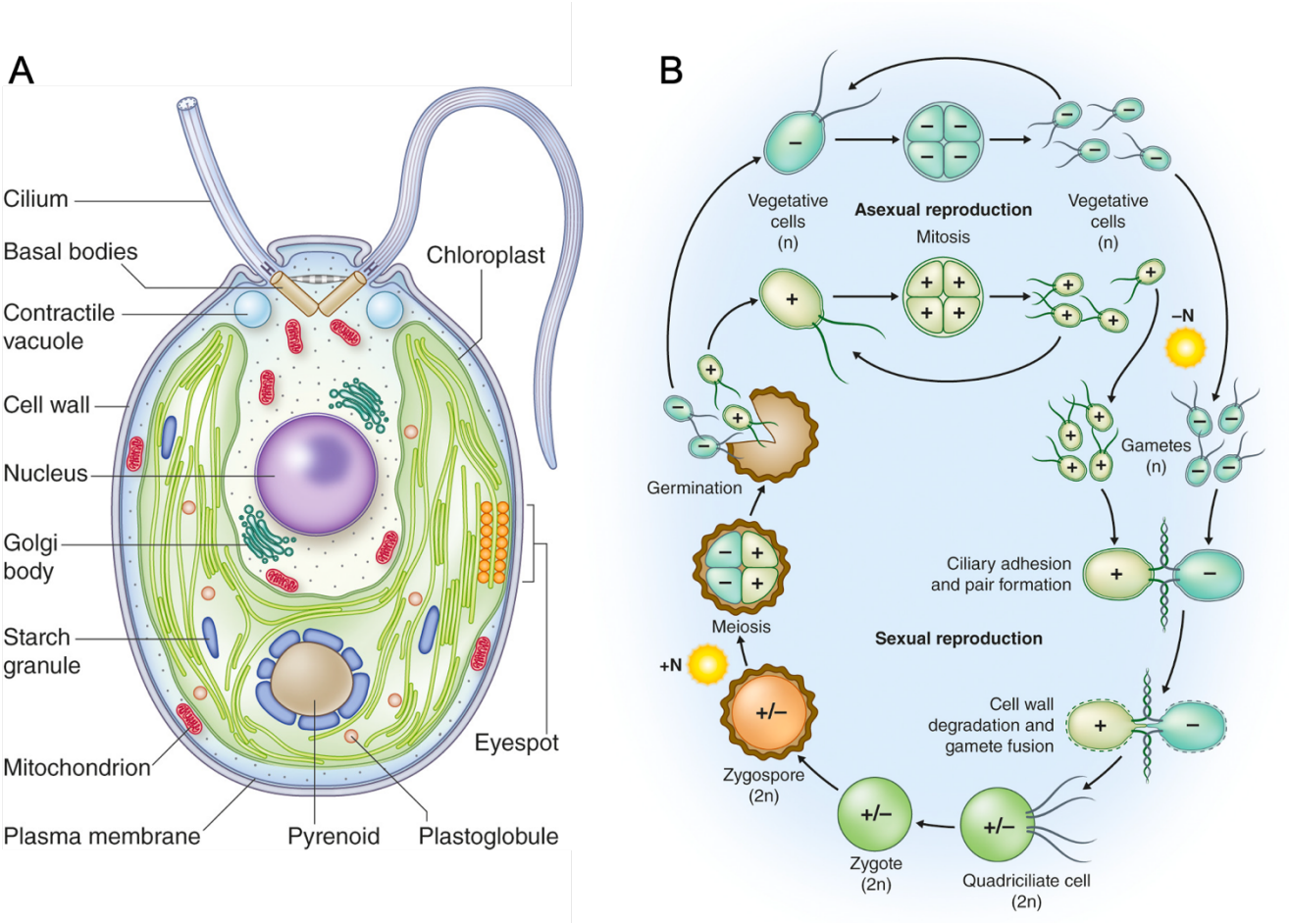


Figure 1.10: A. Structure of Chlamydomonas cells. B. Asexual and Sexual reproduction of Chlamydomonas cells. N: nitrogen. Both images were retrieved from Sasso et al., 2018.

technique requires expensive equipment and time for optimal setup (Guzmán-Zapata et al., 2019). Also, heterologous gene expression has resulted to be rather tricky because Chlamydomonas features a very efficient gene silencing mechanism, that prevents transcription or post-transcriptional processing of nuclear transgenes. Alternatively, chloroplasts have been adopted for heterologous gene expression. Although this strategy requires purification of protein products from cells, it overcomes the gene silencing issue, and also is compatible with post-translational modifications (Schroda, 2019). Nevertheless, many laboratories are putting a lot of effort in both understanding the cause of failures in the application of these techniques and in setting up reproducible protocols that will give high levels of mutants (Schroda, 2019; Sizova et al., 2021).

Chlamydomonas has also been important for the development of optogenetics, a technique to control or monitor the activity of cells (or specific cell pathways) by light, with the discovery of channelrhodopsins (Hegemann & Nagel, 2013). These are ion channel photoreceptors (opsins) that can be engineered and expressed in other cells to control biological processes with light; as optogenetics is a very precise and minimally invasive process, engineered opsins have been expressed in neurons to study neuron functions and neuronal circuits, and also allowed advances in the study of many clinical diseases, such as Alzheimer's disease (Chen et al., 2022).

Recently, Chlamydomonas has gained increasing attention as biofactories, for the production of high-value compounds (such as drugs, antibodies, food additives) mainly for three reasons. First, as mentioned before, Chlamydomonas chloroplasts are being employed for the production of recombinant proteins, since it features a prokaryotic expression system, compatible with post-translational modifications and absence of gene silencing. Second, large-scale production of microalgae biomass is supported by the need for a green economy, which aims to minimize CO_2 production. Additionally, Chlamydomonas is a Generally Recognized As Safe (GRAS) organism (Ma et al., 2022).

Compared to mesophyll cells from Arabidopsis, Chlamydomonas cells are similar in the presence of a chloroplast and the cell wall, but also present some differences (Figure 1.10 A). The most evident are the two flagella which allow cell motility and sexual reproduction. Flagella arise from basal bodies located at the anterior part of the cell, and these are fundamental for flagella assembly, and also mitosis (since they can interconvert to centrioles). In order to assemble flagella, precursors synthesized in the cell body are transported inside the organelle towards the tip where they are assembled (Harris, 2009). This process is called intraflagellar transport (IFT), and occurs in all eukaryotic cilia/flagella, but it was first discovered in Chlamydomonas (Kozminski et al., 1993). In aqueous environments, cell movement is accomplished by a biphasic breast-stroke motion exerted by flagella, while on solid surfaces Chlamydomonas cells can glide with one flagellum leading and the other trailing; these movements are dependent on the intracellular calcium levels (Harris, 2009). Moreover, Chlamydomonas is characterized by a single cup-shaped chloroplast which occupies most of the cell, and that contains at its base a circular structure called pyrenoid. This organelle contains approximately 90% of RuBiSco, and is the site in which CO_2 is fixed (Harris, 2001). Importantly, Chlamydomonas features a carbon concentrating mechanism (CCM), which allows the cell to deal with limited availability of inorganic carbon (Ci) in the environment, and supplies the pyrenoid with concentrated CO_2 that can be used by RuBiSco for the carboxylation reactions. The pyrenoid is surrounded by starch sheaths which are thought to decrease CO_2 leakage from the pyrenoid matrix (Yamano & Fukuzawa, 2009). At the edge of the chloroplast, Chlamydomonas features a specialized structure, the eyespot, which controls phototaxis by detecting directional light. The eyespot is composed of two layers of carotenoid-rich granules (in fact, this structure is seen as an orange spot under the microscope) each one associated with a thylakoid, and also associated with the plasma membrane in correspondence of a channelrhodopsin-rich region. The eyespot carotenoids act as antennas reflecting and amplifying light coming from outside the cell to channelrhodopsin receptors, which in turn trigger changes in flagellar membrane potential, affecting swimming behavior (Hegemann & Berthold, 2009). In addition, Chlamydomonas, as other protists, contains two contractile vacuoles for osmoregulation (Harris, 2001).

Chlamydomonas cells spend most of their life cycle as haploid organisms (Figure 1.10 B); if the conditions are favorable, cells grow and reproduce asexually by mitosis generating from 2 to 8 cells

depending on the cell size and light conditions; during light-dark cycles, cells grow in size during the day and divide in the dark. However, Chlamydomonas can also reproduce sexually: under nitrogen (N) starvation conditions cells undergo gametogenesis. Competent gametes (from compatible mating types) pair using their flagella, and secrete gametolysin to digest their cell wall to facilitate cell fusion. The fusion of two haploid gametes leads to the formation of a quadriflagellate diploid cell, which turns into a zygote once flagella are resorbed. If environmental conditions remain unfavorable, zygotes can develop into highly resistant zygospores, characterized by the formation of a hard impermeable wall, disintegration of the chloroplast with loss of chlorophyll and the formation of lipid bodies. In the presence of N, zygospores germinate in the light, and undergo meiosis generating 4 haploid cells (Sasso et al., 2018).

Chlamydomonas yellow-in-the-dark mutants: a model to study light and retrograde signaling during de-etiolation

Chlamydomonas *yellow-in-the-dark* (*y*) refers to a number of mutant strains which are unable to synthesize chlorophyll in the dark. The first (*y-1*) was originated back in the fifties and employed for early chloroplast biogenesis studies by Ruth Sager, who brought what can be considered the first TEM image of a dark-developed plastid (Sager & Palade, 1954). This “etiolated” plastid is characterized by absence of thylakoid membranes and the pyrenoid, although traces of thylakoidal membranes were observed in the form of irregular vesicles and tubules, and also some of the elements of the pyrenoids are still formed in the dark. In addition, numerous starch granules were observed inside the plastid (Figure 1.11 A,B,C), while the yellowish appearance is given by accumulation of carotenoids which are still synthesized in the dark (Ohad et al., 1967; Sager & Palade, 1954). However, PLB and PT structures, first described a few years after Sager’s works in barley by von Wettstein (von Wettstein, 1959), are absent in *y-1* etiolated plastids. Later works showed that *y* mutants have no photosynthetic capacity and lack photosynthetic machinery, as etiolated cells from angiosperm plants. In particular, it was observed that dark-grown etiolated *y-1* cells feature very low PSII capacity, and completely lack PSII and PSI polypeptides (Malnöe et al., 1988; White & Hoober, 1994). Importantly, when dark-grown *y-1* cells are exposed to light, chloroplast is restored: thylakoid membranes are assembled and stacked into grana, starch sheaths are regularly rearranged around the pyrenoid, and regular layers of carotenoid globules are rebuilt (Figure 1.11 D,E,F). During this process starch is consumed, suggesting that this could be the energy source for the buildup of the chloroplast (Ohad et al., 1967; Sager & Palade, 1954). Moreover, during chloroplast biogenesis PSII photosynthetic capacity is restored, while PSII and PSI polypeptides are gradually accumulated, reaching wild type levels (Malnöe et al., 1988; Ohnishi & Takahashi, 2008; White & Hoober, 1994). Interestingly, in both wild type and *y-1* strains, photosystem nuclear transcripts accumulate with exposure to light, but light does not affect the steady-state level of chloroplast transcripts, although

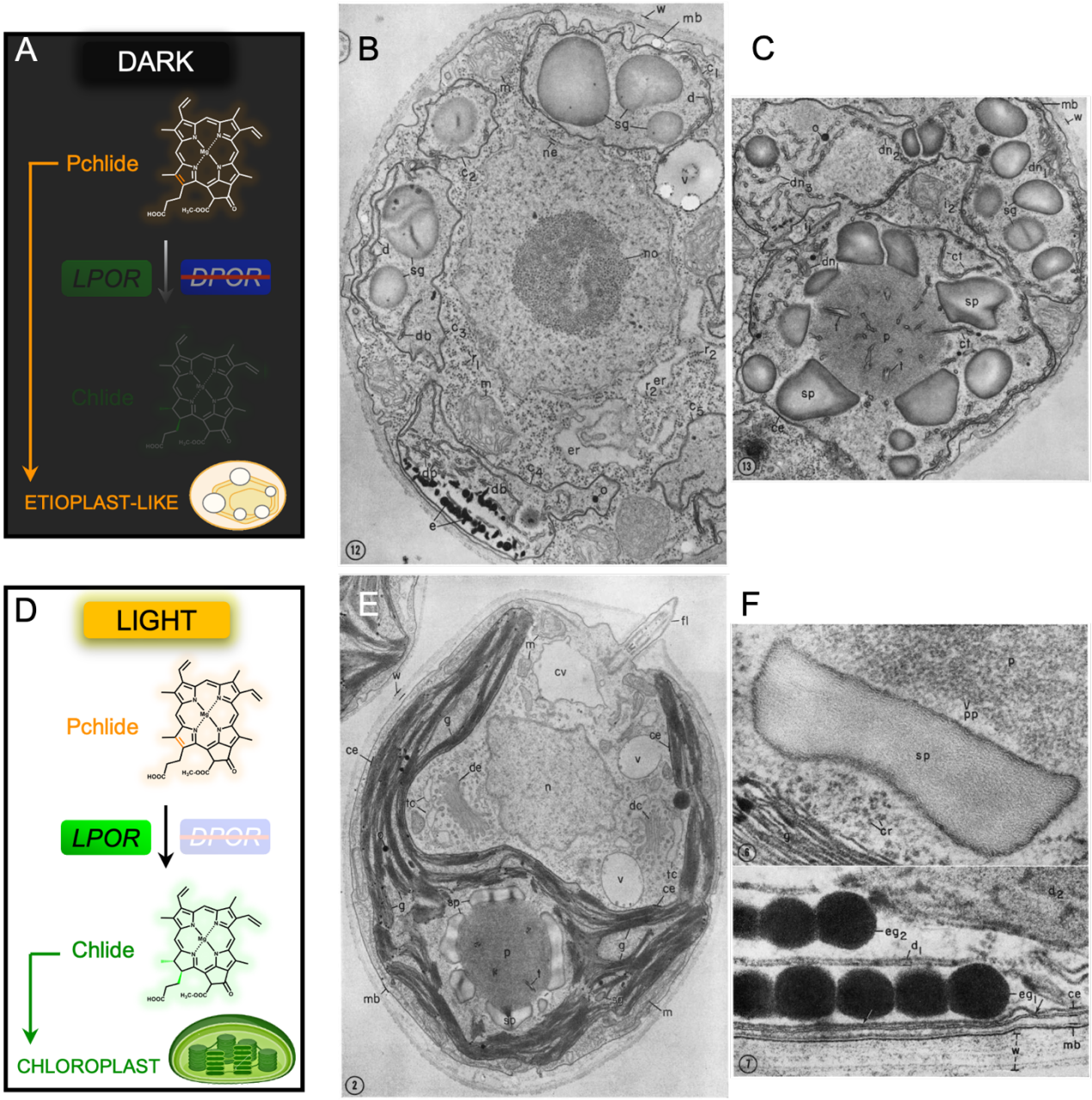


Figure 1.11: Cell morphology of dark- (A-C) and light-grown (D-F) *y-1* mutant cells. A,D Schematic view of Pchlide to Chlide conversion in *y* mutants: *y* mutants lack DPOR and, consequently, are not able to produce chlorophyll in the dark, where they form an etioplast-like plastid, which lacks thylakoids and accumulates Pchlide; upon exposure to light, chlorophyll is produced, and a functional chloroplast is restored. A TEM image exhibiting the apical region of a dark-grown *y-1* mutant cell (B) shows full undifferentiation of chloroplast, which is present in 5 lobes ("c1-5"), that lack thylakoid membranes and grana stacks, reduced to a few disc remnants ("db", v shape, "dp" paired), feature a disorganized eyespot ("e") and are abundant in starch granules ("sg"); the cytoplasm is highly dense in ribosomes ("r1", free, "r2", attached). In the basal part (C), the irregular form of this "etiolated" plastid is evident by the presence of cytoplasmic islands ("i1","i2"), while the pyrenoid ("p") is surrounded by irregular starch plates ("sp") and penetrated by tubules ("t"). In a light-grown *y-1* mutant cell (E), a fully developed chloroplast has a regular cup shape delimited by the chloroplast envelope ("ce"), and is much more abundant in thylakoid membranes, which are stacked in grana ("g"); the chloroplast also features many plastoglobules ("o"), small sg, while the pyrenoid is surrounded by regular starch plates ("sp"). In particular, in this TEM image a contractile vacuole ("cv") and a flagellum ("f") can be observed. A close-up TEM image of the pyrenoid (F, up) shows the regular shape of the starch plates, and pyrenoid particles; importantly, many chloroplast ribosomes can be observed compared to dark-grown *y-1* cells. The eyespot of a light-grown *y-1* cell (F, down) has two rows of regularly disposed carotenoid-rich granules ("eg"), separated by a single chloroplast disc ("d2"). "mb": plasma membrane; "w": cell wall; "n": nucleus; "ne": nuclear envelope; "m": mitochondria; "v": vacuole; "dc": dictyosome; "er": endoplasmic reticulum. TEM images obtained from Siekevitz & Palade, 1967.

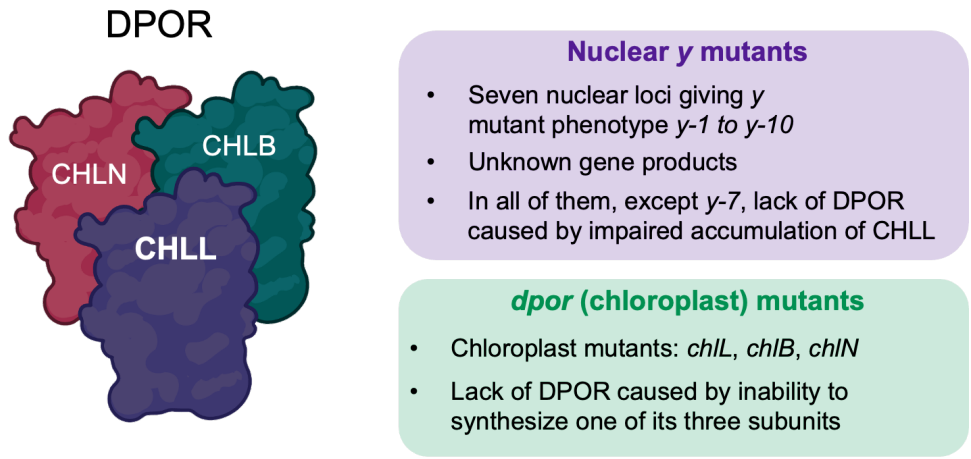


Figure 1.12: *y* mutants are unable to accumulate DPOR enzyme, responsible for Pchlide conversion in the dark. This enzyme is composed of three chloroplast-encoded subunits, named CHLL, CHLB and CHLN. *y* mutants can be classified in two groups. The first group is represented by *y* mutants that carry a mutation in a nuclear locus; these were obtained from UV mutagenesis or spontaneous mutations and are seven, *y-1* (*y-1a*), *y-5*, *y6-1*, *y-7*, *y-8*, *y-10*: the genetic identity of these mutants is still unknown, but later it was shown that all of them, except *y-7*, are unable to accumulate CHLL subunits. The second group are *dpor* mutants, which carry a mutation in one of its three chloroplast-encoded subunits (*chlL*, *chlB*, *chlN*).

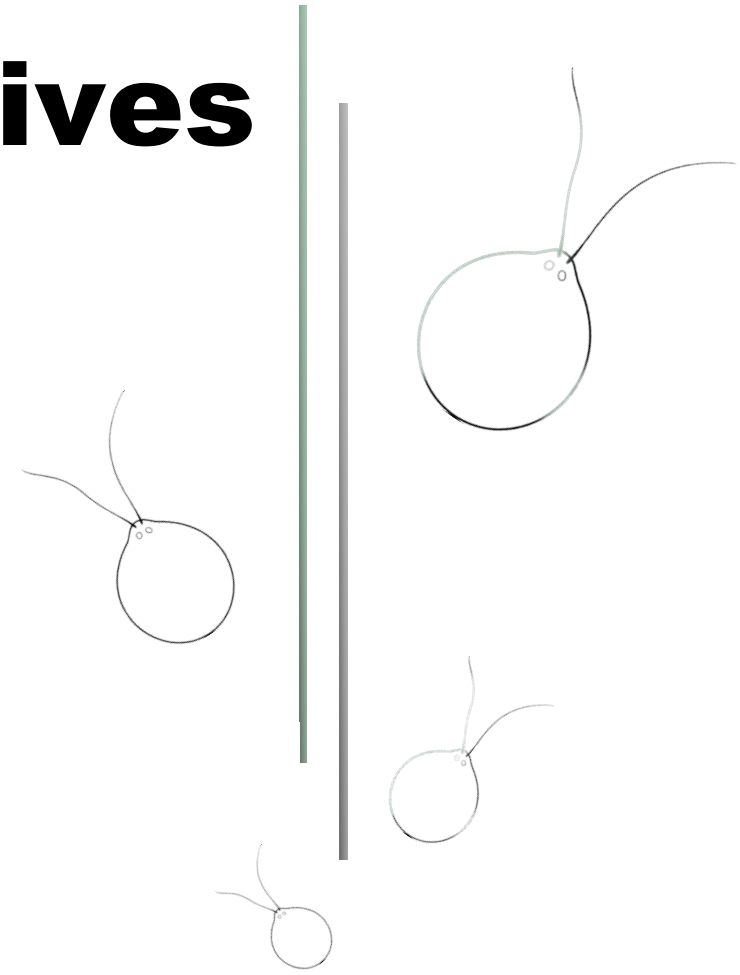
chloroplast polypeptides are actively synthesized in *y-1* cells during chloroplast biogenesis (Malnöe et al., 1988). Limited changes in plastid transcript accumulation were also reported in de-etiolating tobacco leaves (Armarego-Marriott et al., 2019), while light-induced expression of *PhANGs* and synthesis of photosynthetic machinery polypeptides during chloroplast biogenesis have been shown in many de-etiolation experiments (Armarego-Marriott et al., 2019; Dubreuil et al., 2018; Pipitone et al., 2021; Rudowska et al., 2012).

Besides *y-1*, other strains with the *y* phenotype (Figure 1.12) were either isolated from spontaneous mutations (as the *y-1*) or generated by UV mutagenesis; in total, the gene products of seven nuclear loci (named *y-1* to *y-10*) were observed to cause the *y* phenotype, but the specific identity and function in which these genes could be involved were unknown (Ford et al., 1981, 1983; Ford & Wang, 1980, 1982). Only in the beginning of the ‘90s, it was discovered that lack of DPOR is responsible for the *y* phenotype (Choquet et al., 1992), and since DPOR is composed of three chloroplast-encoded subunits, three types if *dpor* mutants with *y* phenotype were generated: *chlN* (Choquet et al., 1992), *chlL* (Suzuki & Bauer, 1992), *chlB* (Li et al., 1993). Therefore, to date these three mutants are the only *y* mutants with known identity of their genetic mutation. Instead, the genetic cause of all seven *y* nuclear mutants remains unknown, but it was demonstrated that all of them (except *y-7*) have defects in accumulating CHLL subunits, but not CHLL transcripts. This finding suggests nuclear mutants may feature defects in proper post-transcriptional regulation of CHLL (Cahoon & Timko, 2000).

Independently of the genetic cause of the mutation, y mutants highly resemble angiosperm plants in their capacity to etiolate by developing a dark adapted plastid with no photosynthetic capacity, and to de-etiolate, by restoring a fully functional chloroplast upon light exposure; also similar is the transcriptional and post-transcriptional regulation of photosynthesis transcripts during de-etiolation.

Remarkably, this occurs without many master regulators of light and RS during this process, such as PIFs, GLKs and GUN1. In this work, we applied transcriptomics to understand how regulation of these two signaling pathways is achieved during de-etiolation in Chlamydomonas *y* mutants. But first, we needed to setup a *y* mutant de-etiolation system that gather the ideal conditions for their study. This will be presented in the following chapter.

Objectives



De-etiolation has been widely characterized in angiosperm plants, at both cellular and molecular level. During the last decades, many works have established the main components of the light signaling pathway, that can be classified into photoreceptors, mainly phytochromes and cryptochromes, which perceive light and transcriptional regulators, such as PIFs, GLKs and HY5, which mediate de-etiolation response by regulating the expression of thousands of genes, that not only regulate chloroplast biogenesis but also whole plant development. Photomorphogenesis is a very complex process, and although these TFs are essential for its proper execution, it is likely that many other TFs are involved.

In contrast, the RS pathway that regulates de-etiolation is still not very well understood. It is known that GUN1 plays a fundamental role not only in chloroplast biogenesis but also in whole seedling development, but how this is achieved is still not very clear. Also, many evidences show that both light and RS pathways coordinate to regulate proper de-etiolation in angiosperm plants: where chloroplast is subjected to stress, GUN1-dependent biogenic RS can affect the expression of main TF involved in LS, giving most optimal biological response.

Remarkably, y mutants of Chlamydomonas resemble angiosperm plants in their ability to etiolate, forming a dark adapted plastid, and de-etiolate, restoring a fully functional chloroplast upon transfer to light, without many key master regulators of light and RS pathways, in particular phytochromes, PIFs, GLKs, and GUN1. De-etiolation in these particular strains have been deeply characterized at the cellular level, and mildly at the molecular level in the past century, where we only have data regarding expression and protein profiles of a few photosynthesis genes in this process. On the other hand, RS has been explored in Chlamydomonas during dark-to-light transition, but these experiments were all carried out in strains that already feature a fully developed chloroplast in the dark.

Here, our goal is to perform transcriptomics to characterize all main events regulated by light and RS pathways during de-etiolation of y mutant cells. We also aim to understand which evolutionary advantage represented the emergence of those essential master regulators of these signaling pathways that are absent in Chlamydomonas. In addition, we want to predict potential novel TFs involved in both pathways. For this purpose, we set the following specific objectives:

1. **Setup of a Chlamydomonas *y* mutant based de-etiolation system**

   In this first objective we aim to 1) setup the optimal conditions (strains, media, light intensity, etc.) that allow us to have perfectly etiolated y mutant cells in the dark with no photosynthetic activity, and healthy de-etiolating cells that fully restore the chloroplast, and also 2) setup a proper experimental design that allows us to characterize of light and retrograde signaling in Chlamydomonas (i.e. election of stress conditions for RS).

2. **Transcriptomic analysis of light signaling**

   In this part, we aim to study main light regulated events during de-etiolation, evaluate which specific advantage represented the emergence of PIFs and GLKs during this process, and also predict novel TFs involved.

3. **Transcriptomic analysis of retrograde signaling**

   In this part, instead, our goal is to study main events regulated by RS during de-etiolation, and especially to study its crosstalk with light signaling. As no homologs of GUN1 have been identified in Chlamydomonas, we will evaluate what advantage this master regulator conferred to angiosperm plants during de-etiolation. Finally, a strategy for the identification of novel *gun* mutants in Chlamydomonas will be presented.

Setup of a y mutant de-etiolation system

CHAPTER 2

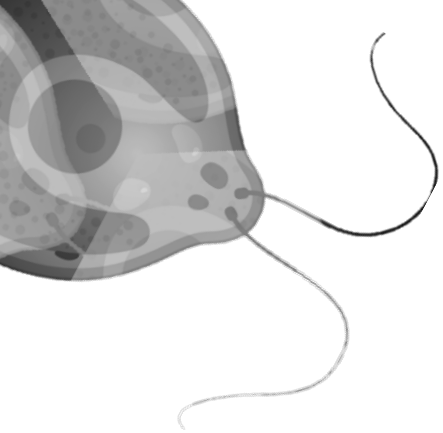
Setup of a *y* mutant based de-etiolation system

Introduction 37-40

Materials and Methods 41-44

Results 44-57

Discussion 57-62



2 Chapter

Introduction

De-etiolation is a key developmental process undergone by angiosperm plants following germination, that starts with an elongating seedling in the dark, with closed cotyledons and non-photosynthetic etioplasts, battling to reach the surface under heterotrophic metabolism, and culminates with the development of a fully autotrophic seedling with green and expanded cotyledons, and fully developed chloroplasts (Gommers & Monte, 2018; Symons & Reid, 2003). Etiolation represented an evolutionary innovation of first angiosperm plants, which during land expansion had to face the inconvenient of an increasing canopy and germination in soil: by suppressing photomorphogenesis in the dark, these plants were able to direct limited energy sources supplied by the seed to maximize elongation until reaching favorable light conditions (Pfeiffer et al., 2016).

To understand the molecular mechanism behind this process, de-etiolation studies have been traditionally conducted in Arabidopsis seedlings (Figure 2.1 A). As light triggers de-etiolation, many efforts were invested in identifying light signaling components, and for this purpose Arabidopsis seedlings were employed to find mutants which were photomorphogenic in darkness (Seluzicki et al., 2018). By analyzing the overall seedling morphology and more closely the plastid architecture, COP1, SPAs, PIFs were identified as key repressors of photomorphogenesis in darkness, in fact their absence generates the so called constitutive photomorphogenesis (*cop*) phenotype (Deng & Quail, 1992; Leivar et al., 2008; Laubinger et al., 2004). Conversely, mutants that exhibit skotomorphogenic growth in light (called albino mutants) were also identified: an example is hemera (HMR), a key factor required for the expression of chloroplast genes during its biogenesis (Chen et al., 2010); similarly, HY5 (a key positive regulator of photomorphogenesis) was identified through a mutation that causes elongated hypocotyls in light (Oyama et al., 1997). Other key components of light signaling have been identified in Arabidopsis: activity of HY5 is highly regulated by BBOX transcription factors (TFs) (Gangappa & Botto, 2014), while GLKs have been involved in regulating chloroplast biogenesis in the cotyledons (Zhang et al., 2021), and more recently in regulating whole seedling development through direct regulation exerted by HY5 (Zhang et al., 2024). Evaluation of skoto- and photomorphogenic

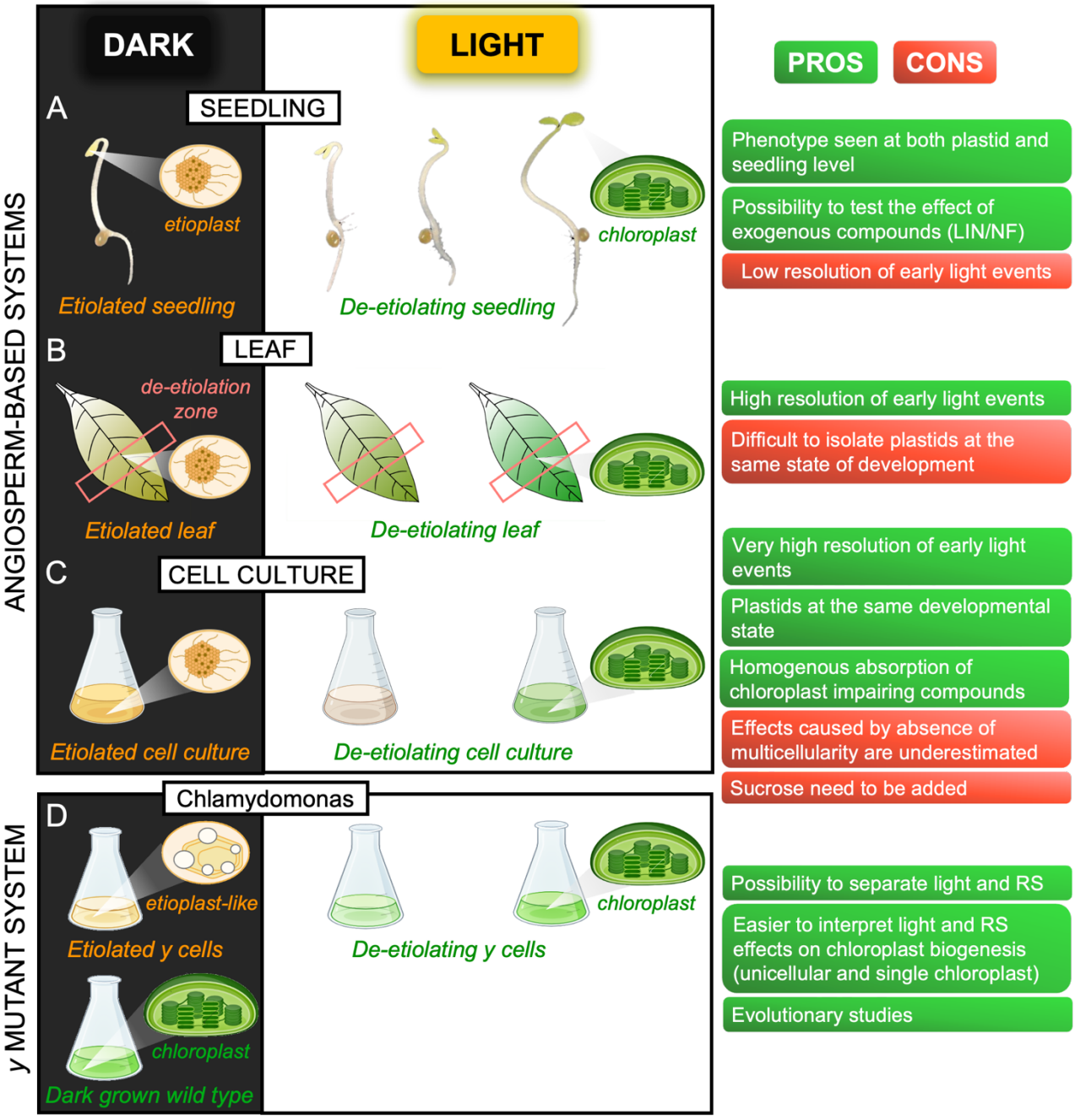


Figure 2.1: De-etiolation systems based on angiosperm plants (A-C) and Chlamydomonas *y* mutants (D). A. Arabidopsis seedlings have been important for the identification of main components of light and RS pathways during de-etiolation. B. Leaf based systems were developed to better characterize early light events during etioplast-to-chloroplast transition, however in these systems, a gradient of chloroplast development is observed along the leaf and only a specific region undergoes de-etiolation, making it difficult to isolate plastids at the same state of development. C. Alternatively, an Arabidopsis cell culture system was developed, where de-etiolation occurs very slowly giving an unprecedented high resolution of early light events; other advantages include homogenous chloroplast biogenesis in all cells, and also uniform absorption of chemical compounds that affect chloroplast activity for RS studies. However, important limitations include underestimation of absence of multicellularity, and the need to add exogenous sucrose which is known to alter light signaling. D. Chlamydomonas *y* mutants represent an interesting alternative system which overcomes many limitations of angiosperms, for instance a) the possibility to separate light conditions from plastid state, individually characterizing light and RS contributions, b) it is a much simpler organism (one cell, one chloroplast), with no developmental cues associated with multicellularity, c) since Chlamydomonas is a very early divergent photosynthetic organism, novel or evolutionary conserved components still not identified might be regulating the ability of *y* mutants to repress photomorphogenesis.

phenotypes in Arabidopsis seedlings also allowed to identify phytochromes (PHYA and PHYB) and cryptochromes (CRY1 and CRY2) as the main red and blue light photoreceptors which trigger the signaling pathway that leads de-etiolation (Dehesh et al., 1993; McCormac et al., 1993; Yang et al., 2000).

But light signals are not alone in regulating de-etiolation: the chloroplast itself can detect if environmental conditions are not favorable, and send RS to the nucleus to regulate the expression of thousands of genes involved in this process (Chan et al., 2016). For instance, when de-etiolating Arabidopsis seedlings encounter conditions that impair chloroplast activity, such as the presence of the carotenoid biosynthesis inhibitor norflurazon, the RS activates and represses the expression of many *PhANGs*. A genetic screen for mutants in which this repression is absent, allowed the identification of several mutants defective in chloroplast-to-nucleus communication, called *gun* (Susek et al., 1993). Of all *GUN* genes so far discovered, *GUN1* is being the most studied as it does not encode for an enzyme of the tetrapyrrole biosynthesis pathway as all the other *GUN2-6* genes (Shimizu & Masuda, 2021), but instead encodes a chloroplast pentatricopeptide repeat protein that is able to regulate many different chloroplast biological processes, such as plastid gene expression, plastid protein import and tetrapyrrole biosynthesis (Richter et al., 2022). More recently it has been shown that it can bind plastid RNA, indicating a role in RNA maturation (Tang et al., 2024). Importantly, GUN1 have been found to regulate not only chloroplast biogenesis during de-etiolation but also whole seedling development through downstream regulation of *GLK1* expression in high light conditions (Martín et al., 2016).

Besides the discovery of main light and RS components involved in de-etiolation, Arabidopsis seedlings have also been important for the characterization of chloroplast biogenesis at both morphological and metabolic level (Pipitone et al., 2020). Alternatively, to get a higher resolution of early light events during etioplast-to-chloroplast transition, alternative systems were developed. For instance, de-etiolation of adult angiosperm leaves (Figure 2.1 B) in tobacco (Armarego-Marriott et al., 2019) and maize (Dubreuil et al., 2018; Sharpe et al., 2011) brought significant contributions to our understanding of the early dynamics of both photosynthetic and metabolic changes during chloroplast biogenesis. However, it is extremely difficult to isolate cells where plastids are in the same developmental state. This drawback was overcome with the recent development of an Arabidopsis cell culture de-etiolation system (Figure 2.1 C) (Dubreuil et al., 2018), where plastid development is synchronized in all cells. This system is also particularly useful for retrograde signaling studies, since assimilation of chemical compounds used to disrupt chloroplast activity is faster and equal for all cells, compared to seedling based systems, where absorption of these compounds takes time, so the actual dose that reaches each tissue and cell might not be initially homogenous. As de-etiolation in Arabidopsis cells is much more slower than the other systems, it gives a high resolution of early light events, and when setup it allowed to define two gene regulatory phases in chloroplast biogenesis: a first phase with rapid changes in gene expression and metabolic profile, and a second phase with

more deep changes in nuclear gene expression that lead to full chloroplast maturity, which is theorized to be triggered by a positive RS (Dubreuil et al., 2018). However, this system also has its own drawbacks: although the apparent high resolution of early chloroplast biogenesis events, cells are grown in an artificial environment, where absence of multicellularity effects and developmental cues on chloroplast are underestimated; also cells need to grow in the presence of an exogenous carbon source, such as sucrose, which is known to affect light signaling, and could generate misleading results (Armarego-Marriott et al., 2020; Dijkwel et al., 1997).

Compared to these angiosperm-based systems, *yellow-in-the-dark* (*y*) mutants of the green microalgae *Chlamydomonas reinhardtii* represent an interesting alternative to study de-etiolation. These mutants in fact do not produce chlorophylls in the dark and resemble angiosperm species in their ability to etiolate, forming a dark adapted plastid with no photosynthetic capacity, and to de-etiolate forming a fully functional chloroplast upon transfer to light (Sager & Palade, 1954). What especially takes our attention, is the capacity of this strain to perform chloroplast biogenesis without many essential components of light and RS above presented, in particular phys, PIFs, GLKs and GUN1 which are absent in Chlamydomonas and other microalgae (Han et al., 2019, Nishiyama et al., 2018). This opens the intriguing question of how these processes are regulated in Chlamydomonas, and what advantage represented the emergence of these master regulators in angiosperm plants. In addition, there are many technical advantages compared to angiosperm-based de-etiolation systems (Figure 2.1 D): a) as a unicellular organism, no developmental traits associated with multicellularity are present, which eases interpretation of light and RS that regulate de-etiolation; b) as a cell culture system, chloroplast developmental state is expected to be synchronized in all cells, and also absorption of chloroplast inhibitor compounds necessary for RS studies is homogenous for all cells; c) the presence of a single chloroplast eases interpretation of RS effects, as in higher plants we cannot discard that the contribution to RS of each chloroplast inside one cell could be different; d) in Chlamydomonas we can better study the crosstalk between light and RS during de-etiolation, as we can compare *y* mutants cells having an etioplast-like plastid in the dark with wild type cells having a fully developed chloroplast in this condition, therefore separating the contribution of RS involved in chloroplast biogenesis on light signaling, a situation that is impossible to find in angiosperm pants where presence or absence of light is directly linked to the developmental state of the chloroplast.

In this chapter we developed a Chlamydomonas *y* mutant based de-etiolation system, selecting the best strain, and environmental conditions that allows us to have perfectly etiolated cells in the dark with no photosynthetic capacity, and healthy de-etiolating cells that restore their chloroplast and photosynthetic activity upon transfer to light. Also, we choose the best experimental design that allows us to characterize light and RS involved in de-etiolation: our final aim, in fact, is to perform a transcriptomic analysis of both light signaling pathways, which will be covered in the following chapters.

Materials and Methods

Strains and culture conditions

All Chlamydomonas strains used for the experiments were obtained from the Chlamydomonas Resource Center (CRC). These strains included the wild type strains 137c- (CC-124) and CC-3269 and the *yellow-in-the-dark* mutant strains CC-1168 (Ford & Wang, 1980), and CC-3840 (Suzuki & Bauer, 1992), hereafter called *y-2* and *y-4*, respectively. All the strains were maintained in Tris-acetate-phosphate (TAP) -agar plates with homemade trace elements (Gorman & Levin, 1965; Kropat et al., 2011) and stored in a plant growth chamber (ARALAB 1200) at 21ºC and 30 µmol m^{-2} s^{-1} of LED light intensity. Strains were re-streaked onto fresh TAP-agar plates one week before preparation of cell cultures for de-etiolation.

De-etiolation setup

In order to obtain the etiolated material and/or dark acclimated cultures, *y* mutant and/or wild type colonies were inoculated in Sueoka's high salt medium plus acetate (HSA) (Sueoka, 1960), and grown for 5 days at 23ºC in the dark. In the first de-etiolation trials (Figures 2.3-to-2.7), the following day the medium was fully replaced with fresh HSA or HSM, the concentration set at 1-2 million cells mL^{-1} and de-etiolation was performed by transferring cells in light at 50 µmol m^{-2} s^{-1}. In addition, "always light" (AL) controls of *y-2* and *y-4* strains were prepared as de-etiolation cultures in HSM, but always keeping the cells in light conditions at 50 µmol m^{-2} s^{-1}.
The final trials and RNA-seq experiment (Figures 2.8-to-2.10), included a dark acclimation step before de-etiolation, which consisted in two steps: 1) at the end of the fifth day of the preparation of the etiolated material, the medium of all the cultures was fully replaced with fresh HSA, and half of them were also supplemented with 0.5 mM lincomycin hydrochloride; 2) next day, the medium of all cultures was replaced with HSM minimal medium (HSA without sodium acetate) with or w/o lincomycin and kept in the dark for 3 hours. De-etiolation was performed as for trials, but setting final concentration at 2.5 million cells mL^{-1}. As before, the "always light" *y* mutant cultures were prepared in the same way as the de-etiolation cultures, but always keeping the cells in light conditions at 50 µmol m^{-2} s^{-1}.

Photosynthesis measurements

Chlorophyll fluorescence measurements (Fv/Fm and ΦPSII) were carried out with Imaging PAM (Walz, Germany) (Peers et al. 2009; Maxwell & Johnson, 2000); samples were prepared by loading approximately 1 million cells onto two pieces of 692 grade glass microfiber filters (VWR International Eurolab, S.L.), and kept in the dark for 15 minutes. Fm measurements for Fv/Fm and ΦPSII values were determined using a saturating pulse of light; ΦPSII was evaluated without and at different increasing actinic lights (20, 110 and 280 µmol m^{-2} s^{-1}) in intervals of 30 s.

Chlorophyll and protochlorophyllide measurements

Chlorophyll content was determined as follows: 1 mL sample of de-etiolating cultures was centrifuged at 12000 r.p.m. for 3 min, the pellet was resuspended in methanol and re-centrifuged at maximum speed for 3 min; supernatant was transferred into single use plastic cuvettes and absorbance at 652, 665 and 750 nm was measured with SpectraMax® Plus 384 Microplate Reader spectrophotometer (Molecular Devices, LLC). Chlorophyll a and b content was determined using the equations of Porra et al., 1989.

Protochlorophyllide content of *y-4* cells was evaluated as follows: samples of 6 mL at 4 million cells mL^{-1} were centrifuged at 4500 r.p.m. for 5 min, discarding the supernatant. The extraction of chlorophyll precursors was performed in strict dark conditions and keeping all the reagents in ice. The pellet was resuspended in 1 mL of acetone:NH_4OH 0.1 M (9:1 v/v), centrifuged again at max speed and the supernatant was mixed with equal volumes of petroleum ether. After a quick centrifugation, two phases were distinguishable: a) the organic phase on top containing chlorophylls and carotenoid pigments and b) the polar phase at the bottom containing chlorophyll precursors (chlorophyllide and protochlorophyllide); the latter was collected, transferred into a glass cuvette and the fluorescence spectrum at 440 nm emission in the range of 500-750 nm in intervals of 5 nm was measured with the SpectraMax® spectrophotometer.

Growth measurements

Growth was monitored during etiolation and de-etiolation steps in two different ways: A) cell turbidity and B) cell concentration. A) Triplicates of 100 µL from each culture were loaded into a 96-well transparent and flat bottom plate, and added to previously loaded 50 µL of a suspension of Tween 20 in HSA or HSM medium at 0.67% concentration (v/v). Triplicates of HSA or HSM medium were used as the blank. Cell turbidity was determined by measuring the sample absorbance at 730 nm with the SpectraMax® spectrophotometer. B) Samples of 200 µL were transferred to a 1.5 mL tube. To immobilize cells, 20 µL of 0.25% (v/v) iodine / ethanol solution were added. A 10 µL volume of immobilized cells was loaded into an hemocytometer and cell number was determined by manually counting a significant number of cells (at least 50). At least 3 counts for sample were performed to obtain an accurate cell concentration.

Microscopy

To assess cell morphology and greening of de-etiolating *y*-mutant and wild type cells, 200 µL sample were taken and immobilized cells were prepared as described in the previous section. To test cell viability, a 200 µL sample was mixed with an equal volume of trypan blue solution (0.4%) and incubated at room temperature for 5 min. A volume of 10 µL of immobilized cells or trypan blue-treated cells was employed for microscopic analysis. Light micrographs were taken through a Leica DM6

Upright Microscope (Leica Microsystems) using a 40X objective, while image parameters were adjusted using the Leica LAS X Software.

Reverse transcription-quantitative polymerase chain reaction (RT-qPCR)

RNA extraction was carried out using Maxwell® RSC Plant RNA Extraction Kit (Promega). Approximately 2.5 million cells were collected from each sample, and processed following manufacturer's instructions. During RNA extraction procedures, samples were treated with 5 µL DNaseI. A NanoDrop® ND-1000 Spectrophotometer was employed to quantify RNA, and to check A_{260}/A_{230} and A_{260}/A_{280} ratios were above 1.8. Synthesis of cDNA was performed using NZY First-Strand cDNA Synthesis Kit (NZYTech), and following the manufacturer's instructions. We employed 1 µg of RNA in a total volume of 20 µL cDNA reaction. After cDNA synthesis, samples were treated with 1 µL of RNaseH from the kit for 20 min at 37ºC. RT- controls for qPCR were prepared by diluting in nuclease free water the same amount of RNA and without performing the cDNA reaction.
RT-qPCR reactions were performed using SYBR™ Green (ThermoFisher). For these reactions we employed 10 ng of cDNA or RT- and 3 pmol of each primer in a total volume of 10 µL SYBR™ Green reaction. Technical and biological triplicates were prepared for each condition. Primers used are shown in Table 2.1, and were designed for 4 target genes (*LHCBM1*, *PSBR1*, *LHCA7* and *PSAD1*), while *GBLP* was used as control gene for RT-qPCR analysis (Petroutsos et al., 2016). RT-qPCR reactions were performed in LightCycler® 480 System (Roche) and the qPCR and melting curve programs for SYBR™ Green with no extension were set according to the manufacturer's instructions. C_T values were calculated using the second derivative maximum method of the LightCycler® 480 Software. Gene expression values were determined with the $2^{-\Delta\Delta CT}$ method, and values of each time point in light were referenced towards dark 0h.

RNA quality control and sequencing

RNA samples for transcriptomic analysis were obtained as described in the previous section. The NanoDrop® ND-1000 Spectrophotometer was employed to quantify all samples, and to check A_{260}/A_{230} and A_{260}/A_{280} ratios were above 2. RNA integrity was evaluated in all the samples by

Table 2.1: Primers used for RT-qPCR analysis. *GBLP* was used as internal control for gene expression. Cre: *Chlamydomonas reinhardtii*.

Gene	*Cre* ID	Primer Forward	Primer Reverse	References
GBLP (*RACK1*)	Cre06.g278222_4532	CAAGTACACCATTGGCGAGC	CTTGCAGTTGGTCAGGTTCC	Petroutsos et al., 2016
LHCBM1	Cre01.g066917_4532	AGAACCTGTCCGACCACCTG	AGACGACCCAAATAAACCGCT	-
PSBR1	Cre06.g261000_4532	ATGTAGCGCATCCTAGCGTC	ACCCGAAACACAAAACTGGC	-
LHCA7	Cre16.g687900_4532	CAGACCCTGAAGTGGTACGTC	GAGGTGAGGATGATGCCAGC	-
PSAD1	Cre05.g238332_4532	CATGATGTCGCCTGCTGAGA	TCAATCAGCGAAATCGGCCA	-

electrophoresis, by running 200-600 ng of RNA in a 1% agarose electrophoresis gel. In some samples RNA integrity was also assessed through bioanalyzer analysis using Agilent RNA 6000 Nano kit, and following the manufacturer's instructions. A total 3 µg of RNA for each sample was processed and stored at room temperature in GenTegra® RNA screw cap tubes, as indicated by the manufacturer. RNA samples were sent to the sequencing company Novogene (Beijing, China), where library preparation and transcriptome sequencing were conducted.

Results

Strain election and de-etiolation medium were key parameters of the Chlamydomonas y mutant based system that required optimization

In order to reach the ideal setup for our transcriptomic analysis that fulfils the traits mentioned in the introduction, we performed several de-etiolation trials in which we tested different strains, as well as several cell culture parameters (such as the temperature, medium, light conditions, etc.). The full system consists in two main steps (Figure 2.2): 1) etiolation step, where *y*-mutant cells are grown in the dark until they lose all photosynthetic capacity, at the same time the cell culture reaches the characteristic yellowish appearance due to absence of chlorophylls in the etiolating cells; 2) de-etiolation step, where etiolated *y*-mutant cells are transferred to light conditions, where they restore their chloroplast in parallel to the recovery of their photosynthetic capacity. Many parameters in both steps had to be set and tested. Fortunately, the majority of these didn't require much optimization (Figure 2.2, black circles), as these are common growth conditions for this species, and also because Chlamydomonas can well-perform in a wide range of light, temperature and metabolic conditions, so that slight variations in the setup of these parameters wouldn't compromise success of the experimental setup. For instance, we chose 23ºC as the temperature for our setup and 50 $\mu mol^{-2}\ s^{-1}$ as light conditions for de-etiolation, as these conditions work very well for photobiology experiments in this species (Hui et al., 2022). For heterotrophic growth during etiolation step, an acetate supplemented medium was required. Although TAP is the most common acetate-supplemented medium for this species, we chose instead HSA as medium for etiolation step (Figure 2.2 c) for several reasons: a) growth rate was slightly higher in HSA compared to TAP in the dark (data not shown); b) it allows to keep salt composition of the medium in both etiolation and de-etiolation steps, in case the latter is performed in a minimal medium (as it will be shown later in this chapter), since HSM is the most common minimal medium used for Chlamydomonas and HSA is the same medium with the addition of acetate; c) we observed that in our conditions prolonged growth of Chlamydomonas cells in TAP cause alkalinization of the medium (pH > 8 after 3 days without medium replacing), while HSA had a better buffering capacity. The two parameters of the de-etiolation setup that required

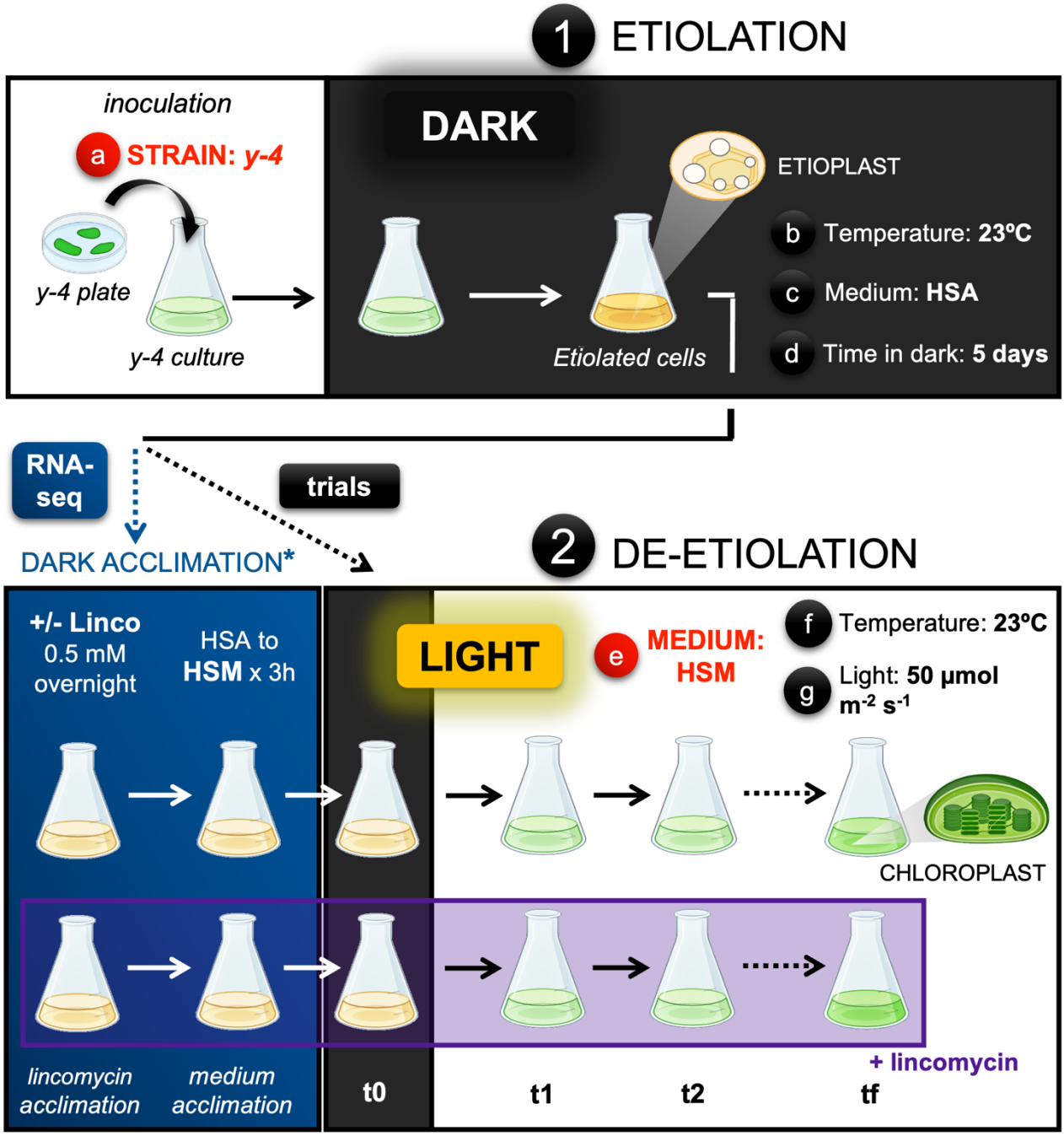


Figure 2.2: Schematic representation of the Chlamydomonas *y* mutant based de-etiolation system. One-week-old *y* mutant cells are inoculated in HSA (acetate supplemented) medium and transferred to dark for etiolation. During the first trials (Figures 2.3-to-2.7), once cells were etiolated they were transferred to light for de-etiolation. For the final trials and the RNA-seq experiment (Figures 2.8-to-2.10), once cells were etiolated, they were pre-acclimated in the dark: first cells were transferred in fresh medium and half of them were overnight treated with lincomycin; second, the following they, before the start of de-etiolation all cells were acclimated in HSM (minimal, w/o acetate) for 3h. Conditions of the setup that didn't require optimization are indicated in black (b-d for etiolation; f,g for de-etiolation), whereas conditions that required optimization are the *y* mutant strain and the de-etiolation medium, indicated in red.

optimization (Figure 2.2, red circles) were the *y* mutant strain and the de-etiolation medium. Two *y* mutant strains were tested: *y-2*, which carries a nuclear mutation that impairs accumulation of CHLL subunit of the DPOR, and the *y-4* which is a chloroplastic *chlL* mutant. Also, two de-etiolation mediums were tested: HSM minimal medium and HSA, which is the same HSM medium but acetate

supplemented. The election of one or the other option is critical since it deeply affects our interpretation of light and RS effects during de-etiolation: for our setup, it is clear that the best choice would be *y-4* as the *y* mutant strain, since here the genotype is the direct cause of the *y* phenotype, and HSM as de-etiolation medium, since it is known that a carbon source alters light signaling. For this reason, and unlike the other parameters, here we are not looking for the best performing option, but rather to check that the preferred option can successfully etiolate and healthily de-etiolate as with the other conditions.

Both y-2 and y-4 mutant cells are able to restore a fully functional chloroplast upon light exposure without the need for carbon supplemented medium

The aim of the first de-etiolation trials was to test both *y-2* and *y-4* mutant strains in HSA and HSM de-etiolation mediums. For this purpose, we obtained data for several physiological parameters, including growth, photosynthesis (measured by means of Pulse-Amplitude-Modulation (PAM) fluorometry), chlorophyll content and cell morphology, in the dark and at several time points in light during de-etiolation. In addition to *y-2* and *y-4* etiolated cells, we included a control consisting in *y-2* and *y-4* cells that were prepared as the etiolated material, but always grown in light conditions, called always light (AL).

We first observed that by growing these strains in the dark in HSA at 23ºC, 5 days was enough time to obtain yellow etiolated cells that show null photosynthetic activity, and absence of chlorophylls (Figure 2.3 B,C,E,F; Figure 2.4 A). Once transferred to light, both *y-2* and *y-4* increased their photosynthetic activity in both HSA and HSM mediums until reaching their maximum levels after 2 days, which coincides with the FvFm values of *y-2* and *y-4* AL controls (Figure 2.3 B,E). Some differences were observed in the dynamics of FvFm recovery: in *y-2* cells this occurs faster, reaching almost AL levels by 12 h in both mediums; *y-4* cells increase their FvFm slightly slower compared to *y-2*, and being HSM slower than HSA for this strain. Chlorophyll content also increases during de-etiolation in both strains until almost reaching AL levels by 2 days (Figure 2.3 C,F): no clear differences were found between both strains, but in *y-4* de-etiolating cells accumulation of chlorophylls is slightly slower in HSM compared to HSA. Visually, both *y-2* and *y-4* etiolated cultures look completely green after 1 day in HSM (Figure 2.4 B). Light micrographs at the middle section of de-etiolating *y-2* and *y-4* cells in both medium conditions, also show the increase in greening with exposure to light, and also the formation of their characteristic cup-shaped chloroplast from a more de-differentiated and disorganized plastid in dark (Figure 2.3 G,H). The dynamics of cell growth and division during de-etiolation, instead, changes depending on the strain and medium: in *y-2* and *y-4* cells de-etiolating in HSA ODs increase throughout the time course, whereas in HSM ODs decrease (Figure 2.3 A). This might be an indicator of cell death in HSM cultures. Interestingly, this is not reflected by the cell number (Figure 2.3 D): de-etiolating cultures of both *y* strains, in fact, increase in

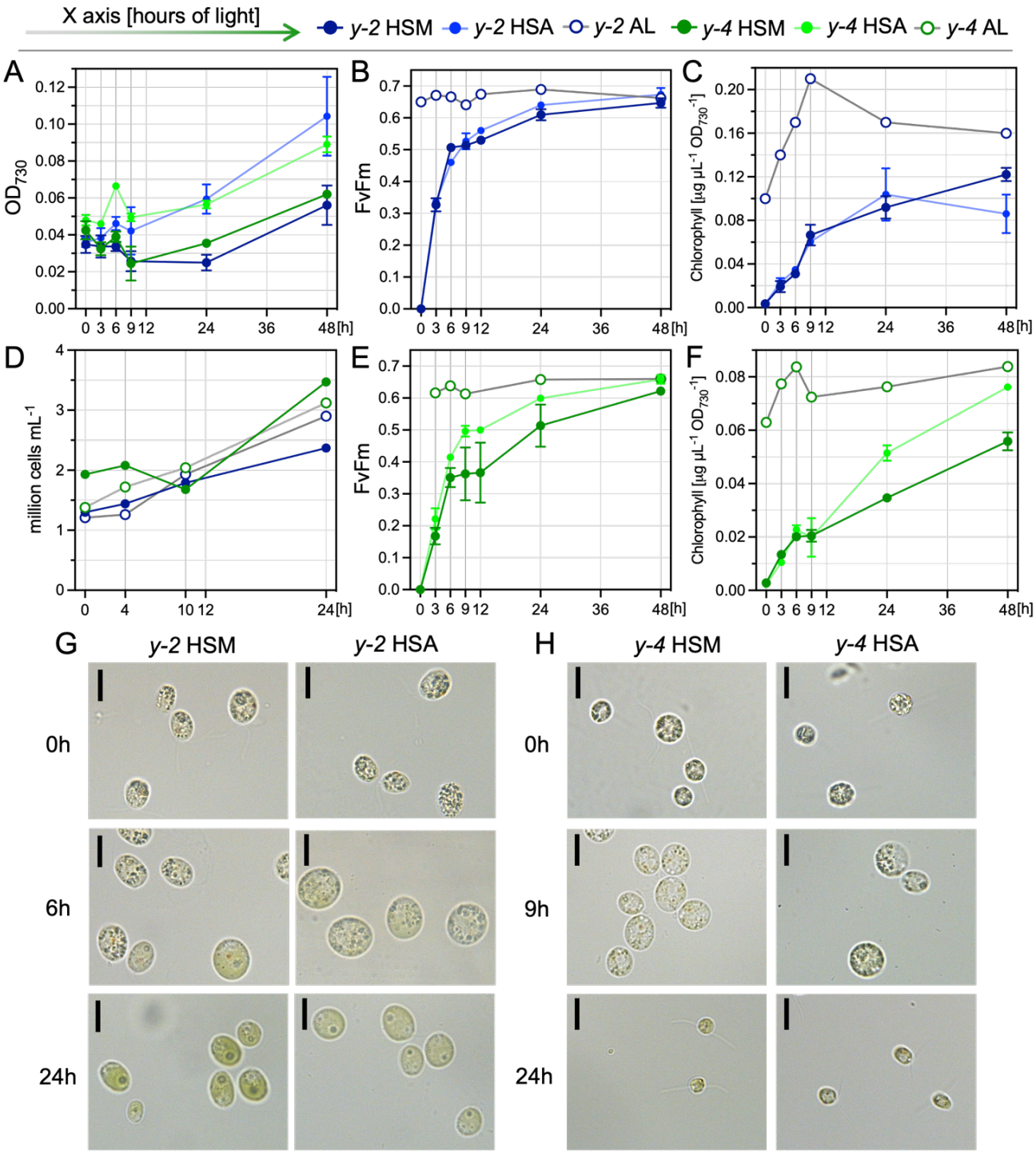


Figure 2.3: De-etiolation trial of *y-2* (blue) and *y-4* (green) mutant strains in acetate supplemented (HSA, light color) or acetate depleted (HSM, dark color) conditions. A control of *y-2* and *y-4* cells always grown in light conditions (AL) and de-etiolating in HSM (empty circle) was added. Growth, cell morphology and photosynthesis measurements were taken in the dark and at several time points upon transfer to light. A,D: Growth of *y-2* and *y-4* strains was assessed in terms of cell turbidity (A) or cell concentration (D). B,E: Maximum quantum yield of PSII (FvFm) was used to determine the photosynthetic performance of *y-2* (B) and *y-4* (E) strains. C,F: Total chlorophylls of *y-2* (C) and *y-4* (F) strains, referenced to cell turbidity. G,H: Light micrographs of *y-2* (G) and *y-4* (H) de-etiolating vegetative cells taken at the middle section to shown general cell architecture. Scale bars of all micrographs: 10 µm.

cell number after 24h, but whereas in *y-2* cultures this increase is small, *y-4* cultures almost duplicate in cell number. This different behavior of both strains is reflected in their morphology (Figure 2.3 G,H): whereas *y-2* cells are similar in size to the starting etiolated cells, *y-4* cells appear considerably smaller compared to their etiolated counterpart.

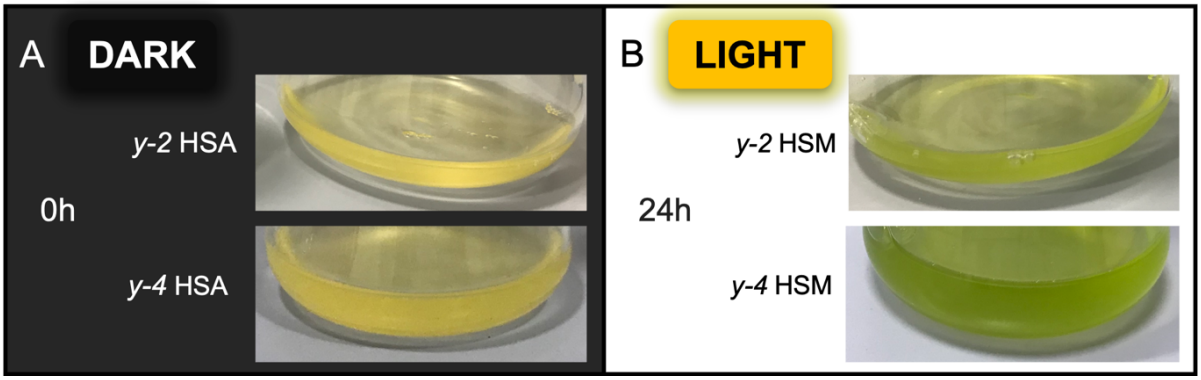


Figure 2.4: Appearance of *y-2* and *y-4* mutant cultures which have been etiolated for 5 days in the dark in HSA medium (A), and after 1 day of de-etiolation in light and HSM (B).

Although the dynamics of de-etiolation can change depending on the strain and the de-etiolation medium, in all the cases this process is fully and healthily completed. Overall, these results suggest that both *y* mutant strains are able to restore a fully functional chloroplast upon light exposure, without the need of a carbon source. Therefore, we chose HSM as de-etiolation medium for our setup, and performed following trials with this medium.

Wild type cells of Chlamydomonas exhibit less photosynthetic activity and chlorophyll content in the dark

An important aspect of our experimental design is the inclusion of wild type cells, since these feature a fully developed chloroplast even when grown in the dark. The comparison between etiolated y-4 cells and wild type cells in the dark is of special interest for our transcriptomic analysis as it allows us to evaluate 1) how the chloroplast state of development influence biogenic RS in the dark, if this signaling pathway is active in this conditions, and 2) at which degree de-etiolation is dependent on light or RS, and therefore if the transcriptome of wt cells in the dark is similar to etiolated or de-etiolated y-4 cells.

In this section, we aimed to evaluate how wt cells of Chlamydomonas behave when grown in the dark and upon light exposure. For this purpose, two wt strains were selected: the CC-124, a common use wt, and the CC-3269, which corresponds to the *y-4* wt background. These cells were prepared the same way as *y* mutant cells in the dark, and transferred to light conditions in HSM. Interestingly, although these cells feature a fully functional chloroplast in the dark where they show photosynthetic activity, FvFm values are below their maximum in light (Figure 2.5 A), while chlorophyll levels were less than half their levels in light (Figure 2.5 B). This low chlorophyll content is reflected by a less intense greening of wild type cells in the dark (Figure 2.5 C,D), which still can be clearly differentiated from the transparent aspect of y etiolated cells, and also maintain the cup-shaped chloroplast structure. No differences in photosynthesis were found between strains (Figure 2.5 A), but CC-3269 cells show higher chlorophyll content in light compared to CC-124, but not in dark (Figure 2.5 B). Also cell morphology is different between wt strains: CC-3269 cells look much smaller in light compared to

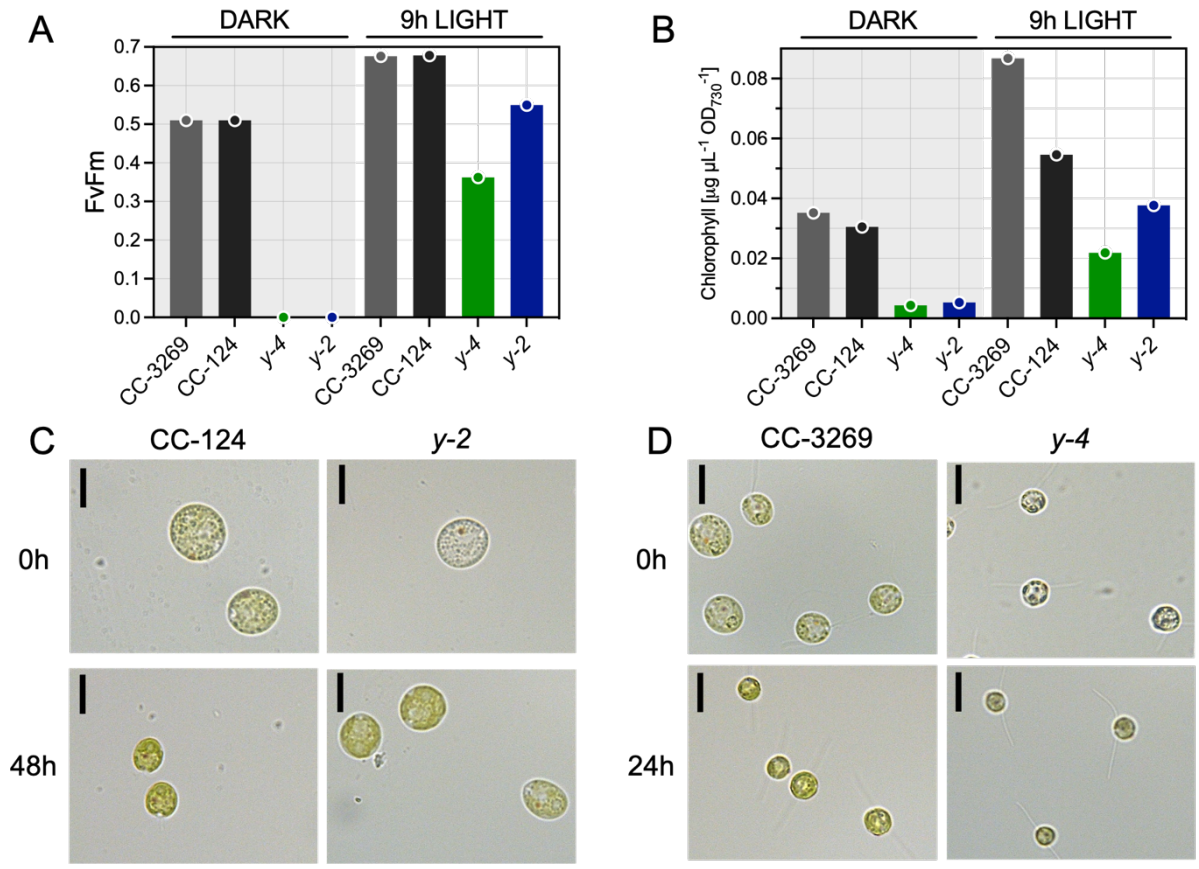


Figure 2.5: Evaluation of de-etiolation in wt strains. In addition to *y-4* (green) and *y-2* (blue), two wt strains were employed for de-etiolation trials, CC-3269 (grey), wt background for *y-4*, and CC-124 (black), a common use wild type used as a control for *y-2* de-etiolation trials. Maximum quantum yield of PSII (A) and total chlorophylls (B) was evaluated for all these strains, in the dark and during de-etiolation at 9h of light. Light micrographs of de-etiolating *y-2* and CC-124 (C), and *y-4* and CC-3269 (D) vegetative cells were taken after 1 or 2 days of de-etiolation to show cell greening. Scale bars of all micrographs: 10 µm.

dark, similarly to de-etiolating *y-4* cells, and these two strains show visible and long flagella (Figure 2.5 D); CC-124 cells are generally bigger and round shaped, and are comparable in size to *y-2* cells (Figure 2.5 C). These results indicate that Chlamydomonas can partially repress photomorphogenesis in the dark, no matter its capacity to synthesize chlorophyll in this condition.

Accumulated Pchlide in y-4 etiolated cells is quickly converted into Chlide upon exposure to light

A major concern of our de-etiolation setup was the capacity of de-etiolating *y-4* cells to process the accumulated Pchlide in the dark. In Arabidopsis, it is known that excess levels of this precursor can cause lethal bleaching upon transfer to light (Leivar et al., 2009), and is characteristic of *pifq* mutants. PIFs are key repressors of photomorphogenesis and, in particular, no *PIFs* homologs have been identified in Chlamydomonas; since these proteins regulate the levels of Pchlide in the dark, we thought initially that *y* mutants could be accumulating critical levels of PChlide during the preparation of the etiolated material. Therefore we tested the capacity of *y* mutant cells to convert all their accumulated PChlide upon transfer to light.

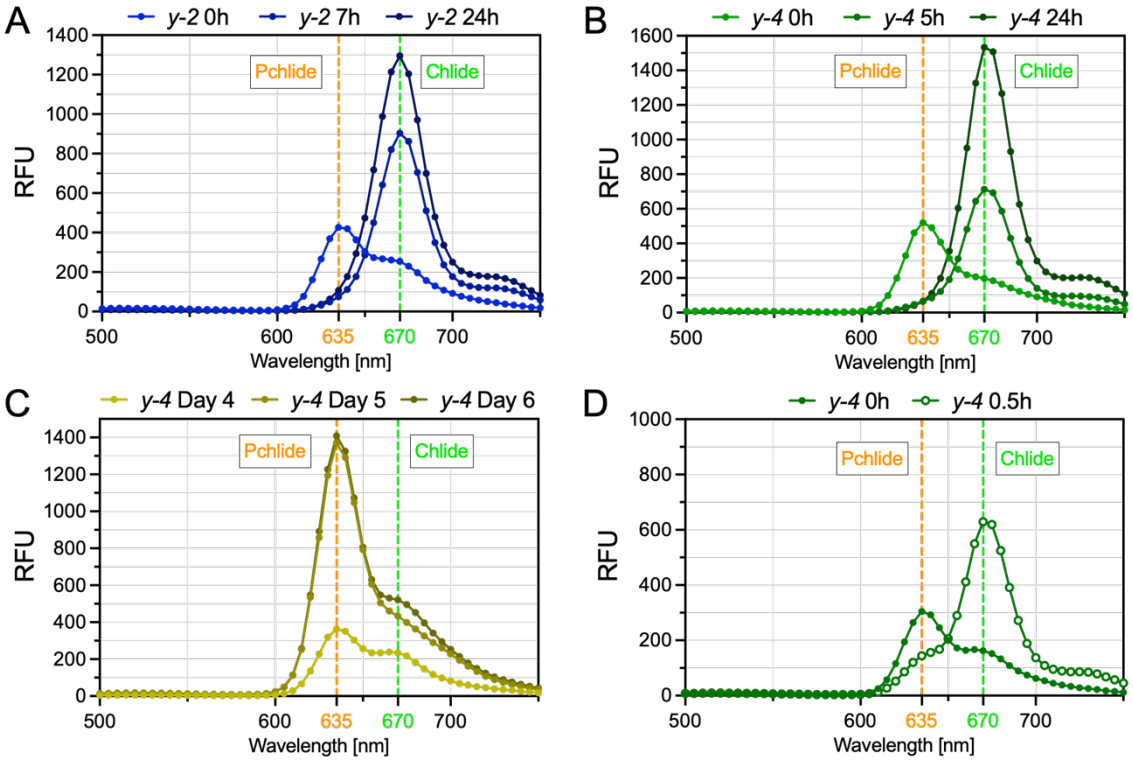


Figure 2.6: Protochlorophyllide content of de-etiolating *y-2* (A), and *y-4* cells (B,D), and during the preparation of the etiolated material for *y-4* cells (C). Plots represent the fluorescence spectrum at 440 nm wavelength emission of the polar phase of the pigment extract (which contains the chlorophyll precursors) for each strain and condition. Pchlide and Chlide peaks can be observed at 635 and 670 nm, respectively. RFU: relative fluorescence units.

For this purpose, Pchlide and Chlide content was measured using their fluorescence properties: these precursors can absorb light at 440 nm and give each a unique emission peak, which corresponds to 635 nm for PChlide and 670 nm for Chlide. We found that both *y-2* and *y-4* cells can convert all the accumulate Pchlide into Chlide when transferred to light in HSM conditions (Figure 2.6 A,B), with no signs of Pchlide content after 7h in *y-2* and 5h in *y-4*. In these cases, we observed that the levels of Pchlide are always lower compared to Chlide in light conditions, which indicates that *y* mutant cells do not accumulate much Pchlide in dark conditions, and that the full chlorophyll biosynthetic pathway is activated in light. Pchlide measurements also allowed us to check the amount of time in the dark needed to obtain fully etiolated *y-4* cells (Figure 2.6 C): whereas with 4 days in the dark, both a Pchlide and a Chlide peak are detected, with 5 days in this condition the accumulation of Pchlide is at its maximum and doesn't change with 6 days, at the same time no Chlide peak is observed. Therefore these results indicate that 5 days in the dark Is the minimum time required to obtain fully etiolated *y-4* cells. These cells are able to convert almost all the accumulated Pchlide in just 30 min upon exposure to light (Figure 2.6 D). These results indicate that both *y-2* and *y-4* cells do not suffer the effects of Pchlide photobleaching during de-etiolation. As both strains can healthily de-etiolate in our conditions, we decided to setup our de-etiolation system with the *y-4* strain, and this was used for our final de-etiolation trials.

Etiolated y-4 cells induce photosystem genes upon exposure to light

In order to choose the best time points to capture early and late light events in the transcriptomic analysis, we evaluated the expression of photosystem genes, which are key genes induced during de-etiolation and required for chloroplast biogenesis in angiosperm based systems (Dubreuil et al., 2018). In Chlamydomonas, photosystem transcripts progressively accumulate during light in 12:12 (light-dark) photoperiod conditions with a maximum at 8-9h (Zones et al., 2015), so that these genes are ideal to define a range for our experimental design that captures main light events during de-etiolation.

In this part, we tested gene expression of four different photosystem genes by RT-qPCR in *y-4* cells before de-etiolation in the dark and at different early and late time points upon light exposure. These are: *LHCBM1* (antenna, PSII), *LHCA7* (antenna, PSI), *PSBR1* (core, PSII) and *PSAD1* (core, PSI). All gene expression values are referenced towards dark. We found that all photosystem genes are induced at 3h of de-etiolation (Figure 2.7), except *LHCBM1* whose expression remains constant in the first 3h. This increase in expression is much higher for *PSBR1* and *LHCA7* (3 fold), compared to *PSAD1* (2 fold). A drop in gene expression is observed in all four genes at 10h of de-etiolation: in *LHCA7* and *PSBR1*, which showed the highest induction, the levels of gene expression at 10h match dark, while *LHCBM1* and *PSAD1* are repressed at 10h compared to dark. Peak of induction of *LHCBM1* and *PSBR1* is likely to be observed in a time point between 3h and 10h; unlikely, it is found before 3h as this would no correlate with recovery of the PSII capacity. These data suggest that main light events involved in de-etiolation are captured by 10h, and that likely maximum peak of expression of these genes is found between 3h and 10h.

De-etiolating y-4 cells treated with lincomycin are unable to perform photosynthesis, but can still convert Pchlide and remain viable at least during the first 24h

A widely employed method to study biogenic RS during de-etiolation consists in impairing chloroplast activity and, for this purpose, lincomycin, a drug that specifically inhibits chloroplast protein translation, has been used to induce RS in angiosperm-based de-etiolation systems (Koussevitzky et al., 2007; Dubreuil et al., 2018). In particular, it was shown that RS induced by this compound not only affect chloroplast biogenesis, but also repress whole seedling photomorphogenesis in the presence of light (Martín et al., 2016). In this section, we tested the effects of this drug during de-etiolation in Chlamydomonas. Starting from these last trials, we took into consideration the time that cells require to absorb this compound and produce the desired effect, which is a limiting factor of seedling based de-etiolation systems. Also, we reasoned that it would be desirable to eliminate metabolic effects in our transcriptomic analysis when comparing dark to light, as in the previous trials etiolated cells are immediately transferred to light once HSA is replaced with HSM for de-etiolation. For these reasons, we added a dark acclimation step in our setup before de-etiolation (Figure 2.2), which includes an

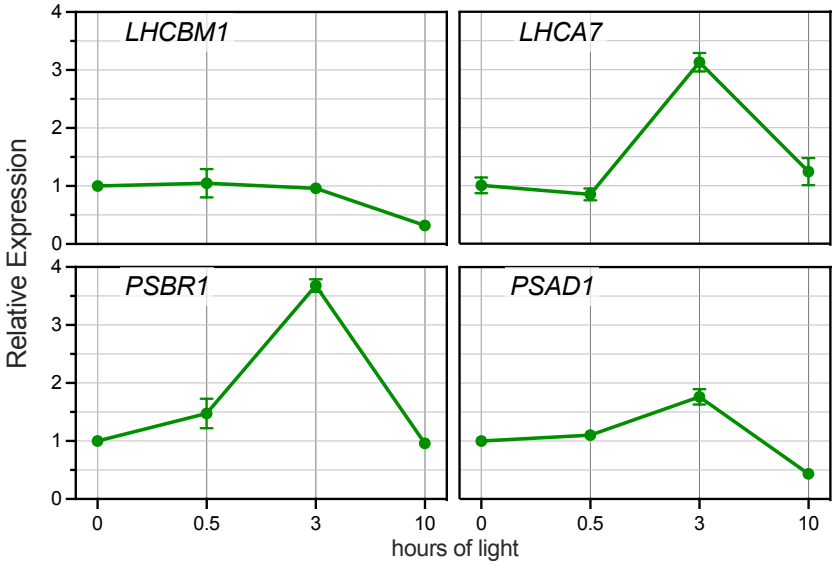


Figure 2.7: Expression levels of four representative photosystem genes in de-etiolating *y-4* cells in HSM conditions, determined through RT-qPCR. Genes here assessed are, PSII: *LHCBM1* (antenna), *PSBR1* (core); PSI: *LHCA7* (antenna), *PSAD1* (core). All values are referenced towards dark (0h) and calculated with the $2^{-\Delta\Delta CT}$ method using *GBLP* as reference gene. Two biological replicates were used for each time point.

overnight treatment with 0.5 mM lincomycin and a 3h acclimation in HSM before de-etiolation. The duration of lincomycin treatment in the dark was designed to give cells more than enough time to absorb the compound, and without affecting growth and yield during the preparation of the etiolated material. A shorter acclimation was thought for HSM medium as cells might suffer stress from starvation, if grown in a minimal medium in the absence of light for too much time. To test this design, we performed de-etiolation trials without and with lincomycin (named Light and Light + Linco), and following the two acclimations mentioned. Dark acclimation in HSM didn't affect the way *y-4* cells de-etiolate, compared to previous experiments: cells grow and divide by 24h (Figure 2.8 A, green), fully recover photosynthetic activity by 24h (Figure 2.8 B, green) and convert almost all the accumulated Pchlide after 1h (Figure 2.8 C); also cell morphology was not affected by HSM acclimation (Figure 2.8 E, left), as cells undergo greening during de-etiolation and cells look smaller after 24h, though this difference in size is less dramatic compared to first de-etiolation trials (Figure 2.3 H, left). Etiolated *y-4* cells that were also treated with lincomycin were completely impaired in their capacity to recover photosynthetic activity during de-etiolation (Figure 2.8 B). However, they were still able to grow during the first 24h, though much more slowly compared to non-treated cells (Figure 2.8 A). Interestingly, lincomycin does not affect the capacity of de-etiolating cells to convert Pchlide into Chlide, as very similar fluorescence profiles are observed for both Light and Light + Linco cultures (Figure 2.8 C,D), being almost all Pchlide already converted by 1h of de-etiolation in both conditions. This result suggests that lower growth in Light + Linco cultures is not caused by Pchlide photobleaching effects. No clear differences in cell morphology were observed between conditions (Figure 2.8 E), but we further tested viability of de-etiolating *y-4* cells using trypan blue, a dye that stains dead cells, in both Light and Light + Linco cultures (Figure 2.8 F). Although it seems that cells incorporated some of the

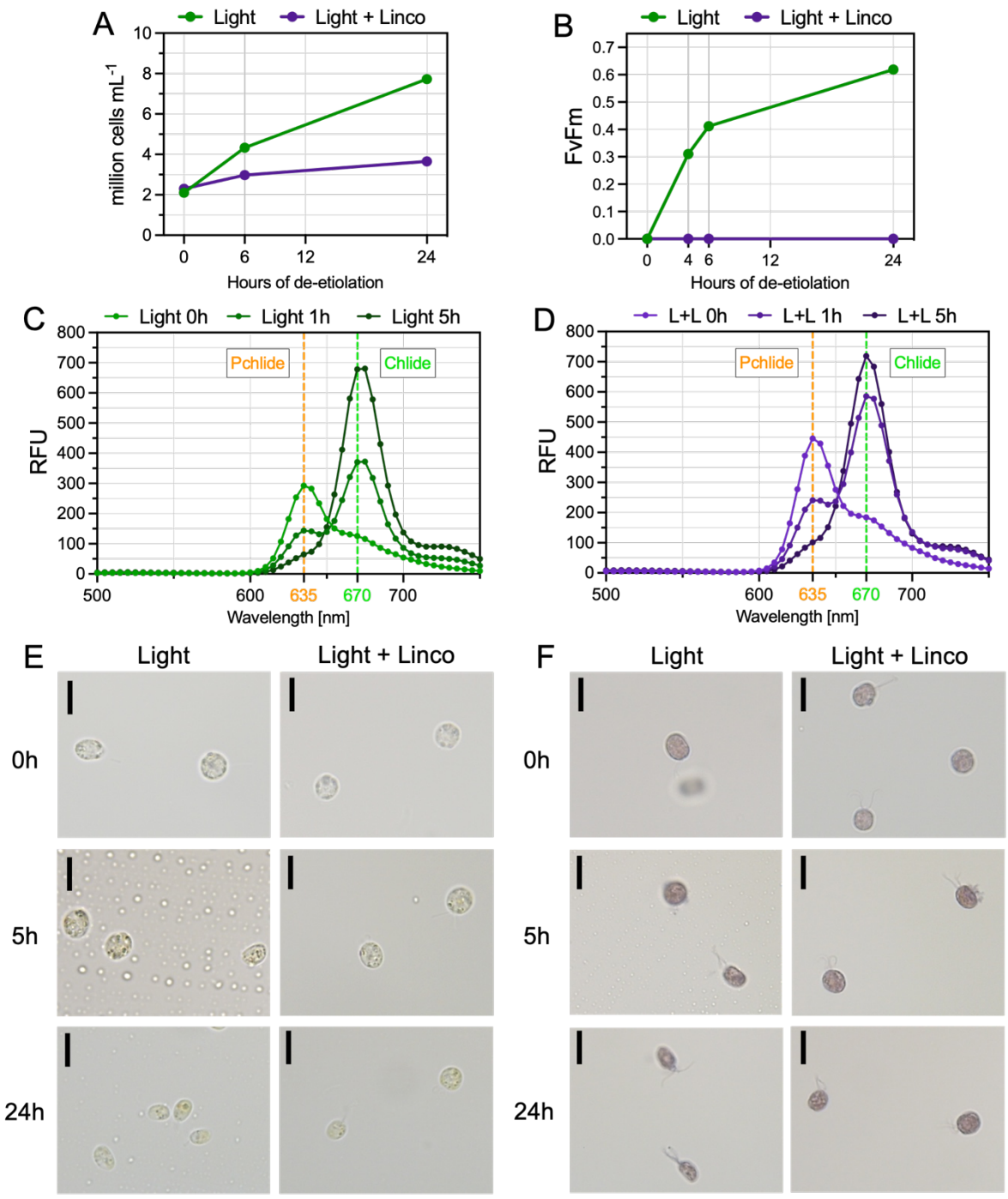


Figure 2.8: De-etiolation trial with pre-acclimation in the dark and lincomycin treatment in *y-4* cells. At the end of the fifth day during the preparation of the etiolated material half of the cultures were pre-treated with 0.5 mM of lincomycin (Linco) and grown overnight, and the following day all the cultures were also pre-acclimated with HSM for 3h before de-etiolation with this same medium. Growth, cell morphology and photosynthetic parameters were measured in de-etiolating *y-4* cells non-treated (Light) and treated with lincomycin (Light+Linco, L+Lin). Growth (A) and maximum quantum yield of PSII (B) of Light (green) and Light+Linco cultures (purple). Pchlide content was determined as before in Light (C) and Light+Linco (D) cultures. E,F: Light micrographs of Light (left) and Light+Linco (right) cultures, taken at the middle section in samples non-treated (E) or treated with Trypan Blue (F), to assess cell viability. Scale bars of all micrographs: 10 µm.

dye, no differences were found in the staining between Light and light + Linco cells. Moreover, the trypan blue staining allowed to show with better contrast in the micrographs the flagella, which are retained by Light and Light+Linco cells even after 24h. This is consistent with the presence of cell motility in the not stained cells for both conditions (not shown). Overall, these results prove that the

designed dark acclimation works very well in our conditions, as cells can healthily de-etiolate and in the same way as previous trials. Also lincomycin treatment is appropriate for our purposes, as it strongly affects photosynthetic capacity, but without compromising cell viability.

The RNA-seq de-etiolation experiment

The final de-etiolation experiment for transcriptomic analysis was designed to capture main light and RS events that occur during this process, and also to assess how RS is regulated in the dark, in different plastid states. Therefore our final setup (Figure 2.9) included: de-etiolating *y-4* cells (*y-4* Light) non-treated, and treated with lincomycin (*y-4* Light + Linco); etiolated *y-4* cells in the dark, prior to their transfer to light for de-etiolation, (*y-4* Dark) non-treated, and treated with lincomycin (*y-4* Dark + Linco); dark grown wild type CC-124 cells, grown the same way as *y-4* etiolated material (WT Dark) non-treated, and treated with lincomycin (WT Dark + Linco); *y-4* cells that were prepared in the same way as the *y-4* etiolated material but always keeping the cells in light conditions (*y-4* Always Light, AL from now on). Although CC-3269 was better wild type strain for this setup since it is *y-4* genetic background, it was impossible in our conditions to generate enough yield for transcriptomic analysis. Since both strains had a similar behavior during dark-to-light transition (Figure 2.5), and CC-124 cells could grow at the same rate as *y-4* etiolating cells, we finally chose CC-124 as wild type strain for our setup.

In the final de-etiolation experiment for transcriptomic analysis, *y-4* cells etiolated cells grew and fully recovered chloroplast functions as in previously executed trials. In particular, FvFm reached AL levels by 12h (Figure 2.10 B), and even higher FvFm levels were observed after 1 and 2 days. Although PSII maximum quantum yield of *y-4* de-etiolating cells was very close to AL levels during 6-12h, the PSII was not functioning at full efficiency (Figure 2.10 G,H): repeated saturating pulses of light with several increasing actinic lights, in fact, caused Y(II) values of *y-4* Light cells to fall at lower levels compared to AL, and without or with a lower Y(II) recovery when the actinic light was switched off; overall PSII efficiency was fully recovered only after 2 days of de-etiolation, with a higher capacity compared to AL. These results indicate that maximum photosynthetic capacity is mostly reached at 9-12h, but two days are required for the PSII to work at full efficiency, which likely depends on the assembly of the rest of the components of the electron transport chain (ETC). Unlike PSII activity, accumulation of total chlorophylls occurred slower (Figure 2.10 C), reaching half of the chlorophyll content of AL cells at 12h, and full content after 2 days. In terms of growth, *y-4* de-etiolating cultures duplicated in cell number after 1 and 2 days (Figure 2.10 A); cell division started at 12h of de-etiolation, and was not observed during the first 9h. Cells that were treated with lincomycin were considerably affected in all the above mentioned parameters, and in the same way as previous trials: lincomycin completely eliminated photosynthetic capacity (not shown), but still cells maintained the capacity to synthesize chlorophylls even after 2 days, although at lower lever compared to *y-4* Light samples (Figure 2.10 C); cell growth in *y-4* Light + Linco cultures was severely compromised, but cell number

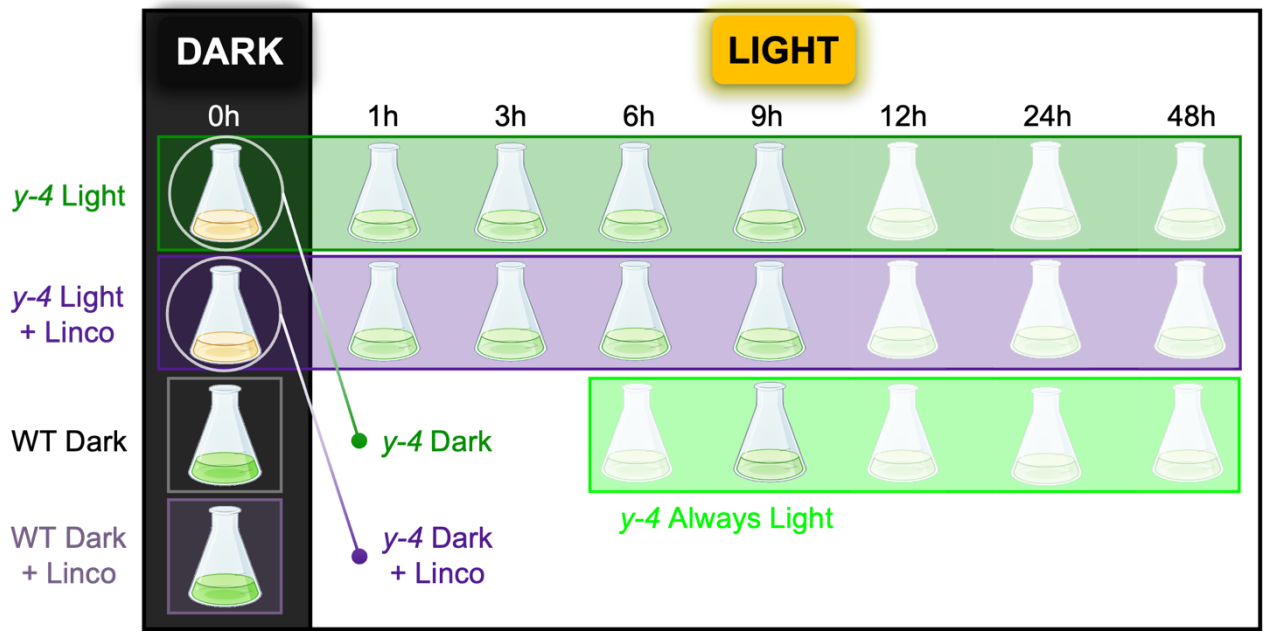


Figure 2.9: RNA-seq setup. Our final de-etiolation experimental setup for transcriptomic analysis included 5 different conditions: "*y-4* Light" consists of etiolated *y-4* cells that are transferred to light for de-etiolation, while "*y-4* Light + Linco" is the same de-etiolation experiment but with the addition of 0.5 mM lincomycin to stress the chloroplast and impair its biogenesis; "WT Dark" consists of CC-124 wild type cells grown in the dark as a control of a fully developed chloroplast in this condition, while "WT Dark + Linco" is the same experiment but with the addition of 0.5 mM lincomycin; "*y-4* Always Light" was prepared as *y-4* Light but always keeping the cells in light conditions during the preparation steps, and serve as a control of a fully developed *y-4* chloroplast that never encountered absence of light. Faded flasks correspond to samples that were not processed for RNA-seq. Biological triplicates for each condition were prepared.

was still increasing after 2 days (Figure 2.10 A). These results indicate that lincomycin affected chloroplast functionality but without compromising cell viability. Additionally, we tested the expression of *PSBR1*, as we previously verified it is induced by light (Figure 2.7). In did, a 3-fold induction of this gene was observed at 3h in *y-4* Light samples, as expected (Figure 2.10 D), but interestingly, AL levels of *PSBR1* were comparable to *y-4* Dark Cultures (Figure 2.10 F). In *y-4* Light + Linco cultures induction at 3h of *PSBR1* was repressed by lincomycin, but we also detected a 2-fold induction at 9h and a slight induction in the dark (Figure 2.10 E). WT Dark cells showed slightly higher expression of *PSBR1* compared to *y-4* Dark etiolated cells, and lincomycin increased levels of *PSBR1* in wild type samples, similarly to *y-4* (Figure 2.10 F).

Altogether, these results indicate that final de-etiolation experiment for transcriptomic analysis worked successfully and as expected from previous trials: *y-4* Light samples fully restored their chloroplast after 2 days of de-etiolation, while *y-4* Light + Linco samples were affected in chloroplast function but remained viable during 2 days. Once this experiment was finally completed, we started up our transcriptomic analysis. Not all the samples were used for RNA-seq: we decided to analyze first light and RS events during de-etiolation before cell division (9h), and use its related AL control (Figure 2.9). These samples were processed before transcriptome sequencing.

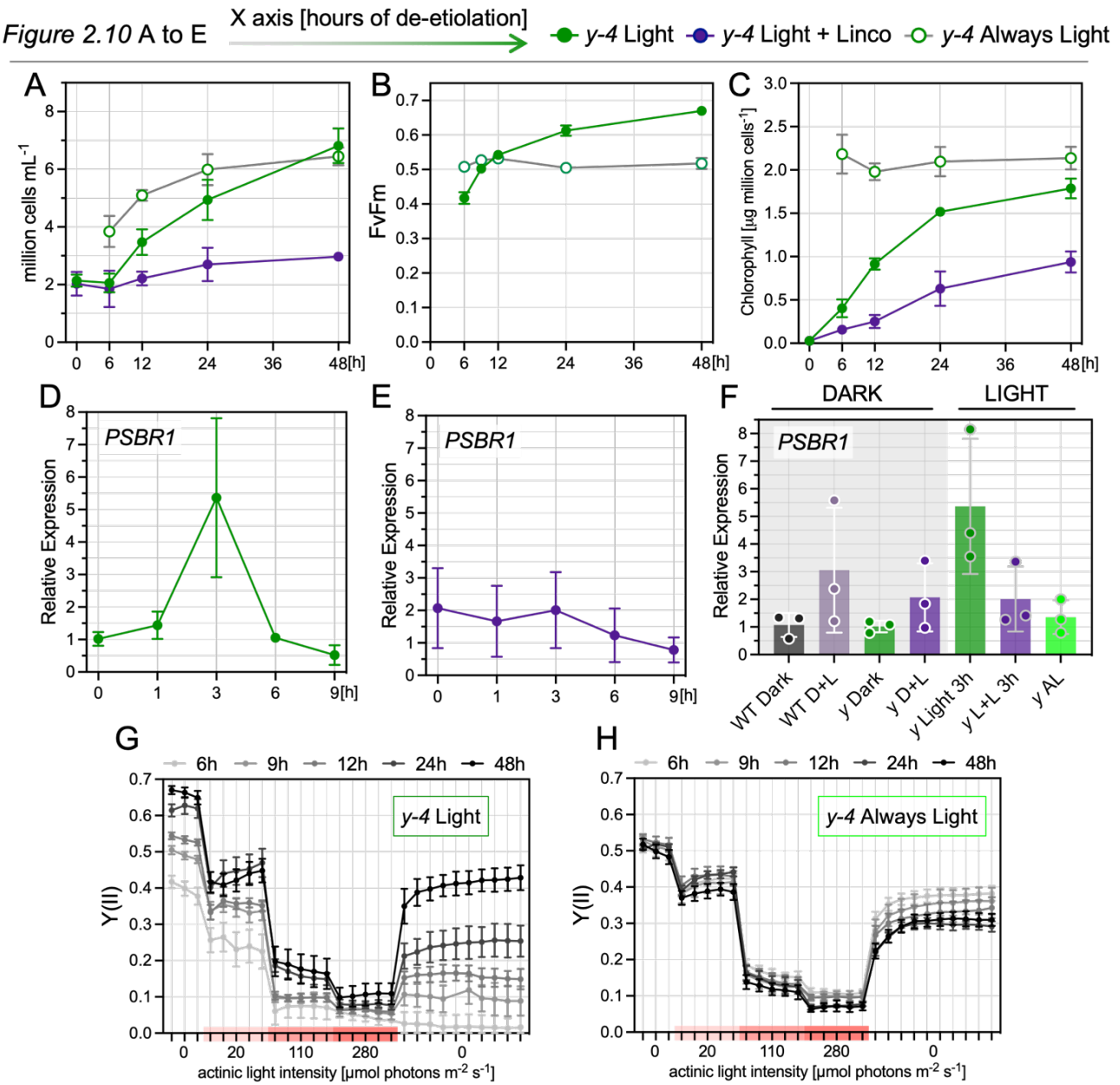


Figure 2.10: RNA-seq de-etiolation experiment based on Figure 2.9. In parallel to the obtention of RNA samples, growth (A), FvFm (B), and chlorophyll content (C) were monitored, in *y-4* Light (green), *y-4* Light+Linco (purple) and *y-4* Always Light (green, empty circles) samples. FvFm of *y-4* Light+linco was null as in previous trials (not shown in the plot). We checked also *PSBR1* expression in *y-4* Light (D), *y-4* Light + Linco (E) samples during the first 9 hours. A comparison of this data with WT samples and Always Light control at 9h is shown in F. We also assessed PSII activity by measuring its maximum quantum yield without and with increasing actinic light intensities in *y-4* Light (G) and *y-4* Always Light (H) samples.

Quality control of RNA-seq samples

In order to verify that all RNA samples taken during RNA-seq de-etiolation experiment featured the appropriate quality for sequencing, several quality control tests were performed. RNA samples were first quantified and checked for purity in a Nanodrop spectrophotometer. All RNA samples were very clean from contaminants as both A_{260}/A_{230} and A_{260}/A_{280} ratios were way above 2 (Figure 2.11 A,B). Interestingly, the yield of RNA increased with the time of de-etiolation and no matter the presence of

lincomycin, while in AL samples the yield of RNA was comparable to *y-4* samples at 1-3h (Figure 2.11 C). Wild type samples in the dark featured higher levels of RNA compared to *y-4* Dark samples. Quality of RNA samples was further assessed with two methods: a) electrophoresis and b) bioanalyzer. Agarose gel electrophoresis of RNA samples showed overall no degradation (Figure 2.11 E), and both 28S rRNA and 18S rRNA bands can be clearly distinguished in the gel, being 28S rRNA band more intense than 18S rRNA. Electrophoresis was performed for all RNA samples obtaining the same results (not shown). Bioanalyzer analysis, instead, was carried out only for 12 representative samples, chosen from all the points and conditions. All these samples featured an excellent RIN number above 8 (Figure 2.11 D), which was way higher than the RIN requested by the sequencing company (above 6). Taken together, these tests showed that RNA samples featured the required quality for RNA-seq and were employed for transcriptome sequencing.

Discussion

Why the election of the y mutant strain and the medium for de-etiolation can deeply mark the interpretation of transcriptomic data?

We achieved to setup a novel de-etiolation system based on Chlamydomonas *y* mutant cells. It is true that these mutants were already employed to study chloroplast biogenesis in the past century, where transition from an etioplast-like plastid to a fully developed chloroplast was characterized both at the cellular level with electron micrographs (Ohad et al. 1967), and biochemically (Kindle 1987; Malnoë et al., 1988; White & Hoober, 1994), but our setup was intended for transcriptomic analysis, and specifically to study gene regulation exerted by light and RS during de-etiolation. This had a fundamental impact in our design, as the election of the proper parameters in both etiolation and de-etiolation steps of our setup (Figure 2.2) would affect not only the way cells de-etiolate, but also how to interpret our transcriptomic results. In this sense, there were two key parameters that could deeply affect our transcriptomic analysis: the election of the *y* mutant strain and the medium for de-etiolation.

As explained in the introduction (Figure 1.12), many *y* mutants have been developed so far and were available for our setup: 3 *dpor* mutants (one for each DPOR subunit *chlL*, *chlN*, *chlB*), and 7 nuclear *loci* in which the mutation indirectly affects accumulation of DPOR. To our knowledge, the great majority of *y* mutant works were conducted in the nuclear *y-1* strain, or other *y* nuclear mutants to characterize chloroplast biogenesis during de-etiolation, both at the cellular and biochemical level (Gyurján et al., 1980; Malnoë et al., 1988; Ohad et al., 1967; White & Hoober, 1994). For our transcriptomic analysis, however, it was not convenient to select the *y-1* or other nuclear mutants since the origin of the mutation is unknown for all these mutants, with the risk of underestimating the influence of this mutation on gene regulation exerted by both signaling pathways during de-etiolation.

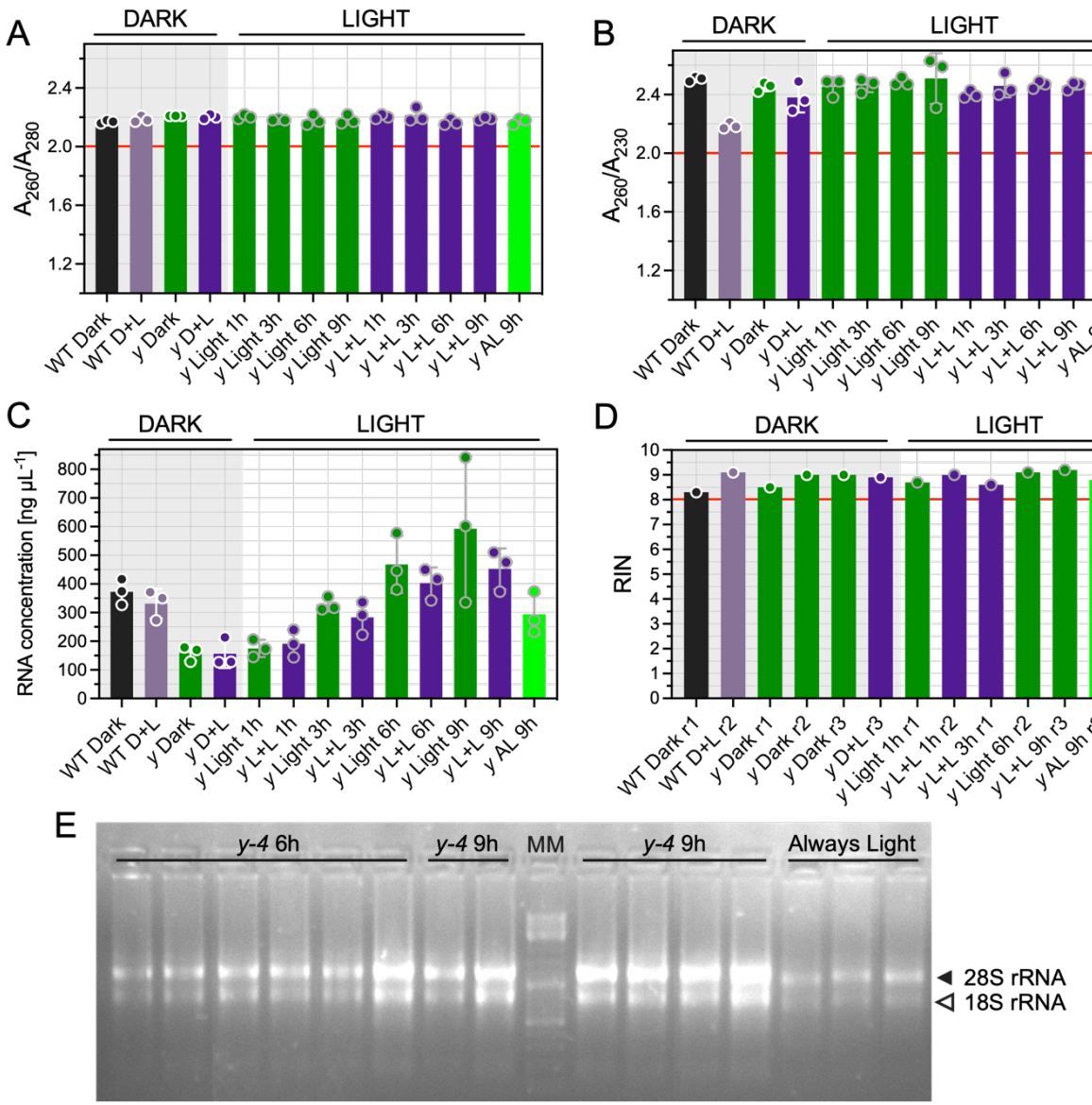


Figure 2.11: Figure 2.11: Quality check of RNA samples for transcriptomic analysis. The degree of purity of RNA samples was determined with A_{260}/A_{280} (A) and A_{260}/A_{230} (B) ratios and had to be higher than 2 (red line) for sequencing. C. RNA yield of samples used for transcriptomic analysis (approximately same number of cells were employed for RNA extractions). Values were obtained from Nanodrop spectrophotometer measurements in A,B,C. D. RNA integrity number (RIN) of a subset of RNA-seq samples, determined by bioanalyzer analysis. RNA integrity is considered excellent for RNA-seq if RIN is above 8 (red line). E. Agarose gel electrophoresis of RNA samples obtained from *y-4* de-etiolating cultures at 6h and 9h, and 9h Always Light cultures; 28S (filled triangle) and 18S (empty triangle) rRNA bands are indicated.

Therefore we initially thought to include a direct *dpor* mutant, and 3 of this type were available. Interestingly, one of the most recent works on *y* nuclear mutants showed that in all of them (except *y-7*) the impaired accumulation of DPOR in the dark is caused by lack of CHLL subunit (Cahoon & Timko, 2000). This means that *chlL* mutant (our *y-4*) is also a better representative of the nuclear *y* mutants, and this motivated the inclusion of this specific strain for our trials. We also included the *y-2* strain, which is a *y-1* mutant with a more stable mutation (Ford & Wang, 1982), in case *y-4* failed to de-etiolate and also as a physiological control for de-etiolation.

The election of the medium for de-etiolation could also affect our RNA-seq analysis. Unlike the preparation of the etiolated material in the dark which can only be done in heterotrophy, de-etiolation

can be set in both autotrophic and mixotrophic conditions. In angiosperm-based systems, most de-etiolation experiments conducted in seedlings were performed in the absence of sucrose (Burko et al., 2020; Pipitone et al., 2021), since the presence of a carbon source affects light signaling and plastid development (Eckstein et al., 2012; Häusler et al., 2014). In the case of Arabidopsis cell cultures, the use of an exogenous carbon source during de-etiolation cannot be overcome and represents an important limitation when interpreting transcriptomic data (Dubreuil et al., 2018). The same can be argued for Chlamydomonas, given that in all *y* mutant de-etiolation studies so far reported, TAP (an acetate supplemented medium) or HSA are used when etiolated cells are transferred to light (Malnoë et al., 1988; Ohad et al., 1967; Wang, 1978). Since the use of an acetate supplemented medium may likely have an effect on gene expression during chloroplast biogenesis, similarly to what shown in angiosperm plants, we tested the possibility to employ HSM minimal medium for de-etiolation in addition to HSA, and observed that this is a very viable medium for de-etiolation as no stress derived from nutrient starvation was detected on cell morphology or photosynthesis parameters.

The presence of an exogenous carbon source affects the kinetics of de-etiolation of y-4 cells

In this chapter we showed that etiolated *y-4* cells can fully restore the chloroplast upon exposure to light and in the absence of an exogenous carbon source. No net increase in OD_{730} was observed in both *y* mutant cultures de-etiolating in HSM after 1 day and even a slight decrease was observed during the first 9h compared to HSA, which might be an indicator of starvation and cell death. However this was not reflected in the actual cell number which progressively increased in *y-2* cultures and remained constant in *y-4* cultures with cell duplication after 1 day. Although light micrographs do not show differences in cell morphology between HSM and HSA, lack of correlation between ODs and cell number measurements can be explained by a decrease in size in cells transferred in minimal medium. The effects of HSM on the growth rate compared to acetate supplemented mediums were already described by Fischer et al., 2006: in addition to cell shrinking, growth rate is lower because it is limited by the uptake of inorganic carbon, which can be overcome by supplementing cultures with CO_2; the availability of acetate as energy source compensates this limitation, resulting in bigger cells and higher growth rates. In our experimental conditions, although depleted of acetate both *y-2* and *y-4* cells could restore a fully functional chloroplast upon transfer to light. So, where does the energy required for chloroplast biogenesis come from? It is likely that starch functions as a backup energy for de-etiolation, such as the cotyledon reserves of angiosperm plants that fuel chloroplast biogenesis when the seedling encounters light. First works on *y* mutants showed that these cells accumulate large amounts of starch in the dark, which is degraded upon transfer to light during chloroplast biogenesis (Ohad et al., 1967; Sager & Palade, 1954). Consistent with this observation, transmission electron micrographs of *y-4* cells taken by our collaborator (Dr. M. A. Ruiz-Sola, University of Sevilla)

also evidenced the formation of many starch granules in the dark, and the apparent absence of these when the chloroplast is fully assembled in light.

In our conditions, AL cells seemed a valid control to evaluate at which degree photosynthesis activity and chlorophyll content recovered during de-etiolation. This was observed for the chlorophyll content, where de-etiolating *y-4* cells progressively accumulated it until reaching AL levels by 48h. In contrast, FvFm values of AL maintained at significantly low levels of 0.5, which were already overcome by *y-4* cells at 12h of de-etiolation and reached 0.7 at 48h. It is likely that AL cells, during their growth in constant light and HSA (+ acetate) conditions for 6 days before de-etiolation, accumulated a high reductive power in the chloroplast stroma, which lead to a state transitions phenomenon. It has been described in fact that to compensate the excessive reductive power, antenna components of the PSII can be transferred to the PSI to reduce photon absorption as a photoprotective mechanism (Fleischmann et al., 1999). As a consequence, when measuring FvFm, AL cells had less reaction centers and showed FvFm levels below optimal. Therefore a better control for de-etiolation could be an AL control with cells always grown in HSM (- acetate) conditions.

Moreover, compared to previous *y* mutant works on chloroplast biogenesis which were carried out in acetate supplemented mediums, kinetics of *y-4* de-etiolation in our conditions occurred much slower: according to Ohad et al, 1967, *y-1* mutant cells fully restore the chloroplast in just 6-8 h, and recovery of photosynthetic activity is paralleled with the synthesis of chlorophylls and thylakoid formation. This also depends on the strain, in fact we also observed a faster de-etiolation in *y-2* cells, no matter the presence of acetate. Still in our conditions *y-2* cells needed 1 day to fully complete de-etiolation, as shown by chlorophyll accumulation. A faster de-etiolation can also be explained by the use of higher temperatures in the mentioned work (25ºC compared to our 23ºC), which speeds the overall kinetics of de-etiolation. In contrast to this work, expression of photosynthesis genes in our de-etiolation setup was consistent with biochemical evidence obtained from de-etiolating *y-1* cells in Malnoë et al., 1988: both antenna and core photosystem nuclear genes feature a peak of expression at 6h, similarly to the peak we observed at 3h for *LHCA7*, *PSBR1* and *PSAD1*, although we cannot discard these genes find their maximum expression later in our setup. In that work, accumulation of photosystem polypeptides both encoded in the nucleus and chloroplast was also evaluated, and interestingly most of them are highly and linearly accumulated during the first 24h upon transfer to light; this indicates that, although many chloroplast physiological parameters can reach their maximum in less than 12h, a fully mature chloroplast is achieved only after 1 day of de-etiolation.

De-etiolation of y-4 cells may undergo two distinct phases

De-etiolation process in angiosperm plants features several important differences compared to our system: 1) at the structural level etioplasts, unlike undifferentiated plastids of dark-grown *y* cells, feature PLB and PT; 2) angiosperm cells contain more than one chloroplast in light conditions, and therefore de-etiolation also includes, chloroplast proliferation. In a recent work from Pipitone et al.,

2021, major structural changes during de-etiolation of Arabidopsis seedlings were described. In particular, they defined two distinct phases of de-etiolation: 1) structure establishment phase, characterized by disassembly of PLB, gradual formation of thylakoids and acquisition of photosynthetic capacity, and 2) chloroplast proliferation phase, characterized by an increase in chloroplast number, in concomitance with cell expansion, grana formation and accumulation of photosynthesis-related polypeptides. We also observed in our de-etiolating *y-4* cells a similar two-step transition. In our setup and their de-etiolation system in fact, maximum photosynthetic capacity starts reaching the plateau at 12h of de-etiolation, when total chlorophylls are still accumulating linearly, and at 12h still the PSII is not functioning at its maximum efficiency. In addition, during the first 12h cells are overall bigger, while at 24h we observed smaller cells with double the amount, but photosynthesis and chlorophyll levels are much higher at 24h compared to 12h. This indicates that chloroplast does not increase in size but continues developing after 12h of de-etiolation, likely by an increase in the ETC components, or density of the thylakoid net. Here, we interpret two possible scenarios: 1) de-etiolation may be a long one-step process that is completed after 24h, but with different kinetics of recovery of the different physiological parameters; 2) de-etiolation may be a more than 1 step process, in this case if other biochemical or molecular parameters show a more than 1-peak profile during this 24h. Eventually, transcriptomic analysis will be useful to clarify this point.

Our setup allows to evaluate the separate contributions of light and retrograde signals to de-etiolation

Our final de-etiolation setup for transcriptomic analysis was designed to analyze light and RS that shape chloroplast biogenesis and likely other non-chloroplast related process in *y* mutants of Chlamydomonas. Although, we report many works that have performed a transcriptomic characterization of these two signaling pathways in de-etiolating Arabidopsis seedlings (Hernández-Verdeja et al., 2020; Martín et al., 2016), our system brings several innovations. First, this system has been optimized for Chlamydomonas, a very early-divergent microalgae species which lacks many key components of light and RS that regulate etiolation and de-etiolation in angiosperm plants, especially phys, PIFs, GLKs, and GUN1 which are essential in angiosperm plants. Therefore, the capacity of *y-4* cells to form an etioplast-like plastid in the dark and restore a fully functional chloroplast in light conditions is very intriguing, and raises many questions: 1) what advantage represented the emergence of key master regulators of light and RS in angiosperm plants and 2) what is the ancestral light and RS pathway that regulates de-etiolation, 3) which are the key components of them and 4) are they conserved in angiosperm plants and playing a fundamental role. Second, compared to angiosperm-based de-etiolation systems where plastid development is directly linked to light conditions, in our system we can also study the case of wt cells having a fully developed chloroplast in the dark. This allows us to evaluate the contribution of plastid state on light signaling during

de-etiolation, and also on RS in dark conditions. In particular, we can evaluate if stress impacts RS in an etioplast-like plastid or a fully developed chloroplast in Chlamydomonas. Third, our system features the advantages of a cell culture system (plastids synchronized in their development, uniform absorption of exogenous compounds such as lincomycin), but without the need for exogenous carbon source, an important drawback of Arabidopsis cell culture systems (Dubreuil et al., 2018); moreover, since Chlamydomonas cells feature a single chloroplast, it eases our analysis as we can discard both chloroplast proliferation effects inside cells, and their different contribution to RS.

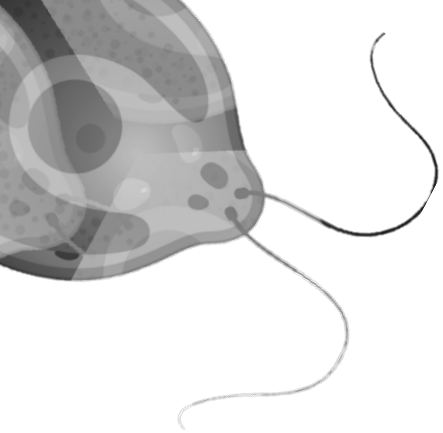
In conclusion, in this chapter we developed a Chlamydomonas de-etiolation system based on y-4 cells, where these developed an etioplast-like plastid in the dark and were able to fully restore the chloroplast in light. We also prepared an experimental design that allows us to capture main light and RS events during de-etiolation. This particular system overcomes many limitations of angiosperm-based systems, and allows us to answer fundamental questions related to both signaling pathways. In the next chapter, we will cover transcriptomic analysis of light signaling.

Transcriptome analysis: LIGHT SIGNALING

CHAPTER 3

Transcriptome analysis: light signaling

Introduction	*65-68*
Materials and Methods	*68-73*
Results	*73-107*
Discussion	*108-114*



3 Chapter

Introduction

When emerging seedlings from the ground first see light, they experience a profound change in their morphology, which enables them to switch from an heterotrophic form of life to a fully photosynthetic autotrophic organism. Transition from skotomorphogenesis (closed non-photosynthetic cotyledons, elongating hypocotyl) to photomorphogenesis (expanded and photosynthetically-active cotyledons, short hypocotyl) is called de-etiolation and is marked at the cellular level by the transformation of dark-adapted etioplasts into fully developed chloroplasts (Arsovski et al., 2012).

At the molecular level light triggers changes in the expression of a third of the transcriptome during de-etiolation, that are specifically required for chloroplast biogenesis (i.e. photosynthesis, tetrapyrrole biosynthesis), or related to plant development or other functions (i.e. ethylene and brassinosteroid biosynthesis, cytoplasmic translation) (Ma et al., 2001). This is achieved through light-mediated activation of soluble cytoplasmic photoreceptors, mainly phytochromes (phy) and cryptochromes (cry), which perceive red and blue light, respectively, and in turn migrate to the nucleus and interact with negative regulators of photomorphogenesis to suppress their activity. Negative regulators include the COP1-SPA ubiquitin ligase complex and the PIF family of transcription factors, which accumulate in the dark to repress positive regulators of photomorphogenesis at both transcriptional (PIFs) and protein level (COP1-SPA) (Xu, 2019). PIFs also negatively regulate the expression of thousands of genes in the dark to prevent photomorphogenesis (Leivar et al., 2009). Positive regulators include several transcription factors, mainly HY5, and GLKs: the first is a central regulator of light signaling, as it has been implicated in many different photomorphogenic responses (chlorophyll and anthocyanin synthesis, lateral root development, hypocotyl elongation arrest) and directly or indirectly regulates the expression of thousands of genes (Lee et al., 2007; Gangappa & Botto, 2014), while GLKs are more specifically involved in chloroplast biogenesis, and regulate the expression of a subset of genes involved in photosynthesis and chlorophyll biosynthesis (Waters et al., 2009). The activity of HY5 is tightly and antagonistically coordinated with PIFs, and these can coexist forming regulatory modules to fine-tune photomorphogenic response (Toledo-Ortiz et al., 2014). HY5 activity is also

modulated by the B-BOX family of transcription factors that feature opposite roles: some members are promoters of photomorphogenesis (i.e. BBX4) and others are suppressors photomorphogenesis (i.e. BBX25) (Gangappa & Botto, 2014). It is important to remark that all of the above mentioned components of the light signaling pathway are essential for proper de-etiolation response: the absence of *pif1345* (*pifq*), *cop1* and *spa1234* mutants feature constitutive photomorphogenic phenotypes in the dark (cop) (Deng & Quail, 1992; Laubinger et al., 2004; Leivar et al., 2008), *hy5* mutants feature elongated hypocotyls in light (Oyama et al., 1997), *glk12* mutants feature defects in greening and reduction of granal thylakoids (Fitter et al., 2002), and *phyA-B* and *cry1* mutant seedlings feature elongated hypocotyls with closed and unexpanded cotyledons (Mazzella & Casal, 2001).

Light signaling has been traditionally explored in angiosperm plants, as these are the only plants that have the ability to etiolate in the dark forming etioplasts, mainly because they are unable to synthesize chlorophylls in the dark. This capacity is instead present in non-angiosperm plants that feature fully developed chloroplasts even after prolonged periods in the absence of light (Reinbothe et al., 2010). Interestingly, many light signaling components that regulate de-etiolation in angiosperm plants are highly conserved among the different green lineages (Han et al., 2019). For instance, phy-PIF module has been identified in the moss *Physcomitrella patens*, and can complement Arabidopsis *pifq* mutant (Possart et al., 2017); also *GLK* homologs have been found both in *P. patens* and in the liverwort *Marchantia polymorpha* with a role in greening and thylakoid biogenesis (Yasumura et al., 2005; Yelina et al., 2023). Sometimes, study of light signaling in non-angiosperm species allowed discovery of novel transcription factors involved in de-etiolation: recently, MYB-related transcription factors have been identified in *M. polymorpha* and have been shown to regulate chloroplast biogenesis synergistically with GLKs, both in this species and in Arabidopsis (Frangedakis et al., 2023). Some components like COP1, SPA and HY5 have emerged even earlier in the evolution with chlorophytes, as gene homologs have been identified in the green microalgae *Chlamydomonas reinhardtii*, but these play a different function in this species, related with photoprotection response (Han et al., 2019). Therefore, light signaling components have an ancient origin that coincides either with the origin of photosynthetic eukaryotes or land adaptation, and their function is conserved in many cases; however, given that non-angiosperm species do not canonically etiolate (meaning generating etioplasts in the dark with no photosynthetic activity), the specific involvement of these light signaling components in regulating de-etiolation should have evolved later, with the emergence of first angiosperm plants (Armarego-Marriott et al., 2020).

But surprisingly *yellow-in-the-dark* (*y*) mutants of Chlamydomonas, unable to synthesize chlorophylls in the dark, can etiolate in this condition developing a dark-adapted plastid with no photosynthetic activity and restore a fully photosynthetic chloroplast upon transfer to light (Ohad et al., 1967; Sager & Palade, 1954). Not much is known about light regulation of this de-etiolation response, but in the past century it has been shown that these mutants induce very little the expression of genes encoding for PSII components during this process, as these are already considerably expressed in the dark,

compared to Arabidopsis, but PSII proteins are progressively accumulated during de-etiolation, indicating post-transcriptional regulation in the synthesis of PSII polypeptides (Kindle et al., 1987; Malnoë et al., 1988). De-etiolation in these mutants is perfectly achieved, though they lack many essential components required for de-etiolation in angiosperm plants. Chlamydomonas in fact lacks the phy-PIF module, GLKs, and many B-BOX proteins, but retains many essential components, as homologs of COP1, SPA, HY5, and CONSTANS have been identified in this species, though they are thought to play a different role, related with light acclimation and photoprotection (Han et al., 2019).

Chlamydomonas plant COP1 (PCOP1) was identified through a forward genetic screen for high light tolerant mutants (Schierenbeck et al., 2015), and has been involved in mediating a UV-B light dependent signal transduction pathway which is triggered by the UVR8 photoreceptor, and causes induction of *LHCSR1* and *PSBS* genes involved in photoprotection (Tilbrook et al., 2016). High light acclimation is also triggered by phototropin (PHOT) blue light photoreceptor which triggers induction of *LHCSR3*, although it is not known if this is mediated by PCOP1 (Petroutsos et al., 2016). However, a suppressor screen of the *phot* mutant that restore the ability to acclimate in high light conditions allowed to identify the CUL4-DDB1^{DET1} E3 ligase complex in regulating this response, through the induction of *LHCSR1* and *LHCSR3A/3B* genes (Aihara et al., 2019). Later, it was shown that induction of *LHCRSs* genes is regulated by a CONSTANS homolog in Chlamydomonas (CRCO), and is dependent on UV-B light: in this condition, UVR8 was shown to interact both with PCOP1 and SPA and trigger their repression to favor accumulation of CRCO; since CUL4-DDB1^{DET1} enhance COP1-SPA ubiquitination activity in land plants, it was proposed that this might also be the case in Chlamydomonas, and use this mechanism to transduce both UV-B and blue light signals during light acclimation (Tokutsu et al., 2019). Furthermore, there are evidences showing that a HY5 homolog in Chlamydomonas (CRHY5) is required for light-dependent induction of photoprotection genes in Chlamydomonas, and that this mechanism is negatively regulated by PCOP1 (Lämmermann et al., 2020).

Both phytochromes and cryptochromes are essential components of light signaling required for de-etiolation in angiosperm plants. Algal genomes do not feature phytochrome genes, but Chlamydomonas retained the capacity to synthesize phytochrome chromophores (phycocyanobilin) which are postulated to mediate chloroplast-to-nucleus retrograde signals necessary for detoxification of reactive oxygen species (ROS), during light acclimation (Wittkopp et al., 2017) (See next chapter). Instead, four cryptochromes are present in Chlamydomonas: a plant type cry (pCRY), an animal type CRY (aCRY) and two DASH type cry (DCRY): pCRY is the Chlamydomonas homolog of CRY1-2 in Arabidopsis, and its role in Chlamydomonas has been associated with the entrainment of the circadian clock and the regulation of life cycle (Kottke et al., 2017); aCRY is a special type not present in higher plants, and interestingly is capable of responding to red, blue and yellow light, influencing transcription of genes involved in different biological processes, such as carotenoid and chlorophyll biosynthesis, photosystem complexes and the entrainment of the circadian clock (Beel et al., 2012);

DCRYs role have remained a mystery until recently, when it has been shown that DCRY1 is present in the chloroplast, where it is thought to balance the photosynthetic machinery architecture: *dcry1* mutants in fact over accumulate chlorophylls, carotenoids and PSII subunits, and also feature hyperstacking of thylakoid membranes (Rredhi et al., 2021). However, no link has been found so far between any of these crys and PCOP1-mediated light signaling pathway involved in photoprotection. It is important to remark that the function of these conserved Chlamydomonas light signaling components has been explored in strains that feature a fully developed chloroplast in the dark, and therefore their involvement in regulating de-etiolation in *y* mutant strains needs to be tested; alternatively, novel TFs that still need to be discovered are regulating this process and could be performing this function in angiosperm species.

In the previous chapter we developed a Chlamydomonas *y* mutant based de-etiolation system that features perfectly etiolated cells with no photosynthetic activity in the dark and that progressively restore chloroplast activity upon exposure to light. We designed this system in a way that allows us to capture main light regulated events during de-etiolation, and in this chapter by means of a transcriptomic analysis of light signaling we aim to 1) determine main light-regulated events in this process and determine if this regulation is conserved compared to angiosperm species, 2) evaluate the evolutionary advantage that represented the emergence of light signaling components not present in Chlamydomonas, and 3) test if known light signaling components in Chlamydomonas also specifically regulate de-etiolation in these mutants and/or predict novel transcription factors involved in de-etiolation, by means of gene co-expression networks (GCN).

Materials and Methods

RNA-seq raw data processing

Paired-end 150 bp libraries from biological triplicates of all the conditions analyzed (See Fig. 2.9) were built and sequenced by Novogene (Beijing, China) on the Illumina NovaSeq platform. We obtained between 13-17 total million reads per sample. Adaptors, low quality and/or excessively short reads were eliminated using Trim Galore (Krueger, 2015): when discarding a read, its paired read was discarded too. In addition, raw reads were filtered from rRNA contamination using SortMeRNA (Kopylova et al., 2012). Clean reads were quasi-mapped against the transcriptome of the Chlamydomonas V6 genome (Craig et al., 2023), and quantified using Salmon (Patro et al., 2017). Raw counts were normalized using DESeq2 (Love et al., 2014) with two methods: median of ratios (hereafter called normalized counts) and transcripts per kilobase million (TPM).

In addition, raw RNA-seq data of dark-to-light transition experiments in both Chlamydomonas cultures grown under 12:12 photoperiod (Strenkert et al., 2019, wt12 Light), and de-etiolating Arabidopsis seedlings (Burko et al., 2020, At Light) were processed following the above mentioned procedure,

except Arabidopsis clean reads were quasi-mapped against the transcriptome of TAIR10 genome: biological triplicate samples at 0,1,3,5 and 9h were analyzed from the first experiment, while biological duplicates from cotyledon samples at 0,1,3,6 and 12h were analyzed from the second.

RNA-seq data analysis

Definition of light responsive genes (LRGs)

For this part, we employed *y-4* Light samples at 0,1,3,6 and 9h (Fig. 2.9). We first determined if the expression of genes significantly changed during the time course by performing DESeq2 likelihood ratio test of one factor (LRT1f). Next, we determined differentially expressed genes (*DEGs*) by performing DESeq2 pairwise comparisons of each time point in light towards dark. In these tests, p-values were adjusted (pAdj) with the Benjamini-Hochberg method. Light responsive genes (*LRGs*) were defined as giving pAdj < 0.05 in the LRT1f and $|\log_2$ fold change$| > 1$ in at least one time point in light. Same criteria were employed to determine *LRGs* in At Light and wt12 Light.

Mfuzz clustering and GO analysis

LRGs obtained from each RNA-seq were grouped into 5 different clusters with similar expression profile using Mfuzz (Kumar & Futschik, 2007). Gene ontology (GO) analysis for biological process was carried out for each cluster, using STRING database (Szklarczyk et al., 2017): to perform this analysis in Chlamydomonas, we created a new database with the proteome data and GO annotations from V6 of the Chlamydomonas genome; for Arabidopsis we employed the already available database. Resulting lists were filtered for redundant and/or obsolete GO terms using Revigo (Supek et al., 2011). To avoid any bias in the selection of the GO terms, we adopted the following criterium for each RNA-seq: we showed the top 20% of GO terms in each list (minimum 5 and maximum 15) with lowest FDR and with at least 3-fold enrichment.

Biased analysis of biological processes

Genes belonging to the most significantly enriched biological processes from GO analysis were manually selected using information from the literature and annotations. These genes were classified into biological process and subprocess (i.e. Photosynthesis, Photosystem II). For each one of these categories the most typical gene expression pattern was determined by calculating the mean Z-score of the $\log_{10}$ TPM values, using the specific mean and standard deviation of each biological process. This was determined if the great majority of genes had similar and consistent $\log_2$FC across the time course, while genes with different expression profile were discarded.

Analysis of chloroplast-associated nuclear genes

Chloroplast-associated nuclear genes (*CpANGs*) were determined using annotations from PB-Chlamy (Wang et al., 2023). Statistical analysis of $\log_2$FC distributions of light-induced and light-repressed between *CpANGs* (Cp) and *non-CpANGs* (Non-Cp) was carried out with unpaired t test analysis. To perform transcriptome analysis of chloroplast biogenesis, main chloroplast biological

processes as well as the majority of genes featured in each one were manually selected using information from literature and annotations. Similarly to the biased analysis, most typical expression profile for each chloroplast biological process was determined by calculating the mean Z-score of the log_{10} TPM values, but using the mean and standard deviation of the full transcriptome. These Z-scores were also employed to determine expression profiles of representative genes for each chloroplast biological process. Highly expressed (HE) and very highly expressed genes (VHE) were determined as the top 5% and 1%, respectively, with the highest TPM levels across the time course.

Transcription factor analysis

In this analysis, we employed the transcription factor (TF) lists from Arend et al., 2023 and AGRIS (Davuluri et al., 2003), for Chlamydomonas and Arabidopsis, respectively. Light responsive transcription factors (*LRTFs*) were determined using the same criteria as for *LRGs*. Hierarchical clustering of standardized TF expression profiles was performed by one minus pearson correlation and average linkage method using Morpheus (https://software.broadinstitute.org/morpheus/).

Analysis of always light cultures

We performed DESeq2 pairwise comparisons of *y-4* always light (*y-4* AL) samples towards *y-4* Dark (*y-4* D0) and *y-4* Light 9h (*y-4* L9). P-values were adjusted with the Benjamini-Hochberg method. *DEGs* in these comparisons were defined as giving $|log_2FC| > 1$ and $pAdj < 0.05$. Statistical analysis of distributions of normalized counts between *y-4* AL and *y-4* D0 or *y-4* L9, for Cp and Non-Cp were performed with Wilcoxon test of matched pairs. For Non-Cp this analysis was performed with a random subset of the same size of Cp.

Analysis of PIF- and GLK- regulated genes

The lists of PIF- and GLK- regulated genes in Arabidopsis were retrieved from Pfeiffer et al., 2014 and Tu et al., 2022, respectively. Chlamydomonas gene homologs of PIF- and GLK- regulated genes were determined through BLASTP, according to Craig et al., 2023. Statistical analysis of distributions of absolute maximum log_2FC between *y-4* Light and At Light were performed with a Wilcoxon test of matched pairs, while differences in distributions of chloroplast (Cp) and non-choroplast (NCp), PIF- or GLK- regulated and light induced genes, between Arabidopsis and Chlamydomonas were tested by means of an ordinary one way ANOVA and Tukey's multiple comparison test. In addition, a control using a random set with same sizes of non-PIF- or non-GLK- regulated genes that fulfilled the rest of the above criteria was prepared and statistically analyzed alike.

Dark adaptation of Arabidopsis seedlings

Plant material and growth conditions

Col-0 seeds were surface sterilized with 70% ethanol and 0.01% Triton X-100 for 12 min, followed by two washes with 100% ethanol. Once dry, seeds were plated on half-strength Murashige and Skoog (0.5X MS) medium without sucrose, stratified in dark at 4ºC for 3 days, incubated in white LED light

at 100 µmol m^{-2} s^{-1} and 21ºC for 3h, and then transferred to the specific conditions required for each experiment. For de-etiolation, seeds were germinated in the dark at 21ºC and seedlings were grown for 2 days in these conditions; next, dark-grown seedlings were incubated in white light at 100 µmol m^{-2} s^{-1} during 1 day. For dark adaptation, seeds were germinated in white LED light at 100 µmol m^{-2} s^{-1} and 21ºC: seedlings were grown for 3 days in these conditions, and then transferred to dark for 1 day.

Photosynthesis and pigments

Photosynthesis measurements were carried out on the cotyledons of approximately 30 seedlings, that were transferred to dark for 30 min before measurements. Chlorophyll fluorescence measurements (Fv/Fm and ΦPSII) were carried out as previously described, except ΦPSII was determined with the default light curve program of the ImagingWin Software.

In order to perform pigment measurements, whole seedling samples were collected before (0h) and at different time points during de-etiolation (1,3,6 and 24h), and ground to powder under frozen conditions. Pigment extraction was performed for each sample as follows: 20 mg of seedlings were combined with 0.5 mL of cold methanol, and this mixture was vortexed, centrifuged at max speed and the supernatant was collected in a separate tube; this procedure was repeated with the same pellet to obtain a combined 1 mL pigment extract. This was transferred into single use plastic cuvettes and absorbance was measured with the same device and settings as described in Chapter 2, but additionally measuring absorbance at 470 nm. Carotenoids as well as total chlorophyll content was determined using the equations from Lichtenhaler & Buschmann, 2001.

RT-qPCR

Whole seedling samples were taken before (0h) and during de-etiolation (1,3,6 and 24h), or dark adaptation at 6h, and ground to powder, as with pigment extraction. RNA extraction and quantification, cDNA synthesis and RT-qPCR were performed following the same procedure described in Chapter 2, but using *PP2A* as control gene (Shin et al., 2013) and 4 different Arabidopsis target genes (*PSB27*, *PSBQ-2*, *PETC*, *LHCB5*), whose expression during de-etiolation or dark adaptation was related towards 0h. Primers are indicated in Table 3.1.

Table 3.1: Primers used for RT-qPCR analysis of Arabidopsis dark adapting seedlings. *PP2A* was used as internal control for gene expression. At: Arabidopsis.

Gene	At ID	Primer Forward	Primer Reverse	References
PP2A	AT1G13320	TATCGGATGACGATTCTTCGT	GCTTGGTCGACTATCGGAATG	Shin et al., 2007
PSB27	AT1G03600	CAATGGCTTCAGCATCAGCG	GAGATACGGAGGAGGCGATG	-
PSBQ-2	AT4G05180	ACACCGTTATCTCCGCTAAGCC	TGATCTCGCCGCATAGTCCAAG	-
PETC	AT4G03280	TATGTGGAAGCAGAGGCTGG	GTGGAGGAGGATGACAAGTGG	-
LHCB5	AT4G10340	TTCAGGGCAGTTTCAAGA	GCTCATCGCTAGTCTCAG	-

Dark adaptation of Chlamydomonas cells

Both wt CC-124 and *y-4* strains were employed for this experiment. Colonies of these strains were inoculated in HSA medium and grown for 5 days at 23ºC under white LED light at 50 µmol m^{-2} s^{-1}. The following day, the medium of all cultures was fully replaced with fresh HSM, the concentration set at 2 million cells mL^{-1}, and cultures were incubated for 3h under white light. Once acclimated, half of the cultures were left in these conditions as a control, and the other half was transferred to dark at 23ºC for 1 day. Photosynthesis measurements as well as RT-qPCR were performed as described in Chapter 2, but for the latter different Chlamydomonas target genes were chosen (*PSB27*, *PSBQ1*, *PETC1*), whose expression during dark adaptation at 6h was related towards its light control at 6h. Primers are indicated in Table 3.2.

De-etiolation in blue and red light

Preparation of the *y-4* etiolated cultures for de-etiolation (including acclimations) was executed in the same conditions as in the RNA-seq experiment (See Chapter 2, De-etiolation setup), except de-etiolation was performed in different regimes of LED light: white, red and blue. The spectrum of all lights was previously determined with a PG200N Spectral PAR meter. White light intensity was set at 50 µmol m^{-2} s^{-1} (as in our RNA-seq experiment), while the intensities of the other lights were adjusted according to their spectrum to match white light, being 11 and 7 µmol m^{-2} s^{-1} of red and blue light, respectively. Light intensities were all adjusted using SpectraPen mini (PSI). Cell concentration, photosynthesis measurements, chlorophyll content and RT-qPCR were carried out as previously explained in Chapter 2, using the primers indicated in Table 3.3.

Gene co-expression networks

A global Chlamydomonas gene co-expression network (GCN) using all transcriptome datasets for this species found in the Sequence Read Archive (SRA) was generated by TOMS Bio lab (ChlamViz platform) and following the already published procedure (Orduña et al., 2023). This global GCN was employed to generate specific subnetworks for each phase of chloroplast biogenesis (See Fig. 3.7). These included all *CpANGs* employed for the expression profiles of the chloroplast biological

Table 3.2: Primers used for RT-qPCR analysis of Chlamydomonas dark adapting *y-4* and wt cells. *GBLP* was used as internal control for gene expression. *Cre*: Chlamydomonas.

Gene	*Cre* ID	Primer Forward	Primer Reverse	References
GBLP (*RACK1*)	Cre06.g278222_4532	CAAGTACACCATTGGCGAGC	CTTGCAGTTGGTCAGGTTCC	Petroutsos et al., 2016
PSB27	Cre05.g243800_4532	AGCTTCGGCAACACCTACTC	GTCGTCCAGCTCCTTTTGGA	-
PSBQ1	Cre08.g372450_4532	TCCTACTGGACTGAGGCTCG	TCAACGGCCTGGATGAACTC	-
PETC1	Cre11.g467689_4532	GGCTCTCAGTACAACGCTGA	AAGTCAGTCTCCGTCCAGGT	-

processes displayed in Fig. 3.7, and the 5 *LRTFs* which showed the highest degree with *CpANGs* (most interacting): these *LRTFs* were selected from early *LRTFs* (*LRTFs* at 1h) for the early phase, early and mid *LRTFs* (*LRTFs* at 3h, 6h) for the mid phase, and all *LRTFs* (including late, *LRTFs* at 9h) for the late phase. LRTFs from each group that interacted with these 5 most interacting were also included (linking nodes), if these in turn showed at list an interaction with *CpANGs*. For *CpANGs* orphan nodes we also included 1-2 most interacting LRTFs, if possible. All networks were generated using Cytoscape (Shannon et al., 2003).

Results

Light triggers 40% of the changes in the transcriptome of de-etiolating y-4 cells

In this chapter, we aimed to study main light-dependent transcriptomic events during de-etiolation. For this purpose, we analyzed the transcriptome of non-photosynthetic etiolated *y-4* cells in the dark, and of de-etiolating *y-4* cells which restore their chloroplast and gain photosynthetic competence upon exposure to light (Figure 3.1 A1, *y-4* Light). We included light samples up to 9h of de-etiolation, since at 12h cells started to divide, and analyzing this time point could lead us to underestimate chloroplast biogenesis effects in favor of mitotic effects. Also, by 9h of de-etiolation cells reached almost maximum photosynthetic capacity in the PSII, while, at 10h, expression of the photosystem genes we evaluated in the previous chapter (*LHCA7*, *PSBR1*, *PSAD1*) was already at dark levels after a peak of induction at 3h; this suggested us that main light regulated events involved in the establishment of the photosynthetic competence were already captured by 9h.

In order to validate our transcriptomic analysis of de-etiolation in Chlamydomonas, we compared our system to a canonical de-etiolation experiment with Arabidopsis seedlings from Burko et al., 2020 (Figure 3.1 A2, At Light), using data from dark-germinated etiolated seedlings and from de-etiolating seedlings upon light exposure (1-3-6-12h); in this study, since the authors separately sequenced and analyzed the transcriptome from cotyledons and hypocotyls, we decided to employ cotyledon data for our comparisons (as chloroplast biogenesis starts here in the early stages of development), although

Table 3.3: Primers used for RT-qPCR analysis of Chlamydomonas de-etiolating *y-4* cells in white, red and blue light. *GBLP* was used as internal control for gene expression. *Cre*: Chlamydomonas.

Gene	*Cre* ID	Primer Forward	Primer Reverse	References
GBLP (*RACK1*)	Cre06.g278222_4532	CAAGTACACCATTGGCGAGC	CTTGCAGTTGGTCAGGTTCC	Petroutsos et al., 2016
LHCSR1	Cre08.g365900_4532	GAGTCTGAGATCACCCACGG	CCGATCTGCTGGAAGTGGTA	Ruiz-Sola et al., 2023
LHCA6	Cre06.g278213_4532	CCTGTTTCCCGGGTTTTTGC	TTCCACTCTGTCCAACCACC	-
"GuCy"	Cre16.g688638_4532	CTGCAATCGACGAAAGCCTG	CAGTAGTCGGGCTCTGCAAC	-
POR1	Cre01.g015350_4532	GCCTACTGGTCGTGGTCTTC	GCAGAGATGTCCCACAGCTT	-

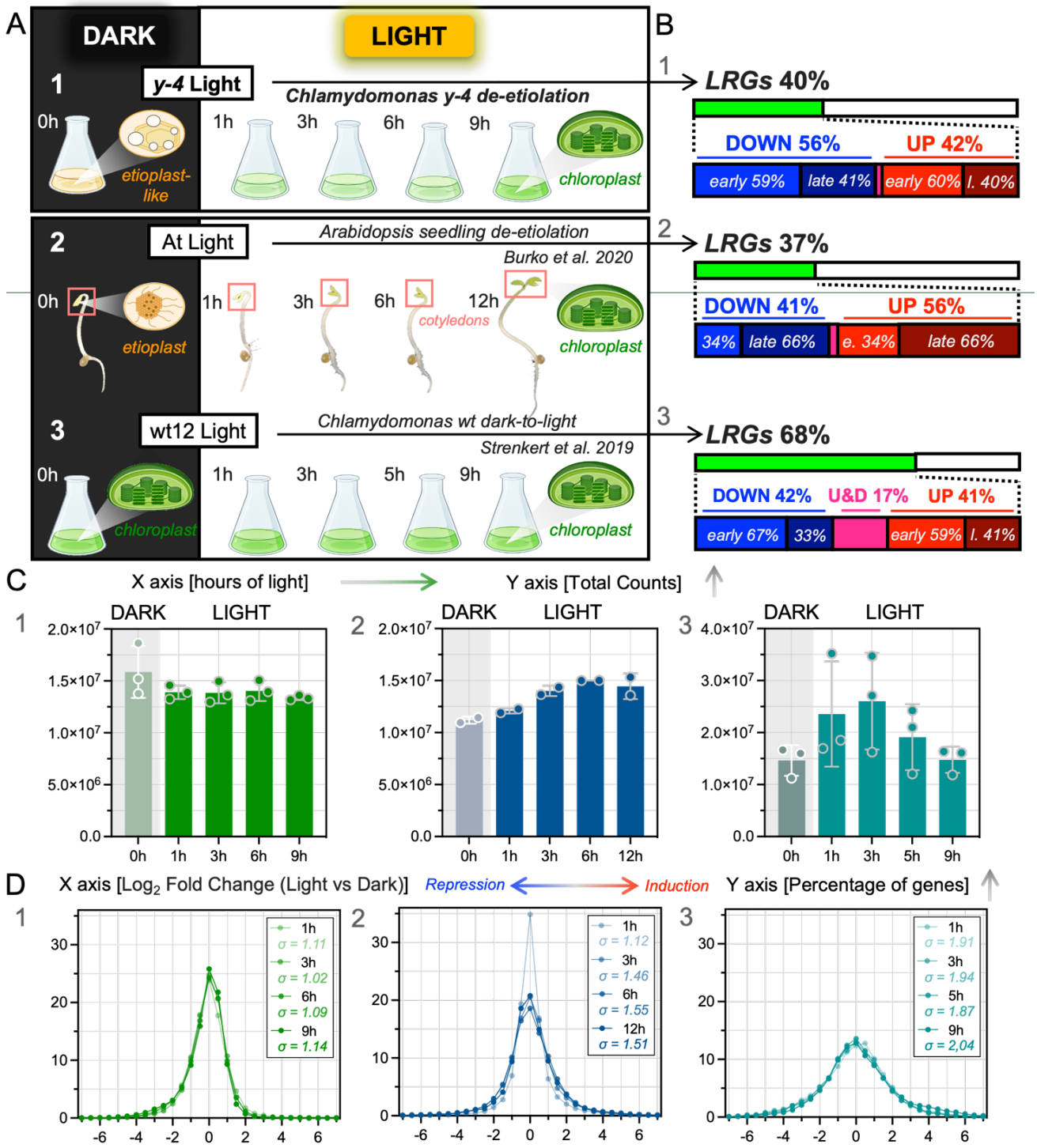


Figure 3.1: A. Schematic representation of samples from our de-etiolation experiment employed for light signaling data analysis in this chapter (*y-4* Light) (1), and two additional RNA-seq experiments used for comparison: (2) de-etiolation performed with Arabidopsis seedlings, from which we employed cotyledon data (At Light) (Burko et al., 2020), and (3) dark-to-light transition of wt cells from Chlamydomonas grown in 12:12 photoperiod (wt12 Light) (Strenkert et al., 2019). B. Summary of light-responsive genes (*LRGs* (green): $|\log_2 fold| \geq 1$ in at least one time point in light towards dark 0h, p-value<0.05) for each experiment, classified in induced ($\log_2 fold > 1$, red), repressed ($\log_2 fold \leq -1$, blue) or both ($\log_2 fold > 1$ & < -1, magenta), and in early ($|\log_2 fold| \geq 1$ at 1h, light color) and late ($|\log_2 fold| \leq 1$ at 1h, & ≥ 1 at 3, 6 or 9h, dark color). C. Total normalized counts of all samples for each RNA-seq experiment. D. Distribution of differential expression (DE) values (in $\log_2$ fold changes) for each time point in light, in each experiment.

data from whole seedling would have been more desirable to study full de-etiolation events. In addition, we compared our de-etiolation system to dark-to-light transition of wt Chlamydomonas cells

grown in diurnal 12:12 (dark/light) conditions from Strenkert et al., 2019 (Figure 3.2 A3, wt12 Light). This comparison serves to both validate the effect of light on the Chlamydomonas transcriptome, but also to evaluate the influence of the plastid state, given that wt cells already feature a fully developed chloroplast in the dark.

In order to make comparisons between transcriptomes more robust, raw data from Strenkert et al., 2019 and Burko et al., 2020 were processed and re-analyzed together with ours using the same criteria to determine light responsive genes (*LRGs*). These were defined as the differentially expressed genes (*DEGs*) giving an absolute log_2 fold change (log_2FC) higher than 1 in at least one time point in light towards dark, and with a pAdj lower than 0.05 using DESeq2 likelihood ratio test of 1 factor. Using these criteria we found that 40% of the transcriptome of our RNA-seq responds to light (Figure 3.1 B1), being the majority downregulated (56%) and 42% upregulated. We also defined as early *LRGs* the ones that reached our criteria at 1h, and late if this occurred starting from 3h. With this definition we observed than more than half *LRGs* are early, in both up- and downregulated subsets. A similar proportion of *LRGs* was found in At Light (37%, Figure 3.1 B2) with our criteria. However, in contrast to *y-4* Light, we observed more up- than downregulated genes (56% up compared to 41% down), and more late *LRGs* than early in both up- and downregulated subsets. In contrast to these de-etiolation systems, the great majority of the transcriptome from wt12 Light is made of *LRGs* (68%) with equal proportions of up- (42%) and downregulated (41%) and a higher proportion of up- & downregulated (17%). Similarly to *y-4* Light, most *LRGs* are early in both up- & downregulated subsets. Overall, similarity in the percentage of *LRGs* between *y-4* Light and At Light both gives strength to our de-etiolation system and eases comparative analysis with Arabidopsis, but the higher proportion of late *LRGs* compared to early in At Light, might be an indication that here light-dependent events are delayed compared to Chlamydomonas. The big proportion of *LRGs* in wt12 Light with our criteria is surprising, considering that these cells already feature a fully developed chloroplast in the dark, and could be explained by the oscillating expression of most of these genes caused by the circadian clock.

We also analyzed total transcript levels at each time point during de-etiolation, here expressed as the sum of the DESeq2 normalized counts of all genes in each sample (Figure 3.1 C). In contrast to the two systems used for comparison, etiolated *y-4* cells in the dark accumulate a higher amount of transcripts compared to light, where the levels are constant (Figure 3.1 C1). This makes more likely and explains why we find more downregulated genes during de-etiolation in *y-4* Light. On the contrary, in At Light the transcript levels are lower in the dark and progressively increase during de-etiolation (Figure 3.1 C2), which also explains why we observed more upregulated and more late genes in this system. In contrast to *y-4* Light, wt12 Light features very low transcript levels in the dark, and these progressively increase during light with a peak at 3h (Figure 3.1 C3), which also indicates a rhythmic pattern in transcript abundance.

Finally, we looked at the distributions of differential expression (DE) values (Figure 3.1 D) in the three systems: in both Chlamydomonas systems, these are constant in light, although towards higher values in wt12 compared to *y-4* Light (Figure 3.1 D1,D3); in Arabidopsis, instead, later time points correlate with higher DE values (Figure 3.1 D2). Overall, this indicates that the degree of regulation exerted by light increases during de-etiolation in Arabidopsis, while in Chlamydomonas this remains stable and independent of the starting plastid state in the dark.

Light regulates same biological processes in Chlamydomonas and Arabidopsis

In order to evaluate how and which biological processes are regulated by light in every system, first we grouped *LRGs* into different gene expression clusters using Mfuzz (Kumar & Futschik, 2007) identifying for each system the 5 most typical patterns. Afterwards, GO analysis for biological process was carried out for each cluster using STRING app (Szklarczyk et al., 2021), aiming to 1) identify the most significantly enriched GO terms for each system, 2) determine which of these are shared between systems, and 3) see if this occurs in clusters with same or similar expression profile. For easiness of representation, here we only show gene clusters which feature shared significantly enriched GO terms between systems. Also, to avoid any bias in the selection of the GO terms here displayed, we adopted a common criteria for GO term representation: first, significantly enriched GO terms (FDR<0.05) were filtered for redundant and obsolete GO terms using Revigo (Supek et al. 2011); next for each cluster we represented the top 20% GO terms (at least 5 and at most 15) with the lowest FDR and fold enrichment (FE) higher than 3, which allowed us to exclude general and less informative categories that contain a high number of genes.

In *y-4* Light, we identified 3 out of 5 clusters with significantly enriched GO terms (Figure 3.2). We found that light induces a high transcriptional and translational activity in the first hours of light (Figure 3.2 A, Early light induced), while repressing cell motility and synthesis of flagella (Figure 3.2 B, Early light repressed). Chloroplast-related biological processes instead, here biosynthesis of tetrapyrroles pigments and photosynthesis-associated genes, are as expected upregulated by light but later during de-etiolation with a 6h peak (Figure 3.2 C, Late light induced). This result agrees with the lag in the recovery of the FvFm during the first 2h of light of de-etiolating *y-4* cells. In At Light we mainly identified three clusters of light induced genes with significantly enriched GO terms (Figure 3.3). More importantly, we found that light upregulates same biological processes compared to *y-4* Light (highlighted in bold), but these are delayed in Arabidopsis: light-dependent induction of transcriptional and translational activity is in fact observed at 6h (Figure 3.3 B), while photosynthesis is slightly more enriched at 12h (Figure 3.3 C), although some photosynthesis genes also feature a 6h peak; in addition, we observed other chloroplast-related processes upregulated at 12h such as photorespiration and starch metabolism. As light events are delayed in Arabidopsis, we defined cluster B and C of Figure 3.3 as Early light induced and Late light induced, respectively. We also

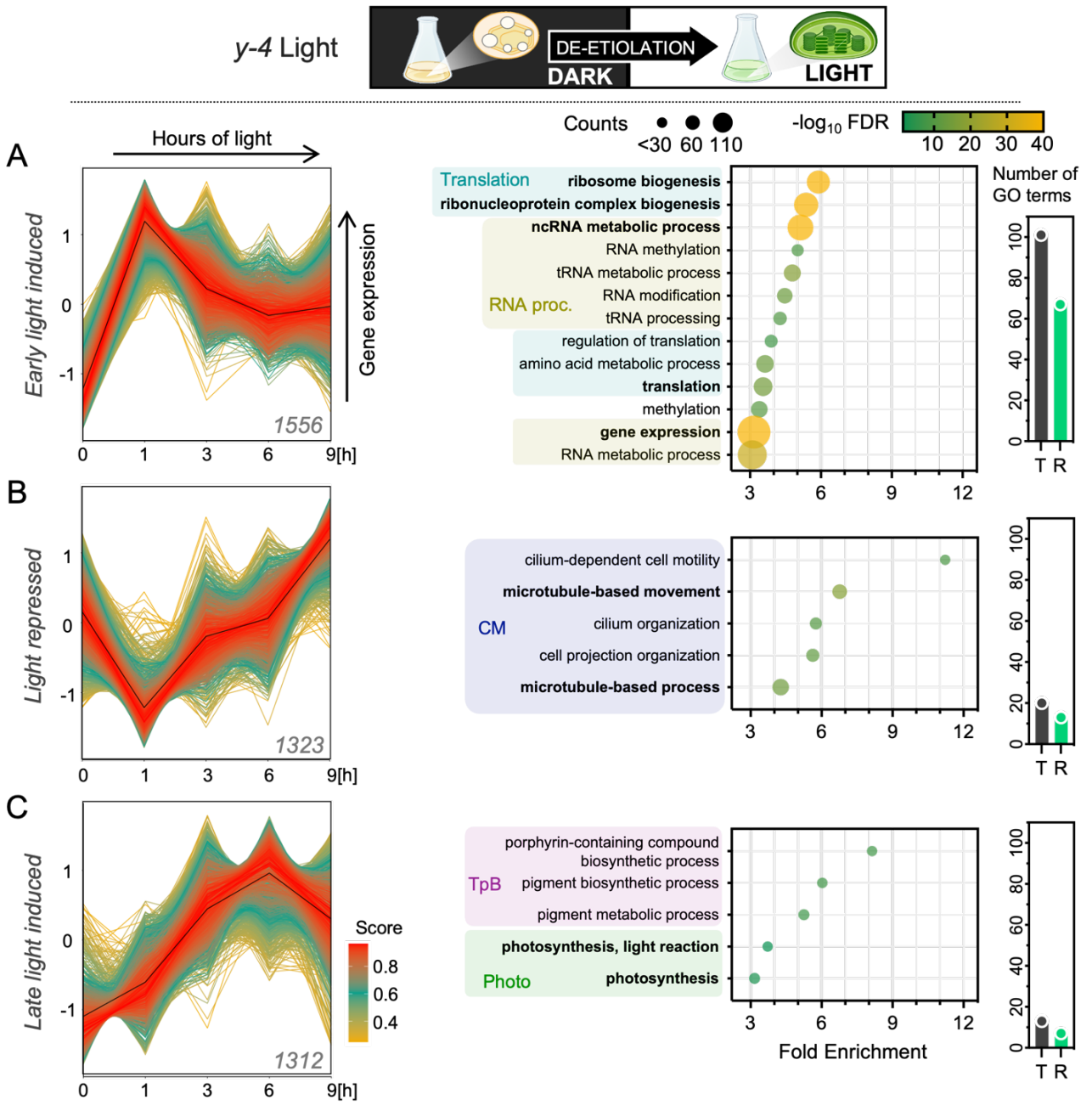


Figure 3.2: Mfuzz clusters of *LRGs* in *y-4* light RNA-seq and GO analysis. Three out of five *LRGs* clusters significantly enriched in GO terms (FDR < 0.05) for biological process are shown and defined as A. early light induced, B. light repressed and C. late light induced. At the bottom right of each cluster profile the total number of genes included is indicated. GO analysis was performed using STRING database (Szklarczyk et al., 2017) with available proteome data and annotations from V6 Chlamydomonas genome (Craig et al., 2023). Many redundant GO terms were excluded using Revigo (Supek et al., 2011). For each cluster, the total number of significantly enriched GO terms (T) and the resulting filtered terms by Revigo (R) is indicated. Here we show the 20% lowest FDR GO terms with at least 3-fold enrichment (minimum 5 and maximum 15). Common GO terms that appear in all the 3 systems analyzed are highlighted in bold. Also, common biological processes between this and Fig. 3.4 and Fig. 3.5 where highlighted: Translation (light blue), RNA processing (yellow), Cell Motility (CM, blue), Tetrapyrrole Biosynthesis (TpB, Pink), Photosynthesis (Photo, green).

found an additional cluster of upregulated genes with a 1-3 h peak that was defined as Very early light induced (Figure 3.3 A): this features processes related to light acclimation and photoprotection such as response to light stimulus and to heat, and also tetrapyrrole biosynthesis, in contrast to *y-4* Light; light also very early induces genes involved in the entrainment of the circadian clock. In wt12

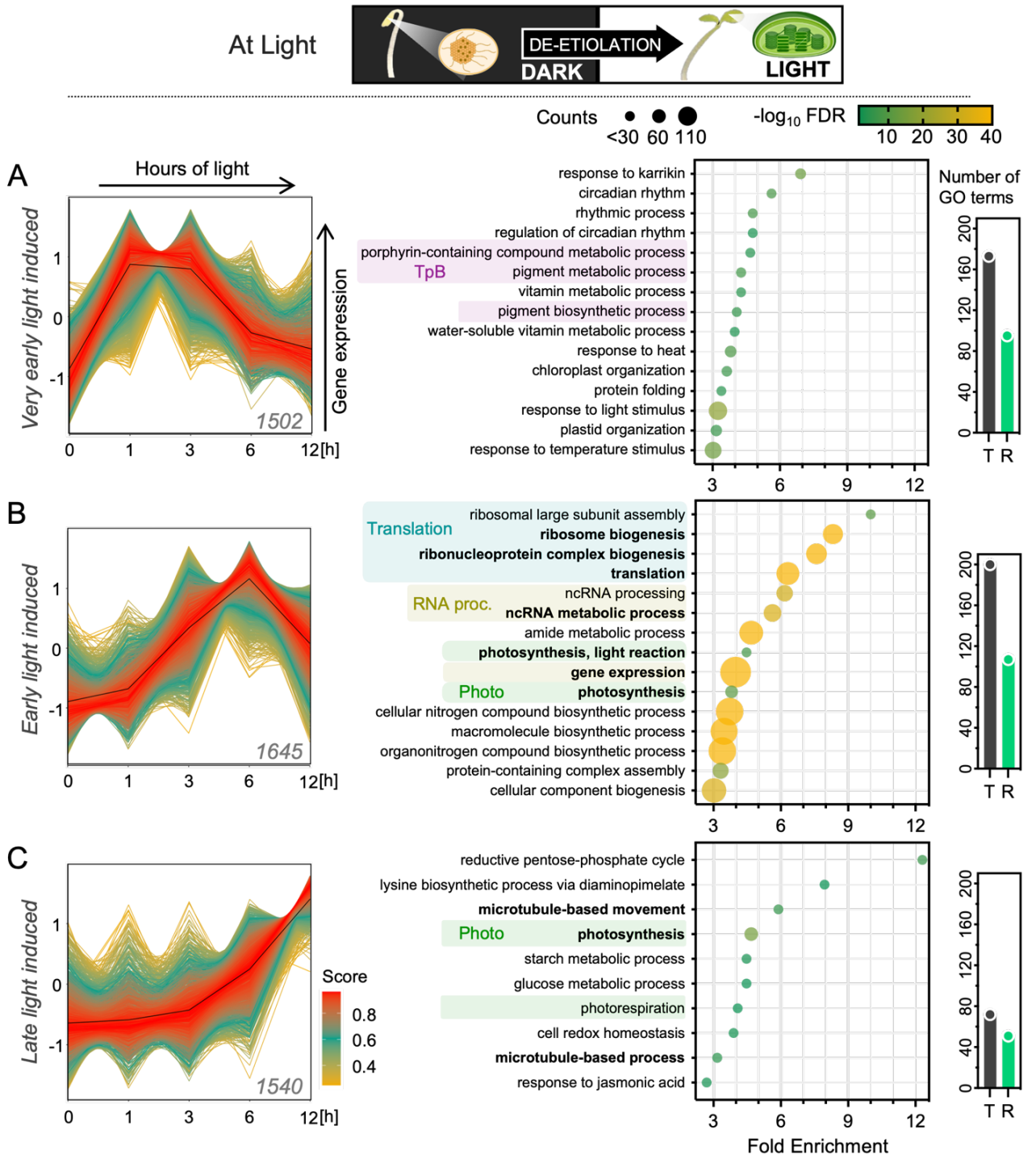


Figure 3.3: Mfuzz clusters of *LRGs* in in At Light RNA-seq and GO analysis. Clusters exhibiting same or similar (and significantly enriched, FDR < 0.05) GO terms found in our *y-4* de-etiolation experiment (3 out of 5) are shown. GO analysis was performed as in Fig. 3.2 but using STRING app with the already available Arabidopsis dataset. Clusters here shown were defined as Very Early Light induced (A), Early light induced (B) and Late light induced (C), depending on how GO terms matched with the ones in y-4 Light clusters.

Light we identified more clusters with significantly enriched GO terms (4 out of 5), probably due to the higher proportion of *LRGs* in this system (Figure 3.4). Here, we also found that light regulates same biological processes compared with *y-4* Light, and with very similar profiles. However, early light induced genes are separated into two clusters: transcriptional activity as well as ribosome biogenesis

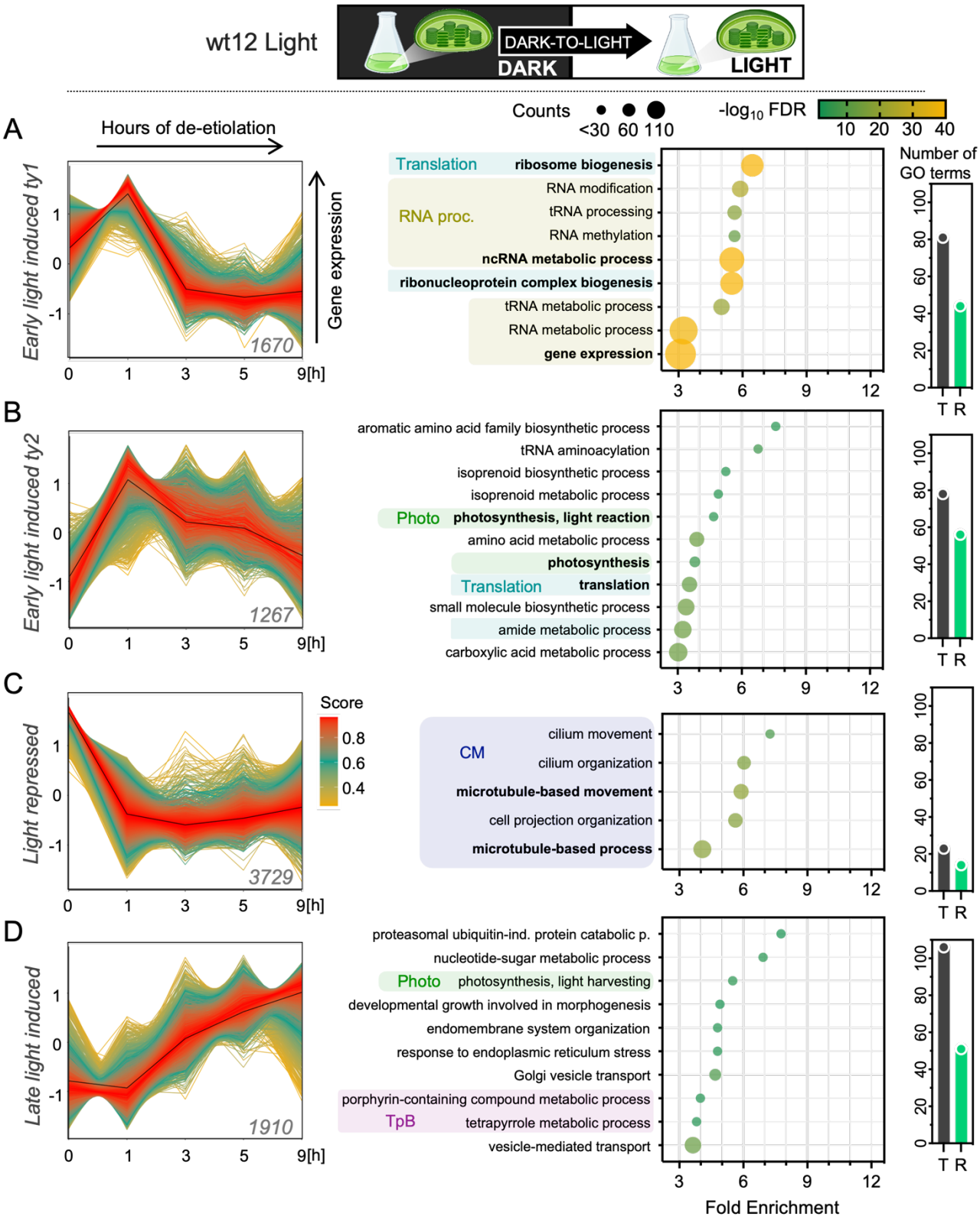


Figure 3.4: Mfuzz clusters of *LRGs* in in wt12 Light RNA-seq and GO analysis. Clusters exhibiting same or similar (and significantly enriched, FDR < 0.05) GO terms found in *y-4* Light (4 out of 5) are shown. GO analysis was performed as in Fig. 3.2. Clusters here shown were defined as Early Light induced type 1 (ty1) (A), Early light induced type 2 (ty2) (B), Light repressed (C) and Late light induced (D), depending on how GO terms matched with the ones in y-4 Light clusters.

is early transiently upregulated by light (Figure 3.4 A, Early light induced ty1), whereas translational activity and amino acid biosynthesis is early sustained upregulated by light (Figure 3.4 B, Early light

induced ty2); the latter features also other biological processes such as isoprenoid biosynthesis (involved in thermotolerance) and some photosynthesis genes. Also similar with *y-4* Light is regulation of cell motility, also early repressed by light (Figure 3.4 C), while chloroplast-related functions, tetrapyrrole biosynthesis and photosynthesis genes, are late light induced (Figure 3.4 D). In addition, this cluster includes glycosylation reactions of the Golgi apparatus.

Altogether, this analysis shows that light upregulates same biological processes during de-etiolation regardless of the species, while in Chlamydomonas plastid-state does not influence overall light regulation. Moreover, while in Chlamydomonas dark-to-light transition occurs in two steps of induction (the first at 1h and the second at 6h), in Arabidopsis this transition is delayed and occurs in three steps (the first at 1-3h, the second at 6h and the third at 12h), with different timing of induction of chloroplast biological processes: here tetrapyrrole biosynthesis is very early induced, whereas photosynthesis genes are induced throughout a wider period between 6h and 12h. We cannot discard the possibility that a group of early light genes or of non-*LRGs* in Chlamydomonas could also be very early induced between 0-1h in our setup.

Interestingly, although all the represented clusters feature a similar number of genes, very big differences in the amount of significantly enriched GO terms were found between them, being also not proportional to the number of genes that made each cluster, especially in Chlamydomonas. This reflects two main issues in this analysis: 1) the function of many genes in both model organisms is unknown, and we are likely underestimating other important biological processes which so far are not well documented and 2) many GO terms are redundant and unequally distributed through the different biological processes, being for instance more likely to obtain significantly enriched GO terms related to nuclear functions, and less related to chloroplast functions.

Light triggers a much higher induction of photosynthesis genes during de-etiolation in Arabidopsis compared to y-4 cells

GO analysis has many limitations mainly due to poor annotation of many genes, especially in Chlamydomonas, and also because many GO terms are not correctly assigned in the genome, which makes it underestimate other biological processes that are not still well documented and/or prone to false positives. Although the first limitation cannot be overcome, we can verify whether light regulates the biological processes obtained from GO analysis. It is worth to point out has this analysis has still the strength of being unbiased, giving as outcome the most significantly enriched biological processes from a defined list of genes. Here, in order to confirm the results obtained from GO analysis, we carried out a biased analysis that goes the opposite way (Fig. 3.5): first, we assigned genes to each biological process obtained from GO analysis using data from the literature and annotations, defining the main category and subcategory (i.e. photosynthesis, photosystem II); next, we defined the most typical trajectory for each category and subcategory (if most genes had similar and consistent fold

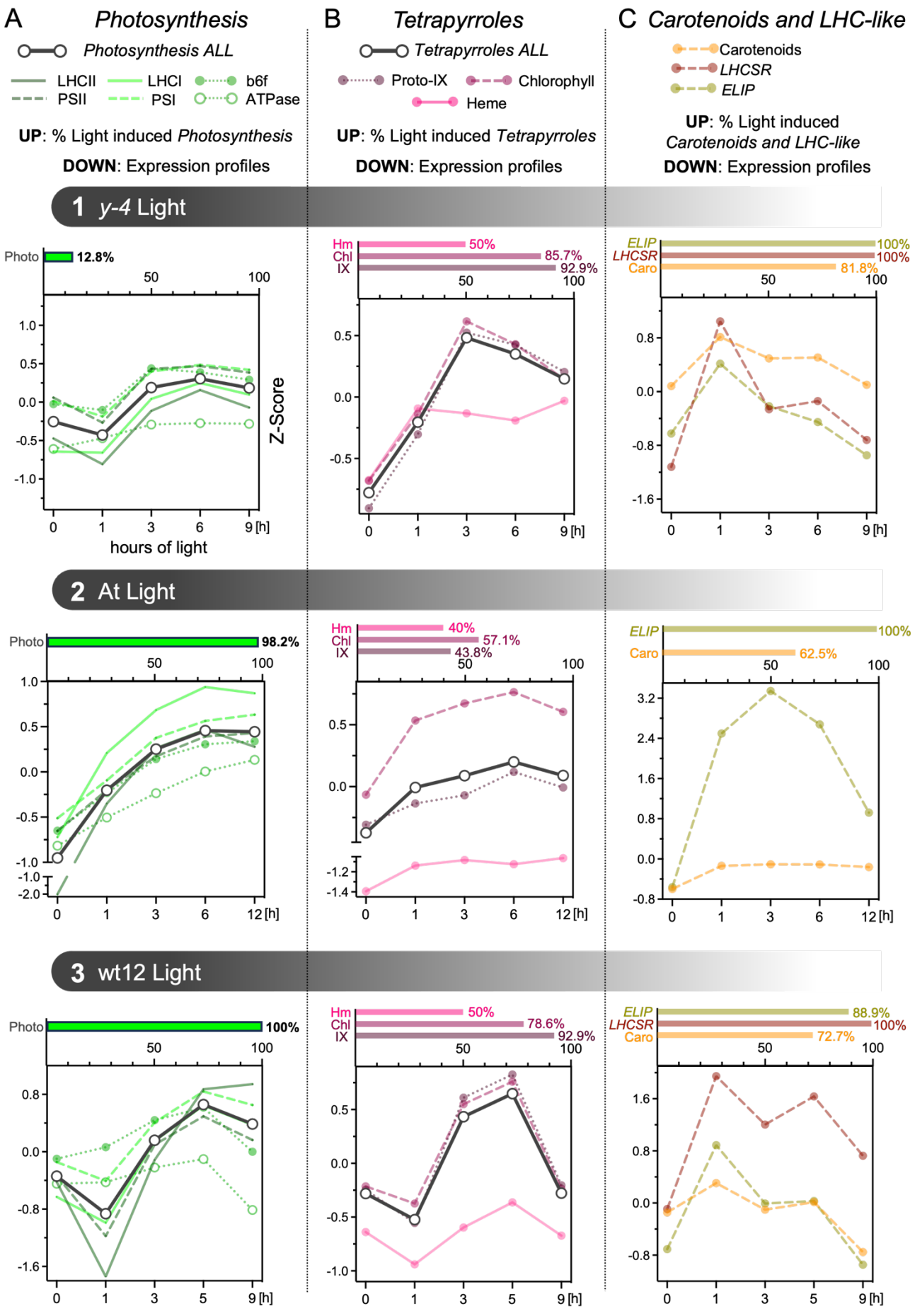
changes across de-etiolation), using TPM data to reflect actual distances between subcategories. In addition, we indicated above the proportion of genes which are *LRGs*. Therefore, the biased analysis allows us not only to verify the results obtained with GO analysis, but also to evaluate the specific trajectories of each biological process and subprocess. We identified six major biological processes with consistent DE values during light in the three systems: photosynthesis, tetrapyrrole biosynthesis, carotenoid biosynthesis and LHC-like, ribosomes, translation factors, and cell motility.

Although photosynthesis is late light induced in *y-4* Light, the expression profile of photosynthesis genes is pretty flat, with a low percentage of *LRGs* (Figure 3.5 A1). Light triggers a higher induction of photosynthesis genes in both At Light (Figure 3.5 A2) and, interestingly, also in wt12 Light (Figure 3.5 A3), where all genes are *LRGs*. In both Chlamydomonas systems the trajectory of photosynthesis genes tends to oscillate, with a minimum at 1h and a peak at 5 or 6h. No big differences were observed in the trajectories of the components of the photosynthetic electron transport chain (PhETC) here represented, in all the three systems. It is worth noticing that these genes are among the genes with highest transcript levels in all three systems (10^2-10^4 TPMs in Arabidopsis and 10^3-10^4 TPMs in Chlamydomonas). Overall, these results indicate that *y-4* cells do not need a strong induction of photosynthesis genes for chloroplast biogenesis, compared to the other systems, and that all components of the PhETC are equally regulated by light.

The enzymes of the tetrapyrrole biosynthesis pathway, instead, are highly upregulated by light in *y-4* cells during de-etiolation (Figure 3.5 B1), with around 90% of the genes upregulated. No differences were found between the profiles of the enzymes involved in synthesis of Proto-IX and chlorophyll, whose induction starts at 1h and registers a 3h peak. Biosynthesis of heme, instead, has a peak of induction at 1h, and then stays flat. Similarly, in wt12 Light tetrapyrrole biosynthesis genes are highly upregulated by light (Figure 3.5 B3), but the individual trajectories follow an oscillating pattern, as with photosynthesis. In Arabidopsis, instead, light induces only half of these genes. Interestingly, biosynthesis of chlorophyll and heme tends to occur very early during de-etiolation with a peak of induction at 1h, while precursors register a peak at 6h (Figure 3.5 B2).

Although not represented in the GO analysis of *y-4* Light, carotenoid biosynthesis genes were significantly enriched and together with LHC-like proteins, they are known to accomplish an important role in photoprotection during early light acclimation (Levin & Schuster, 2023). In Chlamydomonas, this class includes *LHCSR* genes, Chlamydomonas specific genes involved in photoprotection. As expected, almost all of these genes are early upregulated by light in both Chlamydomonas systems (Figure 3.5 C1,3). In Arabidopsis, most but not all carotenoid genes are very early upregulated, while all ELIP genes are early upregulated by light with a peak at 3h (Figure 3.5 C2). Overall, these results indicate that photoprotection response during early light acclimation is conserved.

Translation and ribosome biogenesis GO terms were significantly and consistently enriched in all the three systems. In both Chlamydomonas systems the majority of chloroplast ribosomes are early but transiently induced by light, while the expression of cytoplasm ribosomes remains constant or


A Photosynthesis
Photosynthesis ALL
LHCII
LHCI
b6f
PSII
PSI
ATPase
UP: % Light induced Photosynthesis
DOWN: Expression profiles
B Tetrapyrroles
Tetrapyrroles ALL
Proto-IX
Chlorophyll
Heme
UP: % Light induced Tetrapyrroles
DOWN: Expression profiles
C Carotenoids and LHC-like
Carotenoids
LHCSR
ELIP
UP: % Light induced Carotenoids and LHC-like
DOWN: Expression profiles
1 y-4 Light
Photo 12.8%
Hm 50%
Chl 85.7%
IX 92.9%
ELIP 100%
LHCSR 100%
Caro 81.8%
Z-Score
hours of light
2 At Light
Photo 98.2%
Hm 40%
Chl 57.1%
IX 43.8%
ELIP 100%
Caro 62.5%
3 wt12 Light
Photo 100%
Hm 50%
Chl 78.6%
IX 92.9%
ELIP 88.9%
LHCSR 100%
Caro 72.7%

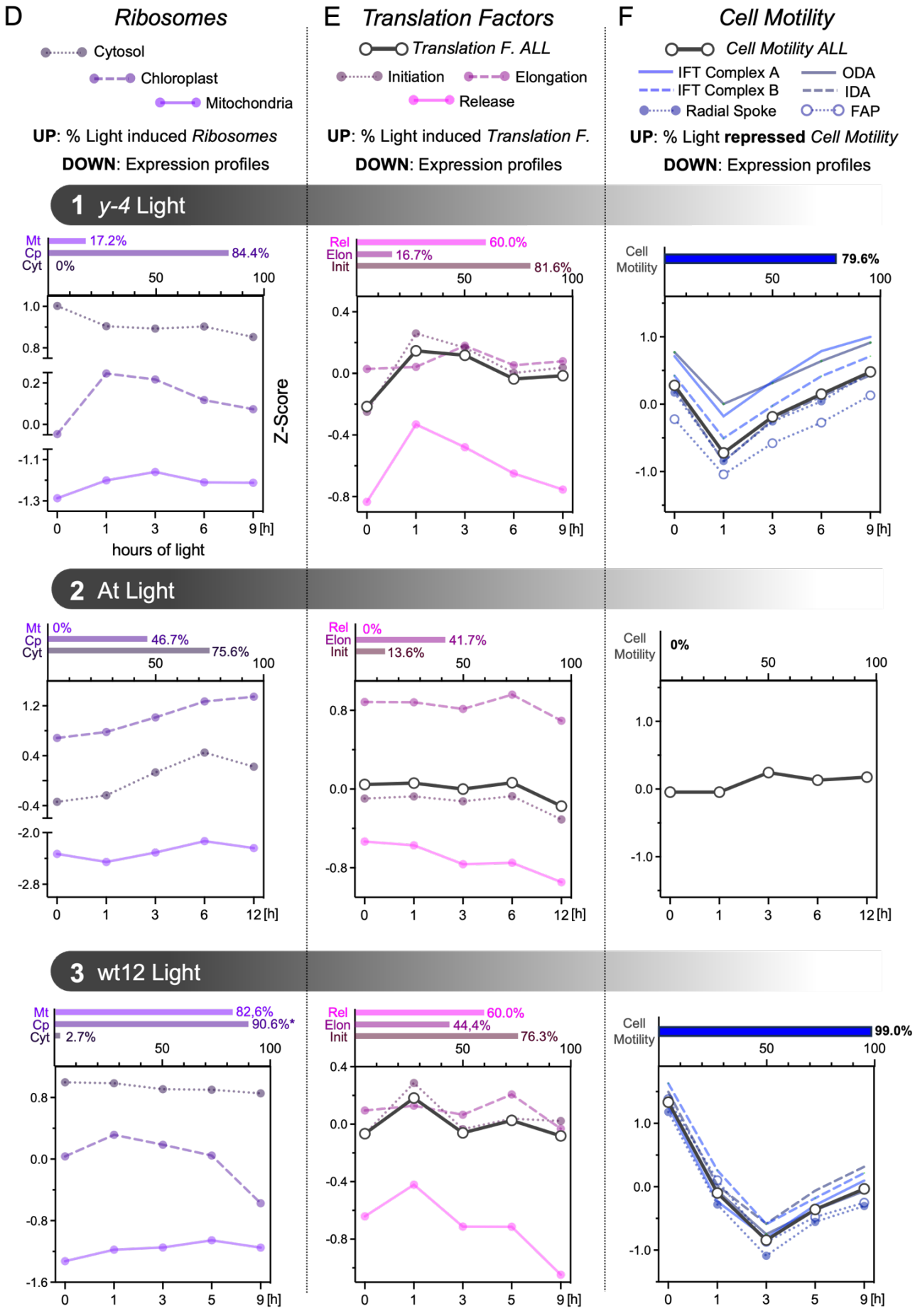

D
Ribosomes
Cytosol
Chloroplast
Mitochondria
UP: % Light induced Ribosomes
DOWN: Expression profiles
E
Translation Factors
Translation F. ALL
Initiation
Elongation
Release
UP: % Light induced Translation F.
DOWN: Expression profiles
F
Cell Motility
Cell Motility ALL
IFT Complex A
IFT Complex B
Radial Spoke
ODA
IDA
FAP
UP: % Light repressed Cell Motility
DOWN: Expression profiles
1 y-4 Light
2 At Light
3 wt12 Light
Mt
Cp
Cyt
Rel
Elon
Init
Cell Motility
Z-Score
hours of light
17.2%
84.4%
0%
60.0%
16.7%
81.6%
79.6%
46.7%
75.6%
41.7%
13.6%
82,6%
90.6%*
2.7%
60.0%
44,4%
76.3%
99.0%

Figure 3.5: Expression profiles of selected genes from significantly enriched biological processes from GO analysis: A. photosynthesis; B. tetrapyrrole biosynthesis; C. carotenoid biosynthesis and LHC-like; D. ribosomes; E. translation factors; F. cell motility. Gene expression profiles were determined for each experiment as the mean Z-score TPM values of all the genes belonging to the biological process (black line, empty circles), or subprocess (colored lines and circles). Genes belonging to each biological process and subprocess were manually selected using information from genome annotations and literature. Above each expression profile the proportion of light induced ($log_2FC > 1$, p-value < 0.05) or light repressed ($log_2FC < -1$, p-value < 0.05) genes included in each biological process or subprocess is represented. Photo: photosynthesis; Hm: heme; Chl: chlorophyll; IX: Proto-IX; Caro: carotenoid biosynthesis; Mt: mitochondria; Cp: chloroplast; Cyt: cytosol; Rel: release factor; Elon: elongation factor; Initiation: factor; IDA-ODA: inner-outer dynein arm; IFT: intraflagellar transport; FAP: flagellar associated protein.

decreases during de-etiolation (Figure 3.5 D1,3); in Arabidopsis, instead, both are progressively induced by light, especially cytoplasm ribosomes (Figure 3.5 D2). Interestingly, we found very high differences in the level of expression of ribosome genes: in Chlamydomonas a big proportion of transcripts is constituted by cytoplasm ribosomes (10^3-10^4 TPMs), and represent together with photosynthesis the genes with the highest transcript levels, while chloroplast ribosomes are considerably less expressed (10^2-10^3 TPMs); in Arabidopsis, these levels are much lower and being chloroplast ribosomes more expressed than cytoplasm (10^2-10^3 and 10^1-10^3 TPMs, respectively). Mitochondria ribosomes, instead, are not or lowly induced by light except in wt12 Light. Translation factors, especially of the initiation and release phase, are early and highly induced by light in both Chlamydomonas systems, while elongation factors are induced later (Figure 3.5 E1,3). Light does not upregulate very much these factors in Arabidopsis, except for the elongation factors which are also early light (6h) induced (Figure 3.5 E2).

Cell motility is instead the only Chlamydomonas-specific biological process regulated by light: all the components of the flagella are equally downregulated by light in both Chlamydomonas systems (Figure 3.5 F1,3), but with slightly different trajectories: in *y-4* light these components are early light downregulated, followed by a progressive induction, while in wt12 Light, these are progressively downregulated until 3h and then upregulated. Arabidopsis has lost almost all of these genes during evolution, except for a little group of putative flagella genes which are not regulated by light (Figure 3.5 E2).

Overall these results confirm that photosynthesis, tetrapyrroles and translation are the major biological processes induced by light during de-etiolation in both Chlamydomonas and Arabidopsis. However, the biased analysis suggests that the ancestral light signaling machinery present in Chlamydomonas regulates these processes in a different way compared to angiosperm plants: while in Arabidopsis de-etiolation relies on a strong induction of photosynthesis genes, and on translation in both cytosol and chloroplast, in Chlamydomonas de-etiolation relies at higher degree in the induction of tetrapyrrole biosynthesis genes and chloroplast translation, and less in the induction of photosynthesis genes, and cytoplasm translation, as transcripts of both biological processes already accumulate at high levels in the dark. In wt12 Light, the high upregulation of photosynthesis genes in cells that already feature a developed chloroplast in the dark could be explained by the additional regulation exerted by the main components involved in the entrainment of the circadian clock;

consistent with this, the expression profiles of photosynthesis and tetrapyrrole biosynthesis genes are both oscillating and synchronized during dark-to-light transition.

Chloroplast biogenesis relies on the upregulation of chloroplast biological processes in three distinct phases during de-etiolation

In order to understand how light signaling regulates biological processes involved in chloroplast biogenesis, we looked at genes encoding for chloroplast-localized proteins. As explained in the introduction, the great majority of these genes are encoded in the nucleus, and are subjected to tight regulation by light and retrograde signaling components during de-etiolation, while a small subset of around 80 genes are chloroplast encoded and are mainly regulated by anterograde signals. In our RNA-seq analysis, we also mapped raw reads to chloroplast and mitochondrial transcriptomes. However, very low transcript levels were detected in our samples, and unfortunately we cannot evaluate how light regulates plastid gene expression. Therefore, we focused our analysis on nuclear genes encoding for chloroplast proteins (*CpANGs*). For this purpose, we defined a high-confident list of these genes using PB-Chlamy, the most recent tool developed to predict subcellular localization in Chlamydomonas (Wang et al., 2023). Using this tool we identified a total 2158 *CpANGs* (Figure 3.6 A): unsurprisingly, more than half of these genes are *LRGs*, and the vast majority of these (72%) are upregulated (Figure 3.6 B). These *LRGs* feature overall higher transcript abundance, compared with *LRGs* from non-*CpANGs* (Figure 3.6 C); however, no significant differences in the degree of induction and repression between these two subsets were found (Figure 3.6 D). This indicates that Chlamydomonas does not particularly prioritize regulation of *CpANGs* during chloroplast biogenesis, over the rest of *LRGs*.

Next, we aimed to identify the specific *CpANGs* that need to be upregulated (and downregulated) in order to assemble a functional chloroplast. For this purpose, we grouped *CpANGs* into specific chloroplast biological processes, determining for each one a representative expression profile (Figure 3.7). This analysis was carried out using the same criteria as for the biased analysis of the previous section, although here we determine global Z-Score values that take into account the transcript levels of all genes, allowing us to compare the trajectories of all of these processes between them, and more importantly, to determine the dynamics of upregulation of all of these processes. In addition, we determined two thresholds for the most highly expressed genes in our time course, named highly expressed (HE, 5% most highly expressed) and very highly expressed (VHE, 1% most highly expressed), which in particular tells us which genes are already upregulated in the dark.

We determined three distinct phases of upregulation of chloroplast biological processes involved in chloroplast biogenesis. The early phase (Figure 3.7 A) mainly features early light transient upregulation of chloroplast biological processes. These include chloroplast translation, LHC-like and carotenoid biosynthesis, fatty acid desaturation and vesicular induced plastid proteins (VIPP).

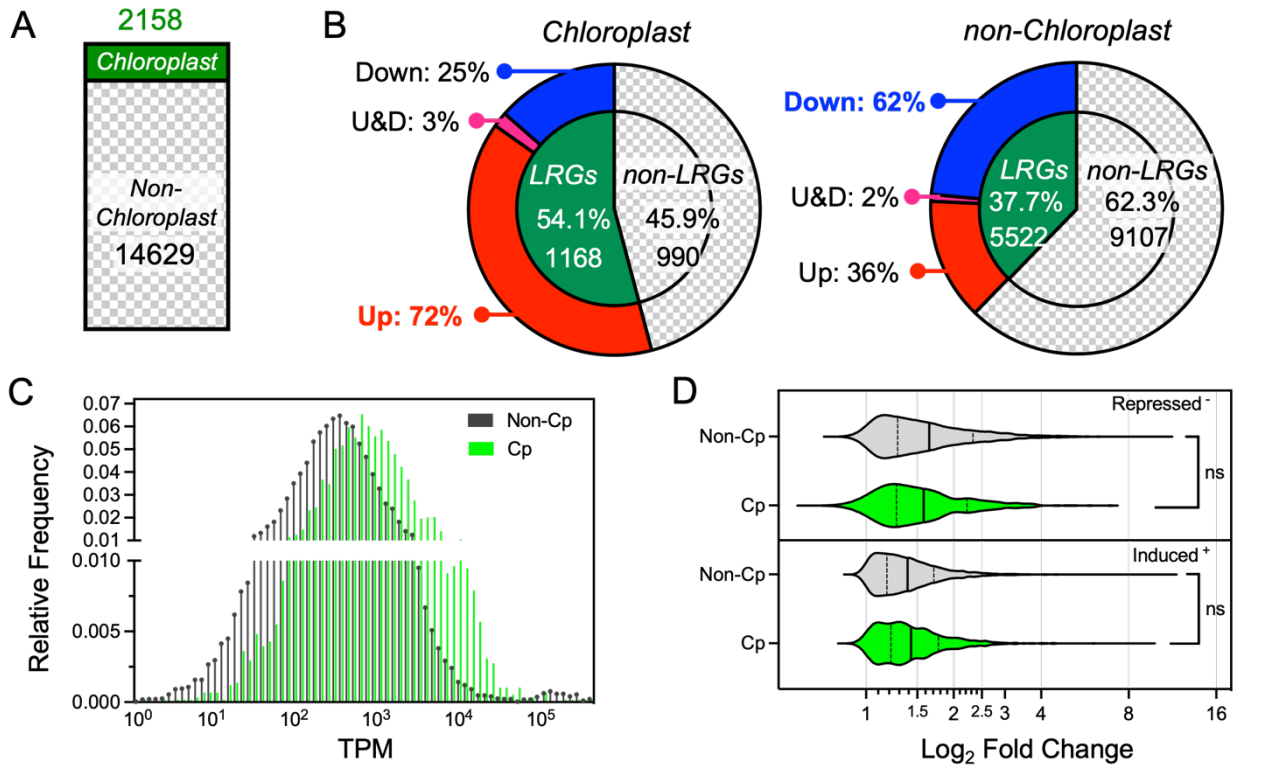
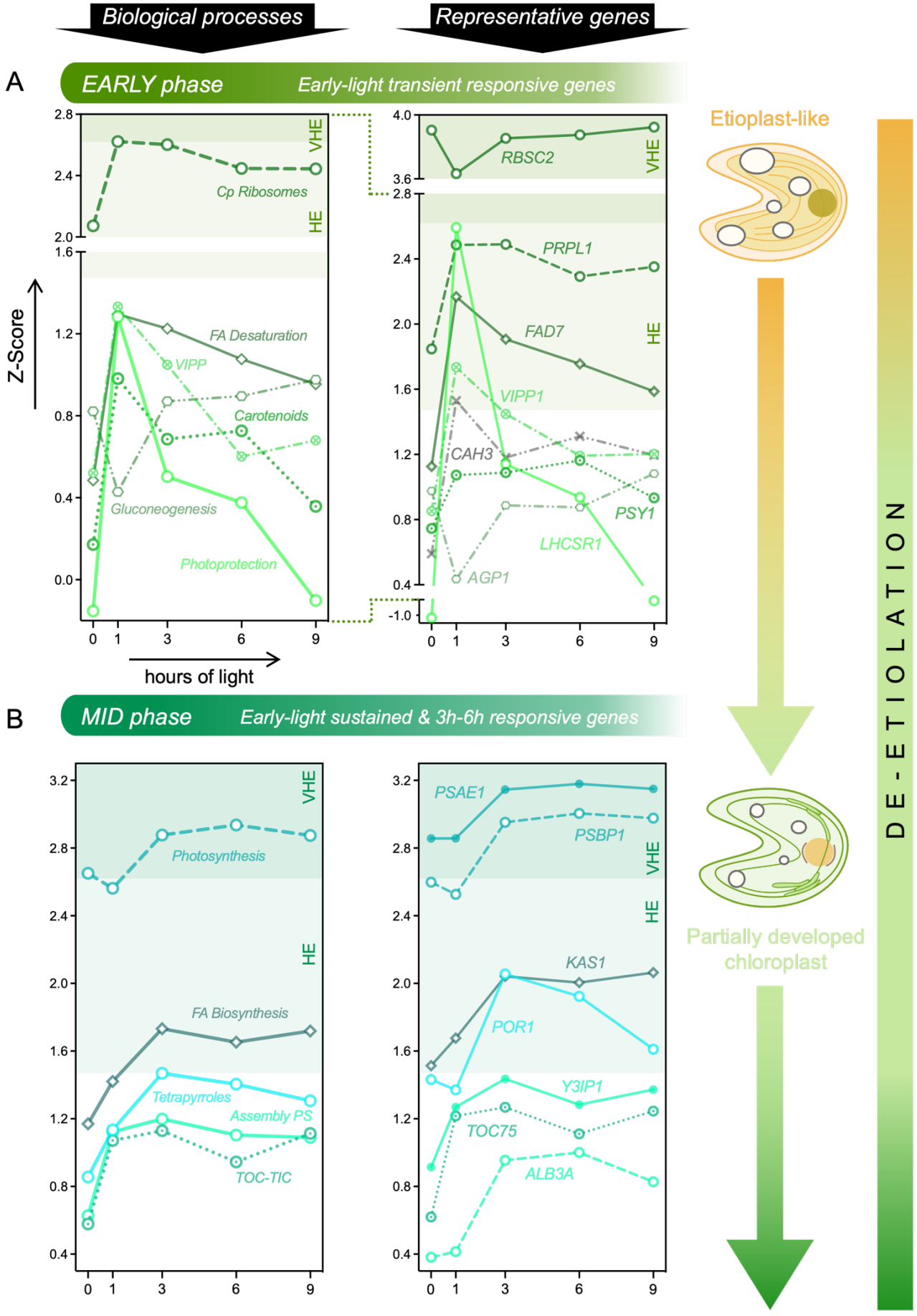


Figure 3.6: Gene expression analysis of nuclear genes coding for chloroplast localized proteins (*CpANGs*). This subset of genes was defined using PB-Chlamy algorithm for protein localization prediction in Chlamydomonas (Wang et al., 2023). A. Proportion of *CpANGs* present in the transcriptome of *y-4* Light samples. B. Summary of differentially expressed genes for both *CpANGs* and *non-CpANGs*. C. Frequency distributions of normalized counts for both *CpANGs* and *non-CpANGs*. D. Distribution of absolute log_2FC values for both light induced and light repressed genes in both subsets. Down: repressed; Up: induced; U&D: Induced and repressed; Cp: chloroplast targeted; Non-Cp: not targeted to the chloroplast

Gluconeogenesis is instead repressed by light. For each category we also included a representative gene: most of them feature a very similar pattern; in particular, we observed that *LHCSR1* (a key regulator of photoprotection) features a considerable variation in transcript levels, from almost absent levels in the dark to be one of the VHE genes at 1h of light, which is indicative of a key role of this gene in photoprotection; *RBSC2* (a RUBISCO subunit), although early downregulated, remains one of the most highly expressed genes of the genome, but, interestingly, the rest of the enzymes from the Calvin cycle do not feature a similar trend in the expression pattern. Altogether these results indicate that in this first phase cells spend energy in form of sugars for translation of chloroplast genes, together with the induction of the photoprotection mechanism for early light acclimation; this energy is also spent in the early light activation of the components needed for the synthesis of thylakoid membranes through VIPP proteins, desaturation of fatty acids, and also synthesis of galactolipids which later register a second peak of induction at 9h (Figure 3.7 C).

The mid-phase (Figure 3.7 B) contains chloroplast upregulated biological processes whose peak of expression is at 3-6 h. These include photosystem assembly (*Y3IP1* and *ALB3A* are involved in the assembly of PSI and PSII, respectively), which precedes induction of photosynthesis (*PSAE1* and *PSBP1* are subunits from PSI and PSII, respectively), tetrapyrrole biosynthesis, translocon at the outer-inner membrane of chloroplasts (TOC-TIC, which is the chloroplast protein import machinery),


Biological processes
Representative genes
A
EARLY phase
Early-light transient responsive genes
Cp Ribosomes
RBSC2
VHE
HE
FA Desaturation
VIPP
Carotenoids
Gluconeogenesis
Photoprotection
PRPL1
FAD7
VIPP1
CAH3
PSY1
LHCSR1
AGP1
Z-Score
hours of light
Etioplast-like
B
MID phase
Early-light sustained & 3h-6h responsive genes
Photosynthesis
FA Biosynthesis
Tetrapyrroles
Assembly PS
TOC-TIC
PSAE1
PSBP1
KAS1
POR1
Y3IP1
TOC75
ALB3A
Partially developed chloroplast
DE-ETIOLATION

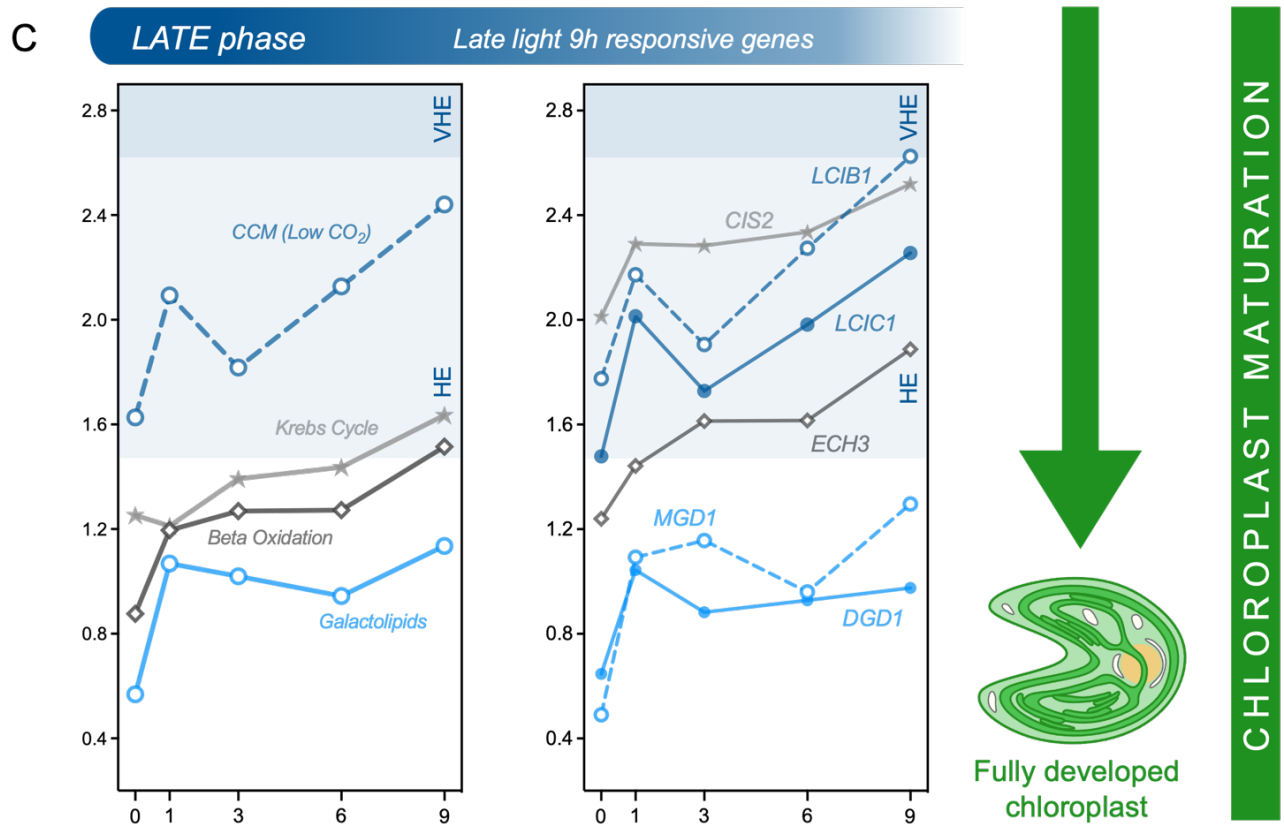


Figure 3.7: Expression profiles (left) of selected genes from chloroplast biological processes (with the exception of beta-oxidation (dark grey)), and of representative genes for each (right, same line style). Expression profiles were determined as the mean Z-score TPM values of all the genes belonging to the biological process. In addition, thresholds for highly expressed genes (HE, light shade) and very highly expressed genes (VHE, dark shade), were defined as belonging to the 5% or 1% highest TPM values in all *y-4* Light samples, respectively. Biological processes were separated into three phases depending on the overall profile shape: A. early phase, featuring biological processes which are transiently light responsive at 1h (green tones); B. mid phase, featuring biological processes which are light induced at 3h, or 6h (aqua green tones); C. late phase, featuring biological processes which show a late peak of induction at 9h (blue tones). In parallel, two phases of chloroplast biogenesis were theorized based on the obtained profiles: 1) de-etiolation phase, and 2) chloroplast maturation phase (See Discussion). Cp: chloroplast; FA: fatty acids; VIPP: vesicle-inducing protein in plastids; TOC-TIC: translocon at the outer-inner membrane of chloroplasts; PS: photosystem; CCM: carbon concentrating mechanism.

and synthesis of fatty acids. As anticipated in the biased analysis, photosynthesis genes are among the genes with the highest transcript levels. Therefore, in the mid phase, cells induce both synthesis and assembly of all the components of the PhETC, and this is accompanied by their import into the forming chloroplast through the TOC-TIC machinery. All these processes contribute for the establishment in the first hours of the photosynthetic capacity.

Finally, we determined a late phase (Figure 3.7 C), consisting in genes that feature a peak of light-induction at 9h, and are likely to keep their induction afterwards: although many *CpANGs* fulfilled this condition, we didn't find a striking majority of these genes belonging to a specific chloroplast localized pathway; instead, we observed the presence of two key genes involved in carbon concentration mechanism in low CO_2 conditions (LCIB1 and LCIC1), and two encoding enzymes for galactolipid biosynthesis (MGD1 and DGD1), the major lipidic component of chloroplast membranes. In addition, we observed induction at 9h of two important metabolic pathways that, although not taking place in the chloroplast, are tightly associated with chloroplast metabolic activities, and between them: Krebs

cycle and beta oxidation of fatty acids. Activation of these two processes suggests a need for production of energy in form of ATP: as energy source, cells might use on one hand newly autotrophically synthesized sugars, thanks to the accumulating CO_2 in the pyrenoid used for the carboxylation reactions, and on the other hand the newly synthesized fatty acids from the mid phase. This energy is likely required for the maturation phase, as reflected by the second induction of galactolipids biosynthesis (See Discussion).

Overall, these results indicate that etioplast-like-to-chloroplast transition in *y-4* cells requires massive changes in the regulation of many chloroplast biological processes. It is worth noticing that in the majority of these, genes feature similar and consistent DE values across the time course, which made possible to group them into the represented categories. This tightly coordinated regulation triggered by light is particularly relevant because it is carried out by a primitive light signaling mechanism that lacks many transcription factors present in angiosperm plants. In the following section we will take a look at them.

Similarly to Arabidopsis, light induces a transcriptional cascade in Chlamydomonas during de-etiolation

In Arabidopsis, the light signaling pathway that regulates de-etiolation features several key transcription factors (TFs), mainly PIF, BBOX, GLK, HY5 and the recently reported MYB (Figure 3.8 A); in the Chlamydomonas genome, although TF families in which these key genes belong are conserved, only homologs for HY5 (CRHY5) and CONSTANS (CRCO) were identified, and these are known to be involved in photoprotection in this species. We observed that in both *y-4* Light and At Light these TFs are early light induced (Figure 3.8 A,B), which might indicate a conserved role in early light response.

We also evaluated the expression of all TFs during de-etiolation: in Arabidopsis, only the expression of 1302 TFs (out of 1775) was detected, while in Chlamydomonas we detected expression of all except for four TFs. Light regulates a similar percentage of TFs (around 30%), being this a little higher for Chlamydomonas, and also a slightly higher percentage of down- to upregulated TFs in both species (Figure 3.8 C,D, left). The percentage of light responsive TFs (*LRTFs*) does not change even when looking at the families shared between species (Figure 3.8 C,D, right). We also observed absence of a specific enrichment in up- or downregulated TFs in any family described in both species. Next, we studied the expression patterns of all TFs in both species, *LRTFs* or not, to evaluate how these globally respond to light. In Arabidopsis, we found groups of TFs that are transiently upregulated by light in each time point starting from dark, which suggests that de-etiolation is dependent on a light-triggered transcriptional cascade (Figure 3.8 E). Interestingly, the same phenomenon was observed in Chlamydomonas (Figure 3.8 F). In Arabidopsis, key regulators of de-etiolation were found upregulated in the dark, such as PIFs, or very early upregulated by light, such as HY5, CO, and the

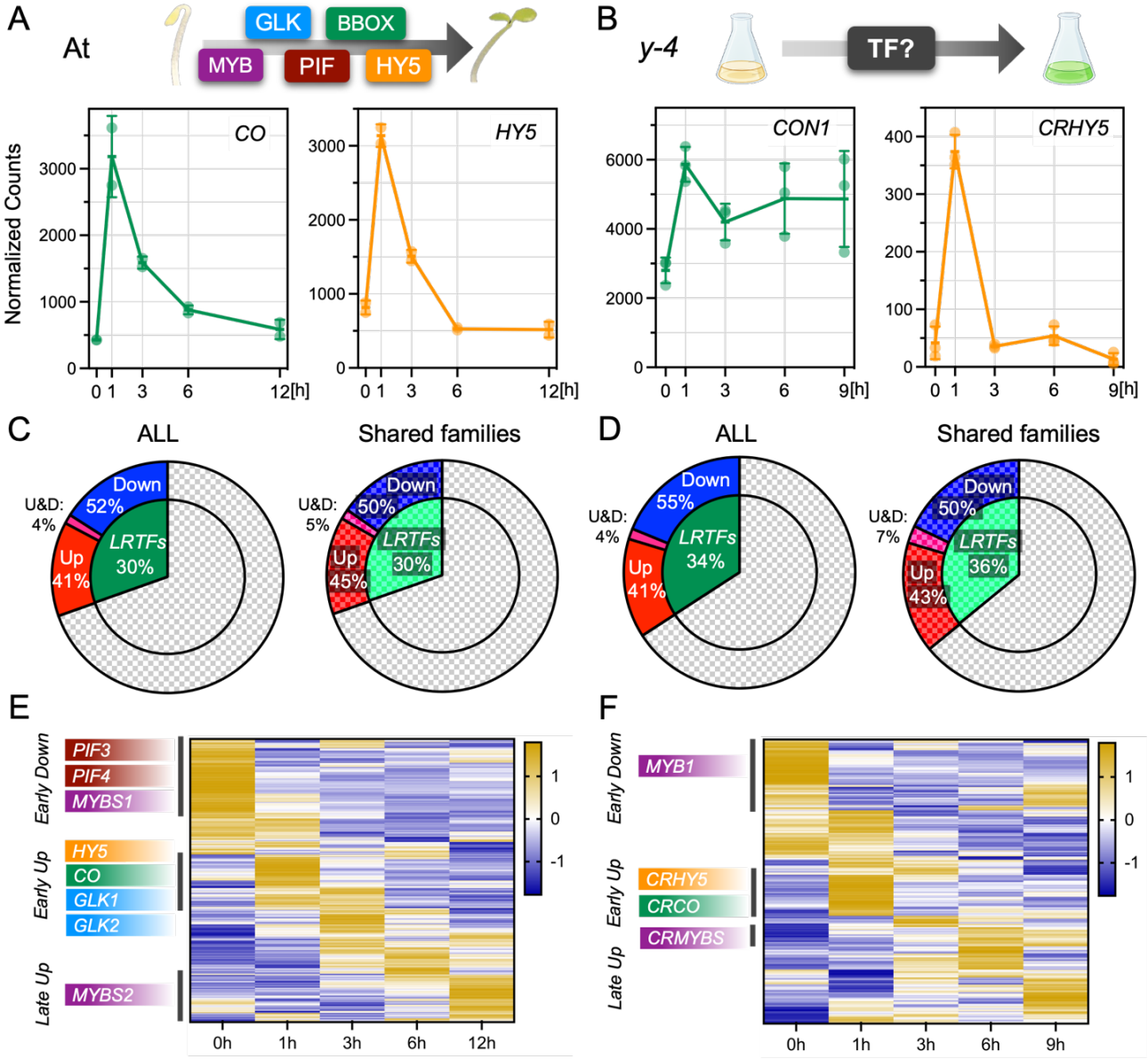


Figure 3.8: Gene expression analysis of transcription factors (TFs) in *y-4* Light and At Light RNA-seq. A total 404 genes were defined as TFs in Chlamydomonas according a recent study (Arend et al., 2023); in Arabidopsis, 1773 TFs are reported according the AtTFDB (Davuluri et al., 2003), but expression was detected only for 1302 of these TFs. Similar expression profiles of CO and HY5 genes in At Light (A) and their homologs in *y-4* Light (B), (CON1 and CRHY5) were observed. Above, main TFs known to regulate de-etiolation. All of them are light responsive (*LRTFs*) in Arabidopsis. Pie charts represent the amount of *LRTFs*, divided in induced (Up) and repressed (Down), in At Light (C) and *y-4* Light (D), for the whole list of TFs in both systems (left), or only the shared families (right, i.e. bHLH, CO-like, MYB, etc.). Heatmaps represent standardized gene expression values for all TFs in At Light (E) and *y-4* Light (F). In addition, main TFs involved in de-etiolation in Arabidopsis and their homolog candidates in Chlamydomonas are highlighted in the heatmaps. In particular, *PIF* genes and *MYBS1* are repressed by light, whereas *HY5* and *CRHY5*, *CO* and *CRCO*, *GLK1*, *GLK2* and *MYBS2* are light induced. U&D: induced and repressed.

GLKs. In Chlamydomonas, CRHY5 and CRCO are early light upregulated similarly to Arabidopsis. Interestingly, a MYBS TFs that has been recently implicated in chloroplast biogenesis (Frangedakis et al., 2023), is late light upregulated in Arabidopsis, and although its homolog in Chlamydomonas is not strictly a *LRTFs*, it seems to late respond to light, which might indicate a conserved role of this TF in this process.

The vast majority of the changes in the transcriptome during dark-to-light transition are caused by light rather than plastid-state

The comparison with wt12 Light is important not only for the validation of genes and biological processes regulated by light, but also to evaluate the influence of the plastid-state on the transcriptome during dark-to-light transition: cells in wt12 Light, in fact, already feature a fully developed chloroplast in the dark, compared to our de-etiolation system.
Although only in our system cells undergo chloroplast biogenesis, both feature 5229 genes *LRGs* in common, almost half of wt12 Light and 85% of *y-4* Light (Figure 3.9). These common *LRGs* are involved in the biological processes already mentioned in the GO and biased analysis: mainly ncRNA processing, ribosome biogenesis, photosynthesis, tetrapyrrole biosynthesis and cell motility. Exclusive *LRGs* subset in wt12 Light is characterized by induction of Golgi-related functions, DNA replication and protein turnover, while in *y-4* Light cells tend to specifically downregulate cytosolic ribosomes. These subsets are not particularly enriched in *CpANGs*, being 8% and 11,4 for *y-4* Light and wt12 Light, respectively. It is worth to point out that analyzing these subsets of specific *LRGs* in each system is prone to false positives, as many of the included genes in wt12 Light could be regulated by light in the same way also in *y-4* Light but does not get past the 2 fold change threshold. Therefore to evaluate actual differences in both transcriptomes, we looked at those common *LRGs* which feature opposite degree of regulation: genes upregulated in y-4 Light and downregulated in wt12 Light (“Subset a”), and viceversa (“Subset b”). Interestingly, “Subset a” features a much higher percentage of *CpANGs* compared to “Subset b” (26% compared to 13%) and more TFs (13 compared to 5) which include several members of the MYB family.
Altogether, these results indicate that the majority of the changes in the transcriptome during dark-to-light transition depend on light rather than the plastid developmental state. Moreover, the specific chloroplast differentiation of *y-4* cells relies on the upregulation of a small subset of genes, nuclear encoded chloroplast proteins and likely of specific TFs.

Prolonged dark induces accumulation of photosynthesis and cytosolic ribosome transcripts in etiolating y-4 cells

To understand how the transcriptome of de-etiolating *y-4* cells compare with the same cells having a fully developed chloroplast and actively growing in photoautrophic conditions, we included the always light control at the last time point of de-etiolation in our analysis (*y-4* AL), and compared with both etiolated *y-4* cells in the dark (*y-4* D0) and with de-etiolating cells at 9h of light (*y-4* L9) (Figure 3.10 A). The number of *DEGs* of *y-4 AL* compared to *y-4* D0 was not as high as our *LRGs* list (3351 compared to 6690). We observed considerably fewer upregulated genes in *y-4* AL (1091 compared with 2260), which were not enriched in GO terms for chloroplast biological processes, but instead in mitochondrial functions (Figure 3.10 B). Interestingly, although more *CpANGs* are upregulated in *y-4*

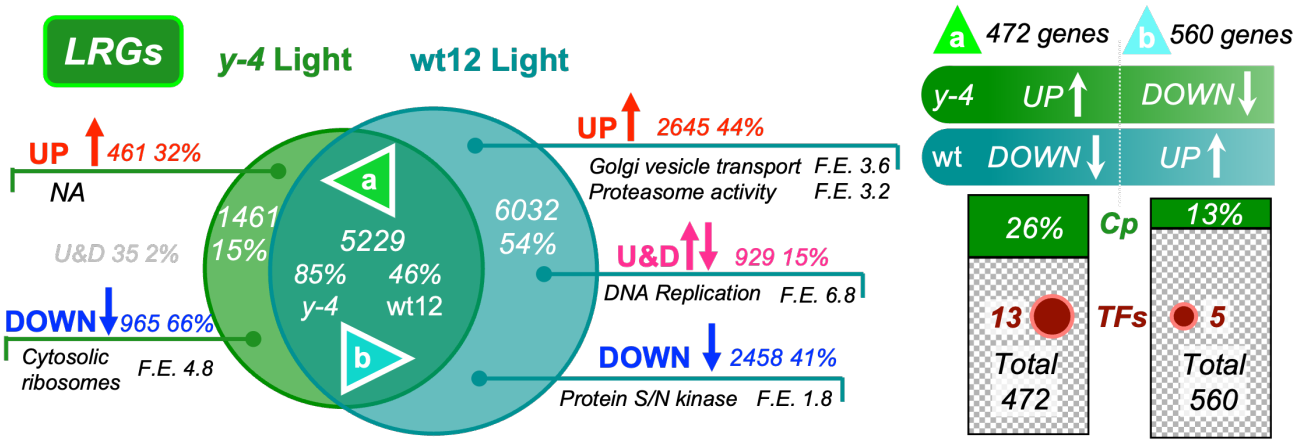


Figure 3.9: Comparison of common and specific *LRGs* in *y-4* Light and wt12 Light, divided in induced (Up), repressed (Down), or induced and repressed (U&D). Number of genes and percentage is specified for each group. In addition, most representative GO biological process terms of all specific significantly enriched GO categories are shown for *LRGs* which are exclusive in one of the two RNA-seq experiments (fold enrichment (F.E.) is also highlighted). Among common *LRGs* between the two systems, two specific subsets with opposite directions of light responsiveness, induced in *y-4* and repressed in wt12 (a), and viceversa (b), were further analyzed: in proportion, there is double the amount of *CpANGs* in subset a, and also more than double the amount of TFs, which could be potentially involved in a specific chloroplast biogenic function absent in wt12 Light.

AL compared to *y-4* D0 (Figure 3.10 C,D), photosynthesis gene transcripts accumulate at higher level in *y-4* D0 (Figure 3.10 E), while other chloroplast biological processes such as tetrapyrrole biosynthesis are upregulated in *y-4* AL. Also, *y-4* D0 feature many more upregulated *non-CpANGs* (Figure 3.10 C); although no significantly enriched biological processes were found in this case, the GO term cytosolic ribosome was significant for cellular component, and strikingly all of these genes were found upregulated in *y-4* D0, although many do not reach our 2 fold change threshold (Figure 3.10 E). These results indicate that prolonged growth in the dark induces the accumulation of photosynthesis and cytosolic ribosome transcripts, which are likely required for chloroplast biogenesis during de-etiolation once cells are exposed to light, while *y-4* cells having their chloroplast fully developed and actively growing in photoautrotrophic conditions, keep the transcript levels of these genes at lower steady state levels. Upregulation of mitochondrial functions in *y-4* AL was confirmed by the induction of most genes from Krebs cycle (Figure 3.10 E), which indicates these cells are actively performing cellular respiration.

Compared instead with *y-4* L9, we found 2002 *DEGs*: genes upregulated in *y-4* L9 were significantly enriched in ribosome biogenesis (Figure 3.10 B), and also featured more *CpANGs* compared to *y-4* AL (Figure 3.10 F); also *CpANGs* overall showed higher expression levels in y-4 L9 (Figure 3.10 G). Overall, genes of main chloroplast biological processes were more upregulated in *y-4* L9, in particular photosynthesis, chloroplast ribosomes and Calvin cycle (Figure 3.10 H). This suggests that many changes in the expression of *CpANGs* only occur during de-etiolation, and once the chloroplast is fully developed these genes return to steady state levels in light: this applies especially for photosynthesis- and translation-associated genes.

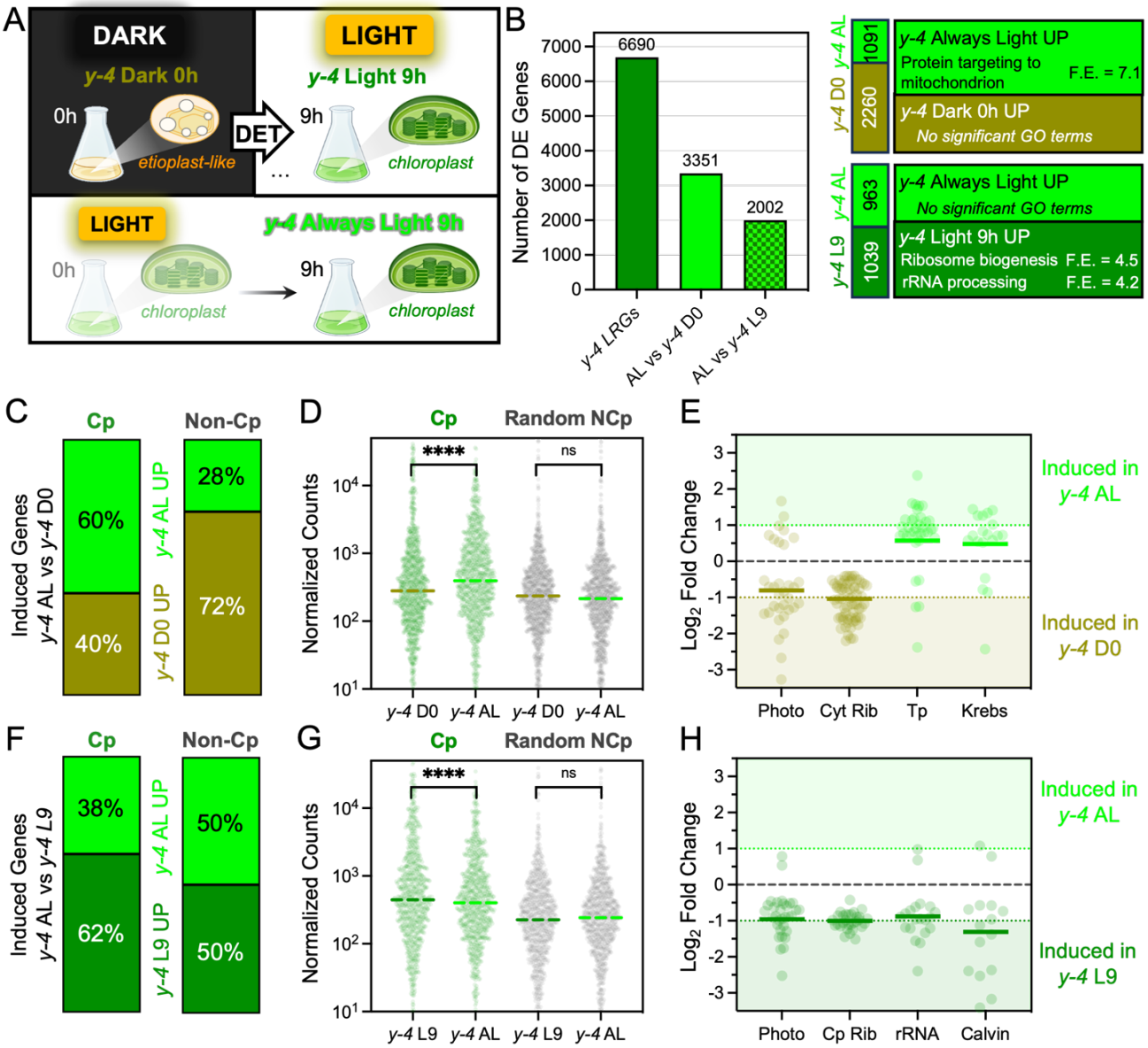


Figure 3.10: Analysis of differentially expressed (DE) genes in always light grown *y-4* cells at 9h (y-4 AL) in our RNA-seq. A. Schematic view of this analysis: *y-4* AL conditions were pairwise compared with etiolated *y-4* cells in dark (*y-4* D0) and our last time of de-etiolation in light (*y-4* L9). B. The number of *DEGs* in the pairwise comparisons before mentioned ($|\log_2 FC| > 1$, p-value < 0.05), and our *LRGs* subset. In addition, most representative GO biological process terms for induced genes (Up) in both pairwise comparisons is shown with its fold enrichment (F.E.). C,F. Proportion of DE *CpANGs* (Cp) and *non-CpANGs* (Non-Cp) in both *y-4* AL vs *y-4* D0 (C) and *y-4* AL vs *y-4* L9 (F) comparisons. D,G. Distribution of normalized counts and median (colored discontinuous line) for significantly induced *CpANGs* (Cp) (only p-value < 0.05) and a random *non-CpANGs* subset with the same size (Random NCp) for both *y-4* AL vs *y-4* D0 (D) and *y-4* AL vs *y-4* L9 (G) comparisons. E,H. Log_2FC distribution and mean (colored continuous line) of significantly DE genes (only p-value < 0.05) belonging to selected biological processes for both *y-4* AL vs *y-4* D0 (E) and *y-4* AL vs *y-4* L9 (H) comparisons. Photo: photosynthesis; Cyt Rib: cytosolic ribosomes; Tp: tetrapyrrole biosynthesis; Calvin: Calvin cycle; Cp Rib: chloroplast ribosomes; Krebs: Krebs cycle; rRNA: rRNA processing.

PIFs and GLKs emerged to confer a higher degree of regulation to nuclear encoded chloroplast light responsive genes during de-etiolation

PIFs and GLKs are two essential regulators of de-etiolation in Arabidopsis: while PIFs accumulate in the dark to repress photomorphogenesis, GLKs accumulate in light to induce this response. Although

these two TFs are absent in Chlamydomonas, etiolated *y-4* cells can fully restore their chloroplast upon transfer to light, and CRHY5 and CRCO might be potentially involved in this response, as their homologs in Arabidopsis (HY5 and CO) are also essential for proper de-etiolation (Figure 3.11 A). This made us wonder what is the evolutionary advantage that represented the emergence of PIFs and GLKs and their role in the de-etiolation response. We hypothesized that these may be involved in regulating at higher degree *LRGs*, given that photosynthesis genes are more induced during de-etiolation in Arabidopsis (Figure 3.11 B), where they progressively increase their expression till 6-12h, compared to a flatter expression profile of these genes in *y-4* cells (Figure 3.11 C,D). In order to test this hypothesis, we evaluated the expression of PIF- and GLK-regulated genes in Arabidopsis and their homologs in Chlamydomonas during de-etiolation. The list of PIF- and GLK-regulated genes was obtained from Pfeiffer et al., 2014, and Tu et al., 2022, respectively. Homologs of these genes in Chlamydomonas were obtained from Craig et al., 2023, using their best BLASTP hit.

We identified a total 597 PIF-regulated genes that share homology between both organisms. Of these more than half (367) are *LRGs* in Arabidopsis. We found that half of these genes (182) are *non-LRGs* in Chlamydomonas (Figure 3.11 E), suggesting that the emergence of PIFs confer them the capacity to respond to light. The other half (179) is made of *LRGs*. In Arabidopsis the majority of these PIF-regulated *LRGs* are upregulated (75%), while in Chlamydomonas these represent a little over half (59%). Moreover, we found that these genes feature higher (but non-significant) FC values in Arabidopsis, and interestingly these values are even higher (and significant) when considering only *CpANGs* (Figure 3.11 F), whereas in Chlamydomonas no difference in FC is observed between *CpANGs* and *non-CpANGs*. It is important to remark that this effect occurs exclusively with PIF-regulated genes: by using the same criteria with a random subset of non-PIF regulated genes we didn't observe any significant difference in the fold changes (Figure 3.11 G). Overall these results confirm that PIFs in Arabidopsis conferred a higher degree of regulation to a subset of chloroplast light-responsive genes during de-etiolation.

This same analysis was repeated with GLK-regulated genes. In this case we identified a total 384 homolog genes, being 239 *LRGs* in Arabidopsis. Similarly with PIF-regulated genes, half of these are *non-LRGs* in Chlamydomonas (120), meaning that GLKs conferred them the capacity to respond to light (Figure 3.11 H). Interestingly, almost all GLK-regulated LRGs are light-induced in Arabidopsis (95%), while in Chlamydomonas we observed a higher proportion of these genes (63%). We also observed significantly higher FC values of chloroplast GLK-regulated light induced genes, compared with Chlamydomonas, although with GLK the difference with *non-CpANGs* is not as striking as with PIFs (Figure 3.11 I). This effect is also exclusive of GLK-regulated genes (Figure 3.11 J). As with PIFs these results confirm that GLKs conferred higher degree of regulation of chloroplast light-responsive genes during de-etiolation. However, with this data we cannot establish whether this higher degree of regulation is caused by a gained repressive effect in the dark or inductive effect in light; this in particular could unveil whether the evolution of light response in higher plants favored a higher

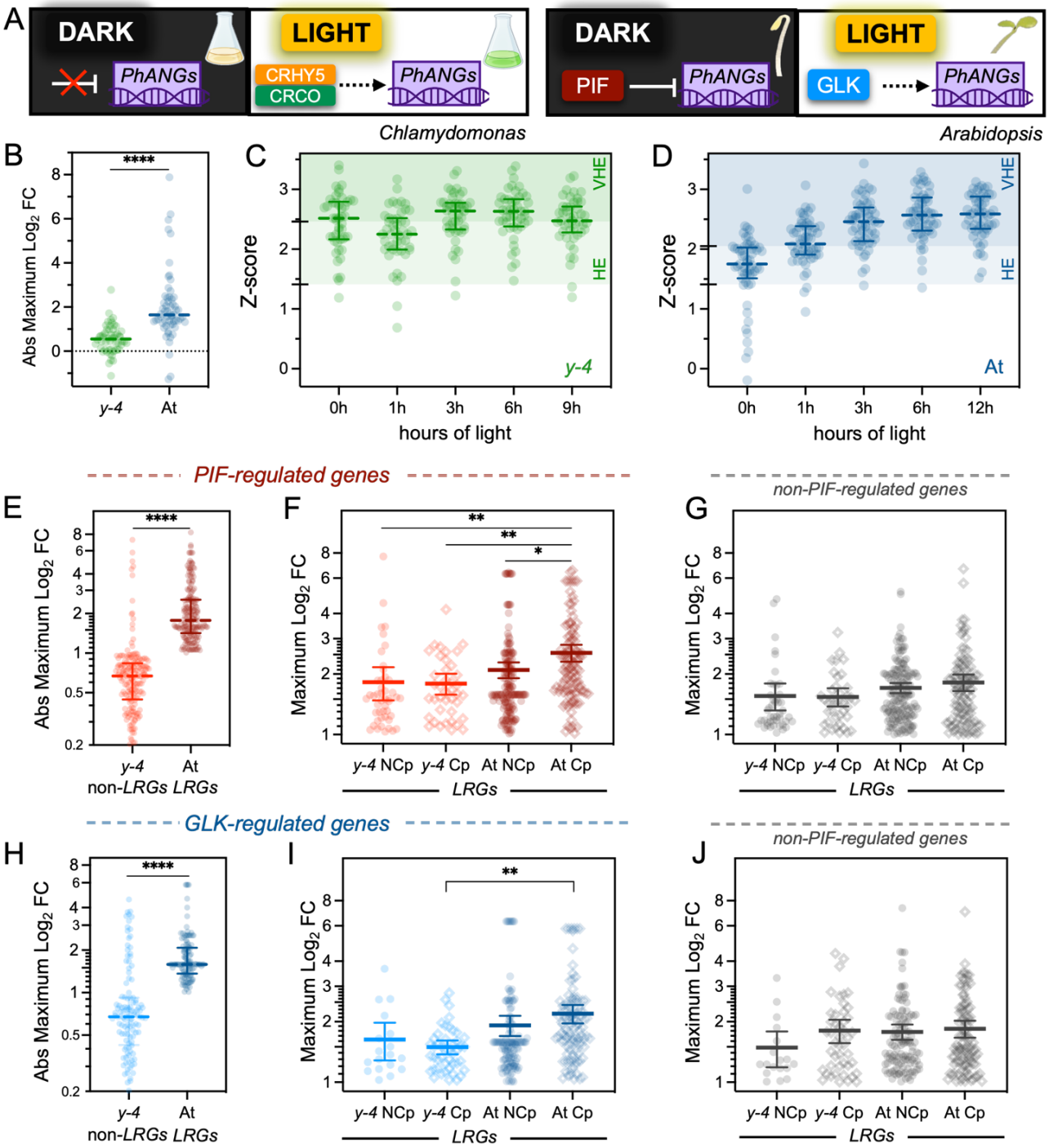


Figure 3.11: Analysis of PIF- and GLK- regulated genes during de-etiolation in At Light and their homologs in *y-4* Light. A. PIFs are well-known Arabidopsis repressors of *PHANGs* in dark, while light triggers their expression through GLKs (and other TFs). Chlamydomonas does not feature PIFs nor GLKs, likely causing absence of *PHANGs* repression in dark, while *CRHY5*, *CRCO* and/or other TFs in light may induce their expression in light. In this and the following figures we tested this hypothesis. B. Distribution of maximum log_2FC values (1h, 3h, 6h, 9h or 12h vs 0h) of *PHANGs* and median (colored discontinuous line) for *y-4* Light (green) and At Light (blue). C,D. Distribution of *PHANGs* expression (each standardized by their Z-score) and median (colored discontinuous line) with interquartile range in both *y-4* Light (B, green) and At Light (C, blue) RNA-seq. Thresholds for highly expressed genes (HE, 5% highest expression values, light shade) and very highly expressed genes (VHE, 1% highest expression values, dark shade) are highlighted. E,F,G. Analysis of PIF-regulated genes. Arabidopsis PIF-regulated genes were obtained from Pfeiffer et al., 2014. H,I,J. Analysis of GLK-regulated genes. Arabidopsis GLK-regulated genes were obtained from Tu et al., 2022. Gene homologs were defined according to Craig et al., 2023. E,H. Distribution of maximum log_2FC values and median (discontinuous line) of PIF- (E, red) and GLK- (H, blue) regulated gene homologs that are *LRGs* in At Light (At, dark color) and *non-LRGs* in *y-4* Light (*y-4*, light color). F,I. Distribution of maximum log_2FC values and mean (continuous line) with 95% confidence interval of PIF- (F, red) and GLK- (I, blue) regulated gene homologs which are *LRGs* in both RNA-seq, separated into *CpANGs* (Cp, circles) and *non-CpANGs* (NCp, diamonds). G,J. Control using non-PIF regulated gene homologs and same parameters as F,I.

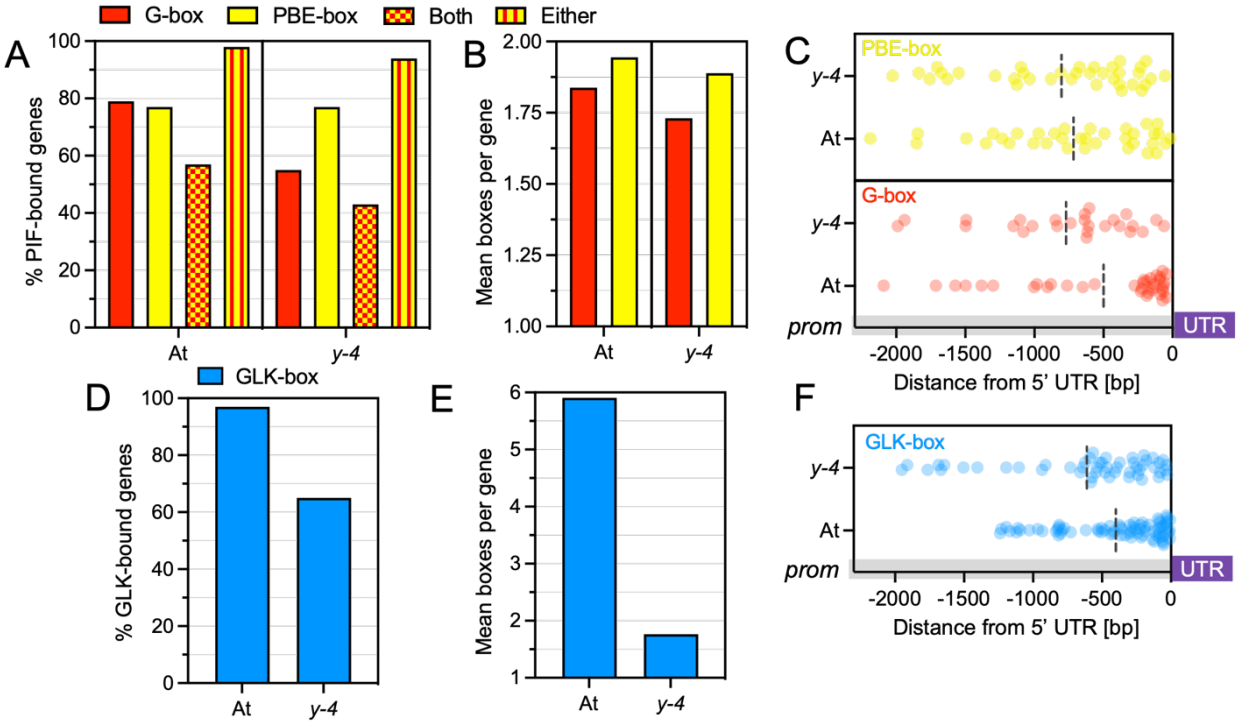


Figure 3.12: Analysis of promoter motifs in GLK- and PIF-bound genes in Arabidopsis and their homologs in Chlamydomonas. PIF- and GLK-bound genes in Arabidopsis were also obtained from Pfeiffer et al., 2014 and Tu et al., 2022, respectively. A region of 2 Kbp upstream of 5' UTR was employed for motif search. We looked for G-boxes (CACGTG) and PBE-boxes (CACATG & CATGTG) in PIF-bound genes, and GLK-boxes (GAATC & GATTC) in GLK-bound genes. A,D. Percentage of genes containing at least one G-box and/or PBE-box in PIF-bound genes (A), and containing at least one GLK-box in GLK-bound genes (D). B,E. Mean number of G-boxes or PBE-boxes in PIF-bound genes (B), and of GLK-boxes in GLK-bound genes (E), in genes that contain at least one box. C,F. Distance distribution in bp from 5'UTR of G-boxes and PBE-boxes in PIF-bound genes (C), of GLK-boxes in GLK-bound genes (F). prom: promoter.

capacity to repress photomorphogenesis, consistent with the role of COP1-SPA and PIFs in the dark or higher capacity to induce this process in light through GLKs, HY5 and BBOX TFs.

Either way, it is important to notice that this higher degree of regulation exerted by PIFs and GLKs is in a reduced number of cases the consequence of their direct regulation, while in the majority of cases is a result of an indirect effect that involves other TFs. This is especially true for PIF-regulated genes where we identified only 37 homolog direct targets, compared with 190 homolog direct targets. PIFs and GLKs direct regulation involves their binding to G-boxes (CACGTG) and PBE-boxes (CACATG & CATGTG), and GLK-boxes (GAATC & GATTC), respectively. We found a higher percentage of PIF-direct targets feature G-boxes compared with Chlamydomonas, but this does not happen with PBE boxes which are equally frequent (Figure 3.12 A). In genes where these boxes are present, no difference was found in the amount of them between species (Figure 3.12 B). Interestingly, Arabidopsis G-boxes and PBE-boxes are closer to the 5' UTR compared with Chlamydomonas, and in the case of G-boxes most of them are found in the first 250 bp upstream of the 5' UTR (Figure 3.12 C). GLK-boxes are found in almost all GLK-regulated genes, while in Chlamydomonas only around 60% feature them (Figure 3.12 D). In particular, the frequency of GLK-boxes in the promoters of these genes in Arabidopsis is much more higher compared to Chlamydomonas (Figure 3.12 E), and also

are found closer to the 5' UTR (Figure 3.12 F). Altogether, these results suggest that sequences of PIF and GLK-direct target genes have evolved for better binding capacity of these TFs, but we cannot discard that their homologs in Chlamydomonas may also have the ability to be regulated by them, especially in the case of PIFs.

A non-PIF dependent light signaling mechanism regulates dark repression of PIF-direct targets in Chlamydomonas

In this section we aimed to evaluate whether lower upregulation of photosynthesis genes in Chlamydomonas is caused by the absence of PIF-mediated repression in the dark, and therefore if emergence of PIFs in higher plants conferred the capacity to repress the expression of these genes in the dark. For this purpose, as we cannot directly compare absolute photosynthesis transcript levels in the dark between different species in different experiments, we tested the capacity of Arabidopsis and Chlamydomonas to repress photosynthesis genes in the dark after their growth in light conditions. For this analysis we chose photosynthesis genes which are PIF-direct targets and homologs between species. We found three genes that fulfilled these specs: *AtPSB27*, *AtPSBQ-2* and *AtPETC* in Arabidopsis, and *CrPSB27*, *CrPSBQ1* and *CrPETC1* in Chlamydomonas.

We first performed a canonical de-etiolation experiment with Arabidopsis seedlings using wt (Col-0) seeds with the aim of confirming the induction of these genes during de-etiolation, as observed in the cotyledons from Burko et al., 2020 RNA-seq. Seedlings were grown for two days in the dark and then transferred to light; de-etiolating seedlings transitioned from skotomorphogenic growth (elongated hypocotyl, closed cotyledons and apical hook) to photomorphogenic growth (hypotocyl elongation arrest, open cotyledons, hook opening and greening), as expected (Figure 3.13 A). Moreover, they recovered photosynthetic capacity upon exposure to light, as shown by the increase in FvFm up to 0.7 after 24h (Figure 3.13 B), and the accumulation of chlorophylls (Figure 3.13 C) and carotenoids (Figure 3.13 D). Light-dependent upregulation of photosynthesis genes in these seedlings was confirmed by q-PCR with *AtPSBQ-2*, *AtPSB27*, and additionally with *AtLHCB5* (a PIF-regulated but not direct target gene), which gradually increased their expression in the first 24h (Figure 3.13 E).

Next, we tested the capacity of Arabidopsis and Chlamydomonas to repress chosen genes in the dark. For Arabidopsis, we germinated Col-0 seeds in light conditions and these were grown for three days in light, before being transferred to light (Figure 3.14 A). Light germinated seedlings had very short hypocotyls, with open and big cotyledons (Figure 3.14 B), and showed maximum photosynthetic capacity and PSII activity (Figure 3.14 C,D). Dark adaptation of these seedlings didn't affect their morphology as well as their photosynthetic activity in the first 6h, while after 24h they showed slightly longer hypocotyls and lower photosynthesis levels. However, since after 24h senescence effects could affect our analysis, we decided to test expression of chosen genes after 6h of darkness. We

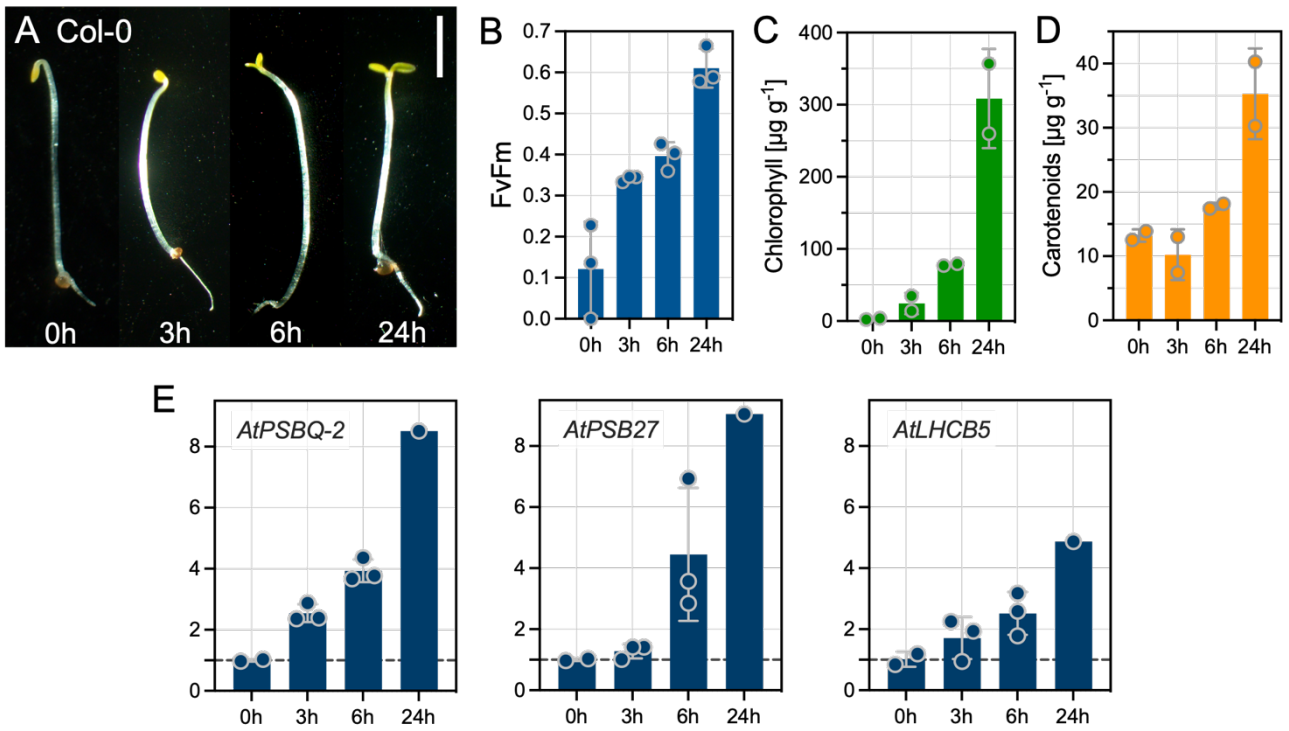


Figure 3.13: Analysis of PIF-regulated genes in de-etiolating Arabidopsis seedlings: 2-day-old wt (Col-0) seedlings were analyzed in the dark and after exposure to light at different time points. A. Representative pictures of wt Arabidopsis seedlings, de-etiolating from dark (0h) to light (3-6-24h). B. FvFm values measured on 20 cotyledons from 3 independent replicates of de-etiolating seedlings, after 30 min dark treatment. C,D. Concentration of total chlorophylls (C) and carotenoids (D) per seedling mass from 2 independent replicates of de-etiolating seedlings were obtained using Lichtenthaler & Buschmann, 2001 procedure. E. Expression of 3 *pifq* regulated genes (*AtPSBQ-2*, *AtPSB27* and *AtLHCB5*) in light (3-6-24h) related to wt dark (Col-0 0h, discontinuous line). Scale bar = 2 mm.

observed lower gene expression levels in the dark of *AtPSBQ-2*, while the rest of the genes didn't feature strikingly lower levels in this condition (Figure 3.14 E).

In Chlamydomonas, we replicated our de-etiolation setup but with opposite light conditions: we started *y-4* and CC-124 wt cultures in light conditions in HSA, and after a 3h acclimation in minimal medium (HSM) these cultures were transferred to dark. To discard effects of carbon starvation in our analysis, we compared our dark adapted cultures with cultures having the same time of acclimation in HSM but in light conditions (Figure 3.15 A). The effect of dark on photosynthetic activity changes between *y-4* and wt cells: in *y-4* cells FvFm value in light is below optimal (which should be around 0.7) and does not change with dark, but dark clearly represses efficiency of PSII (Figure 3.15 B); in wt cells, dark has the opposite effect at 6h, inducing both FvFm and overall PSII activity, compared to light (Figure 3.15 C). Independent on these effects on photosynthesis and surprisingly, in both strains we found a striking repression of chosen photosynthesis genes after 6h in the dark, being this repression even more pronounced compared with Arabidopsis (Figure 3.15 D,E). Interestingly, there seems to be certain degree of correlation in the repression of these genes between species: the most repressed of them is *CrPSBQ1 – AtPSBQ-2*, followed by *CrPSB27 – AtPSB27*, and lastly *CrPETC1 - AtPETC*. Overall, we expected a higher degree of repression of the chosen *PhANGs* in Arabidopsis, where only *AtPSBQ-2* was clearly repressed; however, given that during de-etiolation many light-dependent

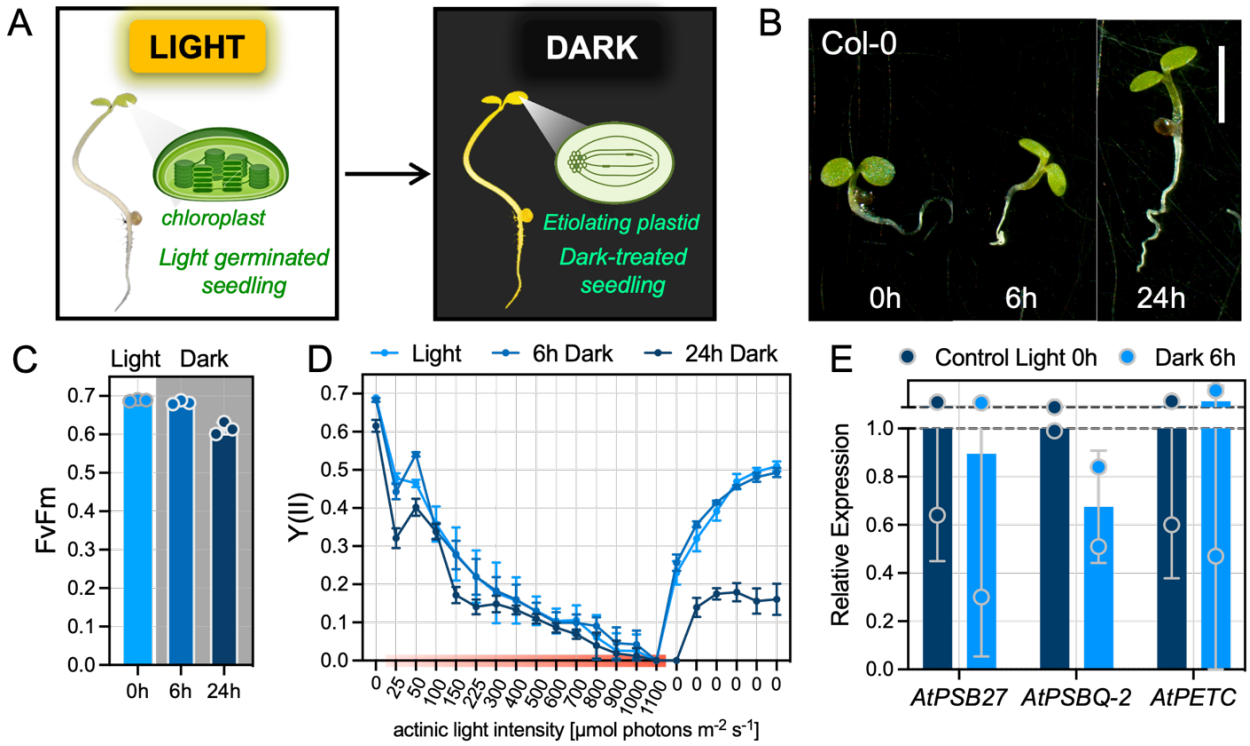


Figure 3.14: Analysis of PIF-regulated genes during dark adaptation in Arabidopsis. A. Light-germinated seedlings were grown for 3 days in light conditions, and then transferred to dark to evaluate repression of PIF-direct target genes in this condition. B. Representative pictures of wt Arabidopsis seedlings in light before dark adaptation (0h), and afterwards at 6h and 24h. C,D. FvFm values (C) and light curve with increasing actinic lights (D) measured on 20 cotyledons from 3 independent replicates of dark adapting seedlings, after 30 min dark treatment. E. Expression of 3 *pifq* direct target genes (*AtPSBQ-2*, *AtPSB27* and *AtPETC*) at 6h of dark adaptation related to light before treatment (Control light 0h). Scale bar = 2 mm.

transcriptomic events are delayed compared with Chlamydomonas, it is likely that this also happens during dark adaptation. Independent on this, dark-triggered repression of these genes in Chlamydomonas is striking, and suggests the presence of an alternative repressive ancestral mechanism in the dark that is not related with PIFs.

Red light can trigger de-etiolation in Chlamydomonas y-4 cells

In Arabidopsis de-etiolation is triggered primarily by the perception of red light by phytochromes which in turn interact with PIFs modulating early light response. Although Chlamydomonas can see red light (Beel et al., 2012), no phytochromes were identified in this species, neither in other microalgae. This opens two possible scenarios: 1) de-etiolation of *y-4* cells may be triggered exclusively by blue light, or 2) red light may also have a role in this process. In either case, this could reveal the primitive light perception mechanism that triggers de-etiolation response. We tested both scenarios by performing a de-etiolation experiment in the same conditions as our RNA-seq setup, but using red light or blue light (Figure 3.16 A). We found that exclusive contributions of blue and, surprisingly, of red light can trigger de-etiolation with almost the same performance as white light. Differences were found in cell division and morphology, obtaining triple and double the amount of cells after 24h, under white and

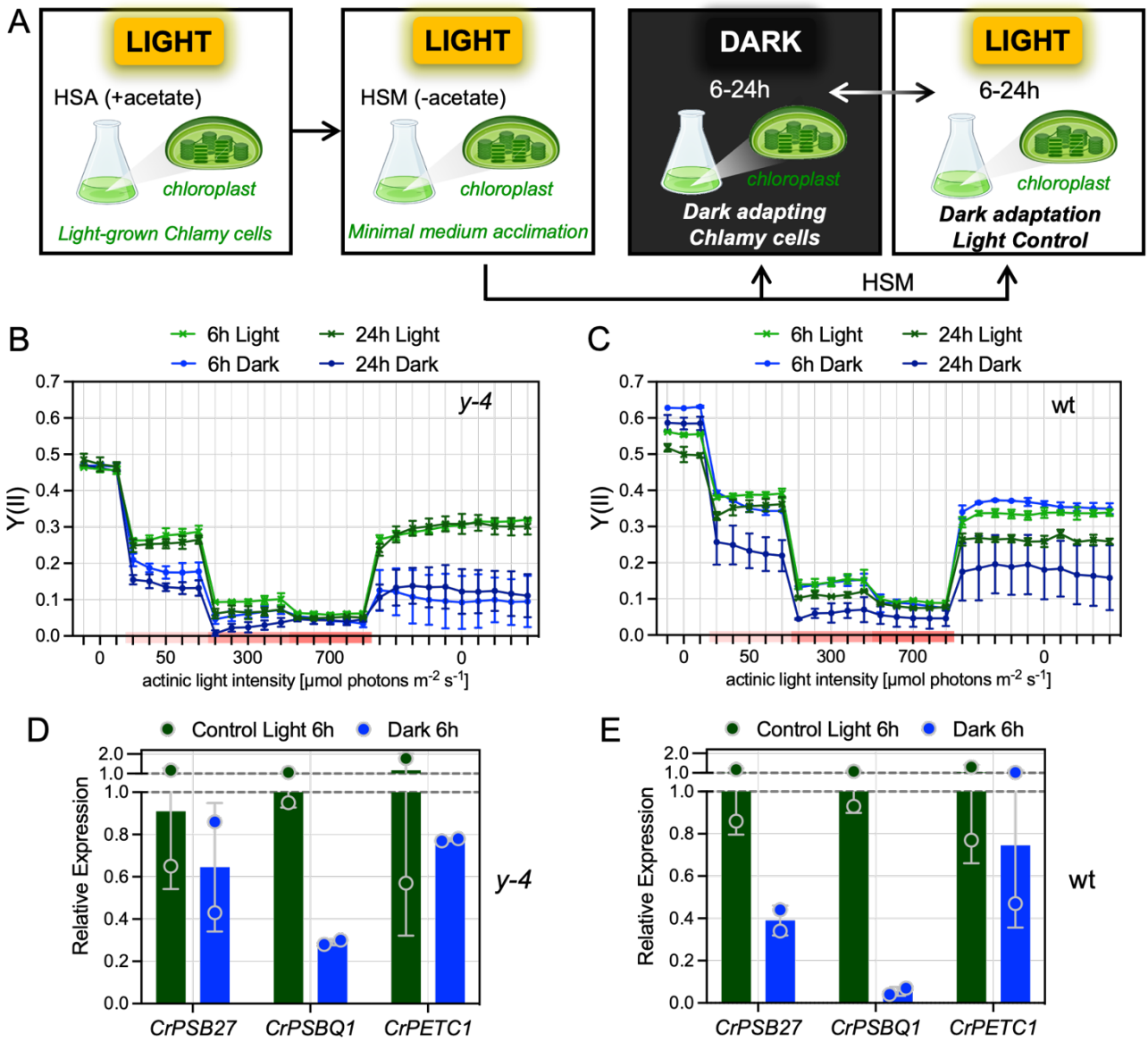


Figure 3.15: Analysis of PIF-regulated gene homologs during dark adaptation in Chlamydomonas. A. Cell cultures for *y-4* and wt (CC-124) strains were prepared and grown in light and the presence of acetate (HSA) for 5 days; next, cultures were subjected to a 3h acclimation in minimal medium HSM, before transfer to dark. To discard carbon starvation effects during this analysis, samples in dark were compared with light samples with the same total time of HSM acclimation. B,C. Light curve with three different increasing actinic lights of dark adapting *y-4* cells (B) and wt cells (C). D,E. Expression of the 3 PIF direct target gene homologs in Chlamydomonas (*CrPSB27*, *CrPSBQ1*, *CrPETC1*) at 6h of dark adaptation related to its control in light (Control Light 6h), for *y-4* cells (D) and wt cells (E).

red light, respectively, while cells under blue light did not divide and were bigger in size (Figure 3.16 B). Recovery of photosynthesis parameters was very similar between light regimes: no differences in the recovery of FvFm were found between white and blue light, while under red light this recovery was slightly slower (Figure 3.16 C); however, maximum PSII efficiency after 24h was only observed with white light, and no differences were found between red and blue (Figure 3.16 D); finally, the rate of accumulation of chlorophylls was identical in the first hours of de-etiolation, but after 24h we observed higher levels for white light, followed by blue and lastly red (Figure 3.16 E). Overall, these results suggests that although with the exclusive contributions of red and blue light cells can de-etiolate, both are required to fully and optimally complete this process.

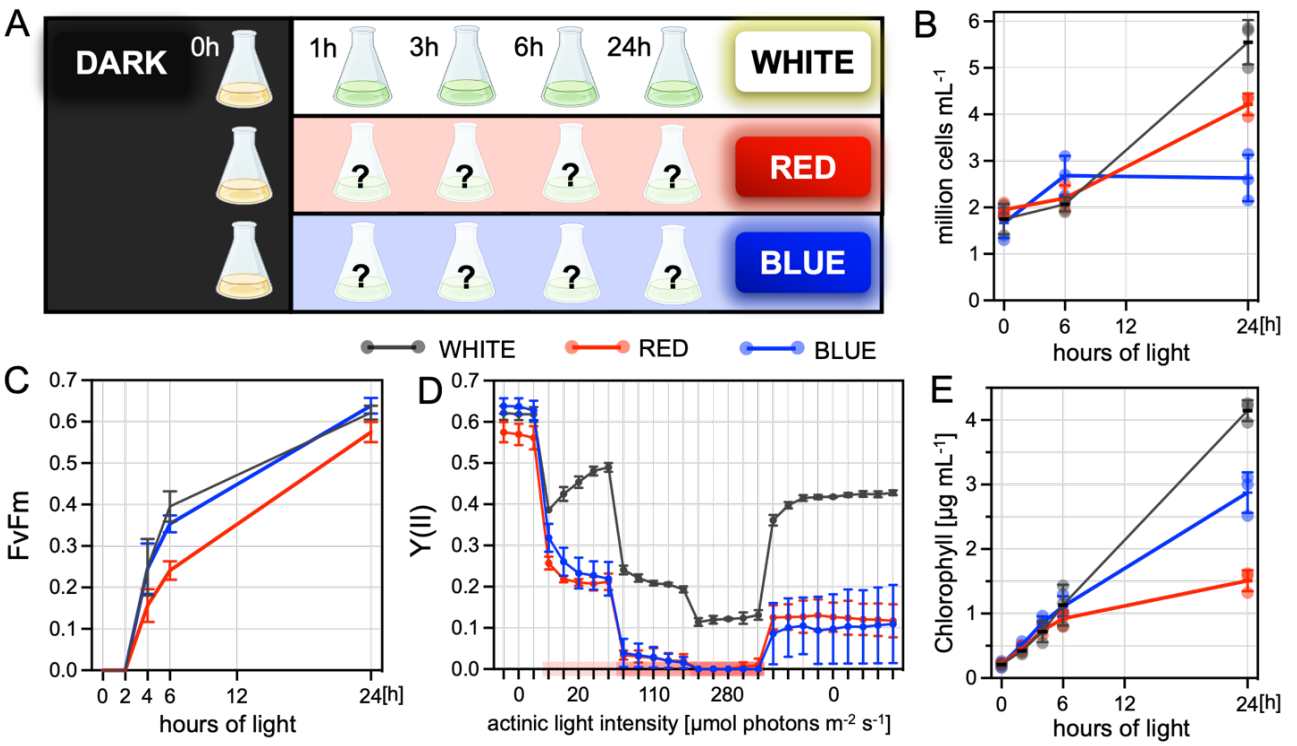


Figure 3.16: Growth and photosynthesis phenotype of de-etiolating dark-grown *y-4* cultures upon red and blue light. A. Schematic view of the experiment: *y-4* cells were grown in the dark in the same conditions (including pre-acclimations) of *y-4* Light RNA-seq; once etiolated, cultures were exposed to red and blue light (and also to white light as a control), and de-etiolation under these light regimes was tested both in terms of photosynthesis and gene expression. Here we measured cell concentration (B), FvFm (C), electron transfer efficiency under increasing actinic lights after 24h of de-etiolation (D) and total chlorophylls (E).

In order to evaluate the effect of each light on the regulation of target genes involved in de-etiolation, we measured the expression of key differently light-regulated genes during this process as observed with our RNA-seq. For this purpose we chose four genes: *LHCSR1* (early light induced), *LHCA6* (late light induced), Cre16.g688638_4532 (early light repressed, hereafter called *GuCy*) and *POR1* (3h light induced). We observed similar expression profiles of these targets genes when de-etiolating with blue and red light, compared with white light (Fig. 3.17 A), and with the expression profiles obtained from our RNA-seq (Fig. 3.17 B). However, the degree of regulation of blue and red light were generally lower compared with white light. In particular, under red light *LHCSR1* levels were higher than blue, and viceversa for *LHCA6*. This is consistent with an overall slower de-etiolation under red light compared with blue and white light, as observed with the recovery of FvFm. Overall, these results suggest that Chlamydomonas features an ancestral light signaling pathway for de-etiolation which is also driven by red light but is not mediated by phytochromes nor PIFs.

A Chlamydomonas gene co-expression network reveals potential novel transcription factors involved in chloroplast biogenesis

In order to predict candidate transcription factors that regulate chloroplast biogenesis during de-etiolation, we built a gene co-expression network (GCN) using all transcriptome datasets available

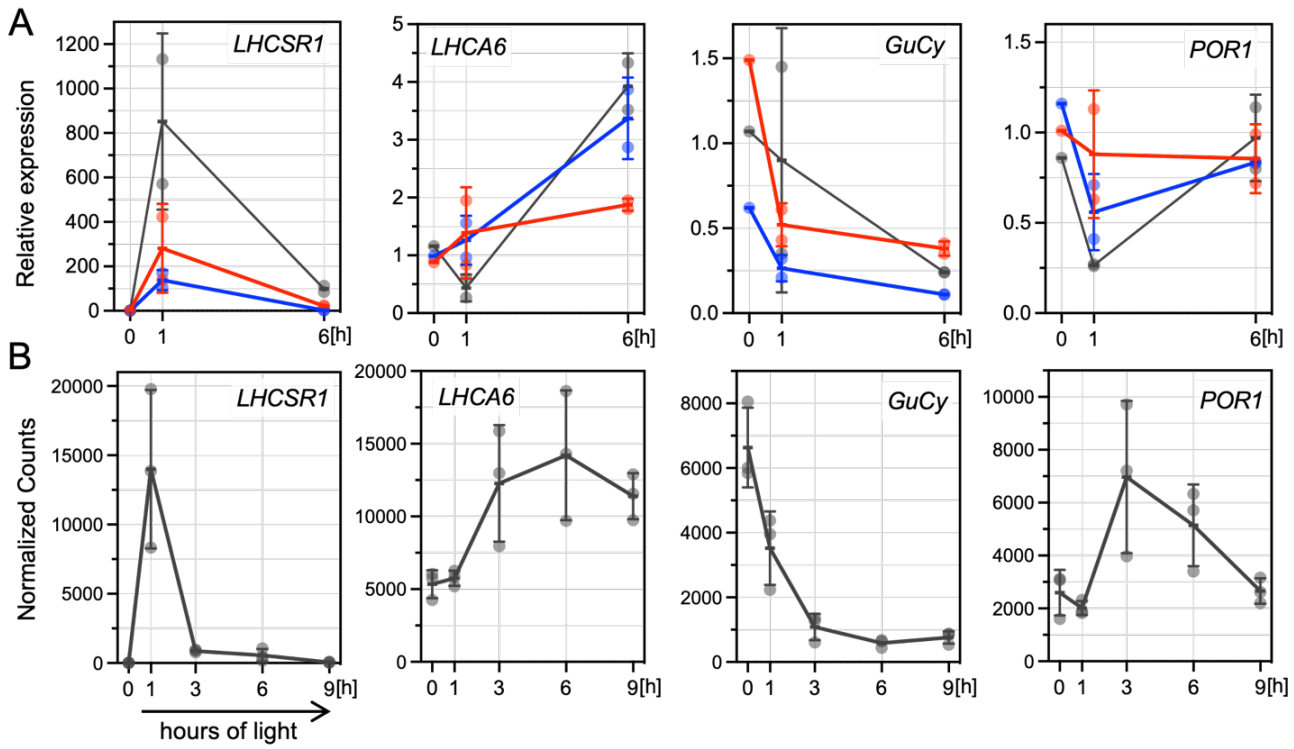


Figure 3.17: Growth and photosynthesis phenotype of de-etiolating dark-grown *y-4* cultures upon red and blue light. A. Schematic view of the experiment: *y-4* cells were grown in the dark in the same conditions (including pre-acclimations) of *y-4* Light RNA-seq; once etiolated, cultures were exposed to red and blue light (and also to white light as a control), and de-etiolation under these light regimes was tested both in terms of photosynthesis and gene expression. Here we measured cell concentration (B), FvFm (C), electron transfer efficiency under increasing actinic lights after 24h of de-etiolation (D) and total chlorophylls (E).

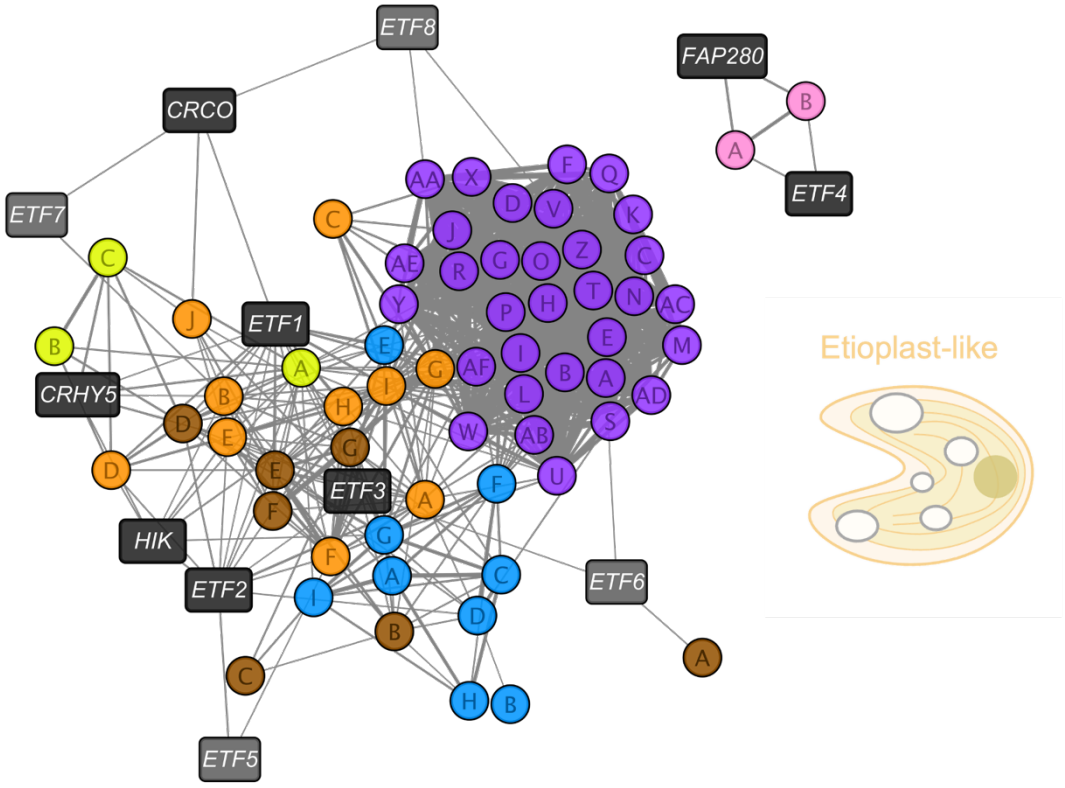
in Chlamydomonas. Here, interactions between genes were established if there was significant correlation in their expression across different transcriptome datasets, according on the “guilt-by-association” principle (Orduña et al., 2023). This global GCN was afterwards employed to build specific subnetworks, one for each phase of chloroplast biogenesis of Figure 3.7 (Figure 3.18). This subnetwork contained all the interactions between all *CpANGs* employed for the expression profiles, plus the five most interacting TFs with these genes obtained from different subsets of LRTFs: only early LRTFs (defined as being LRGs at 1h) for the early phase, early and mid LRTFs (LRGs at 3 and/or 6h), and all LRTFs (therefore including LRTFs at 9h). This was done because we assumed that *CpANGs* are light-responsive as a consequence of the alteration in gene expression of the TFs that regulate them. Many of these most interacting LRTFs also interacted with other TFs, which were included in the networks if these in turn had at least an interaction with a target *CpANG* (linking nodes). For those orphan *CpANGs* nodes we also included the top 1-2 LRTFs that interacted with them, if possible.

By doing so, we found during the early phase (Figure 3.18 A) that chloroplast ribosomes nodes were clustered all together with a high degree of interactions and co-occurrence values (here represented with thicker edges), while the rest of the nodes sparsely clustered by biological process, showing many interactions and in some cases high co-occurrence values with other biological processes. Key

genes involved in early light response such as *LHCSR1* from Photoprotection (A) and *PSY1* from Carotenoid Biosynthesis (H) are in the center of the network and showed the highest number of interactions. Interestingly, gluconeogenesis nodes are highly connected in this network, although these genes are light-repressed, in contrast to the rest of the nodes. Fatty acid desaturation nodes were the sparsest in this network, but some of these nodes show a high degree of interactions and are centered. This indicates that all of these biological processes mentioned are regulated together during the early phase. This task is likely to be performed by CRHY5, which was found among the most interacting LRTFs with these *CpANGs.* This genes was already described as a regulator of early light acclimation during dark-to-light transition: consistent with this, we found that it is highly co-expressed with *LHCSR* and carotenoid genes, which are involved in photoprotection. More importantly, having found *CRHY5* in this network validates the way we are performing this analysis. In contrast, *CRCO*, another key regulator of early light response in Chlamydomonas, showed very little interactions with *CpANGs*, but was highly co-expressed with many TFs, only a few of them though were LRTFs and interacted with *CpANGs* from the early phase. This indicates that the role of CRCO extends beyond regulating early light responses. The most interacting LRTF we found, has not been reported so far and was named as ETF1 (early TF), which was co-expressed with at least one gene from all chloroplast processes of the early phase. Remarkably, this TFs was among the 13 TF which were upregulated in y-4 Light and downregulated in wt12 Light (Figure 3.9), which gives more support to its specific role in chloroplast biogenesis. Among the other most interacting LRTFs found, one is a putative histide kinase photoreceptor (HIK), while the other two (ETF2 and ETF3) have not been reported yet: all of them co-express mainly with genes from carotenoid biosynthesis, gluconeogenesis and fatty acid desaturation processes. The two VIPP genes are highly induced by light at 1h, but are likely regulated in a different manner compared to the rest of the chloroplast biological processes: these two genes didn't show any interaction with the rest of the nodes, neither with the most interacting TFs; also when looking at the TFs that mostly interacted with VIPPs, we found FAP280 and ETF4, which also do not interact with the main network. It is worth to point out that all TFs of the early phase, including linking nodes and TFs of the orphan nodes, are early light upregulated (up & down TFs are upregulated at 1h and downregulated at later time points). It is therefore unlikely that these *CpANGs* are lowly expressed in the dark as a consequence of a repressive mechanism, as occurs in Arabidopsis with PIFs.

In the mid phase (Figure 3.18 B), unsurprisingly photosynthesis and tetrapyrroles biosynthesis nodes form big, but not mixed, cluster with high co-occurrence and high degree of interactions; interestingly, many nodes from fatty acid biosynthesis were deeply embedded in this cluster, indicating that these are highly required in parallel with the synthesis of the components of the ETC, to form the first thylakoid membranes. In the periphery of this giant cluster, we found many genes necessary for the assembly of the photosystem components, and more outside the TOC-TIC genes: this is not surprising, as these genes are already induced at 1h (Fig. 3.7 B), compared to the rest of the biological

A *EARLY PHASE*



Transcription Factor (Most interacting)
Transcription Factor (Linking nodes)
Carotenoid Biosynthesis
Gluconeogenesis
Photoprotection
Fatty Acid Desaturation
VIPP (Vesicle Inducing Plastid Protein)
Chloroplast Ribosomes

Early Up: *CRCO, HIK, FAP280, ETF1, ETF3, ETF4, ETF5, ETF6, ETF7, ETF8*

Early Up & Down: *CRHY5, ETR2*

Transcription Factors	
CRHY5	-
CRCO	-
FAP280	-
HIK	-
Cre01.g002250_4532	*ETF1*
Cre12.g514400_4532	*ETF2*
Cre02.g101150_4532	*ETF3*
Cre13.g586450_4532	*ETF4*
Cre16.g677382_4532	*ETF5*
Cre02.g084550_4532	*ETF6*
Cre02.g087600_4532	*ETF7*
Cre02.g079200_4532	*ETF8*

Chloroplast Ribosomes			
PRPL1	A	*PRPL29*	Q
PRPL3	B	*PRPL31*	R
PRPL4	C	*PRPL32*	S
PRPL7	D	*PRPL33*	T
PRPL9	E	*PRPL34*	U
PRPL11	F	*PRPL35*	V
PRPL13	G	*PRPS1*	W
PRPL15	H	*PRPS5*	X
PRPL17	I	*PRPS6*	Y
PRPL18	J	*PRPS10*	Z
PRPL19	K	*PRPS13*	AA
PRPL21	L	*PRPS15*	AB
PRPL22	M	*PRPS16*	AC
PRPL24	N	*PRPS17*	AD
PRPL27	O	*PRPS20*	AE
PRPL28	P	*PRPS21*	AF

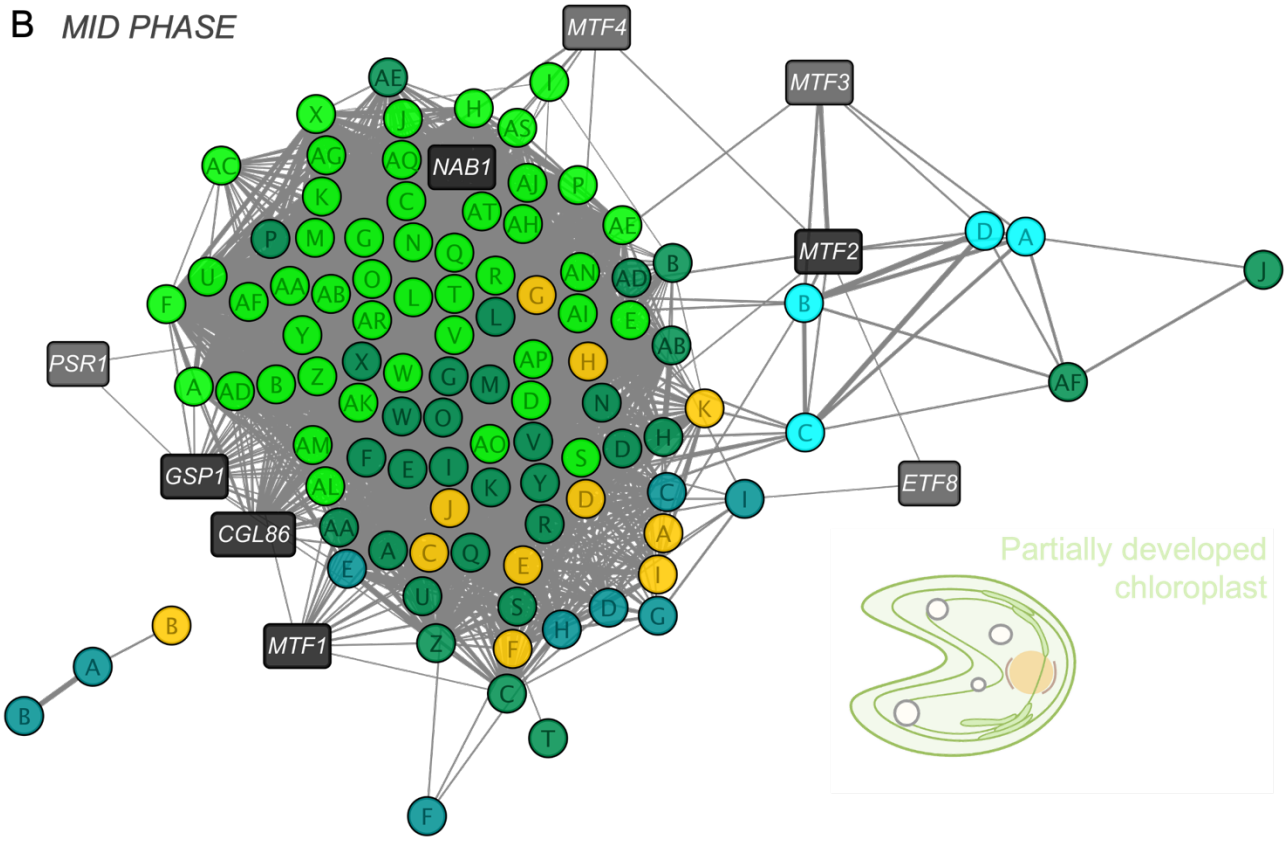
Carotenoid Biosynthesis	
BKT1	A
CHYB1 (BCH)	B
CRTISO1	C
CVDE1	D
LCYB	E
LCYE1	F
PDS1	G
PSY1	H
ZDS1	I
ZEP1	J
PRPS21	AF

VIPP	
VIPP1	A
VIPP2	B

Photoprotection	
LHCSR1	A
LHCSR3A	B
LHCSR3B	C

Gluconeogenesis	
AGP1	A
AGP3	B
AGP4	C
FBA1	D
FBA2	E
FBA3	F
FBP2	G
PGI1	H
PGM1	I

FA Desaturation	
Cre06.g288650_4532	A
FAB2	B
FAD2	C
FAD4	D
FAD5A	E
FAD7	F
FAD9	G



Transcription Factors	
NAB1	-
CGL86	-
GSP1	-
PSR1	-
Cre06.g269100_4532	*MTF1*
Cre02.g101850_4532	*MTF2*
Cre08.g364450_4532	*MTF3*
Cre09.g386753_4532	*MTF4*
Cre02.g079200_4532	*ETF8*

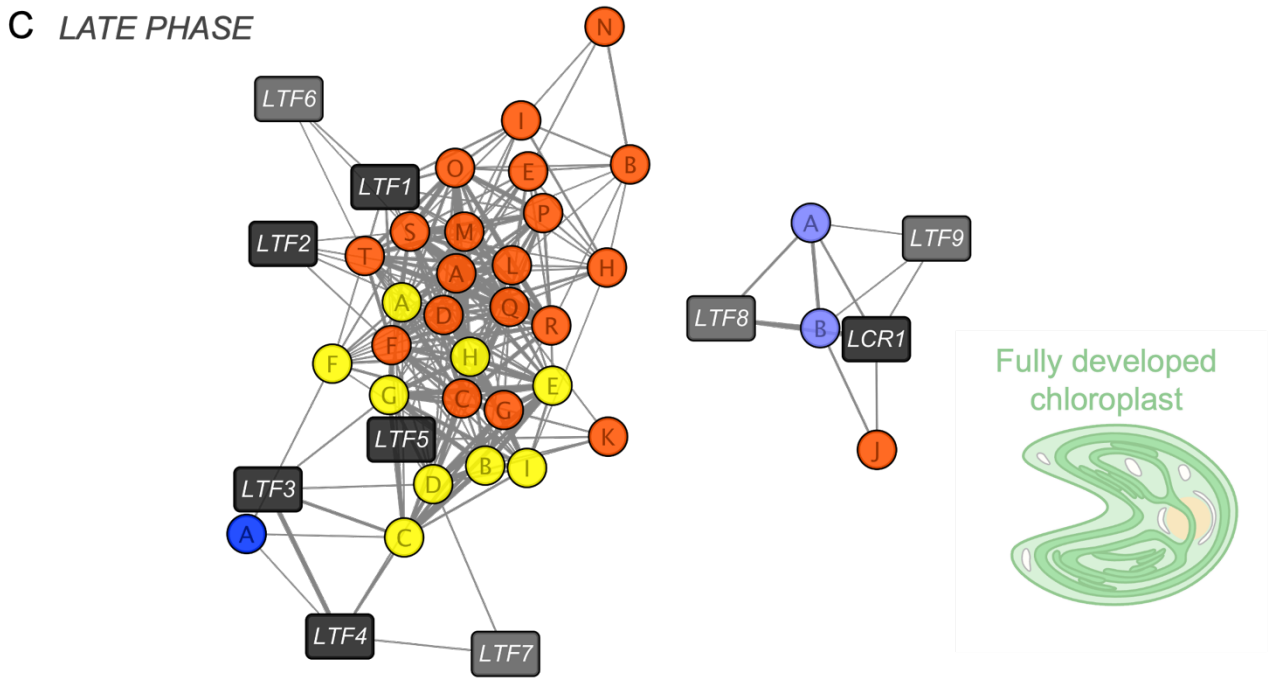
FA Biosynthesis	
ACC1	A
ACP1	B
BC1	C
BCC1	D
BCC2	E
BCX1	F
HAD1	G
KAR1	H
KAS1	I
KAS2	J
KAS3	K

Photosynthesis			
LHCA1	A	*LHCBM4*	X
LHCA2	B	*LHCBM5*	Y
LHCA3	C	*LHCBM6*	Z
LHCA4	D	*LHCBM7*	AA
LHCA5	E	*LHCBM8*	AB
LHCA6	F	*PSB34*	AC
LHCA7	G	*PSBO1*	AD
LHCA8	H	*PSBP1*	AE
LHCA9	I	*PSBQ1*	AF
PSAD1	J	*PSBR1*	AG
PSAF1	K	*PSBW1*	AH
PSAG1	L	*PSBX1*	AI
PSAH1	M	*PSBY1*	AJ
PSAI1	N	*PETC1*	AK
PSAK1	O	*PETM1*	AL
PSAL1	P	*PETN1*	AM
PSAN1	Q	*PETO1*	AN
PSAO1	R	*FDX1 (PETF)*	AO
LHCB4	S	*FNR1 (PETH)*	AP
LHCB5	T	*PCY1*	AQ
LHCBM1	U	*ATPC1*	AR
LHCBM2	V	*ATPD1*	AS
LHCBM3	W	*ATPG1*	AT

Tetrapyrrole Biosynthesis			
ALAD1	A	*CHLD1*	Q
CPX1	B	*CHLG1*	R
CPX2	C	*CHLH1*	S
FLU1	D	*CHLH2*	T
GLTR1 (HEMA1)	E	*CHLI2*	U
GSA1	F	*CHLJ1*	V
GTRBP1	G	*CHLM1*	W
PBGD1	H	*CHLP1*	X
PPX1	I	*DVR1*	Y
TSX1	J	*GUN4*	Z
UROD1	K	*LCAA1*	AA
UROD2	L	*POR1*	AB
UROD3	M	*FEC1*	AC
UROS1	N	*HMOX1*	AD
CAO1	O	*LFO1*	AE
CHL27A	P	*PCYA1*	AF

PS Assembly	
POA2 (PSA2)	A
POA7 (PSA3)	B
PYG7 (CGL71)	C
Y3IP1	D
ALB3A	E
EFG10	F
HCF136	G
LPA1	H
PSB33	I

Chloroplast Protein Import	
TOC34	A
TOC75	B
TIC20	C
TIC100	D



Transcription Factors	
LCR1	-
Cre03.g152150_4532	*LTF1*
Cre13.g580450_4532	*LTF2*
Cre10.g438850_4532	*LTF3*
Cre08.g378800_4532	*LTF4*
Cre01.g001600_4532	*LTF5*
Cre09.g392300_4532	*LTF6*
Cre04.g219600_4532	*LTF7*
Cre03.g212641_4532	*LTF8*
Cre12.g507500_4532	*LTF9*

Krebs Cycle			
ACH1	A	*MME3*	K
CIS1	B	*OGD1*	L
CIS2	C	*OGD2*	M
FUM1	D	*PDC1*	N
IDH2	E	*SCLA1*	O
IDH3	F	*SCLB1*	P
MDH2	G	*SDH1*	Q
MDH3	H	*SDH2*	R
MDH4	I	*SDH3*	S
MDH5	J	*SDH4*	T

Beta Oxidation	
ACX1	A
ACX2	B
ACX3	C
ACX4	D
ECH3	E
HIBCH1	F
KAT1	G
LCS3	H
RED	I

CCM (Low CO_2)	
LCIB1	A
LCIC1	B

Galactolipid Biosynthesis	
MGD1	A

Figure 3.18: Gene co-expression networks (GCN) showing interactions between genes of the main chloroplast biological processes and most interacting *LRTFs* with these genes, separated into each of the three phases of expression during chloroplast biogenesis (See Fig. 3.7): early phase (A), mid phase (B) and late phase (C). Global GCN was created by TOMSBio lab using all Chlamydomonas transcriptome datasets from the Sequence Read Archive (SRA) and following already described procedure (Orduña et al., 2023). Networks for each phase were retrieved from this global GCN, using all selected genes from chloroplast biological processes from Fig. 3.7, plus the 5 most interacting TFs with these genes (Most interacting). In many cases these also interact with other TFs, which were included if these also interacted with chloroplast genes (linking nodes). We also included 1-2 TFs interacting with orphan chloroplast nodes, as in the case of VIPP (A) and CCM low CO_2 (C). TF nodes include the name of the gene if present; otherwise, they were named as (early- (E), mid- (M) or late- (L) TF). IDs of these TFs, as well as the identity of each chloroplast node is indicated downwards. Time and direction of light-responsiveness is also specified for each TF (LR- at 1h – early, 3-6h – mid, 9h – late). For TFs of the late phase an asterisk is put if peak of gene expression is found at 9h. Thickness of the edges is proportional to the co-occurrence values between nodes.

processes, which began to be induced only after 3h. Most interacting LRTFs with mid phase *CpANGs* are NAB1 (the most interacting), GSP1, CGL86 and MTF1 (mid TF). All of them interact mainly with nodes from photosynthesis, tetrapyrrole biosynthesis and fatty acid biological processes. In contrast, photosystem assembly genes are generally lowly co-expressed with these LRTFs, and only ALB3A (involved in the assembly of the PSII, E) interacted with NAB1, GSP1 and MTF1. Some of them neither interact with the main network, such as POA2 and POA7 (A and B, respectively). This indicates that regulation of expression of the components of the two photosystems is different and separated from the factors responsible for their assembly. In contrast to the early phase, these LRTFs are also differently light-regulated: in particular, NAB1 and GSP1 are downregulated, and could represent potential suppressors of mid phase *CpANGs* in the dark. Remarkably, GSP1 is among the five genes downregulated in y-4 Light and upregulated in wt12 Light (Figure 3.9), which makes it a high potential candidate in regulating chloroplast biogenesis. In addition, among the most interacting LRTFs we found MTF2 which is mostly interacting with TOC-TIC components: in particular this LRTFs is early light upregulated, and likely is responsible for the earlier expression of TOC-TIC components, which are necessary for the later import of photosynthesis and tetrapyrrole biosynthesis proteins.

Finally, in the late phase (Figure 3.18 C) the majority of nodes belong to the enzymes of the Krebs cycle and oxidation of fatty acids, which are clustered together and show both a high degree of interactions and co-correlation between them. Only MGD1 (A) from galactolipid biosynthesis interacts with this network, while no interactions were found for DGD1. The two CCM genes of this phase only interact between them and with a Krebs cycle node separated from the main network. Many so far not reported late LRTFs (LTFs) were found interacting with this late network, many of them find their peak of induction at 9h, though reach light-responsiveness before: this is the case of LTF3 and LTF4, which co-express both with FA beta oxidation genes and MGD1, and of LTF1 and LTF5 which only co-express with Krebs cycle genes; instead, LTF2 is early upregulated and only co-expressed with Krebs cycle genes. Here again, we found that LTF2, LTF3 and LTF4 are among the 13 genes upregulated in y-4 Light and downregulated in wt12 Light (Figure 3.9), which highly supports their specific involvement in chloroplast biogenesis. In particular, these novel LTFs reveal a connection between chloroplast maturation and a late change in metabolism, in favor of accumulating energy in the form of ATP.

Altogether, GCN applied for our transcriptomic analysis of chloroplast biogenesis in Chlamydomonas allowed to identify many LRTFs involved in this process, some of them are already described, such as CRHY5, CRCO or NAB1, and further validate our analysis, and some other are novel such as ETF1, MTF2 and LTF3, and may represent ancestral TFs that evolved in angiosperm plants to perform this function, or that have been lost during evolution of green plants. Remarkably, we found in each phase at least one TF which is oppositely regulated by light in our RNA-seq compared to wt12 Light, which strongly supports their specific role in chloroplast biogenesis, and are candidates for their further study in Chlamydomonas.

Discussion

Light upregulates same biological processes in Arabidopsis and Chlamydomonas regardless of the plastid state

In the previous chapter we designed a *y-4* mutant based de-etiolation system that allowed us to capture main light events on the transcriptome during chloroplast recovery and photosynthetic establishment. To our knowledge this is the first transcriptomic study performed in a *y* mutant strain of Chlamydomonas: so far, characterization of light regulation in this species has been very limited, especially because most works were carried out in the past century when -omics technology was at its dawn. Still, we confirmed in this analysis what observed from Malnoë et al. (1988): etiolated *y* mutants do not particularly induce transcription of photosynthesis genes when exposed to light, as they already accumulate at high levels in the dark. As different y mutant strains were used for their (*y-1*, Sager & Palade, 1954) and our (*chlL y-4*, Suzuki & Bauer, 1992) experiment, this is important not only because it validates our de-etiolation system but also because it shows that this behavior (and others) depends on the *y* phenotype (not having chlorophylls in the dark and an undifferentiated plastid), rather than being an artifactual effect of the mutation of each *y* mutant strain.

Comparing our system with a canonical de-etiolation experiment performed in Arabidopsis seedlings (Burko et al., 2020) using the same criteria for transcriptomic data analysis was fundamental to evaluate actual differences between systems in the light regulation of this process. To our surprise, there were actually many similarities: light in fact regulates the same percentage of genes (40%), and upregulates the same biological processes: the great majority of genes involved in photoprotection, ribosome biogenesis, carotenoid and tetrapyrrole biosynthesis, and photosynthesis were all light induced in both systems. However, differences were observed in the degree of upregulation of these processes: in Arabidopsis de-etiolation requires the high and progressive induction of photosynthesis genes, in parallel with translational activity as shown by the parallel induction of both cytoplasm and chloroplast ribosomal subunits; Chlamydomonas already accumulates high levels of photosynthesis transcripts in the dark, and the build-up of the photosynthetic machinery relies more on translational activity (as shown by the high levels of cytoplasmic ribosomal subunits and rRNA processing), and in the induction of chlorophyll biosynthesis, compared with Arabidopsis where this induction is milder and does not involve all genes from this pathway. This observation is consistent with the relatively low levels of PChlide in the dark in Chlamydomonas *y* mutants (Ford & Wang, 1981), while Arabidopsis must accumulate high levels of POR already in the dark to prevent photobleaching effects caused by the high levels of PChlide that accumulate in the etioplasts (Reinbothe et al., 1996); *PORA* and *PORB* in fact have been found downregulated by light during de-etiolation as previously described (Armarego-Marriott et al., 2019). We also observed an overall delay in the induction of these processes. For instance, photoprotection genes in Chlamydomonas are all upregulated at 1h

of light, while in Arabidopsis their maximum is observed in many cases at 3 or 6h: this is particularly evident in the case of *ELIP* genes, which encode proteins that localize to the antenna proteins and prevent photobleaching damage (Levin & Schuster, 2023), or in the case of *PSBS* and *NPQ* genes (here not shown). This delay is also reflected in Arabidopsis in the synthesis of ribosomes which is coupled to induction of photosynthesis genes, although many of these genes and those associated with the Calvin cycle were also upregulated at 12h in a separate cluster; in Chlamydomonas ribosome biogenesis is upregulated at 1h, while photosynthesis genes are all slightly upregulated at 6h with a very similar pattern. We didn't observe in both Chlamydomonas and Arabidopsis a two-phase of expression of photosynthesis genes as reported in other de-etiolation systems (Armarego-Marriott et al., 2019; Dubreuil et al., 2018), but we cannot discard that the second induction peak may be found later; however, expression pattern of genes involved in pigment biosynthesis and photosynthesis was found very similar to chloroplast biogenesis in wheat leaves (Loudya et al., 2021), except carotenoid biosynthesis genes which are induced at 1h in Chlamydomonas, likely because of the key role of these pigments in photoprotection and ROS detoxification (Erickson et al., 2015).

We also compared our system with a dark-to-light transition of wt Chlamydomonas cells growing under a 12:12 day-night cycle (Strenkert et al., 2019), and using the same criteria for data analysis, not only to further validate our system, but also to discern which light events during de-etiolation are specifically associated to the plastid state, as cells from this experiment already feature a fully developed chloroplast in dark conditions. Also, it is important to point out that these cells are also grown in minimal medium avoiding misleading results due to the influence of a carbon source on light signaling (Dijkwel et al., 1997). Interestingly, we observed that a considerably higher proportion of genes is regulated by light in this system (68%), and at higher degree, but this could be explained by the effect of the circadian clock, which is known to affect 70% of transcriptome in Chlamydomonas, compared to angiosperm plants (40%), that have evolved more independent responses to external cues that allowed them to colonize more demanding environments (Petersen et al., 2022). Regardless of this effect, we observed that the same processes are up- and downregulated by light, with the same timing and expression profile, indicating that light is ultimately the major regulator of de-etiolation rather than the plastid state: however the influence of the plastid state on the transcriptome could have increased significantly with the emergence of angiosperm plants, as the transcriptome of Arabidopsis *pifq* mutants in the dark, which are characterized by partially developed plastids in this condition, feature a high degree of de-regulation that affects thousands of genes (Leivar et al., 2009). However, an interesting difference was observed in the upregulation of photosynthesis genes in Strenkert et al. system, with higher fold induction compared to *y-4* cells: this could be explained by the effect of the circadian clock, as the expression profile of these genes feature an oscillating pattern, which is also synchronized with the expression of chlorophyll biosynthesis genes.

Chloroplast biogenesis in de-etiolating y mutant cells occurs in two distinct phases

A fundamental aspect of studying de-etiolation consists in determining the molecular and biochemical processes by which etioplasts transform into fully developed and photosynthetic chloroplasts. Many works have been performed in the last decade to determine how this transition is achieved, and different de-etiolation systems have been employed for this purpose (Armarego-Marriott et al., 2020). Chloroplast biogenesis has also been explored in wheat taking advantage of the gradual plastid developmental stages that monocot leaves feature along their axes, but it is important to remark that this is not strictly a de-etiolation response, but rather a proplastid-to-chloroplast transition (Loudya et al., 2021). Remarkably, most chloroplast biogenesis works agree that this process is achieved in two distinct phases; however, the evidences underlying this definition differ between experiments and in some cases are contradictory. For instance, in Arabidopsis cell culture system the two phases of de-etiolation are supported by two distinct peaks in the expression of photosynthesis genes, one observed immediately after first exposure to light, and the other observed later after the formation of first thylakoid membranes (Dubreuil et al., 2018). Similarly, two phases of expression of photosynthesis genes were also observed in de-etiolating tobacco leaves: the first phase named “de-etiolation phase” coincided with a first induction of photosynthesis genes but in this case it seemed to be more gradual, but necessary for the first synthesis of thylakoid membranes and photosynthesis establishment; the second phase, where a second induction of core photosynthesis genes was observed, was defined as “chloroplast maturation phase”, and corresponds to a linear increase in chlorophyll content, in parallel with an increase in thylakoid stacking and number of grana per plastid, reflected in even higher photosynthetic activity (Armarego-Marriott et al., 2019). However, this two-phased induction of photosynthesis genes was not reflected in the plastid protein accumulation profiles in de-etiolating Arabidopsis seedlings, where it was shown that these accumulate gradually (Pipitone et al., 2020). Here, instead the authors defined a “structure establishment phase” that allows photosynthetic establishment, followed by a “chloroplast proliferation phase” characterized by a high increase in the number of plastids per cell together with grana stacking. In contrast, chloroplast biogenesis in wheat leaves seems is always a two-phased processes but with an apparent opposite path: a first organelle proliferation phase followed by photosynthetic establishment phase (Loudya et al., 2021).

In this work, using our Chlamydomonas *y-4* based de-etiolation system and thanks to the combined physiological and transcriptomic data, we can shed light on some of the controversial points of chloroplast biogenesis, which might be useful to interpret this process in other systems. In particular we performed a targeted analysis of chloroplast biological processes by monitoring the expression of most *CpANGs*, manually grouping them into expression patterns. Here we did not observe two phases of expression of photosynthesis genes, but this is not surprising as Chlamydomonas *y* mutants already express at relatively high levels photosynthesis genes in the dark prior to de-etiolation;

however, neither in de-etiolating Arabidopsis seedlings an early peak was observed (even considering 15 and 30 min time points) (Burko et al., 2020). It is likely that the induction we observed corresponds to the first peak, as we only monitored light events during the first 9 or 12h where chloroplast maturity is not fully completed, whereas in works where these two peaks were observed de-etiolation is performed in much more extended periods in light (Armarego-Marriott et al., 2019; Dubreuil et al., 2018). Our data suggest that chloroplast biogenesis involves a strong early induction of translational activity, in parallel with the induction of genes involved in photoprotection and plastid biogenesis and repair (VIPPs); energy used during the first stages of chloroplast development probably comes from the consumption of starch, which is consistent with the early downregulation of gluconeogenesis genes. Next light-regulated events involve in order the upregulation of TOC-TIC translocon, PS assembly factors (already induced at 1h but with a maximum at 3h), followed by upregulation of tetrapyrrole biosynthesis genes at 3h and photosynthesis at 6h. This late tetrapyrrole pigment induction is consistent with the lag in the recovery of FvFm in de-etiolating *y-4* cells which only starts after 2h of light: although, we also observed conversion of PChlide to Chlide immediately after light exposure, levels of accumulated PChlide are in *y* mutants are low (Ford & Wang, 1981) and likely first converted chlorophylls are not enough to give detectable PSII reaction centers. All these processes correspond to a linear increase in chlorophyll content and recovery of FvFm during the first 9h. We consider this to be the “photosynthesis establishment phase”.

Furthermore, there are many evidences in our experiment that point to the presence of an additional “maturation phase” in *y* mutants, suggesting that the ancestral light signaling mechanism is also capable of planning chloroplast biogenesis in two distinct phases. 1) Although induction of most *CpANGs* is concluded by 6h of de-etiolation, both FvFm and chlorophyll content linearly increase till 24h, while maximum PSII efficiency is not reached until 48h; therefore, we may find a second peak of induction of photosynthesis and/or tetrapyrrole genes after 9h. 2) We found an induction at 9h of galactolipid biosynthesis genes (*MGD1* and *DGD1*): these are a fundamental component of thylakoid membranes and several de-etiolation experiments show these are accumulated just prior to the maturation phase (Armarego-Marriott et al., 2019; Pipitone et al., 2020); moreover, it is likely this induction anticipates the second peak of expression of photosynthesis genes, as it has been recently found that suppression of galactolipid biosynthesis severely impairs expression of these genes (Fujii et al., 2024). 3) Linear increase in chlorophyll content is not caused by cell expansion, given that overall ODs are unaltered, suggesting an increase in number of thylakoids and/or grana formation. 4) Unpublished data of de-etiolating *y-4* cells from our collaborator (Dr. M. A. Ruiz-Sola, University of Sevilla) shows an increase in O2 production, as cells change from an heterotrophic metabolism in the dark to an autotrophic one after light exposure; however, we observed a 9h upregulation of many genes from the Krebs cycle, which together with the induction of CCM enzymes active under low CO_2 and beta oxidation of fatty acids, indicate high requirements of energy in the late phase, which is likely motivated by primary metabolism such as Calvin cycle and photorespiration (Huang et al., 2018).

Novel transcription factors as candidate regulators of chloroplast biogenesis in Chlamydomonas y mutants

In this work we aimed to evaluate the evolutionary advantage that represented the emergence of key essential regulators of light signaling in angiosperm plants, absent in Chlamydomonas, mainly PIFs and GLKs. PIFs are mainly active in the dark as repressors of photomorphogenesis while GLKs are mainly active in light as positive regulators of chloroplast biogenesis during de-etiolation, and both transcription factors regulate directly or indirectly the expression of thousands of genes (Pfeiffer et al., 2014; Tu et al., 2022). We now know that the emergence of these factors allowed Arabidopsis to regulate at higher degree *LRGs*, and especially those nuclear genes encoding chloroplast proteins; however, in the case of photosynthesis genes, whether this higher degree of regulation is caused by a gained repressive effect of PIFs in the dark, or inductive effect in light triggered by GLKs remains elusive: specifically, we found that both *y-4* and wt Chlamydomonas cells grown in continuous light conditions also repress photosynthesis genes upon transfer to dark, as in Arabidopsis, and in contrast to what observed in dark-grown *y-4* and wt cells prior to de-etiolation. There are two possible explanations for this: 1) Chlamydomonas features a non-PIF dependent repressive mechanism that transiently activates in the dark to repress photomorphogenic response, which could be indirectly caused by COP1-SPA (Tokutsu et al., 2019), or by a novel transcription factor; 2) there are two inductive mechanism for photosynthesis genes, one active during light conditions to keep the induction of these genes high, while the other is triggered by extended growth in dark heterotrophic conditions.

Chlamydomonas still features many key TFs that regulate de-etiolation in angiosperm plants, such as HY5 and CONSTANS (Gangappa & Botto, 2014); however, study of these TFs in Chlamydomonas has been explored in wt strains that do not undergo chloroplast biogenesis, while their function has been associated with photoprotection (Lämmermann et al., 2020; Tokutsu et al., 2019). In this chapter, we evaluated whether these TFs could be also involved in chloroplast biogenesis during de-etiolation and also tried to predict novel TFs that might be implicated. For this purpose, we built GCN using all the available transcriptomic data in Chlamydomonas (Orduña et al., 2023). Here, the criterium to associate TFs to their target chloroplast associated genes is by correlation of their gene expression ("*guilt-by-association*"). We observed that similarly to Arabidopsis (Burko et al., 2020), de-etiolation of *y-4* cells is governed by a transcriptional cascade, where groups of TFs from different families are induced at specific time points during this process. Usually this induction is correlated with positive regulation of their target genes: for instance *HY5*, a key regulator of photomorphogenesis, is induced as soon as light is perceived, while *GLK2* is induced later with chloroplast maturation (Dubreuil et al., 2018). In Arabidopsis we also observed repression by light of *PIF3* and *PIF4*; however, it has to be taken into account that this preliminary GCN only allows to

detect positive correlations in gene expression, and therefore we cannot actually predict possible photomorphogenesis repressors similar to PIFs in Chlamydomonas.

To predict main TFs involved in chloroplast biogenesis we looked for those light responsive TFs in our global GCN that showed the highest number of interaction with early, mid and late light regulated chloroplast biological processes. With this approach we identified many that were already reported to play an important role in the regulation of chloroplast functions. For instance CRHY5 showed a high number of interaction with early light upregulated chloroplast processes, including *LHCSR* and carotenoid biosynthesis genes; however, no interactions were observed with photosynthesis or chlorophyll biosynthesis genes, nor with PS assembly genes, which indicate a specific role of CRHY5 in photoprotection during de-etiolation, as already described (Lämmermann et al., 2020). In contrast, CRCO did not feature a high degree of interactions with photoprotection genes, as we expected from previous works (Tokutsu et al., 2019), but interestingly, it was highly connected with many TFs in the global GCN; it is likely that this acts as an upstream regulator of photoprotection during de-etiolation. Of the mid phase we found NAB1 as the most interacting TF with photosynthesis genes, consistent with its well described role in regulating expression of *LHC* genes (Mussgnug et al., 2005). Interestingly, this gene features in our experiment the same expression profile as any other photosynthesis gene, but with overall lower transcript levels. This suggests that NAB1 might be responsible for the high expression in the dark of these specific genes, and constitutes an interesting TF to further study in our system. Lastly, in the late phase we identified LCR1, a MYB-related TF, which is specifically connected with two important components of the CCM mechanism in low CO_2 conditions, *LCIB1* and *LCIC1*, consistent with its function described two decades ago (Yoshioka et al., 2004). However, recently it was shown that *LCR1* also regulates photoprotection (Arend et al., 2023), and this was also confirmed in our global GCN where this interacts with *LHCSR3A/3B*.

However, we also identified several novel TFs regulating chloroplast biogenesis during de-etiolation: in particular, we found a few acetyltransferases in the early and mid phase: ETF1, MTF1, MTF2 all belonging to the GNAT family of TFs. Very recently it was shown that chromatin remodeling is essential for plastome transcriptional activity and determines proper chloroplast biogenesis (Barrero-Gil et al., 2022) in Arabidopsis. This could be also the case in Chlamydomonas and consistent with this hypothesis at least ETF1 and MTF1 are localized in the chloroplast according to PB-Chlamy tool.

Animal type cryptochrome (aCRY1): the ancestral red light photoreceptor that triggers de-etiolation in Chlamydomonas?

Red light and the phy-PIF regulatory module that detects and transduces it represents an essential mechanism in angiosperm plants for proper de-etiolation response (Leivar et al., 2008). It is therefore amazing that Chlamydomonas *y* mutants can perform de-etiolation, while featuring only blue and UV

light type of photoreceptors (Kottke et al., 2017), as green algae light signaling mechanism is adapted to aquatic life where blue is the main component of light cues (Han et al., 2019). However, the animal type of cryptochrome (aCRY1) has been shown to detect also red light, affecting the expression of many genes (Beel et al., 2012). We wondered if red light capable of triggering de-etiolation in *y-4* cells, or if this is mainly dependent on blue light. Surprisingly, only red light could trigger most of the de-etiolation response; this is particularly interesting, as aCRY1 is to our knowledge the only Chlamydomonas photoreceptor known to respond to red light, and indicates that this might be the main photoreceptor that triggers de-etiolation. However, other reports indicate that there might be at least another photoreceptor that can perceive red light, as far-red light has been shown to affect gene expression in Chlamydomonas (Im et al., 2006), and this effect cannot be caused by aCRY1.

Transcriptome analysis: RETROGRADE SIGNALING

CHAPTER 4

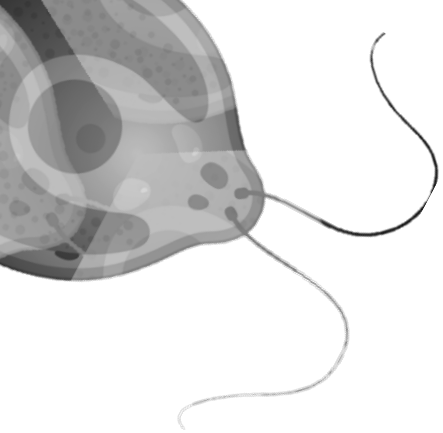
Transcriptome analysis: retrograde signaling

Introduction 117-120

Materials and Methods 120-123

Results 123-144

Discussion 144-148



4

Chapter

Introduction

Retrograde signaling (RS) is an essential mechanism by which chloroplasts communicate to the nucleus their status, triggering changes in gene expression that feedback to chloroplast functions and ultimately allow any photosynthetic organism to adapt in an ever changing environment (Shimizu & Masuda, 2021). RS are not only sent when the mature chloroplast detect changes in the environment (operational control), but also during chloroplast biogenesis (biogenic control) (Richter et al., 2023). The latter is characteristic of angiosperm plants, when dark-developed etioplasts of emerging skotomorphogenic seedlings from the ground transform into fully developed chloroplasts of photomorphogenic seedlings upon exposure to light, a process known as de-etiolation (Gommers & Monte, 2017). Of course light is its major regulator, but since many components of the electron transport chain involved in the photosynthetic reactions are separately encoded in both nuclear and plastid genomes, their expression need to be coordinated by a RS mechanism in the developing chloroplast (Jarvis & López-Juez, 2013).

The components of the biogenic RS pathway are far from being fully elucidated, but a major advance in our knowledge was the identification of GUN1 (Susek et al., 1993), a pentatricopeptide repeat chloroplast protein, which is postulated to accomplish many different molecular functions inside the chloroplast, including regulation of tetrapyrrole biosynthesis, gene transcription, translation, protein import (Shimizu & Masuda, 2021), and very recently it has been demonstrated its ability to bind RNA *in vivo* (Tang et al., 2024). It plays a fundamental role in chloroplast biogenesis as it accumulates in the etioplasts of skotomorphogenic seedlings, preventing its premature development in the dark, by repressing the expression of many positive regulators of photomorphogenesis in the dark (Hernández-Verdeja et al., 2022). Importantly, GUN1 has a major importance in regulating the crosstalk between light and RS during de-etiolation: GUN1-dependent RS and PIF-mediated signals converge to antagonistically regulate the expression of a common subset of photomorphogenesis genes by controlling a common target, GLK1. Also, if de-etiolation is performed under excessive light conditions, GUN1 represses light-dependent hook opening and cotyledon expansion, extending the role of GUN1-biogenic RS in regulating whole plant development, besides chloroplast biogenesis (Martín et al., 2016). Although de-etiolation is exclusive of angiosperm plants, *GUN1* homologs have

been identified in non-angiosperm lineages, including the charophytan algae *Chara braunii* (Nishiyama et al., 2018). *GUN1* sequence is highly conserved in the different lineages, but it has been shown that its ancestral function is not related with RS and that this has emerged more recently in the evolution (Honkanen & Small, 2022), but not necessarily with angiosperm plants (Hills et al., 2015). In contrast, no *GUN1* homologs have been identified in green algae, but remarkably *yellow-in-the-dark* mutant strains of Chlamydomonas, which develop etioplast-like plastids in the dark with no photosynthetic activity due to their inability of synthesizing chlorophylls in this condition, perform chloroplast biogenesis upon transfer to light, fully restoring its photosynthetic apparatus and activity (Sager & Palade, 1954; White & Hoober, 1994). This opens the intriguing question of which major ancestral regulator is regulating chloroplast biogenesis in Chlamydomonas.

Many works aiming to elucidate the components of the RS machinery in Chlamydomonas have been performed in the last decades, and these lead to the identification of components from the tetrapyrrole biosynthesis pathway and chloroplast unfolded protein response (cpUPR) in mediating a RS during early light acclimation, or under certain stress conditions (Richter et al., 2023). The first is the case of HMOX1, an enzyme from the heme branch of the tetrapyrrole biosynthesis pathway, involved in the production of bilins (Duanmu et al., 2013). The *hmox1* mutants are impaired in photoacclimation during dark-to-light transition, and show reduced chlorophyll levels and photosynthetic performance, but these effects can be overcome with the addition of exogenous biliverdin, the reaction product of HMOX1. Also, a pool of genes involved in the detoxification of reactive oxygen species (ROS) is induced during the first 30 min of light, but not when supplemented with biliverdin. Therefore bilins have been postulated as negative RS needed for ROS detoxification during early light acclimation (Duanmu et al., 2013). In addition, GUN4, a regulatory subunit of the Mg-chelatase supercomplex which catalyzes the first reaction of the chlorophyll branch of the tetrapyrrole biosynthesis pathway, has also being involved in RS: *gun4* mutants are photosensitive, accumulate considerably less chlorophylls, and also feature significant changes in the expression of 803 genes including photosynthesis and tetrapyrrole biosynthesis in the dark (Formighieri et al., 2012). Its photosensitive phenotype is due to the inability of *gun4* to sense accumulating ROS in light, in turn triggered by accumulation of the Mg-chelatase precursor Proto-IX, therefore nuclear gene expression changes are due to ROS triggered RS but it is not known whether GUN4 plays a central role in it (Brzezowski et al., 2014). Later it was shown that bilins regulate chlorophyll biosynthesis: specifically, these have been shown to stimulate Mg-chelatase activity by interacting with GUN4, and both are essential for stability of the CHLH1 subunit which is susceptible to Proto-IX phototoxic effects. This work suggests GUN4 and bilins are linked in the same ROS-dependent RS mechanism (Zhang et al., 2021).

The presence of a cpUPR involved in RS in Chlamydomonas has been theorized after the observation that conditional depletion of the plastid protease named ClpP1, involved in maintaining chloroplast protein homeostasis, triggered upregulation of chaperones, heat shock proteins, proteases at both transcript and protein level (Ramundo et al., 2014). This upregulation can also be caused by specific

stress like high light, which triggers ROS-dependent chloroplast protein damage (Ramundo et al., 2014), and in Arabidopsis by lincomycin treatment which specific inhibits chloroplast protein translation, resulting in protein aggregation (Llamas et al., 2017). The cpUPR-mediated RS mechanism requires a system to detect unfolded proteins and also an effector that sends RS to the nucleus (Richter et al., 2023). This might be mediated by VIPP proteins, which are involved in thylakoid biogenesis, and specifically by VIPP2 which is highly upregulated during cpUPR. Although VIPP2 is not a chaperone, it might detect stored curvature elastic (SCE) stress from misassembled membrane proteins and send RS to alleviate it: it has been shown in fact that under high light stress, *vipp2* mutants are unable to upregulate HSP22E/F and LHCSR3 at both protein and transcript levels (Theis et al., 2020). A candidate effector for cpUPR RS could be MARS1 (mutant affected in retrograde signaling), a cytosolic protein identified in a screening for mutants defective in cpUPR response: *mars1* mutants cannot cope with photodamage under high light stress or ClpP1 depletion, and fail to induce key genes of cpUPR response including *VIPP2*, *HSP22E/F* and *CLPB3* (Perlaza et al., 2019).

However, RS has never been explored in *y* mutant strains in Chlamydomonas. As these strains perform chloroplast biogenesis and restore photosynthetic activity similarly to angiosperm plants (Ohad et al., 1967), a RS mechanism able to coordinate expression of nuclear and plastid components is required to avoid potential harmful oxidative damage. Although bilins and cpUPR dependent RS have already been involved in early light acclimation from darkness (Richter et al., 2023), as far as we know all these works have been performed in strains that already feature a fully developed chloroplast in the dark, and therefore their potential implication in the generation of biogenic RS during de-etiolation needs to be tested. Alternatively, Chlamydomonas might possess a primitive RS mechanism specifically involved in chloroplast biogenesis that has not been identified yet. In either case, it is important to remark that this ancestral RS mechanism replaces GUN1 in Chlamydomonas, and so exploring RS in *y* mutants will widen our knowledge of the evolutionary advantage that represented the emergence of GUN1 in angiosperm species, and maybe lead us to the discovery of a new master regulator of this signaling pathway.

We previously developed a Chlamydomonas y mutant based de-etiolation system which allows us to study main events regulated by light and RS. Transcriptomic analysis of de-etiolating *y* mutant cells in light allowed us to identify main biological processes involved in de-etiolation, and predict potential novel TFs involved in light signaling. To study RS in Chlamydomonas cells were treated with lincomycin, a disruptor of chloroplast protein translation used, to activate this signaling pathway. This approach has been widely employed in angiosperm plants to study biogenic RS during de-etiolation (Dubreuil et al., 2018; Koussevitzky et al., 2007; Ruckle et al., 2012). This work will allow us to 1) identify biological processes regulated by biogenic RS, and test whether the above mentioned RS mechanism in Chlamydomonas participate in this process, 2) study the crosstalk between light and

RS in Chlamydomonas, and 3) evaluate if light and RS regulate also biological processes not related with chloroplast biogenesis, as it occurs with angiosperm plants.

Materials and Methods

RNA-seq data analysis

Definition of lincomycin responsive genes (LinRGs)

In this chapter we employed for our analysis *y-4* Light (including Dark) samples of the previous chapter, *y-4* Light + Linco (including Dark + Linco) samples at 0,1,3,6 and 9h (Fig. 2.9), and wt Dark and wt Dark + Linco samples. Raw data from all these samples was processed as explained in the previous chapter. To define lincomycin responsive genes (*LinRGs*) during de-etiolation of *y-4* cells, we first determine if the transcriptome expression profiles in *y-4* Light and *y-4* Light + Linco were significantly different by performing DESeq2 (Love et al., 2014) likelihood ratio test of two factors (LRT2f). Next, we determined differentially expressed genes (*DEGs*) by performing DESeq2 pairwise comparisons of each time point of *y-4* Light towards the same time point of *y-4* Light + Linco. In these tests, p-values were adjusted (pAdj) with the Benjamini-Hochberg method. *LinRGs* were defined as giving pAdj < 0.05 in the LRT2f and $\log_2$FC > 1 (linco inductive effect) or $\log_2$FC < -1 (linco repressive effect) in at least one time point of *y-4* Light + Linco vs *y-4* Light. Early and late *LinRGs* were defined as reaching the mentioned criteria at 1h (regardless of the rest of the time points), and at 3,6,9h, respectively. Combined effect of light and lincomycin during the time course was also evaluated by performing DESeq2 pairwise comparisons of time points in light + linco (1,3,6,9h) towards dark + linco (0h), and we defined light + linco responsive genes (*LLRGs*) as giving $|\log_2 FC| > 1$ in at least 1 time point in light (see Important Remark). Absolute $\log_2$FC values of Light and Light + Linco samples for early and late *LRGs* & *LinRGs* were pairwise compared, and statistical analysis was performed with Wilcoxon test of matched pairs.

Hierarchical clustering and GO analysis

In this part, we defined four different subsets of *LRGs* and *LinRGs* depending on the inductive or repressive effect or light and lincomycin: 1) light induced and linco induced, 2) light induced and linco repressed, 3) light repressed and linco induced and 4) light repressed and linco repressed. We determined two additional subsets of *LRGs* not responsive to linco (light induced and light repressed) and two additional subsets of *LinRGs* not responsive to light (linco induced and linco repressed). For all these subsets hierarchically clustering of Light and Light + Linco $\log_2$FC was performed by one minus pearson correlation and average linkage method using Morpheus online application (https://software.broadinstitute.org/morpheus/). GO analysis for each subset was performed as explained in the previous chapter, but showing in this case the top 30% GO terms with the lowest FDR.

Biased analysis of biological processes

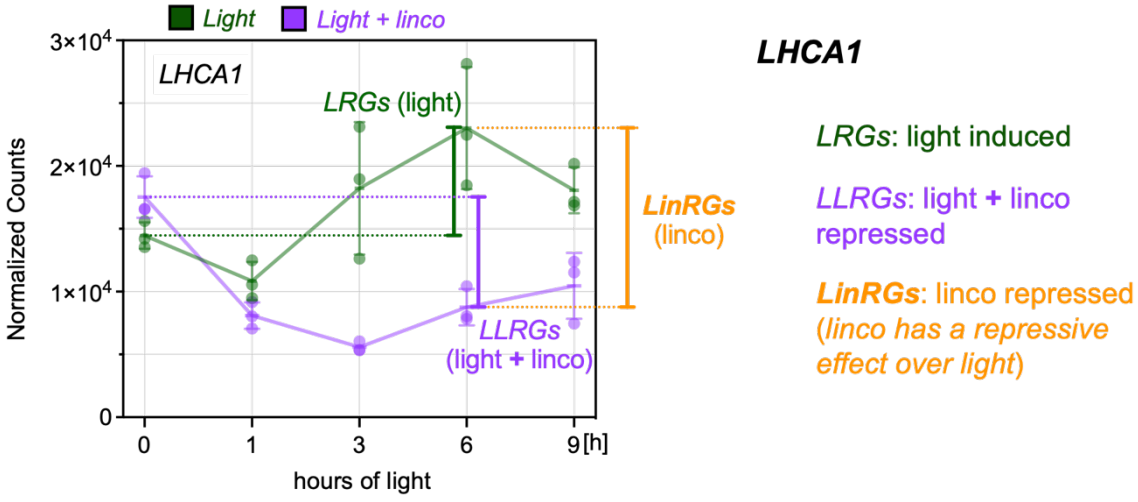
This analysis was performed following the same procedure as in the previous chapter with the following modifications: 1) both light and light + linco expression profiles were determined by calculating the mean Z-score of the log_{10} normalized count values (instead of TPMs); 2) these Z-score values were calculated using the specific mean and standard deviation of each process and subprocess (this means that plots reflect actual distances between light and light + linco expression profiles for the same biological process or subprocess, but not between different subprocesses as in the biased analysis of the previous chapter, as DESeq2 normalized counts do not take into account transcript length).

Analysis of lincomycin responsive chloroplast-associated nuclear genes and transcription factors

Both nuclear genes encoding chloroplast proteins and transcription factors lists were obtained as indicated in the previous chapter. Lincomycin responsive transcription factors (*LinRTFs*) were defined with the same criteria as *LinRGs*. Log_2FC values of *LRTFs* and *LinRTFs* of light and light + linco samples were hierarchically clustered as previously explained.

Analysis of linco-responsive genes on wild type and y-4 etiolated cells in the dark

We performed DESeq2 pairwise comparisons of linco-treated vs non-treated wt Dark and *y-4* Dark samples. P-values were adjusted with the Benjamini-Hochberg method. *DEGs* were defined as giving $|log_2FC|>1$ and pAdj<0.05.



IMPORTANT REMARK: In this chapter the effect of lincomycin during de-etiolation was determined in two complementary ways: 1) by calculating Light + Linco variations towards dark + linco (L+Lin), where we defined *LLRGs* the ones with $|log_2FC| > 1$, and 2) by calculating lincomycin effects on variations caused by light (linco), where we defined *LinRGs* the ones whose trajectories of light and light + linco were significantly different and that reached $|log_2FC| > 1$ in pairwise comparisons between light and light + linco. The first takes into account both light and linco effects during de-etiolation and was employed throughout this chapter to compare expression profiles or specific fold changes with *LRGs*. With this approach, however, we cannot determine if responsiveness is attributed to light, lincomycin or both. Therefore, with the second we can evaluate only linco contributions on light, where these can be inductive if $log_2FC > 1$ in light + linco vs light pairwise comparisons, or repressive if $log_2FC < -1$. Importantly, this analysis was simplified by the fact that not a single gene showed significant differences in the expression levels between Dark and Dark + Linco, a result that will be later discussed in this chapter. In this example, Light and Light + Linco expression profiles are shown for a gene from the antenna complex of the photosystem I (*LHCA1*): this gene is induced by light (*LRGs*, Light Up), and repressed by lincomycin (*LinRGs*, Linco Down).

Analysis of the early effect of lincomycin and high light

Raw RNA-seq data of Chlamydomonas cell cultures growing under 12:12 photoperiod conditions from Knopp et al., 2020 were re-processed as described in the previous chapter. Biological triplicates of samples at 6h of dark phase and after 1h of high light treatment were analyzed from this experiment. High light responsive genes (*HLRGs*) were defined as giving $|\log_2 FC| > 1$ and pAdj < 0.05 in the DESeq2 pairwise comparisons between high light and dark. As a comparison, we first defined early *LLRGs* as giving $|\log_2 FC| > 1$ between *y-4* L+Lin at 1h and *y-4* D+Lin. To discard light effects, common *LLRGs* and *HLRGs* were later filtered keeping those that were *LinRGs* at 1h (*LinRGs* filt). GO analysis for the 1-2 most significant and representative categories was performed using STRING.

Analysis of GUN1-regulated genes

A list of *DEGs* between Arabidopsis Col-0 and *gun1-101* seedlings grown in light + linco conditions was retrieved from Wu et al., 2019. Chlamydomonas gene homologs of GUN1-regulated genes were determined through BLASTP, according to Craig et al., 2023. Genes from this list were evaluated for their maximum $|\log_2 FC|$ values between light and dark in At Light and *y-4* Light, and between light + linco and light in *y-4* Light + Linco and *y-4* Light samples. $|\text{Log}_2 FC| > 1$ values of GUN1 and lincomycin responsive homolog genes were hierarchically clustered by Euclidean distance and average linkage method using Morpheus application. GO analysis was performed on *LinRGs* with $\log_2 FC < -1$ and featuring $\log_2 FC > 1$ in *gun1* linco using STRING and selecting the two most representative GO terms.

Analysis of lincomycin effect in the dark on wild type cells

Wild type CC-124 cells were grown in HSA medium for 3 days in the dark at 23ºC. On the third day the medium of all cultures was replaced with fresh HSA and half of the cultures was treated with 0.5 mM lincomycin hydrochloride; all cultures were grown for other 2 days in the dark at 23ºC. Both PSII maximum quantum yield and total chlorophylls was determined before (0h) and after lincomycin treatment (48h), and following the same procedure as in the previous chapters.

High throughput de-etiolation of y-4 cells

High throughput de-etiolation was setup on 96-well plates (all the procedures were carried out with a multichannel pipet). Wells were filled with HSA and *y-4* cells were inoculated in each well; cultures

Table 4.1: Primers used for RT-qPCR analysis of the high throughput de-etiolation of *y-4* cells. *GBLP* was used as internal control for gene expression. *Cre*: Chlamydomonas.

Gene	*Cre* ID	Primer Forward	Primer Reverse	References
GBLP (*RACK1*)	Cre06.g278222_4532	CAAGTACACCATTGGCGAGC	CTTGCAGTTGGTCAGGTTCC	Petroutsos et al., 2016
VIPP2	Cre11.g468050_4532	AAGAAGGACACGCTCAAGGC	CATCTTATCAAACGCGGCCC	-
HSP22F	Cre14.g617400_4532	TCTGGCGTCTGAGCTGCTTC	ACTCATGCCTGGGCAGTCG	-

were grown for 3 days in the dark at 23ºC, under gentle shaking (150 rpm). On the third day, 100 µL of each culture was discarded and replaced with fresh HSA and cultures were grown in the same conditions for other two days. On the fifth day, plates were centrifuged for 10 min at 2000 rpm, the medium fully replaced with fresh HSA (200 µL) and cells gently resuspended using the pipet; half of the plates were also supplemented with 0.5 mM lincomycin hydrochloride and all plates were incubated in the same dark conditions. Next day, plates were centrifuged as before and the medium was fully replaced with fresh HSM with or w/o 0.5 mM lincomycin; these were incubated in the same dark conditions for 3h. Once acclimated, cultures were transferred to light conditions at 50 µmol m^{-2} s^{-1} and 23ºC for de-etiolation. As a control, de-etiolation of y-4 cells with and w/o lincomycin was also performed using flasks In the same way as the RNA-seq, described in Chapter 2. We monitored the expression of two candidate reporter genes (*VIPP2* and *HSP22F*) at 0,1,3h of de-etiolation by performing RT-qPCR. This was performed as described in Chapter 2 and using the primers shown in Table 4.1. Biological duplicates were prepared for flask samples, while a single sample made with all cultures of a single plate was employed for each time point and treatment in the high throughput de-etiolation. FvFm was monitored during de-etiolation of both flask and plate cultures and determined as previously described.

Results

Not all light responsive genes are targets of retrograde signaling

To study the effect of retrograde signaling during de-etiolation and also evaluate its crosstalk with light signals, we compared *y-4* Light samples of the previous chapter with de-etiolating *y-4* cells treated with lincomycin (linco) at the same time points (*y-4* Light + Linco, Figure 4.1 A). We determined the specific effect of linco during de-etiolation of *y-4* cells, by performing DESeq2 likelihood ratio test of 2 factors (LRT2f) to evaluate if trajectories between light and light + linco were significantly different and also by performing pairwise comparisons at each time point between light + linco and light. Linco responsive genes (*LinRGs*) were defined as those giving pAdj<0.05 from the LRT2f and $|\log_2 FC|>1$ from the pairwise comparisons (see Important Remark). With these filters we obtained 4363 *LinRGs* (Figure 4.1 B) which correspond to 26% of the transcriptome. However, only half of them (2190) were also *LRGs*, and represent a third of this subset, which indicates that only a subgroup of *LRGs* are RS targets. We also defined linco inductive and repressive effect on light of *LinRGs* if $\log_2 FC$ of L + Lin vs Light pairwise comparisons were higher than 1 or lower than -1, respectively. The proportion linco inductive and linco repressed genes depends on the subset of *LinRGs* (Figure 4.1 C): linco has mostly a repressive effect on the *LRGs* and *LinRGs* subset, but has a predominant inductive effect over *LinRGs* that do not respond to light. Moreover, we defined early (E) *LinRGs* those that reached the mentioned criteria starting from 1h, and late (L) *LinRGs* if this happened at 3,6 and/or 9h. We found

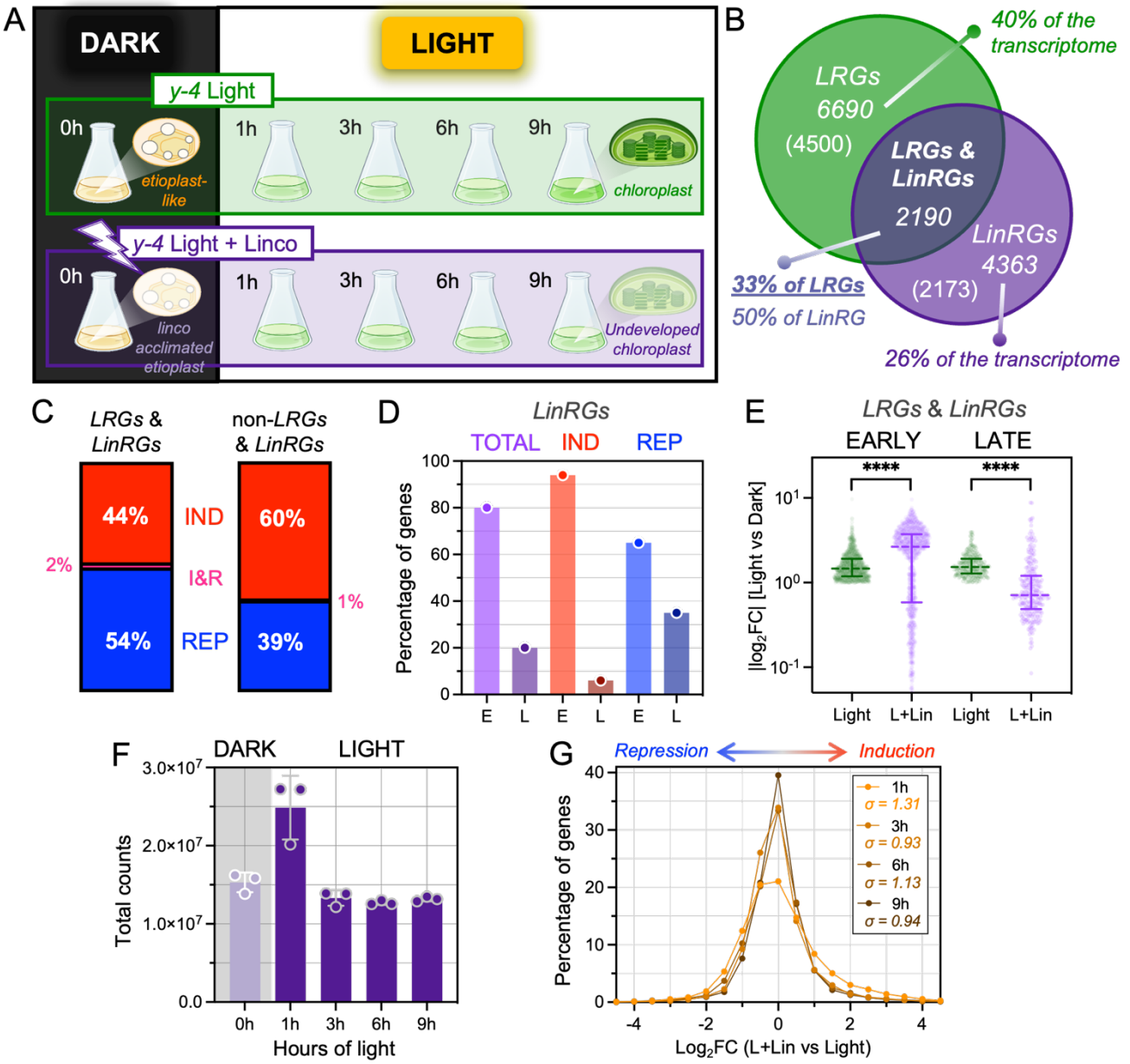


Figure 4.1: A. Schematic representation of samples used for RS data analysis in this chapter: de-etiolation of *y-4* cells in light conditions (*y-4* Light) was also carried out in the presence of lincomycin (linco) (*y-4* Light + Linco) to study the gene targets of RS during this process. B. Venn diagram representing the overlap between *LRGs* (already defined in the previous chapter) and linco responsive genes (*LinRG*, pAdj<0.05 likelihood ratio test of two factors, $|\log_2 FC|>1$ in at least one light vs light + linco pairwise comparison at the same time point). Total *LRGs* and *LinRGs* are indicated in italics, while non-common genes between subsets are indicated inside brackets. C. Percentage of linco induced (IND), repressed (REP) or both (I&R) in the *LRGs* & *LinRGs* and *non-LRGs* & *LinRGs* subsets. D. Percentage of early (E, *LinRG* at 1h of de-etiolation) and late (L, *LinRG* at 3-6-9h of de-etiolation), of all *LinRGs* and separated into linco IND and linco REP. E. Distribution of $|\log_2 FC|$ values for Light and light + linco (L+Lin, see Important Remark) pairwise comparisons, of *LRGs* & *LinRGs* subset divided into early (*LinRGs* at 1h) and late (*LinRGs* at 3-6-9h). The maximum $|\log_2 FC|$ between 3-6-9h was employed for late distributions. Median is indicated with a dashed line, and error bars represent the interquartile range. Statistical analysis was performed between Light and L+Lin samples, using Wilcoxon test for paired values. F. Total normalized counts of all Light + Linco samples. G. Distribution of |log2FC| values of L+Lin vs Light pairwise comparisons in each time point in light.

that linco effect is early in the vast majority of cases (Figure 4.1 D). Also, almost all linco inductive effect is found early, while late effects of linco are mostly repressive. We also evaluated the degree of linco responsiveness inside *LRGs* and *LinRGs* subset (Figure 4.1 E): linco significantly triggers

higher degree of regulation of these genes early at 1h, and lower at later time points, and therefore early RS tend to overpower inductive and repressive effects triggered by light, while late RS tend to lower them. The highly predominant inductive effects of the early *LinRGs* can be explained with a surprising peak of 25 million total normalized counts which is much higher compared to the rest of the samples of our RNA-seq (which is around 15 million) (Figure 4.1 F). Moreover, we found overall higher degrees of induction and repression exerted by linco at 1h compared with the rest of the time points (Figure 4.1 G). It can be observed that at 1h the shape of the histogram is not perfectly symmetric towards 0, but is more opened towards positive values: this means that inductive effects caused by linco feature higher log_2FC compared to repressive effects.

Overall, these results indicate that 1) linco effects are specific, as they significantly affect a quarter of the transcriptome, and only a third of *LRGs*, 2) the majority of these effects are found early at 1h, and are predominantly inductive, while late effects tend to be repressive. In the next section we will evaluate if these tendences are reflected in the biological processes regulated by light and/or linco.

Concerted light and retrograde signals regulate biological processes related and not with chloroplast biogenesis

In this part we evaluated which biological processes are subjected to regulation by RS only, or concertedly with light signals, and which do not require RS regulation under linco stress conditions. For this purpose, we performed GO analysis on different subsets of *LinRGs* and/or *LRGs*. Specifically, *LinRGs* and *LRGs* were divided into four subsets resulting from the combinations of inductive (UP) or repressive (DOWN) effects of light and linco (Figure 4.2): A. light UP & linco UP; B. light UP & linco DOWN; C. light DOWN & linco UP; D. light DOWN & linco DOWN. Similarly, we generated two subsets for only *LRGs* (Figure 4.3: A. light induced and B. light repressed) and for only *LinRGs* (Figure 4.3: C. linco induced and D. linco repressed). All these genes were hierarchically clustered by one minus pearson method and average linkage method and GO analysis was performed as explained in the previous chapter. We kept following the unbiased method for representing GO terms, but here we displayed a slightly higher proportion of GO terms (30% top GO with the lowest FDR).

Inside the group of *LRGs* and *LinRGs* (Figure 4.2), the great majority of GO terms were obtained for light induced genes (Figure 4.2 A,B). Many terms observed for these two subsets are consistent with previously documented effects of linco on de-etiolation in Arabidopsis (Ruckle et al., 2012): in our system linco early triggers oxidative stress, and represses photosynthesis and tetrapyrrole biosynthesis genes. In addition, a few terms indicate induction of translation and repression of rRNA processing, which could be explained by the need for translational activity and for getting rid of accumulating transcripts in the chloroplast, caused by linco biological effect. In contrast, no significant GO terms were obtained for light repressed genes where linco has an inductive effect (Figure 4.2 C), while only a few terms were observed where linco has a repressive effect (Figure 4.2 D). Interestingly,

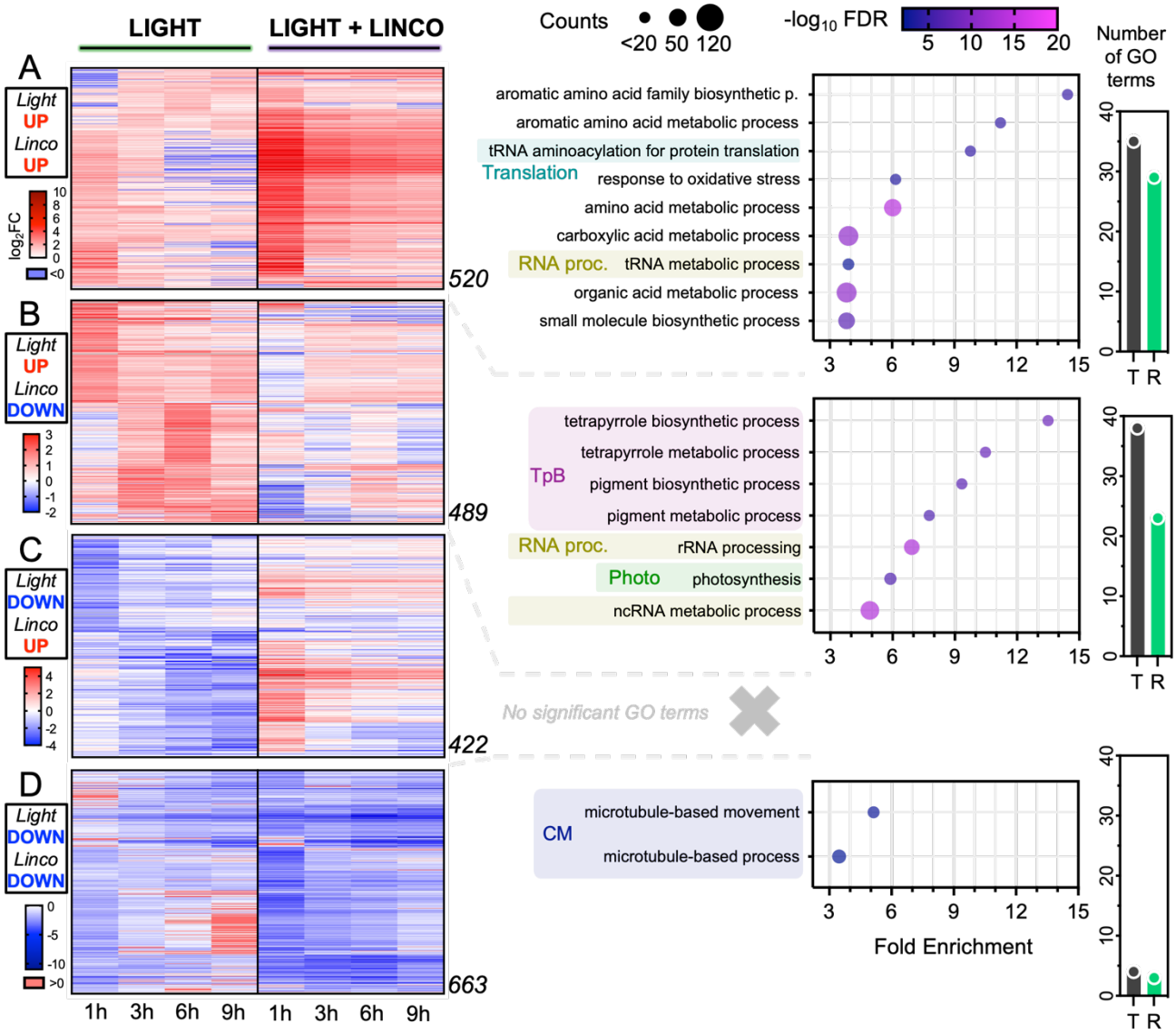


Figure 4.2: Gene clustering and GO analysis of *LRGs* & *LinRGs* genes. For this analysis, this list was divided into light induced and linco induced (A), light induced and linco repressed (B), light repressed and linco induced (C) and light repressed and linco repressed (D). The number of genes belonging to each subgroup is indicated at bottom right in each heatmap. These genes were hierarchically clustered by one minus pearson method and average linkage method, using log_2FC values of Light (light 1-3-6-9h vs dark 0h) and light + linco (light + linco 1-3-6-9h vs dark + linco 0h) pairwise comparisons. GO analysis was performed for each of the four subsets in the same way as in the previous chapter (Fig. 3.3-3.5), but here we show the top 30% lowest FDR GO terms. GO terms associated with biological processes already found in the light signaling analysis are highlighted: Translation (light blue), RNA processing (yellow), Cell Motility (CM, blue), Tetrapyrrole Biosynthesis (TpB, Pink), Photosynthesis (Photo, green). No significantly enriched GO terms were found for subset C.

these are related to flagella functions, and suggest that light and RS concertedly regulate other cellular functions outside chloroplast biogenesis during de-etiolation.

Among the light-induced biological processes not affected by linco (Figure 4.3 A) we found many terms related to translation, ribosome biogenesis and RNA processing. As some of these terms were also found in the previous subsets, it suggests that the effects of linco over these processes is mild, or related to very specific genes. Interestingly, plastid organization is not affected by linco, which might be an indication that cells still restore chloroplast even under adverse conditions, rather than fully suppress its development, as in Arabidopsis. In contrast, no significant GO terms were observed

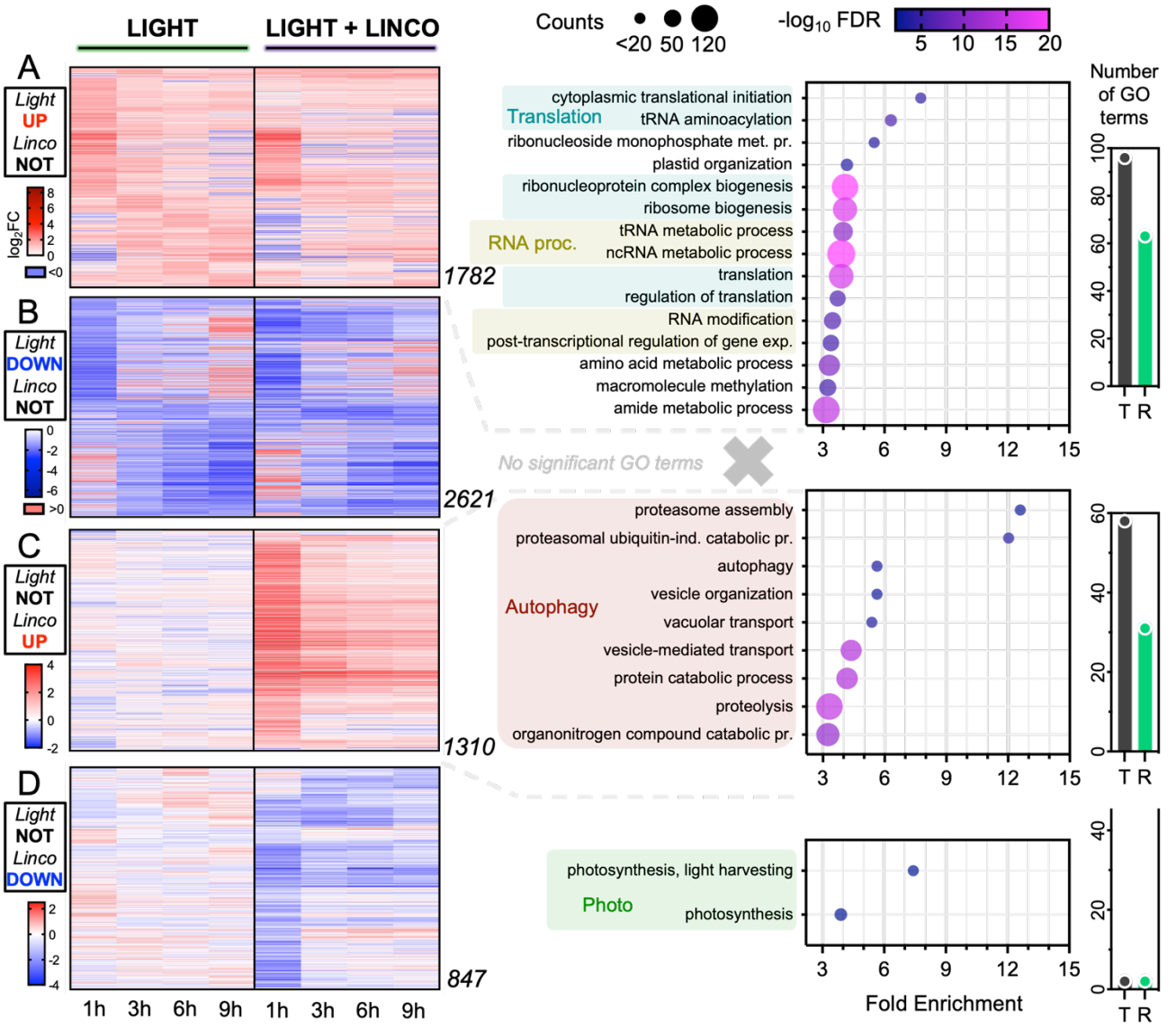


Figure 4.3: Gene clustering and GO analysis of *LRGs non-LinRGs*, separated in light induced (A) and repressed (B), and of *LinRGs non-LRGs*, separated in linco induced (C) and repressed (D). Gene clustering and GO analysis were performed as in Fig. 4.2. GO terms associated with biological processes already found in the light signaling analysis are highlighted In addition, a specific linco induced biological process was observed: Autophagy (Red). No significantly enriched GO terms were found for subset B.

for light repressed genes not affected by linco (Figure 4.3 B), and this further supports that RS regulate cell motility during de-etiolation: since flagella functions are clearly repressed by light, as observed in the previous chapter, the absence of any significant GO term in this subset can be explained by the majority of genes involved in this process being also repressed by linco.

We observed many GO terms for genes that are only induced by linco (Figure 4.3 C): all of them are related to autophagy and protein quality control, suggesting the involvement of the chloroplast unfolded protein response (cpUPR). This can be explained by the impaired protein translation caused by linco, which critically compromises protein homeostasis in the developing chloroplasts and induces all the genes necessary to avoid proteotoxicity. Lastly, only two GO terms were found for genes only repressed by linco (Figure 4.3 D), which are related to photosynthesis function. This is expected, as

these genes are repressed by linco but the great majority of them, although late light induced, do not reach our threshold to be strictly considered *LRGs*. This further indicates linco triggered RS repress photosynthesis during de-etiolation.
Each heatmap here displayed evidences several clusters with variable degree of regulation exerted by light and RS inside each of the eight defined subsets. In the next section we will evaluate how the biological processes obtained relate with these different profiles.

Biogenic retrograde signals strongly but transiently repress light induction of photosynthesis and tetrapyrrole biosynthesis genes during de-etiolation

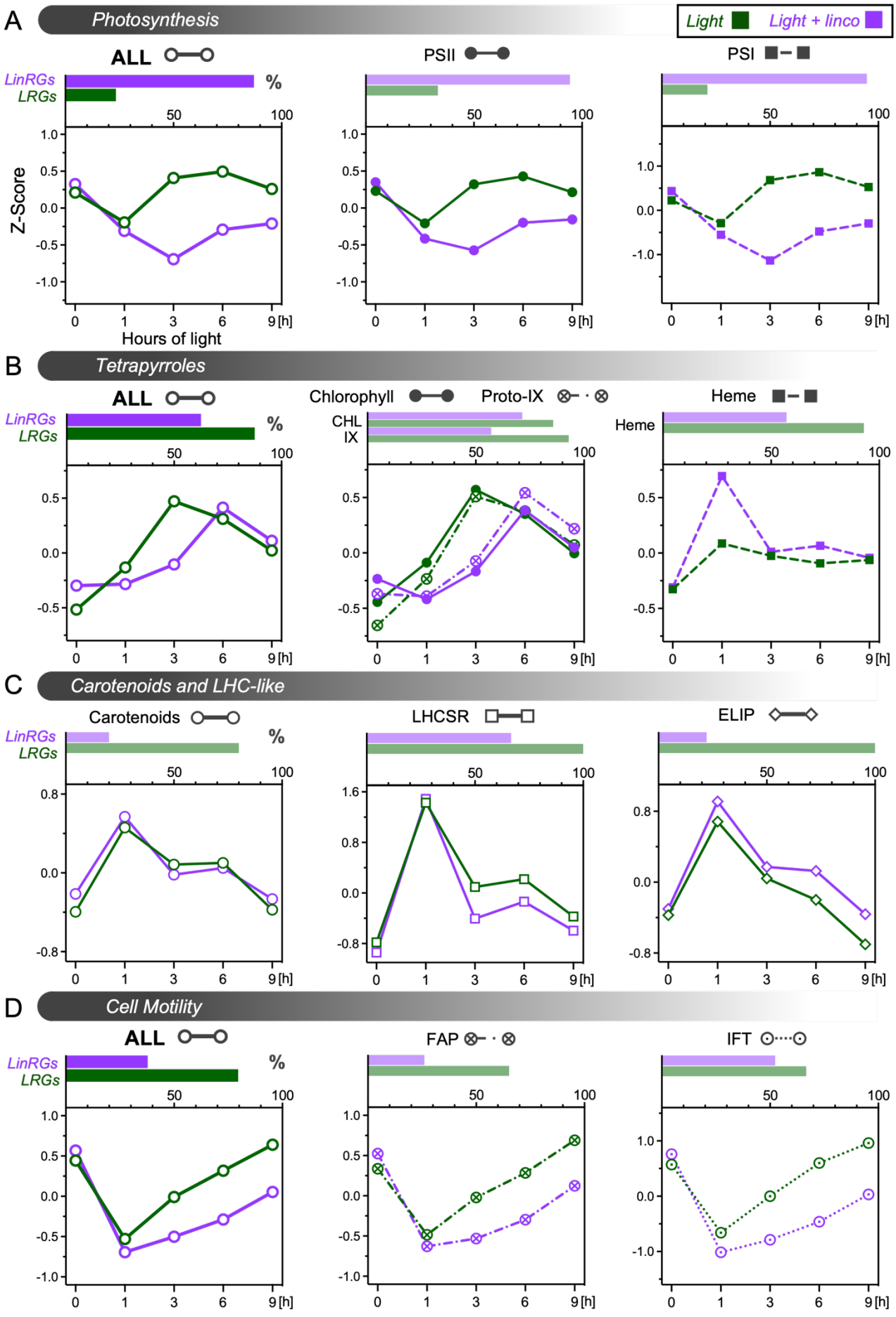
In order to confirm the results obtained from GO analysis and also to evaluate how and at which degree linco affects light regulation during de-etiolation, we further evaluated the expression profiles of biological processes that respond to linco in the previous section. For this purpose, we biasedly selected genes belonging to main biological processes affected by linco, separated into subprocesses (i.e. photosynthesis, photosystem I) and generated the most typical trajectory of light and light + linco for each of them. This was carried out in the same way as the biased analysis performed in the previous chapter, with the main difference that in this case we had to employ normalized counts instead of TPMs to calculate Z-score values, since at 1h there's a drastic increase in total transcript abundance in the light + linco samples (Figure 4.1 F), which deeply affected TPM values of the genes here employed, distorting the overall shape of trajectories. As we employed normalized counts that do not take into account the gene length, expression profiles were standardized for each biological process and subprocess, and therefore comparisons between light and light + linco are valid inside each biological process and subprocess, but are not valid between different ones.
The biological process with the highest degree of linco-triggered repression is photosynthesis (Fig 4.4 A). Almost all photosynthesis genes (90%) are LinRGs and are highly repressed at 3 and 6h, where they are induced by light, with almost identical profiles of photosystem II and I. Interestingly, recovery in the expression of these genes is observed under linco conditions starting from 6h, and tends to light levels. This indicates that linco triggered RS highly repress photosynthesis genes but only transiently, allowing them to increase expression to light levels.
The expression of tetrapyrrole biosynthesis genes is also highly affected by linco (Figure 4.4 B), where 60% of these genes are *LinRGs*. Genes involved in the biosynthesis of chlorophyll and Proto-IX precursors feature almost identical Light and L+Lin profiles; interestingly, linco effect consists in an overall delay in the induction of these genes, whose peak is found at 6h rather than at 3h. Heme biosynthesis genes are also very affected by linco but in a very different way: here linco triggers a strong and transient induction of these genes at 1h, which is consistent with the key role played by bilins in early light photoacclimation in Chlamydomonas (Witkopp et al., 2017). Altogether, light + linco expression profiles of photosynthesis and tetrapyrrole biosynthesis genes indicate that linco triggered

RS cause a strong but transient repression of these processes, resulting in a delayed light-induction of these genes. This effect is very different from what observed in Arabidopsis, where the degree of linco-repression for these genes increases with the time of light and linco exposure, and never recovers (Dubreuil et al., 2018; Ruckle et al., 2012), and could indicate that Chlamydomonas RS are not optimized for the regulation of photosynthesis and chlorophyll biosynthesis genes during de-etiolation.

One of the light-regulated biological processes which are not affected by linco is photoprotection (Figure 4.4 C). Here we show expression profiles for carotenoid biosynthesis, *LHCSR*s and *ELIP* genes, but the same was observed with other key genes involved in photoprotection such as *PSBSs*: all of them are transiently induced by light at 1h and linco does not affect at all this induction. Significant linco affection, however, was observed in the case of *LHCSR1* and *LHCSR3A* but in later time points, but the overall shape of the expression profiles is very similar. This is expected, as de-etiolation of *y-4* cells in linco was performed keeping the same conditions of light, and importantly indicate that linco effects on the transcriptome are specific.

Interestingly, we found a biological process that is regulated by both light and RS and is not related to chloroplast functions, cell motility (Figure 4.4 D). Both synthesis of flagella (IFT), structural proteins (FAP) and motor proteins (dynein) were affected in the same way by linco, with an over-repression at 1h followed by a much slower recovery in light. The percentage of *LinRGs* was not particularly high only because many of these genes did not reach the $|\log_2 FC|>1$ threshold, but indeed all feature the same trajectories. However, at first sight we did not observe differences in presence of absence of flagella in the linco affected cells during de-etiolation, nor differences in their length, and therefore the differences found may be reflected in their movement pattern. This depends on the intraflagellar calcium levels (Wheeler, 2017), and since calcium RS have been described in Chlamydomonas during early light acclimation (Petroutsos et al., 2011), it is likely that this type of RS are active during de-etiolation. Altogether this finding suggests an ancestral capacity of RS to regulate non-chloroplast cellular functions during de-etiolation.

Translation and RNA processing are lowly affected by linco, but with opposite effects. Trajectories of genes involved in RNA processing (here we display rRNA methylations (RRM), small nucleolar ribonucleoproteins (snoRNP) which regulate pre-rRNA processing and RRP components of the cytoplasmic exosome) show that linco suppress their early peak of induction, although the overall increase in their expression during de-etiolation is still observed w/o and with linco (Figure 4.4 E). In contrast, ribosome genes (Figure 4.4 F) are overall induced by linco with some differences: linco triggers a peak of induction of cytoplasmic ribosomes at 1h, a slight induction of chloroplast ribosomes, while does not affect mitochondria ribosomes. Also translation factors are overall slightly induced by linco (Figure 4.4 G). Overall these results indicate that Chlamydomonas cope with impaired chloroplast protein translation by upregulating the levels of cytoplasmic ribosomes and translational activity, as the vast majority of chloroplast proteins are nuclear encoded (especially


A
Photosynthesis
Light
Light + linco
ALL
PSII
PSI
LinRGs
LRGs
%
Z-Score
Hours of light
B
Tetrapyrroles
ALL
Chlorophyll
Proto-IX
Heme
CHL IX
C
Carotenoids and LHC-like
Carotenoids
LHCSR
ELIP
D
Cell Motility
ALL
FAP
IFT
0 1 3 6 9 [h]

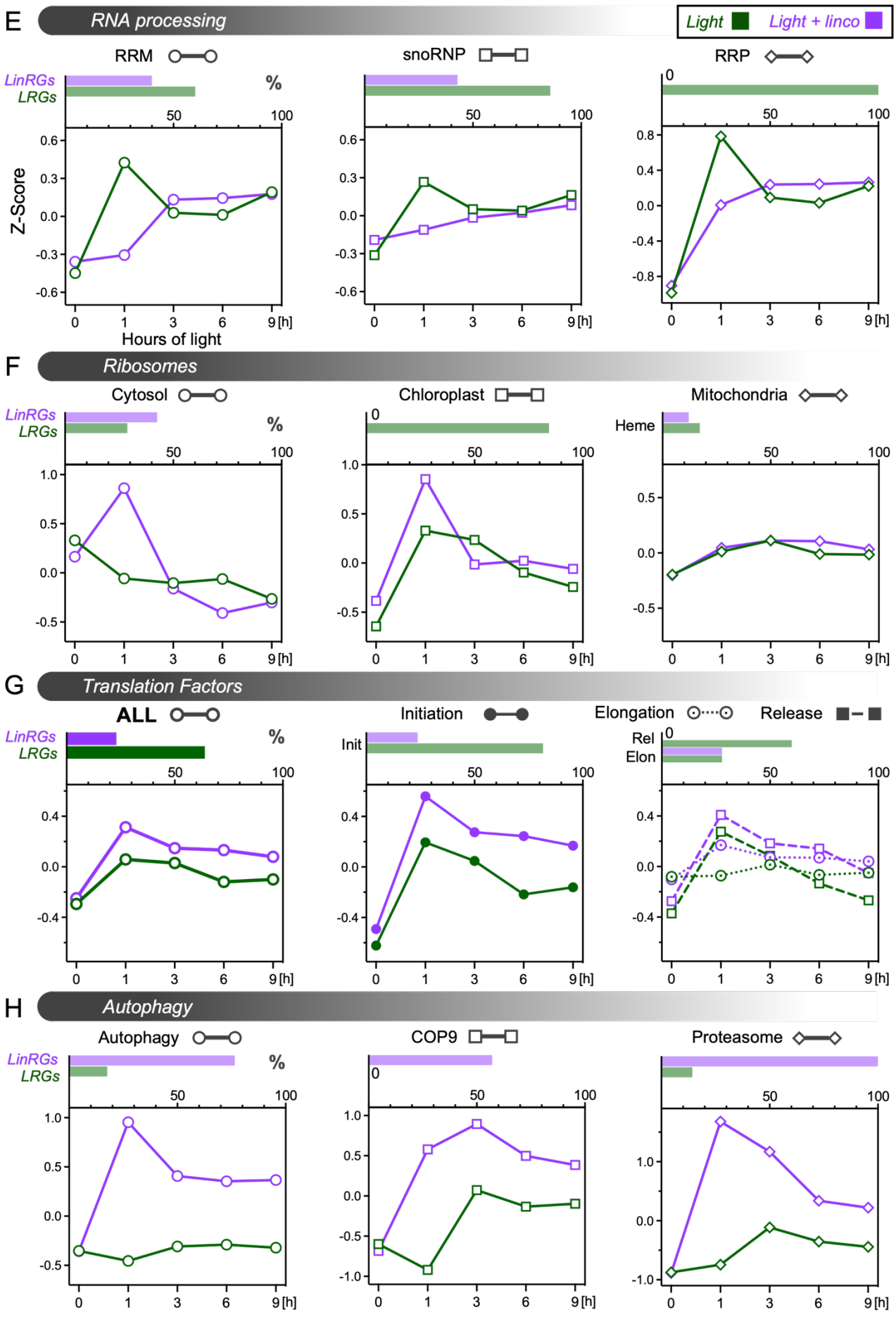

E
RNA processing
Light
Light + linco
RRM
snoRNP
RRP
LinRGs
LRGs
%
Z-Score
Hours of light
F
Ribosomes
Cytosol
Chloroplast
Mitochondria
Heme
G
Translation Factors
ALL
Initiation
Elongation
Release
Init
Rel
Elon
H
Autophagy
Autophagy
COP9
Proteasome
9 [h]

Figure 4.4: Expression profiles of selected genes from significantly enriched biological processes from GO analysis: A. photosynthesis; B. tetrapyrrole biosynthesis; C. carotenoid biosynthesis and LHC-like; D. cell motility; E. RNA processing; F. ribosomes; G. translation factors; H. autophagy. Gene expression profiles were determined for each experiment as the mean Z-score normalized counts values (from both light and light + linco samples) of all the genes belonging to the biological process (ALL), or subprocess (above indicated). Genes belonging to each biological process and subprocess were manually selected using information from genome annotations and literature. Above each expression profile the proportion of *LRGs* (dark green, $|\log_2 FC|>1$ light vs dark) or *LinRGs* (purple, $|\log_2 FC|>1$ linco vs not linco) included in each biological process or subprocess is represented. Photo: photosynthesis; Hm: heme; Chl: chlorophyll; IX: Proto-IX; Caro: carotenoid biosynthesis; Mt: mitochondria; Cp: chloroplast; Cyt: cytosol; Rel: release factor; Elon: elongation factor; Init: Initiation factor; IFT: intraflagellar transport; FAP: flagellar associated protein; RRM: ribosomal RNA methyltransferase; snoRNP: small nucleolar ribonucleoprotein; RRP: component of the exosome complex.

photosystem components as well as the enzymes for tetrapyrrole and carotenoid biosynthesis). As cytoplasmic ribosomes are among the most highly expressed genes in Chlamydomonas, their induction in light could explain the increase in transcript levels at 1h in light + linco samples. The early repression of RNA processing may indicate a need for increasing the availability of RNA transcripts in the cytoplasm.

Finally, we observed a high induction of genes involved in autophagy and protein quality control (COP9 signalosome and proteasome complex) under linco conditions (Figure 4.4 H), as previously described in Arabidopsis (Llamas et al., 2017) and similarly to the effects caused by high light (Ramundo et al., 2014). This further suggests the involvement of the cpUPR during de-etiolation of *y-4* cells.

Altogether these results indicate that linco triggered RS involved in de-etiolation of *y-4* cells 1) strongly but transiently repress light-induced photosynthesis and tetrapyrrole biosynthesis genes 2) regulate the expression of genes involved in cell motility, and 3) compensate defective chloroplast translation by increasing the number of cytoplasmic ribosomes and cytoplasmic translational activity. Also, our results indicate that bilin- and cpUPR-dependent RS are involved in regulating de-etiolation in Chlamydomonas.

Chloroplast associated nuclear genes are not preferentially regulated by retrograde signals

In the previous chapter we evaluated light-responsiveness of the chloroplast associated nuclear genes (*CpANGs*) subset, and found that this was enriched in *LRGs* (55% of *CpANGs* compared to 40% of the whole transcriptome) and that the vast majority of these genes were upregulated. Here, we evaluated if these *CpANGs* are also enriched in *LinRGs*, whether light-responsive or not. We reasoned that since linco affects chloroplast translation during de-etiolation critically compromising chloroplast development, the great part of *CpANGs* should be *LinRGs*. Surprisingly, this was not the case (Figure 4.5 A): most light responsive *CpANGs* are not affected by linco (756), and most *LRGs* and *LinRGs* are not *CpANGs* (1778); in particular, we observed the same proportion of significantly linco affected (*LinRGs*) in the *LRGs* and *CpANGs* subset (35%) as in the *LRGs* and non-*CpANGs* subset (32%), meaning *CpANGs* are not enriched in *LinRGs*. When analyzing inductive and repressive effects of linco, we also couldn't find any tendency (Figure 4.5 B): the only difference found in the *CpANGs* subset was between light-induced (A and B, green, the majority) and repressed (C

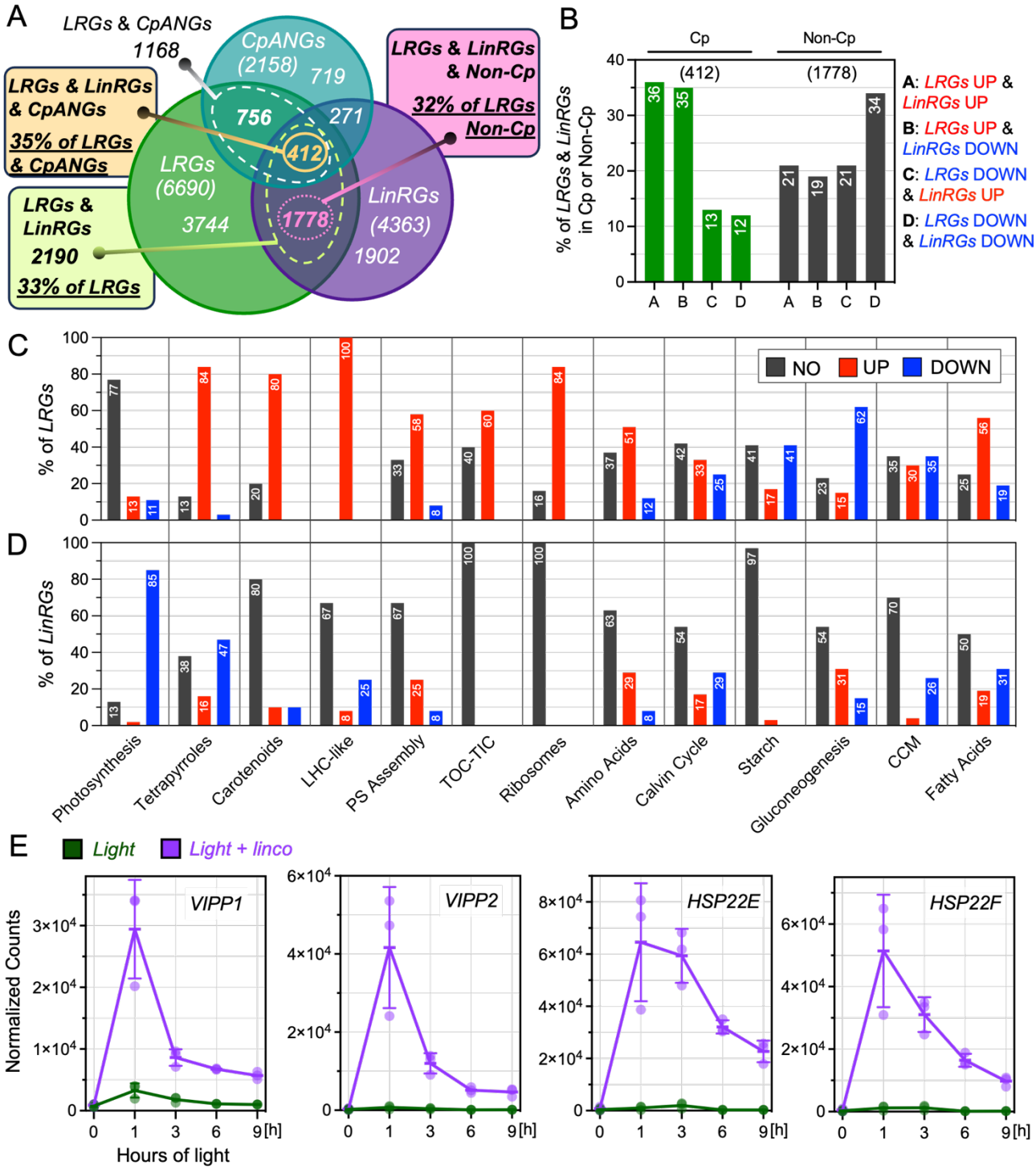


Figure 4.5: Analysis of lincomycin responsive chloroplast associated nuclear genes (*CpANGs*). A. The Venn diagram indicates the overlap between *LRGs*, *LinRGs* and *CpANGs*: total number of genes belonging to these groups is indicated in brackets, whereas the number of genes of each subset is indicated w/o brackets. B. Proportion of upregulated and downregulated *LRGs* and *LinRGs* inside *CpANGs* (green) and *non-CpANGs* (grey) groups. C,D. Proportion of *LRGs* (C) and *LinRGs* (D) for each chloroplast biological process or subprocess (genes belonging to each process were manually annotated using information from genome annotations and literature), divided into upregulated (UP, red), downregulated (DOWN, blue), and non-responsive (NO, grey). E. Expression profiles of genes involved in RS according to Theis et al., 2020 (*VIPP1*, *VIPP2*, *HSP22E*, *HSP22F*).

and D, green) genes, as already shown in the previous chapter; in the non-*CpANGs* subset we observed that light repressed genes are mostly linco repressed (C vs D, grey). This latter group (D, grey) likely features the great majority of cell motility genes, and since Chlamydomonas genome

features more than a thousand of these genes, these are likely to contribute to the observed enrichment.

Next, we looked at the proportion of *LRGs* (Figure 4.5 C) and of *LinRGs* (Figure 4.5 D) in the different chloroplast biological processes, biasedly selecting the genes belonging of these according to the information from the literature and annotations. A high proportion of light induced genes (red bars) was found in the different categories, as already shown in the previous chapter, except for biological processes related to carbon metabolism (Calvin cycle, starch, gluconeogenesis and CCM) which also feature a considerable proportion of light repressed genes; another exception is photosynthesis in which the majority are non-*LRGs*, as these do not reach the $log_2FC>1$ threshold. In contrast, most chloroplast biological processes are non-*LinRGs*, suggesting that many functions are still active under linco conditions. Interestingly, TOC-TIC is not affected, suggesting that the plastid can still import the cytosolic synthesized proteins into the chloroplast. These include carotenoids and LHC-like components involved in photoprotection, chloroplast ribosomes and assembly factors for photosystems, and eventually also photosystem components and tetrapyrrole enzymes when they recover their expression. The plastid still keeps null photosynthetic capacity at any time point tested because many photosynthesis genes are encoded in the chloroplast genome and cannot be translated no matter the presence of assembled ribosomes, as linco specifically blocks their binding with plastid mRNA.

Chlamydomonas VIPPs have been shown to complex with HSP22E/F and send RS to the nucleus under high light conditions to induce their expression. VIPP2 is thought to sense stored curvature elastic (SCE) stress caused by the generation of ROS species, while VIPP1 is known to be involved in the assembly and repair of thylakoid membrane protein complexes (Theis et al., 2020). We evaluated the expression of these genes in our de-etiolation system and found they are all extremely over induced by linco at 1h (Figure 4.5 E). This high over induction is transient, but is kept at least during the first 9h although at lower levels. In particular, *VIPP2*, *HSP22E/F* are the genes with the highest degree of over induction by linco in our transcriptome. As these genes are already induced by light in the absence of linco (*LRGs*), these results suggest that chloroplast biogenesis of *y* mutants highly relies on the regulation by VIPPs-HSP22E/F RS: under ideal conditions these are expressed at low levels to monitor proper thylakoid assembly, while under stress conditions likely caused by the accumulation of ROS (these may be produced by accumulation of free chlorophyll pigments and intermediates which are extremely phototoxic) these components are needed to protect membranes from oxidative damage, and for thylakoid membrane assembly and repair.

Light and retrograde signals converge on FAP280 and ETF4 transcription factors to regulate induction of VIPPs during de-etiolation

We also evaluated if linco significantly affected overall expression of TFs, as defined in the previous chapter (Figure 4.6 A): only a third of all TFs are *LinRGs*, (*LinRTFs*) being half of these also *LRGs* (*LRTFs*). This means that not all *LRTFs* are target of RS, consistent with the specificity of linco effect during de-etiolation. Inside the subset of 53 TFs regulated by light and RS linco effect is stronger at 1h and tends to overpower light-dependent induction or repression (Figure 4.6 B), but this tendency was also found with all light- and linco- responsive genes (Figure 4.1)

Next, we focused on the predicted TFs involved in chloroplast biogenesis from the previous chapter (Figure 4.6 C), and tested if these were significantly affected by linco. Interestingly, of all early transcription factors only those connected to VIPPs, *FAP280* and *ETF4*, were significantly affected by linco, and in the same way as *VIPPs* and *HSP22E/F*. As these *TFs* are also early upregulated by light, they represent two strong candidates in the convergence of light and RS during de-etiolation: in this context, these two signaling mechanisms may act on *FAP280* and *ETF4* to regulate light induction of *VIPPs* and *HSP22E/F*. Specific TFs from the mid phase, *NAB1* and *GSP1*, and late phase, *LCR1* and *LTF2*, were also significantly affected by linco, but in this case linco has a repressive effect. In particular, both Light and L+Lin expression profiles of *NAB1* are identical to their target photosynthesis genes, while in the case of *GSP1* linco suppressed its early light transient induction. However, in both cases Light and L+Lin differences decrease with time in light, consistent with the transient repression of their target photosynthesis and tetrapyrrole biosynthesis genes. Late TFs were highly impacted by linco but overall kept the same profile, and their repression is also consistent with the repression of their target genes (LCR1 with LCIB1 and LCIC1, LTF2 with most Krebs cycle genes). Altogether these results suggest that linco-dependent RS regulate the expression of nuclear target genes by acting on specific (not all) light-regulated TFs.

Importantly two key regulators of light signaling in Chlamydomonas, as CRHY5 and CRCO are not affected by linco (Figure 4.6 C). This suggests that these components are not involved in the crosstalk between light and RS in Chlamydomonas. Regarding HY5, in Arabidopsis this TF is a RS target, as it is significantly induced by linco, and repressed in light in *gun1* mutants (Hernández-Verdeja et al., 2022; Ruckle et al., 2012). It is likely that HY5 gained regulation by RS later in the evolution after the emergence of GUN1.

Lincomycin does not trigger retrograde signaling in the dark

A debated question regarding RS is if this signaling pathway also functions in dark conditions and if it depends on the plastid developmental state. In Arabidopsis it is known that GUN1 accumulates in the cotyledons of etiolated plastids and send RS to the nucleus to prevent premature plastid development in the dark (Hernández-Verdeja et al., 2022). In Chlamydomonas, mutants of RS

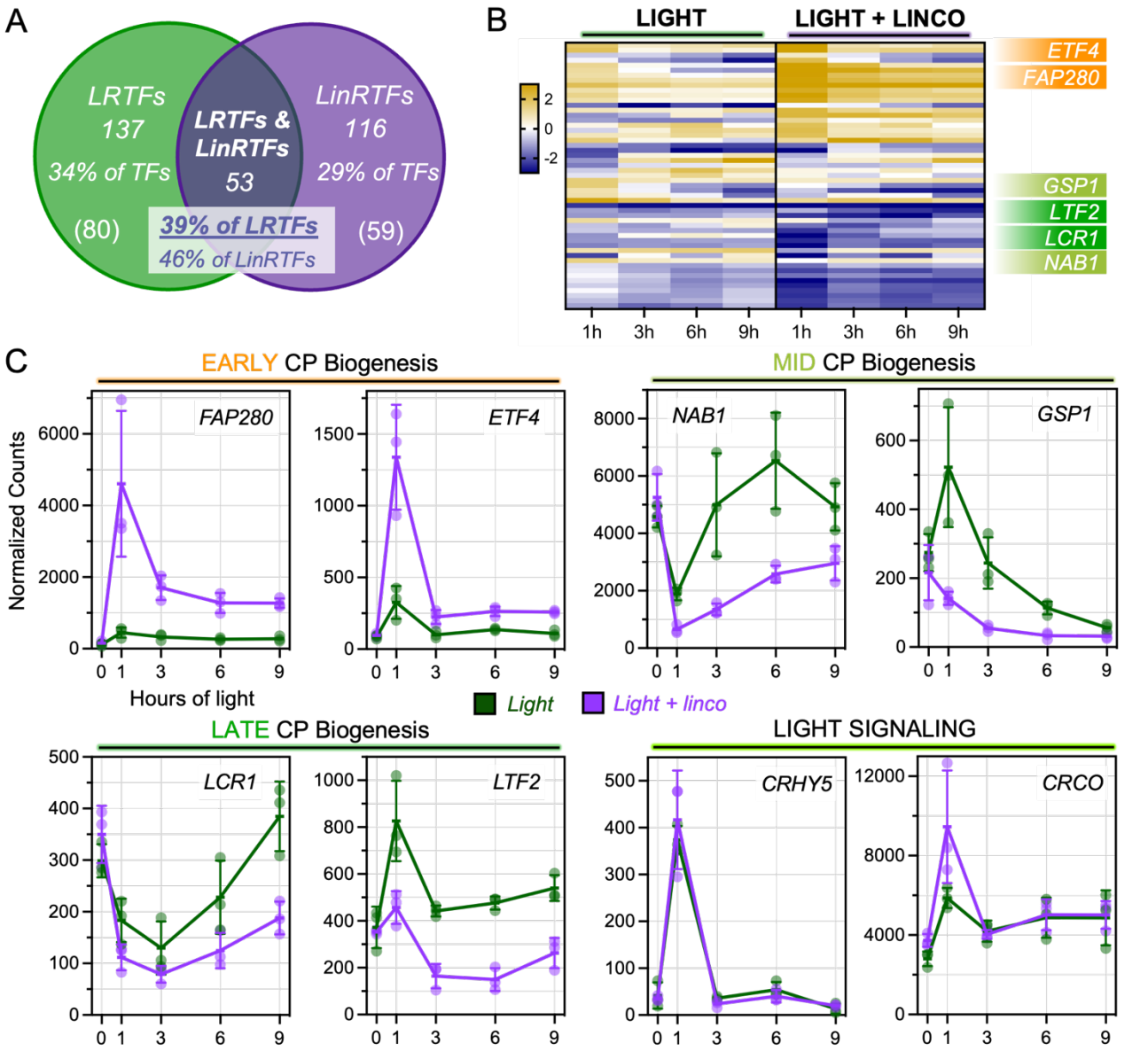


Figure 4.6: Analysis of linco responsive transcription factors (TFs). A. The Venn diagram shows the overlap between light responsive TFs (*LRTFs*) and linco responsive TFs (*LinRTFs*) defined following criteria for *LRGs* and *LinRGs*, respectively. Total *LRTFs* and *LinRTFs* is shown in italics, whereas the number of genes in non-overlapping subsets is shown in brackets. B. Heatmap of log_2FC values for Light and L+Lin pairwise comparisons of all 53 *LRGs* and *LinRTFs*. Genes were hierarchically clustered by one minus pearson method and average linkage method. Next to the heatmap the predicted TFs involved in chloroplast biogenesis (see Chapter 3) which were also significantly affected by linco are indicated. C. Gene expression profiles of Light and L+Lin samples of these linco-regulated TFs separated into each of the three phases of chloroplast biogenesis. In addition, we show the expression profiles of two key regulators of light signaling in Chlamydomonas.

components from tetrapyrrole biosynthesis pathway (*hmox1* and *gun4*) feature significantly differentially expressed genes in the dark (Duanmu et al., 2013; Formighieri et al., 2011); however, these effects on the transcriptome vanish when performing comparisons with their complemented lines instead of using their wt background (Brzezowski et al., 2014; Witkopp et al., 2017). We aimed to solve this question by evaluating linco effects in the dark in both *y-4* and wt cells. Thanks to this approach, we can also evaluate if RS are sent in the dark only when plastids are undeveloped, as in Arabidopsis, or if they are sent also when the chloroplast is fully developed in the absence of light;

this represents an important advantage compared to angiosperm-based de-etiolation systems where light and plastid developmental state are two inseparable variables.

Both *y-4* and wt cells were grown in the same conditions in the dark, with the difference that *y-4* cultures were prepared in bigger flasks as they were later employed for de-etiolation analysis. Linco treatment included overnight acclimation in acetate supplemented medium (HSA) plus 3h of minimal medium acclimation (HSM), making approximately a total 15h of linco exposure, all carried out in dark conditions (Figure 4.7 A). Surprisingly, we didn't find a single *DEG* between linco treated and non-treated cells in both *y-4* and wt strains (Figure 4.7 B). This suggested that RS is not active in the dark in Chlamydomonas; alternatively, the time of linco exposure may not have been enough to cause sufficient effects that trigger RS. To test this last possibility, we extended linco treatment of wt cells for two more days to evaluate how it affected chloroplast parameters (Figure 4.7 C). After two days linco caused slightly more yellowish cultures (Figure 4.7 D), and impaired both maximum PSII quantum yield (Figure 4.7 E) and accumulation of chlorophylls (Figure 4.7 F); however the same effect was observed in non-linco samples, though in a slightly lesser degree. This indicates that repression of photosynthetic activity is caused mainly by dark and mostly overlaps with linco effects in this condition. Interestingly, just a short light treatment caused a high increase of maximum PSII capacity in non-treated samples compared to linco treated samples Figure 4.7 E). It is therefore unlikely that the absence of *DEGs* in the dark is caused by low exposure time to linco conditions. Therefore we propose that linco does not trigger RS in the dark in Chlamydomonas, no matter the degree of plastid affection, while light trigger RS likely as a consequence of the release of ROS species, and the need of the cells to protect from oxidative damage by inducing cpUPR on one hand, and bilin biosynthesis on the other (Figure 4.7 G).

Lincomycin and high light trigger highly similar retrograde signaling response

High light has been shown to impair chloroplast protein homeostasis and trigger the cpUPR in Chlamydomonas. This response is mediated by VIPPs and HSP22E/F in the chloroplast that send RS to the nucleus to induce their expression, as well as the expression of *LHCSR3*, a key photoprotection gene (Theis et al., 2020). As we also observed the induction of these genes in our de-etiolation system under linco conditions, we wondered if high light and linco- dependent RS regulate the same genes during dark-to-light transition. For this purpose, we analyzed transcriptomic data of Chlamydomonas cells exposed to high light treatment from Knopp et al., 2020 (Figure 4.8 A): we processed raw data following the same procedure used for our transcriptomic analysis, and pairwise compared 1h high light treated cells towards dark, this latter condition being the middle of the dark phase of cells grown in a 12:12 (light-dark) photoperiod. High light responsive genes (*HLRGs*) were determined as giving pAdj<0.05 and $|\log_2 FC|>1$ in this comparison; this subset was compared with Light+Linco responsive genes at 1h (*LLRGs*, see Important Remark), which were defined with the same criteria. By doing so, we observed similar numbers of *HLRGs* (6431) and

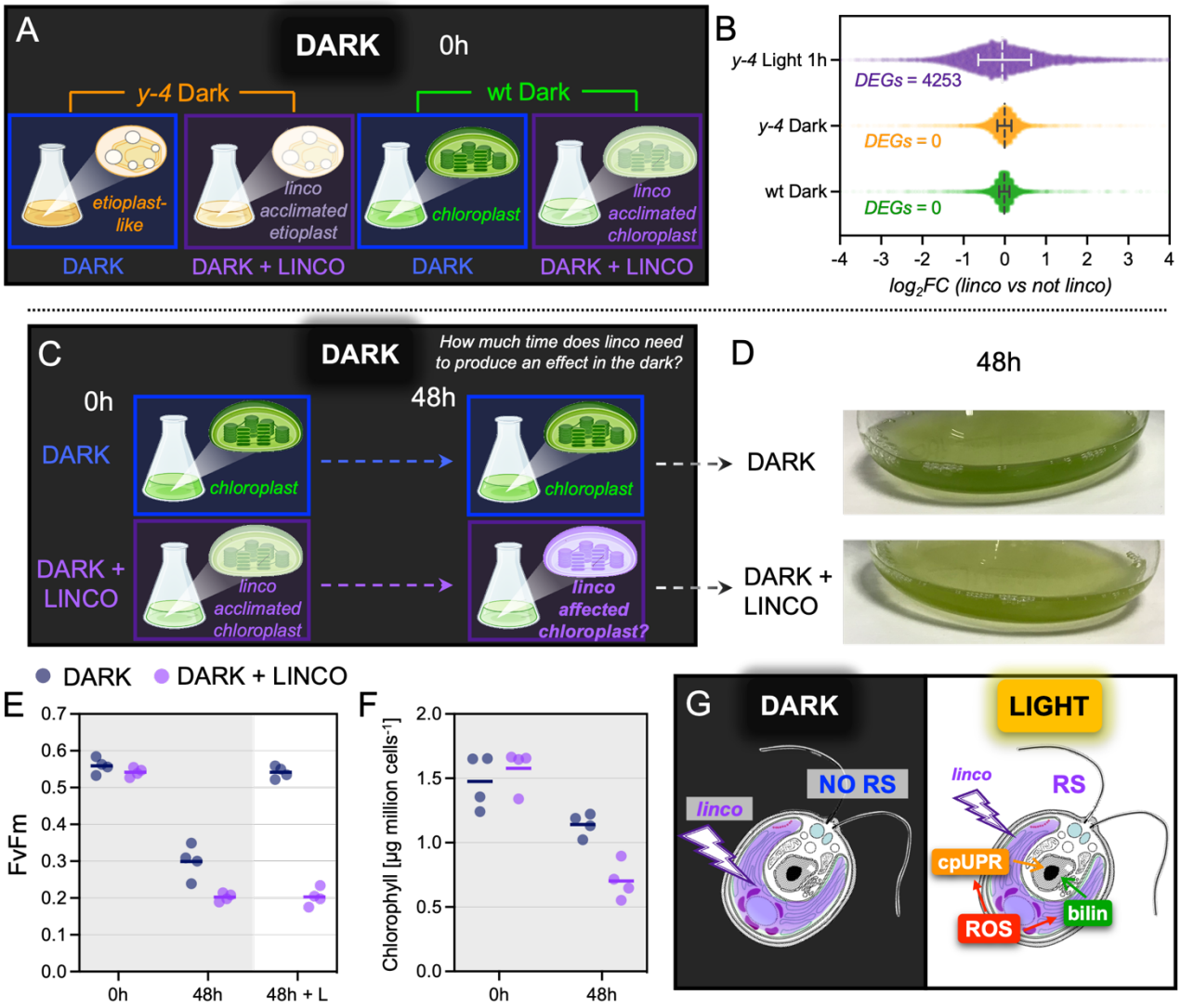


Figure 4.7: Analysis of linco responsive genes in the dark. A. Schematic view of samples from our RNA-seq experiment used for this analysis: the comparison between *y-4* etiolated cells in the dark w/o (y-4 Dark) and with linco (*y-4* Dark + Linco) indicates if an etioplast-like plastid can send linco RS to the nucleus, whereas comparing wt dark-grown cells w/o (wt Dark) and with linco (wt Dark + Linco) indicates if this process needs a fully developed and functional chloroplast instead. B. Distributions of log_2FC values from *y-4* and wt pairwise comparisons as indicated in A (linco vs non-linco treated). To better understand the magnitude of linco affection in the dark, another comparison linco vs not linco at 1h light was added. Dashed line represents the median, whereas error bars indicate the interquartile range. C. The linco effect on wt cells in the dark was later tested by extending the treatment with additional 48h (original acclimation was overnight+3h, see Chapter 2). D. Images of a wt cell culture after 48h of linco treatment in the dark (DARK + LINCO) and its control w/o linco (DARK). E,F. FvFm (E) and total chlorophylls (F) of DARK (blue) and DARK + LINCO (purple) samples before linco treatment (0h) and after 48h of linco treatment. FvFm was also tested after 48h with a short light treatment. G. Model for linco RS in the dark. Consistent with transcriptomic data from other RS works in Chlamydomonas linco did not generate changes in gene expression in the dark (Brzezowski et al., 2014; Witkopp et al., 2017). Upon light exposure ROS accumulate due to presence of free tetrapyrrole pigments that are phototoxic; this in turn triggers synthesis of bilins to cope with photooxidative stress and of the cpUPR response due to ROS-mediated protein damage.

LLRGs (6653), and found a high degree of overlap between both subsets which represents almost 50% of each (Figure 4.8 B). However, this overlap could be explained by the presence of a high number of light regulated genes which are not affected by linco or excess light stress. Therefore, we filtered this common subset for those genes significantly affected by linco in the L+Lin vs Light pairwise comparison at 1h (*LinRGs filt*, Figure 4.8 A). We used this approach and didn't take into account light samples from Knopp et al., 2020 (used in this work to evaluate only excess light effects)

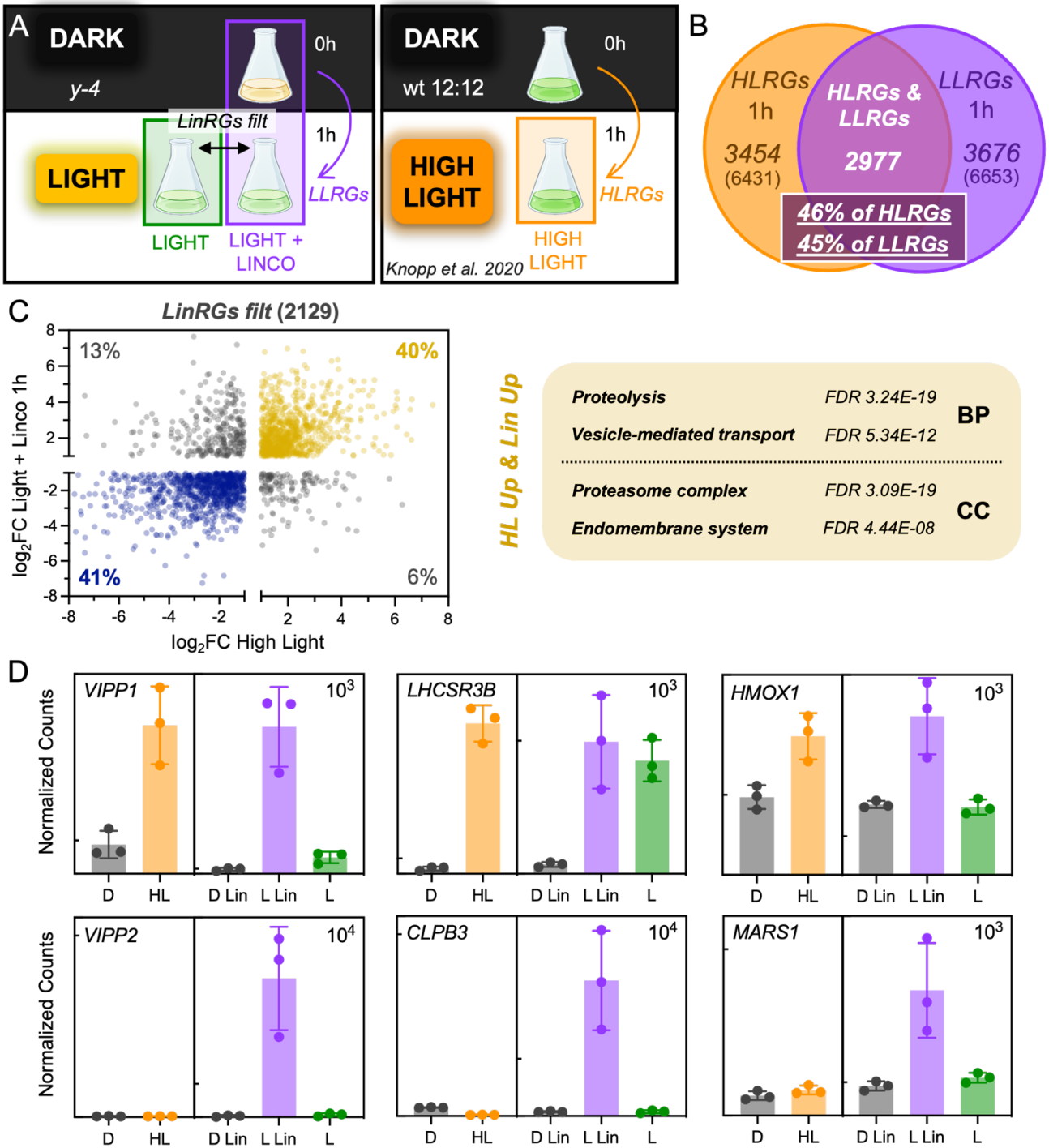


Figure 4.8: Analysis of high light and linco dependent RS during early light response. A. For this part of the analysis, we compared the effects of linco in de-etiolating *y-4* cells in our experiment, with high light stress on wt cells grown in 12:12 photoperiodic conditions (Knopp et al., 2020). We first determined light + linco (*LLRGs*: pAdj<0.05, $|\log_2 FC|>1$ L+Lin vs Dark+Lin at 1h pairwise comparison) and high light effects (*HLRGs*: pAdj<0.05, $|\log_2 FC|>1$ in high light vs dark) on dark grown cells, and later discarded light contributions using *y-4* light samples in our experiment (*LinRGs filt*: pAdj<0.05 in L+Lin vs Light at 1h). B. Venn diagram showing overlap between *LLRGs* and *HLRGs* (without *LinRGs filt*). The number of genes of each subset is shown in italics, whereas total *LLRGs* and *HLRGs* (at 1h) are shown in brackets. C. Correlation plot of $\log_2 FC$ values for L+Lin and high light pairwise comparisons of the *HLRGs* and *LLRGs* subset with *LinRGs* filter. Upregulated and downregulated genes in both comparisons are highlighted in yellow and blue, respectively. For upregulated genes selected GO terms significantly enriched for biological process (BP) and cellular component (CC) are shown (FDR< 0.05). D. Gene expression levels of main RS regulators in Chlamydomonas in the samples from both experiments employed in this analysis. High light experiment: dark (D, black), high light 1h (HL, orange); *y-4* de-etiolation experiment: dark + linco (D Lin, black), light + linco 1h (L Lin, purple), light 1h (L, green). Ticks in the y axes are a reference of the normalized counts levels scaled for each experiment, and the reference values are shown in the upper right corner of each plot.

as these were taken at 6h of light under 12:12 photoperiod, and we would be underestimating the effects of the early light response which in many cases is transient. Interestingly, the number of *HLRGs* and *LLRGs* which were also significantly regulated by linco compared to light was still high (2129). We next evaluated if linco and high light dependent RS also regulate these genes in the same way, and found that in the majority of them (80%) both stresses cause inductive (40%) or repressive (41%) effects (Figure 4.8 C). These results indicate highly similar gene regulation exerted by linco and high light triggered RS. Consistent with this we found that common upregulated genes were significantly enriched in GO terms related to protein homeostasis; in contrast, we didn't find any significantly enriched GO terms in the subset of common downregulated genes. Next, we evaluated the expression of key genes from the cpUPR and also of the bilin RS pathway (Figure 4.8 D): linco significantly induces the expression of all cpUPR genes except *LHCSR3B*, a target gene of this pathway; surprisingly, although upregulated high light genes include many cpUPR targets, certain genes encoding key components described for the cpUPR are not induced by high light, such as *VIPP2*, *CLPB3* (encoding a chaperone) and *MARS1*. These results are in contrast with what has been so far described (Theis et al., 2020), and could indicate that cpUPR can also be executed through an alternative mechanism that is not mediated by *VIPP2* nor *MARS1*, and that high light treatment in this experiment didn't cause SCE stress; in our de-etiolation system, instead, *VIPPs*, *HSP22E/F* and *MARS1* are highly over induced by linco, as these cells suffer from combined effects of featuring undeveloped thylakoid membranes and impaired protein homeostasis caused by linco. *HMOX1* is also induced by high light, but we don't know if in this case light at moderate levels would have induced this gene at the same levels, or if it is a specific effect caused by stress as with linco.
Overall, we found that high light and linco trigger a highly similar retrograde signaling response. Also linco triggers cpUPR response as already reported in Arabidopsis (Llamas et al., 2017). How this cpUPR is achieved likely depends on the plastid developmental state and/or on the degree of the stress (high light, linco or others) that the chloroplast suffers during dark-to-light transition.

A subset of GUN1-regulated genes in Arabidopsis is regulated in the same way in Chlamydomonas by an alternative retrograde signaling pathway

GUN1 is considered a key master regulator of biogenic RS in angiosperm plants that fine-tunes chloroplast biogenesis as well as other developmental responses during de-etiolation (Calderon & Strand, 2021). In particular, GUN1-dependent retrograde signals are described to repress many *CpANGs* during de-etiolation under linco (Koussevitzky et al., 2007) or other conditions that generate stress in the developing chloroplast (Figure 4.9 A). Since Chlamydomonas genome does not feature a *GUN1* homolog, we tested whether these genes are also repressed during de-etiolation of *y-4* cells. For this purpose, we employed the list of GUN1-regulated genes in Arabidopsis from Wu et al., 2018, and DE values obtained from the comparison between Col-0 and *gun1* mutants seedlings germinated

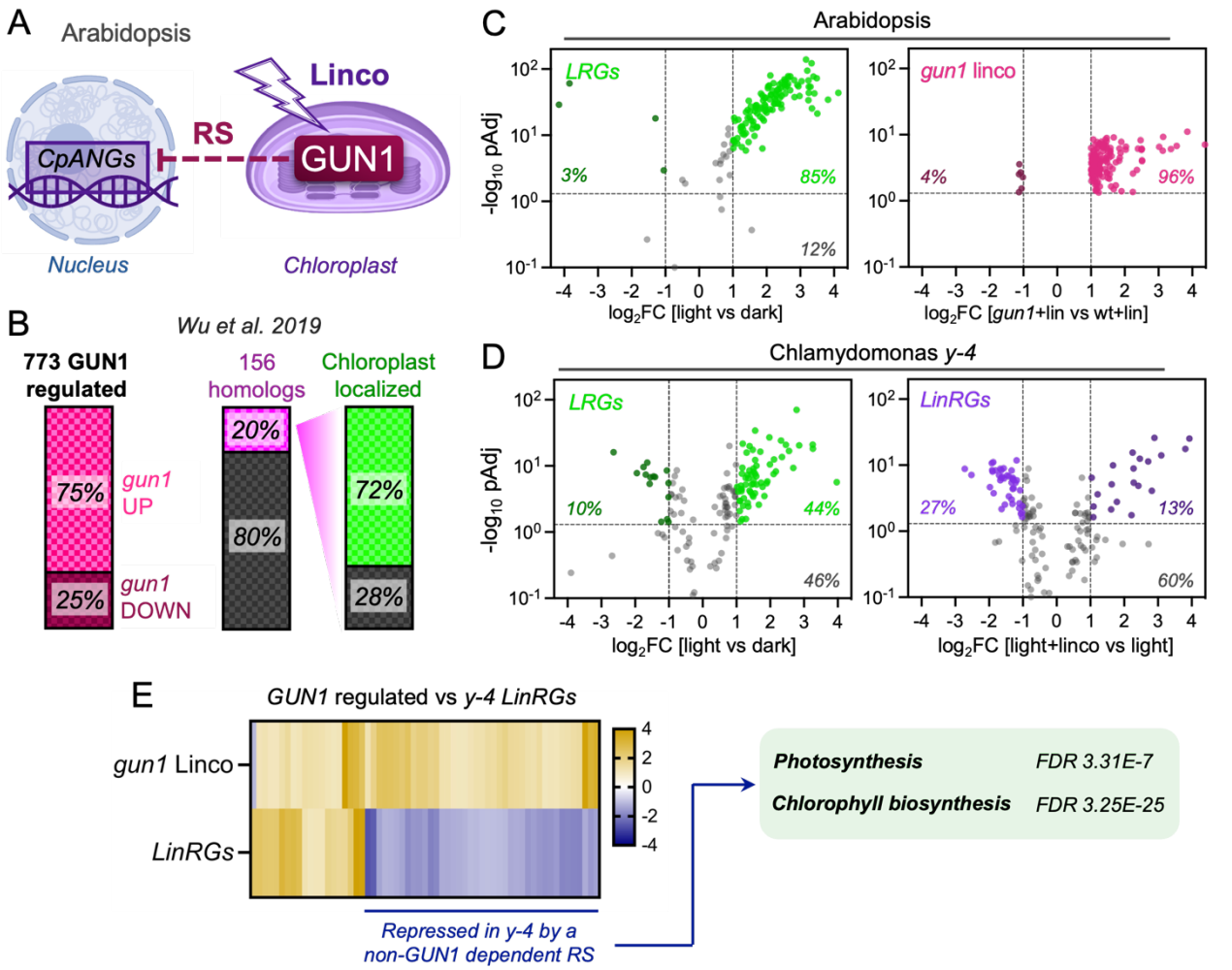


Figure 4.9: Analysis of GUN1-regulated genes in Chlamydomonas. A. In Arabidopsis, stress caused by lincomycin during chloroplast biogenesis triggers GUN1-regulated RS which are sent to the nucleus to repress the expression of many *CpANGs*. B. Number of GUN1-regulated genes in Arabidopsis from Wu et al., 2019 with the percentage of *gun1* upregulated (UP) and downregulated (DOWN) genes. Percentage of all GUN1-regulated genes which share a homolog with Chlamydomonas and percentage of these gene homologs which are *CpANGs*. C,D. Volcano plots of 156 GUN1-regulated and Chlamydomonas homologs genes in Arabidopsis (C) and Chlamydomonas (D). For Arabidopsis, *gun1* linco differentially expressed genes were obtained from Wu et al., 2019, whereas *LRGs* plot values were obtained from seedling de-etiolation experiment used in the previous chapter (Burko et al., 2020), using maximum $|\log_2 FC|$ values of light vs dark pairwise comparisons. For Chlamydomonas, *LRGs* plot values correspond to the maximum $|\log_2 FC|$ values of light vs dark pairwise comparisons, whereas *LinRGs* plot values correspond to the maximum $|\log_2 FC|$ of L+Lin vs Light pairwise comparisons. E. Heatmap represents differential expression values from *gun1* linco and *LinRGs* plots of C and D. These values were hierarchically clustered by Euclidean distance and average linkage method. A cluster of *gun1* linco induced and linco repressed is highlighted. Since Chlamydomonas does not feature any *GUN1* homolog, this cluster represents genes that are repressed by a non-GUN1 dependent RS in Chlamydomonas, and mainly consists in genes involved in photosynthesis and chlorophyll biosynthesis.

in light under linco conditions (Figure 4.9 B): the great majority of GUN1-regulated genes (773) are upregulated in *gun1* in this comparison (75%), meaning GUN1 triggers mostly repressive effects on gene expression. We identified a total 156 GUN1-regulated gene homologs in Chlamydomonas (to determine gene homologs we followed the same approach used for determining PIF- and GLK-regulated genes in the previous chapter), the majority are *CpANGs* (72%). We next evaluated how these 156 homolog genes are regulated in Arabidopsis (Figure 4.9 C) and in Chlamydomonas (Figure 4.9 D). The vast majority are light induced genes (according to Burko et al., 2020 data, as analyzed in the previous chapter), and almost all of them are linco-induced in *gun1*, meaning GUN1 represses

all these genes in this condition. In Chlamydomonas, 44% of GUN1-regulated genes are light-induced in our RNA-seq, although this percentage could be higher considering that many photosynthesis genes do not reach the $|\log_2 FC|>1$ threshold to be considered *LRGs*. We found 27% of these genes are significantly repressed by linco during de-etiolation: these are mainly genes involved in photosynthesis and chlorophyll biosynthesis (Figure 4.9 E). Since Chlamydomonas lacks GUN1, these genes must be repressed by an alternative RS mechanism, which could depend on the cpUPR, the synthesis of bilins, or on novel RS regulators that still need to be discovered.

High throughput de-etiolation as a strategy for the screening of novel biogenic retrograde signaling mutants in Chlamydomonas

Transcriptomic analysis allowed us to predict if already described RS pathways are involved in regulating de-etiolation of *y-4* cells, and to determine main biological processes affected. However, to identify novel regulators of RS we need to generate mutants in which chloroplast-to-nucleus communication is impaired. In this context, a key advantage of our de-etiolation system is that we can characterize the ancestral biogenic RS pathway involved in regulating chloroplast biogenesis, by using *y-4* strains as background to generate novel *gun* mutants that are, for instance, no longer able to fully reconstitute their chloroplast upon light. Here two questions arise: 1) how can we generate RS mutants? and 2) how do we know that these mutants are impaired in RS?

There are two possible strategies to generate RS mutants: 1) to create an insertional mutant library (Cheng et al., 2017) or 2) by random mutagenesis using a mutagen source such as UV light (Schierenbeck et al., 2015) or EMS (Lee et al., 2014); forward genetic screen can be easily performed in the first case by PCR, whereas in the second case whole-genome sequencing need to be performed to identify the mutation.

In either case, to easily detect mutants that are affected in RS in our de-etiolation system, we need to generate a reporter line that shows an easily visible phenotype, such as a fluorescence signal, when RS mechanism is activated (Figure 4.10 A). For this purpose, we need to identify a gene which under RS-triggering conditions, linco in our case, is highly induced compared to light and build a cassette in which a fluorescence marker (such as mVenus) is under the control of the promoter of this gene. We identified two suitable reporter genes in our transcriptome: *VIPP2* and *HSP22F*, which are the most highly induced genes by linco (Figure 4.10 B). In our de-etiolation system the resulting reporter line would show a powerful fluorescence signal under linco conditions, indicative of the activation of RS, while a mutant of this process should suppress this signal in this condition, as chloroplast and nucleus are no longer communicating.

As we aim to detect mutants affected in biogenic RS during de-etiolation of *y-4* cells, we need a strategy to etiolate and de-etiolate possibly hundreds of candidate mutants at the same time during the screening process. For this purpose, we setup a high throughput de-etiolation system in which

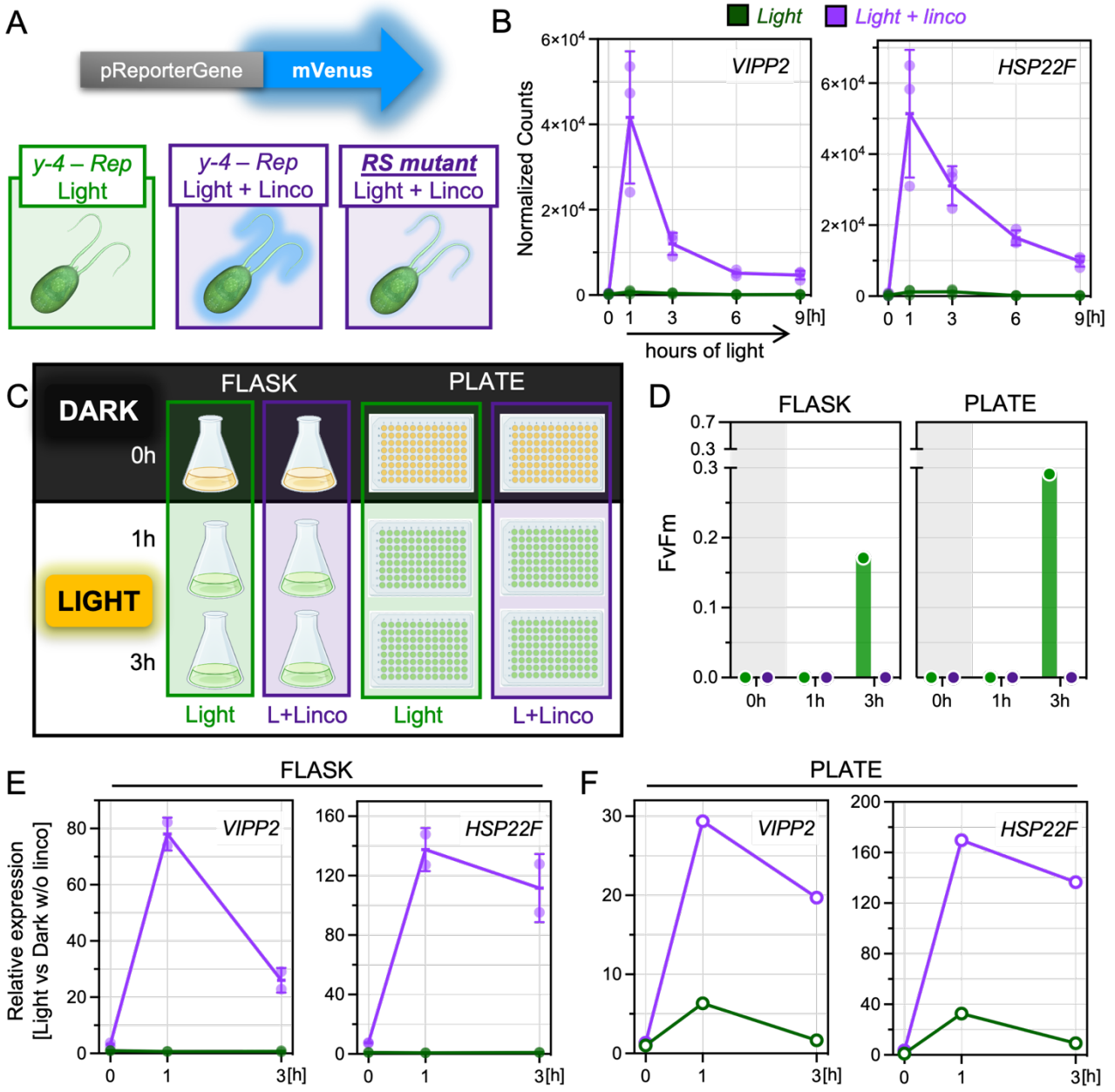


Figure 4.10: Design of a biogenic RS reporter line in Chlamydomonas. A. The first step consists in finding a suitable reporter gene, which has to be only and highly induced in L+Lin conditions. A *y-4* strain expressing a fluorescent tag (such as mVenus) under the control of the promoter of this reporter gene would give fluorescent signal only in conditions where RS is induced, whereas a RS mutant (i.e. generated by UV mutagenesis) would have impaired chloroplast-to-nucleus communication, repressing this signal. B. Two candidate reporter genes were selected, *VIPP2* and *HSP22F*. Here their Light (green) and L+Lin (purple) expression profiles in our RNA-seq is shown. C. Since likely hundreds of colonies need to be screened and checked during de-etiolation, a high-throughput (HT) de-etiolation need to be setup. Here a schematic view of a HT de-etiolation, performed in 96-well plates and in flasks, as a control. D. FvFm of de-etiolating *y-4* cells in flask or plate. E,F. Expression values in Light (green) and L+Lin (purple), relative to dark 0h, of both reporter genes in *y-4* cells de-etiolating in flasks (E) and plate (F).

de-etiolation is performed on 96-well plates (Figure 4.10 C): preparation of the etiolated material, linco treatment and medium acclimations were all performed following the same procedure used for our RNA-seq, with the difference that each step was scaled to the volume that can hold each well (around 200 µL). As a control we also performed de-etiolation in flasks. By doing so, we managed to obtain

perfectly etiolated cells with no photosynthetic capacity also on plate (Figure 4.10 D): here, FvFm recovered upon transfer to light starting at 3h, while linco treated cells were completely impaired in this recovery, as in cells de-etiolating in flasks.
We next monitored the expression of our candidate reporter genes by RT-qPCR in both cells de-etiolating in flask (Figure 4.10 E) and on plate (Figure 4.10 F), and found *VIPP2* and *HSP22F* where much more highly expressed in linco conditions compared to light in both cases, though this difference was more striking in flasks. This indicates that our de-etiolation system is very robust and can be adapted to any volume, and that the setup high throughput de-etiolation is a valid strategy for the screening of biogenic RS mutants in Chlamydomonas.

Discussion

Chlamydomonas retrograde signals have limited capacity to repress chloroplast biogenesis under adverse conditions

In this work we aimed to identify the main events regulated by RS during de-etiolation, and to evaluate at which degree it affects light signaling, as in angiosperm plants both are essential for proper autotrophic seedling establishment (Woodson & Chory, 2008). For this purpose, we followed a similar approach that has been many times employed to study biogenic RS in Arabidopsis, that consisted in treating de-etiolating *y-4* cells with linco, to disrupt chloroplast activity and trigger changes in the RS pathway that regulates de-etiolation (Dubreuil et al., 2018; Koussevitzky et al., 2007; Ruckle et al., 2012). We previously observed that this approach is valid at the physiological level, as linco specifically affected photosynthetic performance and chlorophyll production, but cells remained perfectly viable for at least 24h. In this chapter, we also validated it transcriptomically, as linco effect showed to be very specific: on one hand it significantly affects only 26% of the transcriptome, being half of these *LinRGs* also significantly regulated by light (being a third of *LRGs*), while the other half is only significantly regulated by linco; on the other hand, linco affects very specific biological processes, at different degree and causing both inductive and repressive effects, overall resulting in very distinct expression patterns.
Biological processes which are both induced by light and repressed by linco are photosynthesis and tetrapyrrole biosynthesis genes, which is consistent with similar works performed in Arabidopsis (Dubreuil et al., 2018; Ruckle et al., 2012). This indicates that regulation of chloroplast biogenesis by plastid RS is conserved in Chlamydomonas, which is remarkable considering that this species lacks GUN1. There is however an important difference: in de-etiolating *y-4* cells, linco only transiently represses photosynthesis genes, and expression of these genes recover tending to the levels of non-treated cells, resulting in an overall delay in their induction. This transient repression can be explained by the own nature of Chlamydomonas RS, which are optimized for light acclimation and specifically

to cope with photooxidative damage. Although this precise RS mechanism is still not well understood, it has been demonstrated that both bilins (in particular biliverdin) and the cpUPR, the latter triggered by excess or misassembled proteins in the chloroplast, are involved. Indeed in our conditions, genes involved in heme biosynthesis and autophagy are highly induced by linco, consistently with previous studies (Duanmu et al., 2013; Ramundo et al., 2014), but this induction is transient with a peak at 1h. Our data suggest that Chlamydomonas employs RS dependent on bilins and cpUPR to regulate chloroplast biogenesis in de-etiolating *y-4* mutants, but since their induction is transient their repressive effects on photosynthesis genes is transient too. In Arabidopsis, instead, that evolved a biogenic RS mechanism that tightly regulates this process, the degree of repression exerted by linco on photosynthesis genes increases with the time of exposure to light (Dubreuil et al., 2018; Ruckle et al., 2012). This also gives hints about the evolutionary advantage that represented the emergence of GUN1 in angiosperm plants: as GUN1-regulated gene homologs we identified in Chlamydomonas are related to photosynthesis and chlorophyll biosynthesis, GUN1 may have emerged in angiosperm plants to keep repression of photosynthesis and chlorophyll genes down under adverse conditions for chloroplast biogenesis, while Chlamydomonas RS have limited capacity to repress them because its RS mechanism is not prepared to efficiently regulate chloroplast biogenesis.

Interestingly, we also found that linco significantly affects the expression of flagella genes, but in a different way compared to photosynthesis genes: linco over-repressed these genes at 1h, and also impaired light-dependent recovery in later time points, increasing the gap with non-treated cells. Bilins and cpUPR- dependent RS might be regulating the expression of flagella genes. Alternatively, it could be a secondary effect of calcium-mediated RS, which has been shown to activate in under high light stress triggering upregulation of the Ca^{2+} sensing receptor CAS, which in turn contributes to the secretion of Ca^{2+} from the chloroplast (Petroutsos et al., 2011): as cell motility is highly dependent on the intraflagellar calcium levels (Wheeler, 2017), increase in cytosolic Ca^{2+} might led to change in phototactic movements, that eventually require differential regulation of cell motility genes under linco conditions. Consistent with this, we found that *CAS1* is significantly induced by linco at 1h of de-etiolation.

Chloroplast biogenesis is regulated by VIPP2-dependent RS in Chlamydomonas

Theis et al. (2020) have proposed a model for the role of VIPPs in the chloroplast: under high light stress VIPP1 and VIPP2 form heteroligomers that complex with HSP22E/F, presumably to alleviate SCE stress, to protect plastid proteins from photooxidative damage through a peptide methionine sulfoxide reductase (MSRA) and/or to metabolize excess or misassembled proteins; this complex also would trigger the emission of RS through MARS1 or other mediators to induce *VIPPs*, *HSP22E/F* and *LHCSR3* expression. Many of these responses are consistent with what observed in our de-etiolating *y-4* cells in linco treatment: first, we showed that there is high overlap between high light and linco responsive genes, which indicates that these different stresses trigger the same RS

mechanism, as also shown in Arabidopsis (Llamas et al., 2017); second, in our experiment *VIPPs*, *HSP22E/F* and even a *MSRA* are all extremely over-induced by light at 1h, being *VIPP2* and *HSP22E/F* the ones with the highest degree of linco over-induction in our transcriptome ($log_2FC > 5$). Interestingly, *LHCSR3* as well as other key genes involved in photoprotection responses which are highly induced by light, were completely unaffected by linco. Moreover, we noticed that in some cases high light did not specifically induce the expression of *VIPP2* and *HSP22E/F* (Knopp et al., 2020), but it did in the case of *VIPP1*. It is important to notice that in this particular high light experiment, strains used always feature a fully developed chloroplast in the dark; therefore, an explanation could be that high light conditions generate a minor damage on thylakoid membranes that didn't require to generate VIPPs-HSP22 complex dependent RS. VIPP1 in fact has been assigned a key role in the biogenesis and repair of thylakoid membrane complexes in Arabidopsis (Kroll et al., 2001), and appears to conserve this role and be sufficient in this function in Chlamydomonas (Theis et al., 2020). These combined observations suggest a need for VIPP2-dependent RS to specifically trigger chloroplast biogenesis in *y*-mutant cells. It would be revealing to test whether a *vipp2* mutant in a *y* background loses the capacity to restore the chloroplast during de-etiolation in a condition that stresses but eventually allow these mutants to restore their chloroplast, such as testing with different high light intensities. As *VIPP2* originated from a gene duplication in green algae (Theis et al., 2020) being absent in angiosperm plants, VIPP2 could represent the ancestral RS regulator of chloroplast biogenesis in these *y* mutant strains.

Retrograde signals rewire light signaling pathway through novel transcription factors

It is important to remark that all linco effects shown in this chapter occur only when cells are exposed to light, as we found no *DEGs* in the dark; in addition half *LinRGs* are also *LRGs*. These observations suggest that 1) RS is dependent on light and 2) RS mode of action consists in rewiring light signaling pathway. In the case of photosynthesis genes, repression could be caused by 1) by changing the nature of positive regulators of photomorphogenesis into negative regulators, or 2) by repressing at the transcriptional or post-transcriptional levels these regulators; alternatively, novel repressors of photomorphogenesis are activated by RS. In this chapter, we explored whether candidate TFs involved in chloroplast biogenesis during de-etiolation (which are all *LRGs*) could be rewired by linco triggered RS. Almost all early TFs were not affected, including CRHY5. It is therefore unlikely that CRHY5 participates in the light and RS crosstalk as it does in Arabidopsis (Ruckle et al., 2007), while the possibility that it acts as a transcriptional repressor have been recently refuted (Burko et al., 2020, Cañibano et al., 2021). The only early TFs affected were FAP280 and ETF4 the only two connected to VIPP1 and VIPP2 in our early GCN, which are highly over-induced by linco similarly to these genes. This indicates that VIPP-dependent RS are mediated by these TFs and these in turn may be regulating expression of target genes, including photosynthesis, directly or through repression of other TFs affected by linco such as NAB1 and GSP1.

Retrograde signaling is not active in the dark in Chlamydomonas

In angiosperm plants, the ability to repress photomorphogenesis in the dark forming dark-adapted etioplasts was acquired in parallel with the loss of the capacity to synthesize chlorophylls, and this required massive reprogramming of the RS circuitry to also repress expression of photosynthesis genes (Calderon & Strand, 2021). The presence of an active RS mechanism in the dark has been demonstrated in Arabidopsis: GUN1 accumulates in the dark and prevents premature chloroplast development (Hernandez-Verdeja et al., 2022), and RS are known to repress a common subset of PIF-regulated genes in the dark under stress conditions (Martín et al., 2016), which is indicative of fundamental crosstalk between light and RS also in the absence of light.

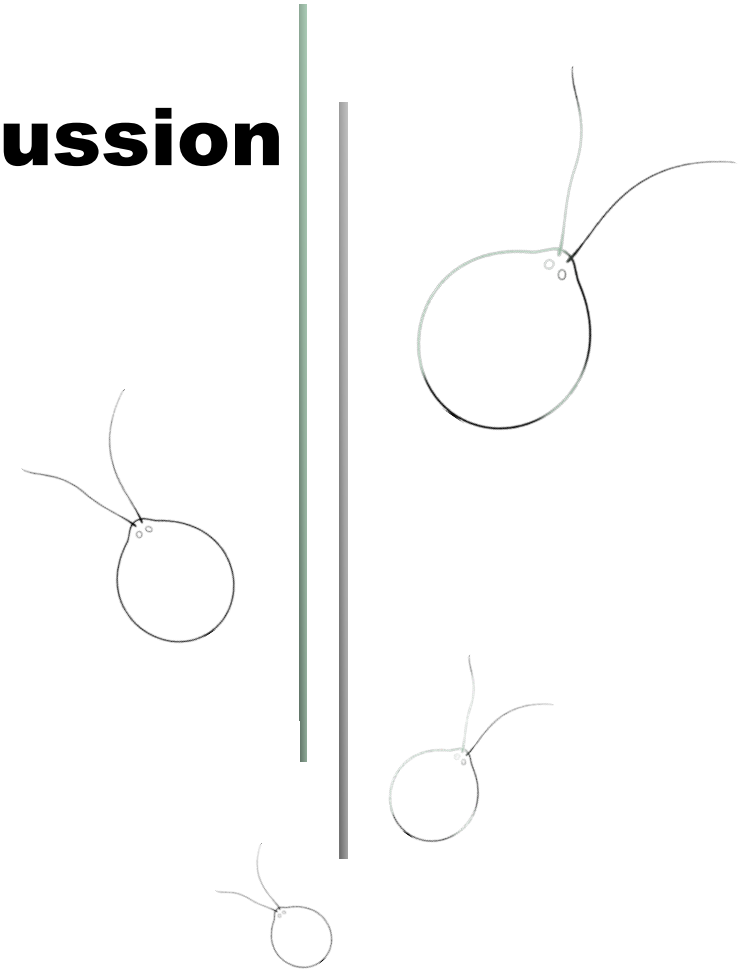
As *y* mutant cells also undergo etiolation in the dark similarly to angiosperm plants, we tested if this is regulated by RS in this condition. For this purpose, we evaluated the transcriptome of *y-4* cells and wt cells treated with linco in the dark, to test if changes seen are dependent on the plastid developmental state. Surprisingly linco treatment didn't trigger any significant change in the transcriptome of both strains tested. In order to discard the possibility that this may be caused by insufficient time of exposure to linco, we extended it for two more days in wt cells: we observed that linco represses PSII capacity and chlorophyll content, but so also did darkness although at lesser level. These results suggest that RS is not active in Chlamydomonas; alternatively, there is a possibility that there is an active RS in the dark but we cannot detect it as both linco and darkness effects on the chloroplast are overlapping.

We initially though that the latter could be the case, as we did obtain more than a thousand *DEGs* when comparing y-4 with wt cells in the dark, suggesting that DPOR could be involved in sending RS in this condition; in particular, we found that photosynthesis genes are upregulated in the wt. However, we eventually decided not to include these results, as this comparison is highly prone to artifactual effects. In *hmox1* mutants the differences in the transcriptome observed in the dark compared with its wt background disappeared when this comparison was done with the complemented lines (Duanmu et al., 2013). Similarly, massive transcriptomic changes were initially documented in the *gun4* mutant in the dark (Formighieri et al., 2011); however, when the role of GUN4 was evaluated during early photoacclimation, many *DEGs* with relatively high fold expression were both observed in *gun4* mutants and its complemented lines compared to the wt background, indicating that the initially found effect on the transcriptome in the dark is not specifically caused by *GUN4* absence (Brzezowski et al., 2014).

We therefore propose that Chlamydomonas RS signaling is absent in the dark and requires light to be activated. In this condition linco 1) by blocking translation of chloroplast-encoded photosystem subunits, cause accumulation of free tetrapyrrole intermediates leading to oxidative stress and the activation of bilin-dependent RS, and 2) induces accumulation of protein aggregates that trigger the cpUPR (Llamas et al., 2017). It is likely that dark RS evolved later in the evolution, and might have

required GUN1 activity to repress photosynthesis genes in the dark. This might have occurred prior to the emergence of angiosperm plants, as a dark RS mechanism that represses *LHC* genes under adverse conditions has been identified in pine (Hills et al., 2015), and is largely independent on light. Although, the involvement of GUN1 in these RS still needs to be proved in pine, absence of GUN1-dependent RS in Chlamydomonas could explain why photosynthesis genes that are already highly expressed in the dark, do not experience linco-mediated repression in this condition.

General Discussion



During the last decades, light and RS that regulate de-etiolation have been studied in Arabidopsis and other angiosperm species (tobacco, tomato, etc.), and using different systems (seedling, leaf, cell culture, etc.) (Armarego-Marriott et al., 2020). Whereas the light signaling pathway involved in this process is pretty well established, how RS regulation is orchestrated and the crosstalk between both signaling pathways is mostly unknown. Light signaling involves light perception mainly by phytochromes (red light photoreceptors) and cryptochromes (blue light photoreceptors), inactivation of photomorphogenesis repressors (COP1-SPA E3 ubiquitin ligase and PIFs) and the consequent activation of positive regulators of photomorphogenesis (HY5, GLKs, BBOX, and others) (Xu, 2019); this in turn triggers massive changes in the transcriptome of de-etiolating plants (Ma et al., 2001). RS mechanism has not been fully deciphered but it highly depends on the activity of GUN1, which has a key role in regulating not only chloroplast biogenesis but also whole plant development, fine-tuning this response depending on the environmental conditions through an active crosstalk with light signals (Hernández-Verdeja et al., 2022; Martín et al., 2016).

As this process and this complex regulatory mechanism is only featured in angiosperm plants, it is definitely a surprise that *y* mutants of an evolutionary distant green microalgae can also etiolate and de-etiolate, without many essential components of light and RS pathways, including phy-PIF module, GLKs and GUN1 (Han et al., 2019, Richter et al., 2023). Therefore, understanding how light and RS is orchestrated in these mutants motivated this work, and to have a thorough vision of main events regulated by these signaling pathways during de-etiolation we decided to perform a transcriptomic characterization, which has been never adopted with *y* mutant strains. There was also another very appealing advantage of using Chlamydomonas for our studies: here in fact we can also study the case of a fully developed chloroplast in the dark, and therefore separate light and plastid contributions on de-etiolation, something impossible to do in angiosperm plants were light conditions are tightly associated with the plastid state. Therefore our aim was to 1) evaluate if light and RS regulate same processes compared to angiosperm species; 2) understand the evolutionary advantage that represented the emergence of light and RS components of angiosperm plants absent in Chlamydomonas, and evaluate the role of conserved components; 3) predict novel regulators of these processes; 4) characterize main transcriptomic events during chloroplast biogenesis in these strains; 5) study the separate contributions of light and RS during de-etiolation.

To perform this transcriptomic analysis first we needed to setup a y mutant de-etiolation system, with the aim of both selecting the best physiological conditions and also design the experiment in the best way to transcriptomically capture light and RS events (Chapter 2). The two critical aspects were the selection of the y mutant strain and the medium for de-etiolation: many *y* mutant strains are available, but we selected the *chlL* (*y-4*) mutant (Suzuki & Bauer, 1992), as here the genotype is directly associated with the phenotype (a direct mutation on a subunit of DPOR), and also because of the three subunits of the DPOR (CHLL, CHLB, CHLN), CHLL is the one whose accumulation is affected

in all *y* nuclear mutants that have been employed in the past century (Cahoon & Timko, 2000); moreover, we managed to setup de-etiolation in the absence of any exogenous carbon source, which is known to alter light signaling, and could give us misleading results (Dijkwel et al., 1997). This system successfully gave us perfectly etiolated cells with no photosynthetic activity, which fully restored their chloroplast upon transfer to light, as any other system (Armarego-Marriott et al., 2019; Dubreuil et al., 2018; Pipitone et al., 2020). In order to evaluate the effect of RS we treated cells with lincomycin and monitored de-etiolation in these conditions, an approach already adopted in Arabidopsis (Dubreuil et al., 2018; Ruckle et al., 2012); lincomycin drastically affected photosynthetic parameters but cells still manage to survive this conditions and grow for at least 48h. Also we did not observed photobleaching effects due to excessive PChlide accumulation in the dark, independently of linco treatment; this was important to test as Chlamydomonas does not feature PIFs, and Arabidopsis *pifq* mutants are known to accumulate harmful levels of PChlide in the dark which lead seedling death upon exposure to light (Leivar et al., 2009). At the end we successfully designed an alternative Chlamydomonas based de-etiolation system that allowed us to study main light and RS events during de-etiolation, that compared to angiosperm-based systems specifically features an evolutionary importance (absence of key light and RS components of angiosperm plants), and also many technical advantages that ease their study (single chloroplast, synchronous plastid development in all cells, uniform absorption of lincomycin, etc.).

In Chapter 3 we performed an exhaustive analysis of light regulated events during de-etiolation of y-4 cells. We found that light regulates the same proportion of genes and the same biological processes compared with Arabidopsis (Burko et al., 2020), with the difference that y mutants the degree of induction of photosynthesis genes is much lower, because transcript levels of these genes are already high in the dark prior to de-etiolation. Moreover, we found that light rather than plastid state is responsible for the great majority of transcriptomic changes occurring during de-etiolation, as same biological processes were also found when comparing our system with dark-to-light transition of wt cells grown in 12:12 photoperiod (Strenkert et al., 2019). We also collected many evidences that point to a two-phased de-etiolation in *y* mutant cells, as shown in angiosperm plants (Armarego-Marriott et al., 2019; Loudya et al., 2021; Pipitone et al., 2020).

If de-etiolation is carried out in a surprisingly similar way to angiosperm plants, then what advantage represented the emergence of PIFs and GLKs? Thanks to available information regarding PIFs- and GLKs- regulated genes (Pfeiffer et al., 2014; Tu et al., 2022), we found that these TFs are responsible for the higher degree of regulation of their targeted (direct and indirect) light regulated genes, especially those that encode chloroplast proteins. However, we do not know if angiosperm plants evolved higher capacity to repress these genes in the dark, induce them in light, or both. Chlamydomonas cells still have a way to repress photosynthesis genes when they are transferred to dark from continuous light conditions: we do not know if this is caused by a repressive mechanism

COP1-SPA dependent or not, or if cells just stop inducing these genes and another mechanism induces their expression in the dark.

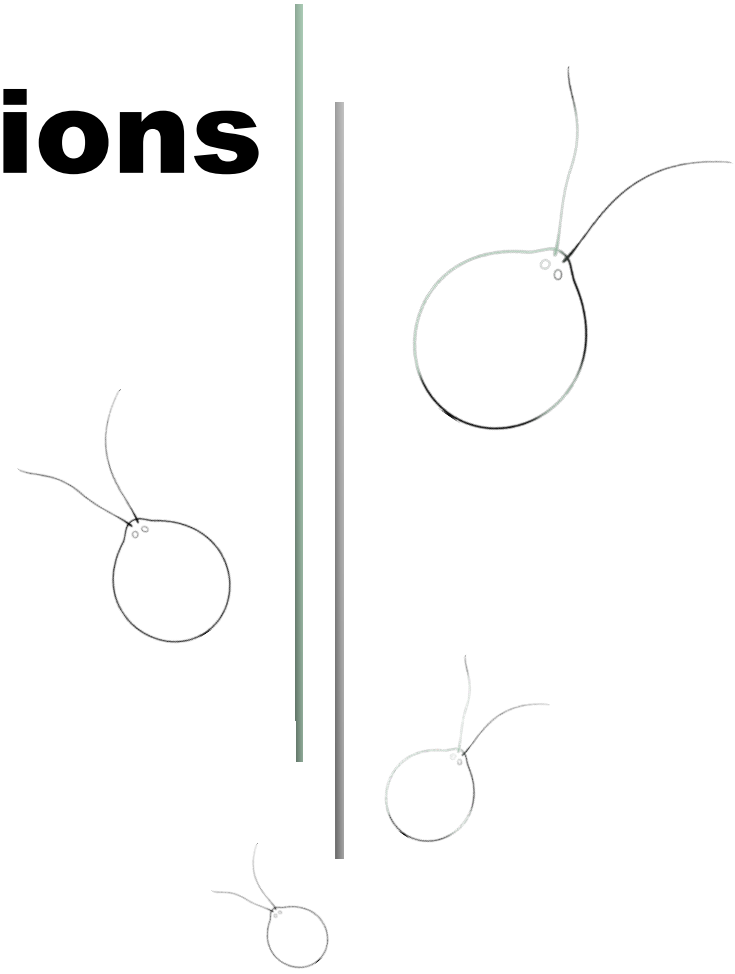
Thanks to a GCN approach, we predicted candidate TFs involved in chloroplast biogenesis in *y-4* cells. We found that several conserved light signaling components are also involved in regulating chloroplast biogenesis, though in a different way compared to angiosperm plants: CRHY5 is mainly associated with key genes involved in the photoprotection response, but not with photosynthesis genes nor with assembly factors which are early light induced; CRCO is highly co-expressed with many other TFs (light responsive or not), and could represent a potential light signaling hub, beyond its well described role in photoprotection (Tokutsu et al., 2019). We also found that NAB1 is highly co-expressed with photosynthesis genes, as previously reported (Mussgnug et al., 2005) and since it features the same expression profile as these genes, it might be also responsible for their accumulation in the dark. We found novel TFs as candidates to regulate chloroplast biogenesis: interestingly, we found several TFs from the GNAT family, that feature acetyltransferase activity, and have been recently reported to play a key role in plastid transcription and chloroplast biogenesis in Arabidopsis (Barrero-Gil et al., 2022). Lastly, it has been reported that Chlamydomonas can see red light through an animal type cryptochrome (aCRY1), which can influence expression of many genes including those involved in chlorophyll and carotenoid biosynthesis (Beel et al., 2012). Here, we show that red light can also trigger de-etiolation at almost the same performance as blue and white light.

Finally in Chapter 4 we studied main events regulated by RS during de-etiolation of y-4 cells. It is important to underline that many RS works have been performed in Chlamydomonas, where RS have been associated with bilins (Duanmu et al., 2013) and cpUPR (Ramundo et al., 2014), but so far all these works have been all performed using strains that feature a fully developed chloroplast in the dark, and therefore the role of bilins- and cpUPR-triggered RS in regulating de-etiolation needs to be demonstrated. Here we used a completely different approach in Chlamydomonas, as we monitored biogenic RS in de-etiolating *y-4* cells under linco treatment, similarly to Arabidopsis (Ruckle et al., 2012). We found that only a subset of *LRGs* is regulated by RS, and that the effect of linco is very specific affecting at different degree different biological processes, light and non-light regulated. Moreover, linco-triggered RS strongly repress photosynthesis and tetrapyrrole biosynthesis genes as in Arabidopsis, but this repression is only transient, and cells restore expression of these genes to non-treated levels; in contrast, these genes are progressively repressed at higher degree with time of exposure to linco in angiosperm plants (Dubreuil et al., 2018; Ruckle et al., 2012). Since we show that many of these genes are regulated by GUN1 in angiosperm plants, we propose that GUN1 has emerged to sustain repression of these genes under adverse conditions for chloroplast biogenesis. Nevertheless, what RS mechanism regulates this transient repression in Chlamydomonas? We found that both *HMOX1* (Duanmu et al., 2013), genes involved in protein homeostasis (Ramundo et al., 2014) and VIPPs-HSP22E/F (Theis et al., 2020) are highly induced by linco, suggesting the

involvement of the already described bilins- and cpUPR-dependent RS mechanisms: however, induction of these genes is transient, and this could explain why repression of photosynthesis and chlorophyll biosynthesis genes is not maintained under linco conditions. Moreover, we propose that VIPPs-HSP22E/F complex might be the main regulator of RS during de-etiolation, as these genes are the most highly over induced by linco in our transcriptome; also, of all ETFs identified in the previous chapter, the two TFs interacting with VIPPs in a separate cluster (FAP280 and ETF4), are the only ones significantly affected by linco.

Interestingly, we did not find evidence of an active RS in the dark, as no genes were significantly affected by lincomycin in the dark independently of the plastid developmental state. Although we cannot discard that lincomycin in the dark might not be able to affect the chloroplast status in Chlamydomonas, this result is in contrast to what has been reported in Arabidopsis (Hernández-Verdeja et al., 2022; Martín et al., 2016). This might indicate that RS in Chlamydomonas depend on light, likely because light triggers phototoxic effects caused by free tetrapyrrole pigments that cannot be incorporated into the photosystem complexes due to the effect of lincomycin. This would in turn generate ROS that could activate bilin biosynthesis (involved in ROS detoxification), while damaged proteins could trigger the cpUPR response.

Conclusions



Chapter 2 - Setup of a y mutant based de-etiolation system

⇒ We setup a novel de-etiolation system based on Chlamydomonas *yellow-in-the-dark* mutants, and designed to study main light and retrograde signaling regulated events. This system, which is based on the *y-4* (*chlL*) mutant, features perfectly dark-adapted cells in the dark with no photosynthetic activity which gradually recover photosynthetic activity and restore their chloroplast upon exposure to light, similarly to angiosperm-based de-etiolation systems. In particular:

- de-etiolation is completed in 48h, but most photosynthetic capacity is already reached by 9h without cell division effects
- full de-etiolation of these cells is achieved without the need for an exogenous carbon source
- etiolated *y-4* cells can convert all the accumulated PChlide into Chlide upon exposure to light without suffering from photobleaching effects
- lincomycin fully impairs photosynthetic activity, represses chlorophyll accumulation and slows cell growth, but cells remain viable for at least 48h

Chapter 3 - Transcriptome analysis: light signaling

⇒ Light triggers changes in the expression of 40% of genes in de-etiolating *y-4* cells, and regulates biological processes associated and not with the chloroplast

⇒ Light upregulates similar biological processes in Chlamydomonas and Arabidopsis

⇒ In Chlamydomonas, the great majority of changes in the transcriptome during de-etiolation are triggered by light rather than the plastid developmental state

⇒ Our data suggest that de-etiolation is achieved in two distinct phases: 1) “photosynthesis establishment phase” characterized by high translational activity of the accumulated photosystem transcripts in the dark, induction of many chloroplast biological processes, in parallel to a rapid increase in FvFm and linear increase of chlorophyll content during the first 9h, followed by 2) “chloroplast maturation phase” characterized by increase in synthesis of galactolipids, in parallel to a linear increase of chlorophylls per cell volume, and change in metabolism in favor of Calvin cycle and photorespiration reactions.

⇒ PIFs and GLKs might have emerged in angiosperm plants to confer higher degree of regulation to chloroplast associated *LIGHT REGULATED GENES*.

⇒ In the absence of light, Chlamydomonas triggers repression of photosynthesis-related genes

⇒ GCN allowed us to predict potential TFs that regulate chloroplast biogenesis in *y-4* mutant cells; already described TFs such as CRHY5, NAB1 and LCR1 are highly co-expressed with chloroplast associated nuclear genes

⇒ Red light triggers de-etiolation in y-4 cells, indicating that Chlamydomonas can sense and respond to red light. Further studies will be needed to determine whether aCRY1 is the red-light photoreceptor that triggers this response.

Chapter 4 - Transcriptome analysis: retrograde signaling

⇒ Only a subset of light responsive genes are regulated by retrograde signaling in Chlamydomonas during de-etiolation. This indicates that the effect of lincomycin is very specific, affecting only certain biological processes and at different degrees.

⇒ Retrograde signaling affects biological processes associated with the chloroplast, but not exclusively. Others include effects on the expression of genes related to flagella movement.

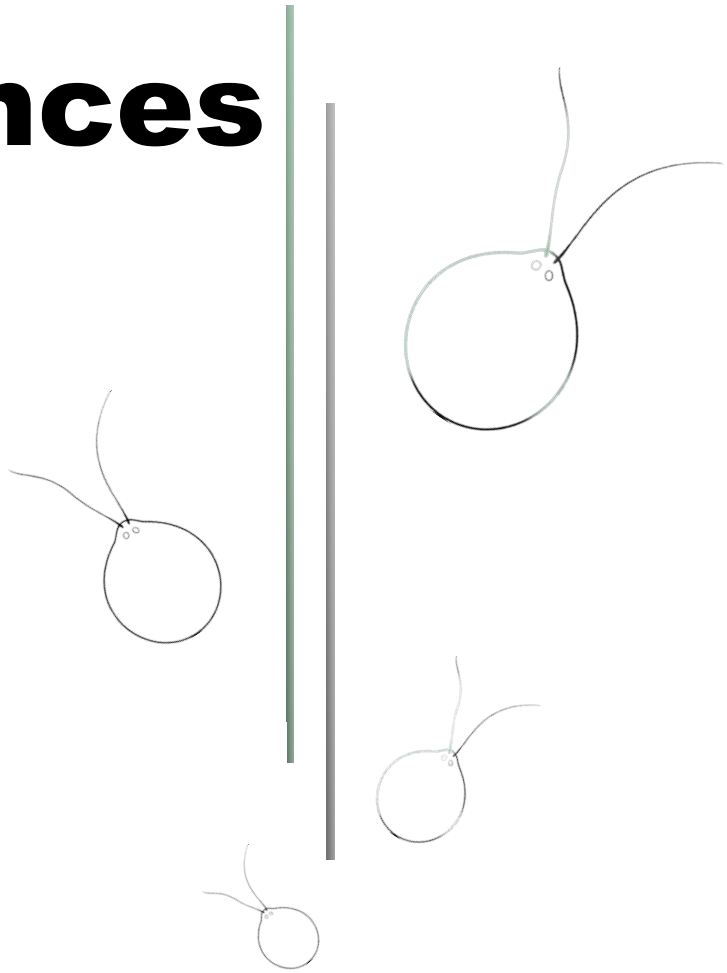
⇒ Biogenic retrograde signals involved in de-etiolation are likely triggered by bilins and cpUPR, given that previously described *HMOX1*, *VIPPs* and *HSP22E/F* genes are highly but transiently induced by lincomycin at 1h of light.

⇒ Lincomycin-dependent RS strongly but transiently affect the expression of photosynthesis and chlorophyll biosynthesis genes in Chlamydomonas, possibly through the transient activation of bilin- and cpUPR-dependent retrograde signal. This is in contrast to the sustained repression reported in Arabidopsis.

⇒ During evolution, we propose that GUN1 appeared in angiosperms to sustainedly maintain repression of photosynthesis and chlorophyll biosynthesis genes under adverse conditions.

⇒ Lincomycin-induced retrograde signaling was not detected in Chlamydomonas in the dark, regardless of the plastid developmental state.

References



Achard, P., Liao, L., Jiang, C., Desnos, T., Bartlett, J., Fu, X., & Harberd, N. P. (2007). DELLAs contribute to plant photomorphogenesis. *Plant Physiology, 143*(3), 1163–1172.

Ahmad, M., & Cashmore, A. R. (1996). Seeing blue: The discovery of Cryptochrome. *Plant Molecular Biology, 30*(5), 851–861.

Aihara, Y., Fujimura-Kamada, K., Yamasaki, T., & Minagawa, J. (2018). Algal photoprotection is regulated by the E3 ligase CUL4–DDB1^{DET1}. *Nature Plants, 5*(1), 34–40.

Arend, M., Yuan, Y., Ruiz-Sola, M. Á., Omranian, N., Nikoloski, Z., & Petroutsos, D. (2023). Widening the landscape of transcriptional regulation of green algal photoprotection. *Nature Communications, 14*(1).

Armarego-Marriott, T., Kowalewska, Ł., Burgos, A., Fischer, A., Thiele, W., Erban, A., … Bock, R. (2019). Highly resolved systems biology to dissect the etioplast-to-chloroplast transition in tobacco leaves. *Plant Physiology, 180*(1), 654–681.

Armarego-Marriott, T., Sandoval-Ibañez, O., & Kowalewska, Ł. (2020). Beyond the darkness: Recent lessons from etiolation and de-etiolation studies. *Journal of Experimental Botany, 71*(4), 1215–1225.

Arsovski, A. A., Galstyan, A., Guseman, J. M., & Nemhauser, J. L. (2012). Photomorphogenesis. *The Arabidopsis Book, 10*.

Artz, O., Dickopf, S., Ranjan, A., Kreiss, M., Abraham, E. T., Boll, V., … Hoecker, U. (2019). Characterization of spa mutants in the moss Physcomitrella provides evidence for functional divergence of SPA genes during the evolution of land plants. *New Phytologist, 224*(4), 1613–1626.

Bai, M.-Y., Shang, J.-X., Oh, E., Fan, M., Bai, Y., Zentella, R., … Wang, Z.-Y. (2012). Brassinosteroid, gibberellin and phytochrome impinge on a common transcription module in Arabidopsis. *Nature Cell Biology, 14*(8), 810–817.

Barrero-Gil, J., Bouza-Morcillo, L., Espinosa-Cores, L., Piñeiro, M., & Jarillo, J. A. (2022). H4 acetylation by the NUA4 complex is required for plastid transcription and chloroplast biogenesis. *Nature Plants, 8*(9), 1052–1063.

Beel, B., Prager, K., Spexard, M., Sasso, S., Weiss, D., Müller, N., … Mittag, M. (2012). A flavin binding cryptochrome photoreceptor responds to both blue and red light in *Chlamydomonas reinhardtii*. *The Plant Cell, 24*(7), 2992–3008.

Blanco-Touriñán, N., Serrano-Mislata, A., & Alabadí, D. (2020). Regulation of DELLA proteins by post-translational modifications. *Plant and Cell Physiology, 61*(11), 1891–1901.

Brzezowski, P., Schlicke, H., Richter, A., Dent, R. M., Niyogi, K. K., & Grimm, B. (2014). The *gun4* protein plays a regulatory role in tetrapyrrole biosynthesis and chloroplast-to-nucleus signalling in *Chlamydomonas reinhardtii. The Plant Journal, 79*(2), 285–298.

Burko, Y., Seluzicki, A., Zander, M., Pedmale, U. V., Ecker, J. R., & Chory, J. (2020). Chimeric activators and repressors define HY5 activity and reveal a light-regulated feedback mechanism. *The Plant Cell, 32*(4), 967–983.

Cahoon, A. B., & Timko, M. P. (2000). *Yellow-in-the-dark* mutants of Chlamydomonas lack the CHLL subunit of light-independent protochlorophyllide reductase. *The Plant Cell, 12*(4), 559.

Calderon, R. H., & Strand, Å. (2021). How retrograde signaling is intertwined with the evolution of photosynthetic eukaryotes. *Current Opinion in Plant Biology*, 63, 102093.

Cañibano, E., Bourbousse, C., García-León, M., Garnelo Gómez, B., Wolff, L., García-Baudino, C., … Fonseca, S. (2021). DET1-mediated COP1 regulation avoids HY5 activity over second-site gene targets to tune plant photomorphogenesis. *Molecular Plant, 14*(6), 963–982.

Cazzonelli, C. I., Hou, X., Alagoz, Y., Rivers, J., Dhami, N., Lee, J., … Pogson, B. J. (2020). A cis-carotene derived apocarotenoid regulates etioplast and chloroplast development. *eLife, 9*.

Cheminant, S., Wild, M., Bouvier, F., Pelletier, S., Renou, J.-P., Erhardt, M., … Achard, P. (2011). DELLAs regulate chlorophyll and carotenoid biosynthesis to prevent photooxidative damage during seedling deetiolation in Arabidopsis. *The Plant Cell, 23*(5), 1849–1860.

Chen, M., & Chory, J. (2011). Phytochrome signaling mechanisms and the control of plant development. *Trends in Cell Biology, 21*(11), 664–671.

Chen, M., Galvão, R. M., Li, M., Burger, B., Bugea, J., Bolado, J., & Chory, J. (2010). Arabidopsis HEMERA/pTAC12 initiates photomorphogenesis by phytochromes. *Cell, 141*(7), 1230–1240.

Chen, W., Li, C., Liang, W., Li, Y., Zou, Z., Xie, Y., … Zhu, X. (2022). The roles of optogenetics and technology in neurobiology: a Review. *Frontiers in Aging Neuroscience, 14*.

Chen, D., Lyu, M., Kou, X., Li, J., Yang, Z., Gao, L., … Zhong, S. (2022). Integration of light and temperature sensing by liquid-liquid phase separation of phytochrome B. *Molecular Cell, 82*(16), 3015-3029.

Chen, H., Shen, Y., Tang, X., Yu, L., Wang, J., Guo, L., … Deng, X. W. (2006). Arabidopsis CULLIN4 forms an E3 ubiquitin ligase with RBX1 and the CDD complex in mediating light control of development. *The Plant cell, 18*(8), 1991–2004

Chen, D., Xu, G., Tang, W., Jing, Y., Ji, Q., Fei, Z., & Lin, R. (2013). Antagonistic basic helix-loop-helix/bZIP transcription factors form transcriptional modules that integrate light and reactive oxygen species signaling in Arabidopsis. *The Plant Cell, 25*(5), 1657–1673.

Cheng, X., Liu, G., Ke, W., Zhao, L., Lv, B., Ma, X., … Huang, K. (2017). Building a multipurpose insertional mutant library for forward and reverse genetics in Chlamydomonas. *Plant Methods, 13*(1).

Choquet, Y., Rahire, M., Girard-Bascou, J., Erickson, J., & Rochaix, J. D. (1992). A chloroplast gene is required for the light-independent accumulation of chlorophyll in *Chlamydomonas reinhardtii*. *The EMBO Journal, 11*(5), 1697–1704.

Christie, J. M. (2007). Phototropin blue-light receptors. *Annual Review of Plant Biology, 58*(1), 21–45.

Craig, R. J., Gallaher, S. D., Shu, S., Salomé, P. A., Jenkins, J. W., Blaby-Haas, C. E., … Merchant, S. S. (2023). The Chlamydomonas Genome Project, version 6: reference assemblies for mating-type plus and minus strains reveal extensive structural mutation in the laboratory. *The Plant Cell, 35*(2), 644–672.

Davies, J. P., & Grossman, A. R. (1998). The use of Chlamydomonas (Chlorophyta: Volvocales) as a model algal system for genome studies and the elucidation of photosynthetic processes. *Journal of Phycology, 34*(6), 907–917.

Davuluri, R. V., Sun, H., Palaniswamy, S. K., Matthews, N., Molina, C., Kurtz, M., & Grotewold, E. (2003). Agris: Arabidopsis gene regulatory information server, an information resource of Arabidopsis cis-regulatory elements and transcription factors. *BMC Bioinformatics, 4*(1).

de Lucas, M., Davière, J.-M., Rodríguez-Falcón, M., Pontin, M., Iglesias-Pedraz, J. M., Lorrain, S., … Prat, S. (2008). A molecular framework for light and gibberellin control of cell elongation. *Nature, 451*(7177), 480–484.

Dehesh, K., Franci, C., Parks, B. M., Seeley, K. A., Short, T. W., Tepperman, J. M., & Quail, P. H. (1993). Arabidopsis HY8 locus encodes phytochrome A. *The Plant Cell, 5*(9), 1081–1088.

Deng, X.-W., & Quail, P. H. (1992). Genetic and phenotypic characterization of COP1 mutants of *Arabidopsis thaliana*. *The Plant Journal, 2*(1), 83–95.

Depège, N., Bellafiore, S., & Rochaix, J.-D. (2003). Role of chloroplast protein kinase STT7 in LHCII phosphorylation and state transition in Chlamydomonas. *Science, 299*(5612), 1572–1575.

Dijkwel, P. P., Huijser, C., Weisbeek, P. J., Chua, N. H., & Smeekens, S. C. (1997). Sucrose control of phytochrome A signaling in Arabidopsis. *The Plant Cell, 9*(4), 583–595.

Dobrogojski, J., Adamiec, M., & Luciński, R. (2020). The Chloroplast Genome: A Review. *Acta Physiologiae Plantarum, 42*(6).

Duanmu, D., Bachy, C., Sudek, S., Wong, C.-H., Jiménez, V., Rockwell, N. C., … Worden, A. Z. (2014). Marine algae and land plants share conserved phytochrome signaling systems. *Proceedings of the National Academy of Sciences, 111*(44), 15827–15832.

Duanmu, D., Casero, D., Dent, R. M., Gallaher, S., Yang, W., Rockwell, N. C., … Lagarias, J. C. (2013). Retrograde Bilin signaling enables Chlamydomonas greening and phototrophic survival. *Proceedings of the National Academy of Sciences, 110*(9), 3621–3626.

Dubreuil, C., Ji, Y., Strand, Å., & Grönlund, A. (2017). A quantitative model of the phytochrome-PIF light signalling initiating chloroplast development. *Scientific Reports, 7*(1).

Dubreuil, C., Jin, X., Barajas-López, J. de, Hewitt, T. C., Tanz, S. K., Dobrenel, T., … Strand, Å. (2018). Establishment of photosynthesis through chloroplast development is controlled by two distinct regulatory phases. *Plant Physiology, 176*(2), 1199–1214.

Eckstein, A., Zięba, P., & Gabryś, H. (2011). Sugar and light effects on the condition of the photosynthetic apparatus of *Arabidopsis thaliana* cultured in vitro. *Journal of Plant Growth Regulation, 31*(1), 90–101.

Erickson, E., Wakao, S., & Niyogi, K. K. (2015). Light stress and photoprotection in *Chlamydomonas reinhardtii*. *The Plant Journal, 82*(3), 449–465.

Fan, T., Roling, L., Hedtke, B., & Grimm, B. (2023). FC2 stabilizes POR and suppresses ALA formation in the tetrapyrrole biosynthesis pathway. *New Phytologist, 239*(2), 624–638.

Favero, D. S. (2020). Mechanisms regulating PIF transcription factor activity at the protein level. *Physiologia Plantarum, 169*(3), 325–335.

Feng, S., Martinez, C., Gusmaroli, G., Wang, Y., Zhou, J., Wang, F., … Deng, X. W. (2008). Coordinated regulation of Arabidopsis thaliana development by light and gibberellins. *Nature, 451*(7177), 475–479.

Fischer, B. B., Wiesendanger, M., & Eggen, R. I. (2006). Growth condition-dependent sensitivity, photodamage and stress response of *Chlamydomonas reinhardtii* exposed to high light conditions. *Plant and Cell Physiology, 47*(8), 1135–1145.

Fitter, D. W., Martin, D. J., Copley, M. J., Scotland, R. W., & Langdale, J. A. (2002). GLK gene pairs regulate chloroplast development in diverse plant species. *The Plant Journal, 31*(6), 713–727.

Fleischmann, M. M., Ravanel, S., Delosme, R., Olive, J., Zito, F., Wollman, F.-A., & Rochaix, J.-D. (1999). Isolation and characterization of photoautotrophic mutants of *Chlamydomonas reinhardtii* deficient in state transition. *Journal of Biological Chemistry, 274*(43), 30987–30994.

Ford, C., Mitchell, S., & Wang, W. (1981). Protochlorophyllide photoconversion mutants of *Chlamydomonas reinhardtii*. *Molecular and General Genetics MGG, 184*(3), 460–464.

Ford, C., Mitchell, S., & Wang, W. (1983). Characterization of NADPH: protochlorophyllide oxidoreductase in the *y-7* and *pc-1 y-7* mutants of *Chlamydomonas reinhardtii*. *Molecular and General Genetics MGG, 192*(1–2), 290–292.

Ford, C., & Wang, W. (1980). Three new yellow loci in *Chlamydomonas reinhardtii*. *Molecular and General Genetics MGG, 179*(2), 259–263.

Ford, C., &; Wang, W. (1982). Instability at the *y-1* locus of *Chlamydomonas reinhardtii*. *Molecular and General Genetics MGG, 187*(2), 286–290.

Formighieri, C., Ceol, M., Bonente, G., Rochaix, J.-D., & Bassi, R. (2012). Retrograde signaling and photoprotection in a *gun4* mutant of *Chlamydomonas reinhardtii*. *Molecular Plant, 5*(6), 1242–1262.

Frangedakis, E., Yelina, N. E., Billakurthi, K., Schreier, T., Dickinson, P. J., Tomaselli, M., … Hibberd, J. M. (2023). Synergistic control of chloroplast biogenesis by MYB-related and Golden2-like transcription factors. bioRxiv. https://doi.org/10.1101/2023.08.11.552970

Fujii, S., Wada, H., & Kobayashi, K. (2024). Orchestration of photosynthesis-associated gene expression and galactolipid biosynthesis during chloroplast differentiation in plants. *Plant And Cell Physiology*.

Gangappa, S. N., & Botto, J. F. (2014). The BBX family of plant transcription factors. *Trends in Plant Science, 19*(7), 460–470.

Gommers, C. M., & Monte, E. (2017). Seedling establishment: A dimmer switch-regulated process between dark and light signaling. *Plant Physiology, 176*(2), 1061–1074.

Gorman, D. S., & Levine, R. P. (1965). Cytochrome f and plastocyanin: their sequence in the photosynthetic electron transport chain of *Chlamydomonas reinhardi*. *Proceedings of the National Academy of Sciences, 54*(6), 1665–1669.

Greiner, A., Kelterborn, S., Evers, H., Kreimer, G., Sizova, I., & Hegemann, P. (2017). Targeting of photoreceptor genes in *Chlamydomonas reinhardtii* via zinc-finger nucleases and CRISPR/Cas9. *The Plant Cell, 29*(10), 2498–2518.

Gutman, B. L., & Niyogi, K. K. (2004). Chlamydomonas and Arabidopsis. A dynamic duo. *Plant Physiology, 135*(2), 607–610.

Guzmán-Zapata, D., Sandoval-Vargas, J., Macedo-Osorio, K., Salgado-Manjarrez, E., Castrejón-Flores, J., Oliver-Salvador, M., … Badillo-Corona J. A. (2019). Efficient editing of the nuclear *APT* reporter gene in *Chlamydomonas reinhardtii* via expression of a CRISPR-Cas9 module. *International Journal of Molecular Sciences, 20*(5), 1247.

Han, X., Chang, X., Zhang, Z., Chen, H., He, H., Zhong, B., & Deng, X. W. (2019). Origin and evolution of core components responsible for monitoring light environment changes during plant terrestrialization. *Molecular Plant, 12*(6), 847–862.

Han, X., Huang, X., & Deng, X. W. (2020). The photomorphogenic central repressor COP1: conservation and functional diversification during evolution. *Plant Communications, 1*(3), 100044.

Harris, E. H. (2001). Chlamydomonas as a model organism. *Annual Review of Plant Physiology and Plant Molecular Biology, 52*(1), 363–406.

Harris, E. H. (2009). Motility and Behavior. In *The Chlamydomonas Sourcebook* (2nd ed., Vol. 1, pp. 89-117). Academic Press.

Häusler, R. E., Heinrichs, L., Schmitz, J., & Flügge, U.-I. (2014). How sugars might coordinate chloroplast and nuclear gene expression during acclimation to high light intensities. *Molecular Plant, 7*(7), 1121–1137.

Hegemann, P., & Berthold, P. (2009). Sensory photoreceptors and light control of flagellar activity. In: EH Harris, DB Stern, GB Witman (Eds.), *The Chlamydomonas sourcebook* (2nd ed., Vol. 3, pp. 395-429). Academic Press.

Hegemann, P., & Nagel, G. (2013). From channelrhodopsins to optogenetics. *EMBO Molecular Medicine, 5*(2), 173–176.

Hernández-García, J., Briones-Moreno, A., Dumas, R., & Blázquez, M. A. (2019). Origin of gibberellin-dependent transcriptional regulation by molecular exploitation of a transactivation domain in DELLA proteins. *Molecular Biology and Evolution, 36*(5), 908–918.

Hernández-Verdeja, T., & Lundgren, M. R. (2023). GOLDEN2-LIKE transcription factors: a golden ticket to improve crops? *Plants, People, Planet*.

Hernández-Verdeja, T., Vuorijoki, L., Jin, X., Vergara, A., Dubreuil, C., & Strand, Å. (2022). GENOMES UNCOUPLED 1 plays a key role during the de-etiolation process in Arabidopsis. *New Phytologist, 235*(1), 188–203.

Hernández-Verdeja, T., Vuorijoki, L., & Strand, Å. (2020). Emerging from the darkness: interplay between light and plastid signaling during chloroplast biogenesis. *Physiologia Plantarum, 169*(3), 397–406.

Hills, A. C., Khan, S., & López-Juez, E. (2015). Chloroplast Biogenesis-associated nuclear genes: Control by plastid signals evolved prior to their regulation as part of photomorphogenesis. *Frontiers in Plant Science, 6*.

Honkanen, S., & Small, I. (2022). The GENOMES UNCOUPLED1 protein has an ancient, highly conserved role but not in retrograde signalling. *New Phytologist, 236*(1), 99–113.

Hornitschek, P., Kohnen, M. V., Lorrain, S., Rougemont, J., Ljung, K., López-Vidriero, I., … Fankhauser, C. (2012). Phytochrome interacting factors 4 and 5 control seedling growth in changing light conditions by directly controlling auxin signaling. *The Plant Journal, 71*(5), 699–711.

Hui, C., Schmollinger, S., Strenkert, D., Holbrook, K., Montgomery, H. R., Chen, S., … Merchant, S. S. (2022). Simple steps to enable reproducibility: Culture conditions affecting *Chlamydomonas* growth and elemental composition. *The Plant Journal, 111*(4), 995–1014.

Hwang, Y., Han, S., Yoo, C. Y., Hong, L., You, C., Le, B. H., … Chen, M. (2022). Anterograde signaling controls plastid transcription via sigma factors separately from nuclear photosynthesis genes. *Nature Communications, 13*(1).

Im, C., Eberhard, S., Huang, K., Beck, C. F., & Grossman, A. R. (2006). Phototropin involvement in the expression of genes encoding chlorophyll and carotenoid biosynthesis enzymes and LHC apoproteins in *Chlamydomonas reinhardtii*. *The Plant Journal, 48*(1), 1–16.

Inoue, K., Nishihama, R., & Kohchi, T. (2017). Evolutionary origin of phytochrome responses and signaling in land plants. *Plant, Cell & Environment, 40*(11), 2502–2508.

Ito, S., Song, Y. H., & Imaizumi, T. (2012). LOV domain-containing F-Box Proteins: Light-dependent protein degradation modules in Arabidopsis. *Molecular Plant, 5*(3), 573–582.

Jarvis, P., & López-Juez, E. (2013). Biogenesis and homeostasis of chloroplasts and other plastids. *Nature Reviews Molecular Cell Biology, 14*(12), 787–802.

Kim, C., Kwon, Y., Jeong, J., Kang, M., Lee, G. S., Moon, J. H., … Choi, G. (2023). Phytochrome B photobodies are comprised of phytochrome B and its primary and secondary interacting proteins. *Nature Communications, 14*(1).

Kindle, K. L. (1987). Expression of a gene for a light-harvesting chlorophyll a/b-binding protein in *Chlamydomonas reinhardtii*: effect of light and acetate. *Plant Molecular Biology, 9*(6), 547–563.

Kindle, K. L., Schnell, R. A., Fernández, E., & Lefebvre, P. A. (1989). Stable nuclear transformation of Chlamydomonas using the Chlamydomonas gene for nitrate reductase. *The Journal of Cell Biology, 109*(6), 2589–2601.

Kiontke, S., Göbel, T., Brych, A., & Batschauer, A. (2020). DASH-type cryptochromes - solved and open questions. *Biological Chemistry, 401*(12), 1487–1493.

Knopp, M., Garg, S. G., Handrich, M., & Gould, S. B. (2020). Major changes in plastid protein import and the origin of the Chloroplastida. *iScience, 23*(3), 100896.

Kopylova, E., Noé, L., & Touzet, H. (2012). SortMeRNA: fast and accurate filtering of ribosomal RNAs in metatranscriptomic data. *Bioinformatics, 28*(24), 3211–3217.

Kottke, T., Oldemeyer, S., Wenzel, S., Zou, Y., & Mittag, M. (2017). Cryptochrome photoreceptors in green algae: Unexpected versatility of mechanisms and functions. *Journal of Plant Physiology, 217*, 4–14.

Koussevitzky, S., Nott, A., Mockler, T. C., Hong, F., Sachetto-Martins, G., Surpin, M., … Chory, J. (2007). Signals from chloroplasts converge to regulate nuclear gene expression. *Science, 316*(5825), 715–719.

Kozminski, K. G., Johnson, K. A., Forscher, P., & Rosenbaum, J. L. (1993). A motility in the eukaryotic flagellum unrelated to flagellar beating. *Proceedings of the National Academy of Sciences, 90*(12), 5519–5523.

Kropat, J., Hong-Hermesdorf, A., Casero, D., Ent, P., Castruita, M., Pellegrini, M., … Malasarn, D. (2011). A revised mineral nutrient supplement increases biomass and growth rate in *Chlamydomonas reinhardtii*. *The Plant Journal, 66*(5), 770–780.

Kropat, J., Oster, U., Rüdiger, W., & Beck, C. F. (1997). Chlorophyll precursors are signals of chloroplast origin involved in light induction of nuclear heat-shock genes. *Proceedings of the National Academy of Sciences, 94*(25), 14168–14172.

Krueger F. (2014). Trim Galore: a wrapper tool around Cutadapt and FastQC to consistently apply quality and adapter trimming to FastQ files, with some extra functionality for MspI-digested RRBS-type (Reduced Representation Bisufite-Seq) libraries. https://www.bioinformatics.babraham.ac.uk/projects/trim_galore

Lämmermann, N., Wulf, D., Chang, K. S., Wichmann, J., Jang, J., Jin, E., … Kruse, O. (2020). Ubiquitin ligase component LRS1 and transcription factor CRHY5 act as a light switch for photoprotection in Chlamydomonas. bioRxiv. https://doi.org/10.1101/2020.02.10.942334

Larkin, R. M., Alonso, J. M., Ecker, J. R., & Chory, J. (2003). GUN4, a regulator of chlorophyll synthesis and intracellular signaling. *Science, 299*(5608), 902–906.

Laubinger, S., Fittinghoff, K., & Hoecker, U. (2004). The SPA quartet: a family of WD-repeat proteins with a central role in suppression of photomorphogenesis in Arabidopsis. *The Plant Cell, 16*(9), 2293–2306.

Lee, B., Choi, G.-G., Choi, Y.-E., Sung, M., Park, M. S., & Yang, J.-W. (2014). Enhancement of lipid productivity by ethyl methane sulfonate-mediated random mutagenesis and proteomic analysis in *Chlamydomonas reinhardtii*. *Korean Journal of Chemical Engineering, 31*(6), 1036–1042.

Lee, J., He, K., Stolc, V., Lee, H., Figueroa, P., Gao, Y., … Deng, X. W. (2007). Analysis of transcription factor HY5 genomic binding sites revealed its hierarchical role in light regulation of development. *The Plant Cell, 19*(3), 731–749.

Legris, M., Ince, Y. Ç., & Fankhauser, C. (2019). Molecular mechanisms underlying phytochrome-controlled morphogenesis in plants. *Nature Communications, 10*(1).

Leister, D., & Kleine, T. (2016). Definition of a core module for the nuclear retrograde response to altered organellar gene expression identifies GLK overexpressors as gun mutants. *Physiologia Plantarum, 157*(3), 297–309.

Leivar, P., Monte, E., Oka, Y., Liu, T., Carle, C., Castillon, A., … Quail, P. H. (2008). Multiple phytochrome-interacting bHLH transcription factors repress premature seedling photomorphogenesis in darkness. *Current Biology, 18*(23), 1815–1823.

Leivar, P., Tepperman, J. M., Monte, E., Calderon, R. H., Liu, T. L., & Quail, P. H. (2009). Definition of early transcriptional circuitry involved in light-induced reversal of PIF-imposed repression of photomorphogenesis in young Arabidopsis seedlings. *The Plant Cell, 21*(11), 3535–3553.

Leivar, P., Tepperman, J. M., Cohn, M. M., Monte, E., Al-Sady, B., Erickson, E., & Quail, P. H. (2012). Dynamic antagonism between phytochromes and PIF family basic helix-loop-helix factors induces selective reciprocal responses to light and shade in a rapidly responsive transcriptional network in Arabidopsis. *The Plant Cell, 24*(4), 1398–1419.

Levin, G., & Schuster, G. (2023). LHC-like proteins: The guardians of photosynthesis. *International Journal of Molecular Sciences, 24*(3), 2503.

Li, J., Goldschmidt-Clermont, M., & Timko, M. P. (1993). Chloroplast-encoded *chlB* is required for light-independent protochlorophyllide reductase activity in *Chlamydomonas reinhardtii*. *The Plant Cell, 5*(12), 1817.

Li, J., Nagpal, P., Vitart, V., McMorris, T. C., & Chory, J. (1996). A role for brassinosteroids in light-dependent development of Arabidopsis. *Science, 272*(5260), 398–401.

Li, X., Zhang, R., Patena, W., Gang, S. S., Blum, S. R., Ivanova, N., … Jonikas, M. C. (2016). An indexed, mapped mutant library enables reverse genetics studies of biological processes in *Chlamydomonas reinhardtii*. *The Plant Cell, 28*(2), 367–387.

Lichtenthaler, H. K., & Buschmann, C. (2001). Extraction of phtosynthetic tissues: chlorophylls and carotenoids. *Current Protocols in Food Analytical Chemistry, 1*(1).

Llamas, E., Pulido, P., & Rodriguez-Concepcion, M. (2017). Interference with plastome gene expression and CLP protease activity in Arabidopsis triggers a chloroplast unfolded protein response to restore protein homeostasis. *PLOS Genetics, 13*(9).

Loudya, N., Mishra, P., Takahagi, K., Uehara-Yamaguchi, Y., Inoue, K., Bogre, L., … López-Juez, E. (2021). Cellular and transcriptomic analyses reveal two-staged chloroplast biogenesis underpinning photosynthesis build-up in the wheat leaf. *Genome Biology, 22*(1).

Love, M. I., Huber, W., & Anders, S. (2014). Moderated estimation of fold change and dispersion for RNA-seq data with DESeq2. *Genome Biology, 15*(12).

Ma, L., Li, J., Qu, L., Hager, J., Chen, Z., Zhao, H., & Deng, X. W. (2001). Light control of Arabidopsis development entails coordinated regulation of genome expression and cellular pathways. *The Plant Cell, 13*(12), 2589–2607.

Ma, K., Deng, L., Wu, H., & Fan, J. (2022). Towards green biomanufacturing of high-value recombinant proteins using promising cell factory: *Chlamydomonas reinhardtii* chloroplast. *Bioresources and Bioprocessing, 9*(1).

Malnoë, P., Mayfield, S. P., & Rochaix, J. D. (1988). Comparative analysis of the biogenesis of photosystem II in the wild-type and *y-1* mutant of *Chlamydomonas reinhardtii*. *The Journal of Cell Biology, 106*(3), 609–616.

Martín, G., Leivar, P., Ludevid, D., Tepperman, J. M., Quail, P. H., & Monte, E. (2016). Phytochrome and retrograde signalling pathways converge to antagonistically regulate a light-induced transcriptional network. *Nature Communications, 7*(1).

Martínez-García, J. F., Huq, E., & Quail, P. H. (2000). Direct targeting of light signals to a promoter element-bound transcription factor. *Science, 288*(5467), 859–863.

Mathews, S. (2006). Phytochrome-mediated development in land plants: red light sensing evolves to meet the challenges of changing light environments. *Molecular Ecology, 15*(12), 3483–3503.

Maxwell, K., & Johnson, G. N. (2000). Chlorophyll fluorescence—a practical guide. *Journal of Experimental Botany, 51*(345), 659–668.

Mazzella, M. A., & Casal, J. J. (2001). Interactive signalling by phytochromes and cryptochromes generates de-etiolation homeostasis in *Arabidopsis thaliana*. *Plant, Cell & Environment, 24*(2), 155–161.

McCormac, A. C., Wagner, D., Boylan, M. T., Quail, P. H., Smith, H., & Whitelam, G. C. (1993). Photoresponses of transgenic Arabidopsis seedlings expressing introduced phytochrome B-encoding cDNAs: evidence that phytochrome A and phytochrome B have distinct photoregulatory functions. *The Plant Journal, 4*(1), 19–27.

Merchant, S. S., Prochnik, S. E., Vallon, O., Harris, E. H., Karpowicz, S. J., Witman, G. B., … Grossman, A. R. (2007). The Chlamydomonas genome reveals the evolution of key animal and plant functions. *Science, 318*(5848), 245–250.

Mochizuki, N., Brusslan, J. A., Larkin, R., Nagatani, A., & Chory, J. (2001). Arabidopsis genomes uncoupled 5 (GUN5) mutant reveals the involvement of Mg- chelatase H subunit in plastid-to-nucleus signal transduction. *Proceedings of the National Academy of Sciences, 98*(4), 2053–2058.

Mochizuki, N., Susek, R., & Chory, J. (1996). An intracellular signal transduction pathway between the chloroplast and nucleus is involved in de-etiolation. *Plant Physiology, 112*(4), 1465–1469.

Monte, E., Tepperman, J. M., Al-Sady, B., Kaczorowski, K. A., Alonso, J. M., Ecker, J. R., … Quail, P. H. (2004). The phytochrome-interacting transcription factor, PIF3, acts early, selectively, and positively in light-induced chloroplast development. *Proceedings of the National Academy of Sciences, 101*(46), 16091–16098.

Moon, J., Zhu, L., Shen, H., & Huq, E. (2008). PIF1 directly and indirectly regulates chlorophyll biosynthesis to optimize the greening process in Arabidopsis. *Proceedings of the National Academy of Sciences, 105*(27), 9433–9438.

Müller, B., & Eichacker, L. A. (1999). Assembly of the D1 precursor in monomeric photosystem II reaction center precomplexes precedes chlorophyll a-triggered accumulation of reaction center II in barley etioplasts. *The Plant Cell, 11*(12), 2365.

Mussgnug, J. H., Wobbe, L., Elles, I., Claus, C., Hamilton, M., Fink, A., … Kruse, O. (2005). NAB1 is an RNA binding protein involved in the light-regulated differential expression of the light-harvesting antenna of *Chlamydomonas reinhardtii*. *The Plant Cell, 17*(12), 3409–3421.

Nishiyama, T., Sakayama, H., de Vries, J., Buschmann, H., Saint-Marcoux, D., Ullrich, K. K., … Rensing, S. A. (2018). The Chara genome: secondary complexity and implications for plant terrestrialization. *Cell, 174*(2).

Oh, E., Zhu, J.-Y., & Wang, Z.-Y. (2012). Interaction between BZR1 and PIF4 integrates brassinosteroid and environmental responses. *Nature Cell Biology, 14*(8), 802–809.

Ohad, I., Siekevitz, P., & Palade, G. E. (1967). Biogenesis of chloroplast membranes. *The Journal of Cell Biology, 35*(3), 521–552.

Ohlrogge, J., & Browse, J. (1995). Lipid biosynthesis. *The Plant Cell, 7*(7), 957–970.

Ohnishi, N., & Takahashi, Y. (2008). Chloroplast-encoded PsbT is required for efficient biogenesis of photosystem II complex in the green alga *Chlamydomonas reinhardtii*. *Photosynthesis Research, 98*(1–3), 315–322.

Orduña, L., Santiago, A., Navarro-Payá, D., Zhang, C., Wong, D. C., & Matus, J. T. (2023). Aggregated gene co-expression networks predict transcription factor regulatory landscapes in grapevine. *Journal of Experimental Botany, 74*(21), 6522–6540.

Oyama, T., Shimura, Y., & Okada, K. (1997). The Arabidopsis HY5 gene encodes a bZIP protein that regulates stimulus-induced development of root and hypocotyl. *Genes & Development, 11*(22), 2983–2995.

Paik, I., & Huq, E. (2019). Plant photoreceptors: Multi-functional sensory proteins and their signaling networks. *Seminars in Cell & Developmental Biology, 92*, 114–121.

Patro, R., Duggal, G., Love, M. I., Irizarry, R. A., & Kingsford, C. (2017). Salmon provides fast and bias-aware quantification of transcript expression. *Nature Methods, 14*(4), 417–419.

Pedmale, U. V., Huang, S. C., Zander, M., Cole, B. J., Hetzel, J., Ljung, K., … Chory, J. (2016). Cryptochromes interact directly with PIFs to control plant growth in limiting blue bight. *Cell, 164*(1–2), 233–245.

Peers, G., Truong, T. B., Ostendorf, E., Busch, A., Elrad, D., Grossman, A. R., … Niyogi, K. K. (2009). An ancient light-harvesting protein is critical for the regulation of algal photosynthesis. *Nature, 462*(7272), 518–521.

Perlaza, K., Toutkoushian, H., Boone, M., Lam, M., Iwai, M., Jonikas, M. C., … Ramundo, S. (2019). The MARS1 kinase confers photoprotection through signaling in the chloroplast unfolded protein response. *eLife, 8*.

Petersen, J., Rredhi, A., Szyttenholm, J., & Mittag, M. (2022). Evolution of circadian clocks along the green lineage. *Plant Physiology, 190*(2), 924–937.

Petroutsos, D., Busch, A., Janßen, I., Trompelt, K., Bergner, S. V., Weinl, S., … Hippler, M. (2011). The chloroplast calcium sensor CAS is required for photoacclimation in *Chlamydomonas reinhardtii*. *The Plant Cell, 23*(8), 2950–2963.

Petroutsos, D., Tokutsu, R., Maruyama, S., Flori, S., Greiner, A., Magneschi, L., … Minagawa, J. (2016). A blue-light photoreceptor mediates the feedback regulation of photosynthesis. *Nature, 537*(7621), 563–566.

Pfeiffer, A., Janocha, D., Dong, Y., Medzihradszky, A., Schöne, S., Daum, G., … Lohmann, J. U. (2016). Integration of light and metabolic signals for stem cell activation at the shoot apical meristem. *eLife, 5*.

Pfeiffer, A., Shi, H., Tepperman, J. M., Zhang, Y., & Quail, P. H. (2014). Combinatorial complexity in a transcriptionally centered signaling hub in Arabidopsis. *Molecular Plant, 7*(11), 1598–1618.

Pipitone, R., Eicke, S., Pfister, B., Glauser, G., Falconet, D., Uwizeye, C., … Demarsy, E. (2021). A multifaceted analysis reveals two distinct phases of chloroplast biogenesis during de-etiolation in Arabidopsis. *eLife, 10*.

Podolec, R., & Ulm, R. (2018). Photoreceptor-mediated regulation of the COP1/SPA E3 ubiquitin ligase. *Current Opinion in Plant Biology, 45*, 18–25.

Podolec, R., Demarsy, E., Ulm, R. (2021). Perception and signaling of ultraviolet-B radiation in plants. *Annual Review of Plant Biology, 72*(1), 793–822.

Pontier, D., Albrieux, C., Joyard, J., Lagrange, T., & Block, M. A. (2007). Knock-out of the magnesium protoporphyrin IX methyltransferase gene in Arabidopsis. Effects on chloroplast development and on chloroplast-to-nucleus signaling. *Journal of Biological Chemistry, 282*(4), 2297–2304.

Porra, R. J., Thompson, W. A., & Kriedemann, P. E. (1989). Determination of accurate extinction coefficients and simultaneous equations for assaying chlorophylls a and b extracted with four different solvents: verification of the concentration of chlorophyll standards by atomic absorption spectroscopy. *Biochimica et Biophysica Acta (BBA) - Bioenergetics, 975*(3), 384–394.

Possart, A., Xu, T., Paik, I., Hanke, S., Keim, S., Hermann, H.-M., … Hiltbrunner, A. (2017). Characterization of phytochrome interacting factors from the moss *Physcomitrella patens* illustrates conservation of phytochrome signaling modules in land plants. *The Plant Cell, 29*(2), 310–330.

Pribil, M., Labs, M., & Leister, D. (2014). Structure and dynamics of thylakoids in land plants. *Journal of Experimental Botany, 65*(8), 1955–1972.

Quail, P. H. (2021). Photobodies reveal their secret. *Nature Plants, 7*(10), 1326–1327.

Quail, P. H., Boylan, M. T., Parks, B. M., Short, T. W., Xu, Y., & Wagner, D. (1995). Phytochromes: Photosensory perception and signal transduction. *Science, 268*(5211), 675–680.

Ramundo, S., Casero, D., Mühlhaus, T., Hemme, D., Sommer, F., Crèvecoeur, M., … Rochaix, J. D. (2014). Conditional depletion of the Chlamydomonas chloroplast ClpP protease activates nuclear genes involved in autophagy and plastid protein quality control. *The Plant Cell, 26*(5), 2201–2222.

Ranjan, A., Dickopf, S., Ullrich, K. K., Rensing, S. A., & Hoecker, U. (2014). Functional analysis of COP1 and SPA orthologs from Physcomitrella and rice during photomorphogenesis of transgenic Arabidopsis reveals distinct evolutionary conservation. *BMC Plant Biology, 14*(1).

Rascio, N., Mariani, P., & Orsenigo, M. (1984). Photosynthetic apparatus differentiation in *Ginkgo biloba* L. *Advances in Photosynthesis Research*, 661–664.

Reinbothe, C., Bakkouri, M. E., Buhr, F., Muraki, N., Nomata, J., Kurisu, G., … Reinbothe, S. (2010). Chlorophyll biosynthesis: spotlight on protochlorophyllide reduction. *Trends in Plant Science, 15*(11), 614–624.

Reinbothe, S., Reinbothe, C., Lebedev, N., & Apel, K. (1996). PORA and PORB, two light-dependent protochlorophyllide-reducing enzymes of angiosperm chlorophyll biosynthesis. *The Plant Cell*, 763–769.

Richardson, L. G., & Schnell, D. J. (2019). Origins, function, and regulation of the TOC–TIC general protein import machinery of plastids. *Journal of Experimental Botany, 71*(4), 1226–1238.

Richter, A. S., Nägele, T., Grimm, B., Kaufmann, K., Schroda, M., Leister, D., & Kleine, T. (2023). Retrograde signaling in plants: a critical review focusing on the GUN pathway and beyond. *Plant Communications, 4*(1), 100511.

Rredhi, A., Petersen, J., Schubert, M., Li, W., Oldemeyer, S., Li, W., … Mittag, M. (2021). DASH cryptochrome 1, a UV-A receptor, balances the photosynthetic machinery of *Chlamydomonas reinhardtii*. *New Phytologist, 232*(2), 610–624.

Ruckle, M. E., Burgoon, L. D., Lawrence, L. A., Sinkler, C. A., & Larkin, R. M. (2012). Plastids are major regulators of light signaling in Arabidopsis. *Plant Physiology, 159*(1), 366–390.

Ruckle, M. E., DeMarco, S. M., & Larkin, R. M. (2007). Plastid signals remodel light signaling networks and are essential for efficient chloroplast biogenesis in Arabidopsis. *The Plant Cell, 19*(12), 3944–3960.

Rudowska, Ł., Gieczewska, K., Mazur, R., Garstka, M., & Mostowska, A. (2012). Chloroplast biogenesis — correlation between structure and function. *Biochimica et Biophysica Acta (BBA) - Bioenergetics, 1817*(8), 1380–1387.

Sager, R., & Palade, G. E. (1954). Chloroplast structure in green and yellow strains of Chlamydomonas. *Experimental Cell Research, 7*(2), 584–588.

Sassi, M., Lu, Y., Zhang, Y., Wang, J., Dhonukshe, P., Blilou, I., … Xu, J. (2012). COP1 mediates the coordination of root and shoot growth by light through modulation of PIN1- and PIN2-dependent auxin transport in Arabidopsis. *Development, 139*(18), 3402–3412.

Sasso, S., Stibor, H., Mittag, M., & Grossman, A. R. (2018). From molecular manipulation of domesticated *Chlamydomonas reinhardtii* to survival in nature. *eLife, 7*.

Schierenbeck, L., Ries, D., Rogge, K., Grewe, S., Weisshaar, B., & Kruse, O. (2015). Fast forward genetics to identify mutations causing a high light tolerant phenotype in *Chlamydomonas reinhardtii* by whole-genome-sequencing. *BMC Genomics, 16*(1).

Schroda, M. (2019). Good news for nuclear transgene expression in Chlamydomonas. *Cells, 8*(12), 1534.

Shannon, P., Markiel, A., Ozier, O., Baliga, N. S., Wang, J. T., Ramage, D., … Ideker, T. (2003). Cytoscape: A software environment for integrated models of Biomolecular Interaction Networks. *Genome Research, 13*(11), 2498–2504.

Sharpe, R. M., Mahajan, A., Takacs, E. M., Stern, D. B., & Cahoon, A. B. (2010). Developmental and cell type characterization of bundle sheath and mesophyll chloroplast transcript abundance in maize. *Current Genetics, 57*(2), 89–102.

Shen, H., Zhu, L., Castillon, A., Majee, M., Downie, B., & Huq, E. (2008). Light-induced phosphorylation and degradation of the negative regulator PHYTOCHROME-INTERACTING FACTOR1 from Arabidopsis depend upon its direct physical interactions with photoactivated phytochromes. *The Plant Cell, 20*(6), 1586–1602.

Shimizu, T., & Masuda, T. (2021). The role of tetrapyrrole- and GUN1-dependent signaling on chloroplast biogenesis. *Plants, 10*(2), 196.

Shin, K., Lee, R.-A., Lee, I., Lee, S., Park, S. K., & Soh, M.-S. (2013). Genetic identification of a second site modifier of CTR1-1 that controls ethylene-responsive and gravitropic root growth in *Arabidopsis thaliana*. *Molecules and Cells, 36*(1), 88–96.

Sizova, I., Kelterborn, S., Verbenko, V., Kateriya, S., & Hegemann, P. (2021). Chlamydomonas POLQ is necessary for CRISPR/Cas9-mediated gene targeting. *G3 (Bethesda, Md.), 11*(7).

Solymosi, K., & Schoefs, B. (2010). Etioplast and Etio-chloroplast formation under natural conditions: The dark side of chlorophyll biosynthesis in angiosperms. *Photosynthesis Research, 105*(2), 143–166.

Strand, Å., Asami, T., Alonso, J., Ecker, J. R., & Chory, J. (2003). Chloroplast to nucleus communication triggered by accumulation of Mg-protoporphyrinIX. *Nature, 421*(6918), 79–83.

Strenkert, D., Schmollinger, S., Gallaher, S. D., Salomé, P. A., Purvine, S. O., Nicora, C. D., … Merchant, S. S. (2019). Multiomics resolution of molecular events during a day in the life of Chlamydomonas. *Proceedings of the National Academy of Sciences, 116*(6), 2374–2383.

Sueoka, N. (1960). Mitotic replication of deoxyribonucleic acid in *Chlamydomonas reinhardi*. *Proceedings of the National Academy of Sciences, 46*(1), 83–91.

Sun, T. (2011). The molecular mechanism and evolution of the GA–GID1–DELLA signaling module in plants. *Current Biology, 21*(9).

Sun, T., Zeng, S., Wang, X., Owens, L. A., Fe, Z., Zhao, Y., … Li, L. (2022). GLKs directly regulate carotenoid biosynthesis via Interacting with GBFs in nuclear condensates in plants. bioRxiv. https://doi.org/10.1101/2022.09.09.507346

Supek, F., Bošnjak, M., Škunca, N., & Šmuc, T. (2011). Revigo summarizes and visualizes long lists of gene ontology terms. *PLoS ONE, 6*(7).

Susek, R. E., Ausubel, F. M., & Chory, J. (1993). Signal transduction mutants of Arabidopsis uncouple nuclear CAB and RBCS gene expression from chloroplast development. *Cell, 74*(5), 787–799.

Susek, R., & Chory, J. (1992). A tale of two genomes: Role of a chloroplast signal in coordinating nuclear and plastid genome expression. *Functional Plant Biology, 19*(4), 387.

Suzuki, J. Y., & Bauer, C. E. (1992). Light-independent chlorophyll biosynthesis: involvement of the chloroplast Gene *chlL* (*frxC*). *The Plant Cell, 4*(8), 929.

Symons, G. M., & Reid, J. B. (2003). Interactions between light and plant hormones during de-etiolation. *Journal of Plant Growth Regulation, 22*(1), 3–14.

Szklarczyk, D., Kirsch, R., Koutrouli, M., Nastou, K., Mehryary, F., Hachilif, R., … von Mering, C. (2022). The string database in 2023: Protein–protein association networks and functional enrichment analyses for any sequenced genome of interest. *Nucleic Acids Research, 51*(D1).

Tadini, L., Peracchio, C., Trotta, A., Colombo, M., Mancini, I., Jeran, N., … Pesaresi, P. (2019). GUN1 influences the accumulation of NEP-dependent transcripts and chloroplast protein import in Arabidopsis cotyledons upon perturbation of chloroplast protein homeostasis. *The Plant Journal, 101*(5), 1198–1220.

Tadini, L., Pesaresi, P., Kleine, T., Rossi, F., Guljamow, A., Sommer, F., … Leister, D. (2016). GUN1 controls accumulation of the plastid ribosomal protein S1 at the protein level and interacts with proteins involved in plastid protein homeostasis. *Plant Physiology, 170*(3), 1817–1830.

Tang, Q., Xu, D., Lenzen, B., Brachmann, A., Yapa, M. M., Doroodian, P., … Kleine, T. (2024). Arabidopsis GENOMES UNCOUPLED PROTEIN1 binds to plastid RNAs and promotes their maturation. bioRxiv. https://doi.org/10.1101/2024.02.08.579428

Terry, M. J., & Smith, A. G. (2013). A model for tetrapyrrole synthesis as the primary mechanism for plastid-to-nucleus signaling during chloroplast biogenesis. *Frontiers in Plant Science, 4*.

Theis, J., Niemeyer, J., Schmollinger, S., Ries, F., Rütgers, M., Gupta, T. K., … Schroda, M. (2020). VIPP2 interacts with VIPP1 and HSP22E/F at chloroplast membranes and modulates a retrograde signal for HSP22E/F gene expression. *Plant, Cell & Environment, 43*(5), 1212–1229.

Tian, F., Yang, D. C., Meng, Y. Q., Jin, J., & Gao, G. (2020). PlantRegMap: charting functional regulatory maps in plants. *Nucleic acids research, 48*(D1), D1104–D1113.

Tilbrook, K., Dubois, M., Crocco, C. D., Yin, R., Chappuis, R., Allorent, G., … Ulm, R. (2016). UV-B perception and acclimation in *Chlamydomonas reinhardtii*. *The Plant Cell, 28*(4), 966–983.

Tokutsu, R., Fujimura-Kamada, K., Matsuo, T., Yamasaki, T., & Minagawa, J. (2019). The CONSTANS flowering complex controls the protective response of photosynthesis in the green alga Chlamydomonas. *Nature Communications, 10*(1).

Toledo-Ortiz, G., Johansson, H., Lee, K. P., Bou-Torrent, J., Stewart, K., Steel, G., … Halliday, K. J. (2014). The HY5-PIF regulatory module coordinates light and temperature control of photosynthetic gene transcription. *PLoS Genetics, 10*(6).

Tran, N. T., & Kaldenhoff, R. (2020). Achievements and challenges of genetic engineering of the model green alga *Chlamydomonas reinhardtii*. *Algal Research, 50*, 101986.

Tu, X., Ren, S., Shen, W., Li, J., Li, Y., Li, C., … Zhong, S. (2022). Limited conservation in cross-species comparison of GLK transcription factor binding suggested wide-spread Cistrome divergence. *Nature Communications, 13*(1).

Veciana, N., Martín, G., Leivar, P., & Monte, E. (2022). BBX16 mediates the repression of seedling photomorphogenesis downstream of the GUN1/GLK1 module during retrograde signalling. *New Phytologist, 234*(1), 93–106.

Vedalankar, P., & Tripathy, B. C. (2018). Evolution of light-independent protochlorophyllide oxidoreductase. *Protoplasma, 256*(2), 293–312.

von Wettstein, D. (1959). The formation of plastid structures. In *The photochemical apparatus, its structure and function* (Vol. 11, pp.138-159). Brookhaven National Laboratory.

Vothknecht, U. C., Otters, S., Hennig, R., & Schneider, D. (2011). VIPP1: A very important protein in plastids?! *Journal of Experimental Botany, 63*(4), 1699–1712.

Wang, W. (1978). Effect of dim light on the *y-1* mutant of *Chlamydomonas reinhardtii*. *Plant Physiology, 61*(5), 842–846.

Wang, Q., & Lin, C. (2020). Mechanisms of cryptochrome-mediated photoresponses in plants. *Annual Review of Plant Biology, 71*(1), 103–129.

Wang, C., Liu, Y., Li, S.-S., & Han, G.-Z. (2015). Insights into the origin and evolution of the plant hormone signaling machinery. *Plant Physiology, 167*(3), 872–886.

Wang, W., Paik, I., Kim, J., Hou, X., Sung, S., & Huq, E. (2021). Direct phosphorylation of HY5 by SPA kinases to regulate photomorphogenesis in Arabidopsis. *New Phytologist, 230*(6), 2311–2326.

Wang, L., Patena, W., Van Baalen, K. A., Xie, Y., Singer, E. R., Gavrilenko, S., … Jonikas, M. C. (2023). A chloroplast protein atlas reveals punctate structures and spatial organization of biosynthetic pathways. *Cell, 186*(16).

Wang, L., Tian, Y., Shi, W., Yu, P., Hu, Y., Lv, J., … Bai, M.-Y. (2020). The miR396-GRFs module mediates the prevention of photo-oxidative damage by brassinosteroids during seedling de-etiolation in Arabidopsis. *The Plant Cell, 32*(8), 2525–2542.

Waters, M. T., Wang, P., Korkaric, M., Capper, R. G., Saunders, N. J., & Langdale, J. A. (2009). GLK transcription factors coordinate expression of the photosynthetic apparatus in Arabidopsis. *The Plant Cell, 21*(4), 1109–1128.

Weiner, I., Atar, S., Schweitzer, S., Eilenberg, H., Feldman, Y., Avitan, M., … Yacoby, I. (2018). Enhancing heterologous expression in *Chlamydomonas reinhardtii* by transcript sequence optimization. *The Plant Journal, 94*(1), 22–31.

Wheeler, G. L. (2017). Calcium-dependent signalling processes in Chlamydomonas. *Chlamydomonas: Molecular Genetics and Physiology*, 233–255.

White, R. A., & Hoober, J. K. (1994). Biogenesis of thylakoid membranes in *Chlamydomonas reinhardtii y1* (a kinetic study of initial greening). *Plant Physiology, 106*(2), 583–590.

Wittkopp, T. M., Schmollinger, S., Saroussi, S., Hu, W., Zhang, W., Fan, Q., … Lagarias, J. C. (2017). Bilin-dependent photoacclimation in *Chlamydomonas reinhardtii*. *The Plant Cell, 29*(11), 2711–2726.

Woodson, J. D., Perez-Ruiz, J. M., & Chory, J. (2011). Heme synthesis by plastid ferrochelatase I regulates nuclear gene expression in plants. *Current Biology, 21*(10), 897–903.

Wu, G.-Z., Meyer, E. H., Wu, S., & Bock, R. (2019). Extensive posttranscriptional regulation of nuclear gene expression by plastid retrograde signals. *Plant Physiology, 180*(4), 2034–2048.

Wu, G., & Spalding, E. P. (2007). Separate functions for nuclear and cytoplasmic cryptochrome 1 during photomorphogenesis of Arabidopsis seedlings. *Proceedings of the National Academy of Sciences, 104(47)*, 18813–18818.

Wulf, D., Krüger, F. J., Klages, L. J., Viehöver, P., Jin, E., Wobbe, L., … Bräutigam, A. (2023). Multiple transcription factors mediate acclimation of Chlamydomonas to light stress. bioRxiv. https://doi.org/10.1101/2023.10.30.564712

Xu, D. (2019). COP1 and BBXs-HY5-mediated light signal transduction in plants. *New Phytologist, 228*(6), 1748–1753.

Xu, X., Chi, W., Sun, X., Feng, P., Guo, H., Li, J., … Zhang, L. (2016). Convergence of light and chloroplast signals for de-etiolation through ABI4–HY5 and COP1. *Nature Plants, 2*(6).

Yamano, T., & Fukuzawa, H. (2009). Carbon-concentrating mechanism in a green alga, *Chlamydomonas reinhardtii*, revealed by transcriptome analyses. *Journal of Basic Microbiology, 49*(1), 42–51.

Yamawaki, S., Yamashino, T., Nakanishi, H., & Mizuno, T. (2011). Functional characterization of HY5 homolog genes involved in early light-signaling in *Physcomitrella patens*. *Bioscience, Biotechnology, and Biochemistry, 75*(8), 1533–1539.

Yang, H.-Q., Wu, Y.-J., Tang, R.-H., Liu, D., Liu, Y., & Cashmore, A. R. (2000). The C termini of Arabidopsis cryptochromes mediate a constitutive light response. *Cell, 103*(5), 815–827.

Yasumura, Y., Moylan, E. C., & Langdale, J. A. (2005). A conserved transcription factor mediates nuclear control of organelle biogenesis in anciently diverged land plants. *The Plant Cell, 17*(7), 1894–1907.

Yelina, N. E., Frangedakis, E., Schreier, T. B., Rever, J., Tomaselli, M., Haseloff, J., & Hibberd, J. M. (2023). Streamlined regulation of chloroplast development in the liverwort *Marchantia polymorpha*. bioRxiv. https://doi.org/10.1101/2023.01.23.525199

Yoon, H. S., Hackett, J. D., Ciniglia, C., Pinto, G., & Bhattacharya, D. (2004). A molecular timeline for the origin of photosynthetic eukaryotes. *Molecular Biology and Evolution, 21*(5), 809–818.

Yoshioka, S., Taniguchi, F., Miura, K., Inoue, T., Yamano, T., & Fukuzawa, H. (2004). The novel Myb transcription factor LCR1 regulates the CO2-responsive gene cah1, encoding a periplasmic carbonic anhydrase in *Chlamydomonas reinhardtii*. *The Plant Cell, 16*(6), 1466–1477.

Yu, X., Klejnot, J., Zhao, X., Shalitin, D., Maymon, M., Yang, H., … Lin, C. (2007). Arabidopsis cryptochrome 2 completes its posttranslational life cycle in the nucleus. *The Plant Cell, 19*(10), 3146-3156.

Zhang, Y., Mayba, O., Pfeiffer, A., Shi, H., Tepperman, J. M., Speed, T. P., & Quail, P. H. (2013). A quartet of PIF bHLH factors provides a transcriptionally centered signaling hub that regulates seedling morphogenesis through differential expression-patterning of shared target genes in Arabidopsis. *PLoS Genetics, 9*(1).

Zhang, W., Willows, R. D., Deng, R., Li, Z., Li, M., Wang, Y., … Duanmu, D. (2021). Bilin-dependent regulation of chlorophyll biosynthesis by GUN4. *Proceedings of the National Academy of Sciences, 118*(20).

Zhao, X., Huang, J., & Chory, J. (2019). GUN1 interacts with MORF2 to regulate plastid RNA editing during retrograde signaling. *Proceedings of the National Academy of Sciences, 116*(20), 10162–10167.

Zheng, B., Xing, K., Zhang, J., Liu, H., Ali, K., Li, W., … Ren, H. (2022). Evolutionary Analysis and functional identification of ancient brassinosteroid receptors in *Ceratopteris richardii*. *International Journal of Molecular Sciences, 23*(12), 6795.

Zhong, S., Shi, H., Xi, Y., & Guo, H. (2010). Ethylene is crucial for cotyledon greening and seedling survival during de-etiolation. *Plant Signaling & Behavior, 5*(6), 739–742.

Zhong, S., Shi, H., Xue, C., Wei, N., Guo, H., & Deng, X. W. (2014). Ethylene-orchestrated circuitry coordinates a seedling's response to soil cover and etiolated growth. *Proceedings of the National Academy of Sciences, 111*(11), 3913–3920.

Zones, J. M., Blaby, I. K., Merchant, S. S., Umen, J. G. (2015). High-resolution profiling of a synchronized diurnal transcriptome from *Chlamydomonas reinhardtii* reveals continuous cell and metabolic differentiation. *The Plant Cell, 27*(10), 2743–2769.